AD_____

Award Number: W81XWH-07-1-0543

TITLE: New Radiation Therapy Systems: Applications to Human Cancer Treatment and Novel Drug Discovery

PRINCIPAL INVESTIGATOR: Giuseppe Pizzorno

CONTRACTING ORGANIZATION: Nevada Cancer Institute
Las Vegas, NV 89135

REPORT DATE: July 2010

TYPE OF REPORT: Final Addendum

PREPARED FOR: U.S. Army Medical Research and Materiel Command
Fort Detrick, Maryland 21702-5012

DISTRIBUTION STATEMENT: Approved for public release; distribution unlimited

REPORT DOCUMENTATION PAGE

Form Approved
OMB No. 0704-0188

1. REPORT DATE *(DD-MM-YYYY)*	**2. REPORT TYPE**	**3. DATES COVERED** *(From - To)*
01-07-2010	Final Addendum	15 JUL 2009 - 14 JUN 2010

4. TITLE AND SUBTITLE
New Radiation Therapy Systems: Applications to Human Cancer Treatment and Novel Drug Discovery

5a. CONTRACT NUMBER

5b. GRANT NUMBER
W81XWH-07-1-0543

5c. PROGRAM ELEMENT NUMBER

6. AUTHOR(S)
Giuseppe Pizzorno

E-Mail: gpizzorno@nvcancer.org

5d. PROJECT NUMBER

5e. TASK NUMBER

5f. WORK UNIT NUMBER

7. PERFORMING ORGANIZATION NAME(S) AND ADDRESS(ES)
Nevada Cancer Institute
Las Vegas, NV 89135

8. PERFORMING ORGANIZATION REPORT NUMBER

9. SPONSORING / MONITORING AGENCY NAME(S) AND ADDRESS(ES)
U.S. Army Medical Research and Materiel Command
Fort Detrick, Maryland 21702-5012

10. SPONSOR/MONITOR'S ACRONYM(S)

11. SPONSOR/MONITOR'S REPORT NUMBER(S)

12. DISTRIBUTION / AVAILABILITY STATEMENT
Approved for Public Release; Distribution Unlimited

13. SUPPLEMENTARY NOTES

14. ABSTRACT
A significant portion of prostate cancer patients fails standard hormonal therapy and will result in developing locally advanced or metastatic disease. Neither surgery nor radiation therapy (RT) achieves long-term remission for many patients. New therapeutic approaches, in combination with RT, are needed. The initial hypothesis was to determine whether the growth inhibition and apoptosis induction by RT in prostate cancer cells may be synergistically enhanced by DNA-methylation inhibitors (DNMTIs) and histone-deacetylase inhibitors (HDACIs). Furthermore, we wanted to evaluate whether prostate cancer cells may possess a novel signaling pathway involving nitric oxide (NO), cGMP and protein kinase G (PKG), which stimulates expression of Inhibitor of apoptosis Proteins (IAPs). The data acquired provide valuable new information on combining radiation therapy and DNMTIs given the effect of this combination on the DNA repair mechanism(s) that could be exploited not only for the treatment of prostate cancer but also in the therapeutic approach of other cancer know to be susceptible to radiation. We have also elucidated the novel role of the NO/cGMP/PKG signaling pathway in regulating apoptotic susceptibility in prostate cancer cells and other types of cancer cells of epithelial origin, including lung cancer and mesothelioma. This new information will be used to develop new agents inhibiting the NO/cGMP/PKG signaling pathway and overall generating better therapeutic approaches for the treatment of epithelial cancers.

15. SUBJECT TERMS
Synergism of radiation therapy and DNA-methylation inhibitors; DNA repair mechanisms; PKG/Src interaction; chemoresistance and resistance to radiation.

16. SECURITY CLASSIFICATION OF:			**17. LIMITATION OF ABSTRACT**	**18. NUMBER OF PAGES**	**19a. NAME OF RESPONSIBLE PERSON**
a. REPORT	**b. ABSTRACT**	**c. THIS PAGE**			USAMRMC
U	U	U	UU	206	**19b. TELEPHONE NUMBER** *(include area code)*

Table of Contents

Introduction

A significant portion of prostate cancer patients fails the standard hormonal ablation therapy and will eventually develop locally advanced or metastatic disease. Long term remission is usually not achieved by additional surgery or radiation therapy. Therefore, the development of new therapeutic approaches or modalities is a spearhead priority of prostate cancer research. We here provide continued evidence for our original research, demonstrating that radiation-induced growth retardation and cell death of prostate cancer cells is synergistically enhanced by DNA-methylation inhibitors (DNMTIs) and histone-deacetylase inhibitors (HDACIs). We have also shown that prostate cancer cells possess a hitherto unknown signaling pathway involving nitric oxide (NO), cGMP and protein kinase G (PKG), which stimulates expression of Inhibitor of Apoptosis Proteins (IAPs), thereby altering susceptibility of these cells to radiation-, DNMTI- and HDACI-induced apoptosis. Our accumulated data provide novel information about the regulatory mechanisms underlying radiation- and DNMTI-induced cell death which could be easily implement in the clinical arena. In addition, we have defined a novel role for the NO/cGMP/PKG signaling pathway in regulating apoptotic susceptibility of prostate cancer cells. Taken together, the research we here present will undoubtedly contribute to the development of novel therapeutic approaches for the treatment of prostate cancer.

Body of Research

Several portions of the initial proposal have been completed during the past 12 months and have been finalized in nine manuscripts that have been either published, under review for publication or being prepared for publication. For clarity we will introduce each of these completed projects as a summary and for more details we will present the whole manuscript as an attachment as indicated.

Original Statement of Work

a. Growth inhibition properties of DNMTIs (5-Azacytidine, decitabine and zebularine) alone and in combination with RT will be determined in prostate cancer (DU145, LnCAP, & PC-3) cell lines.
b. A novel technique pioneered by the Co-PI (Dr. Fiscus), utilizing the new technologies of capillary electrophoresis with laser-induced fluorescence detector (CE-LIF) and microchip electrophoresis (micro-CE), will be used to characterize and quantify levels of apoptotic DNA fragmentation in prostate cancer cell lines induced by the selected treatments.
c. Apoptotic mechanisms of RT and DNMTIs will be determined using CE-LIF, micro-CE, caspase activity assays and PARP cleavage as well as analysis of pathways involving BCL-2, BAX, BID, IAP proteins and death receptors (DR4 and DR5).
d. Using specific inhibitors and siRNA gene knockdown of NOSs/PKGs, the involvement of the NO/cGMP/PKG signaling pathway in regulating the susceptibility of prostate cancer cells to induction of apoptosis by RT, DNMTIs and HDACIs, alone and in combination, will be determined.
e. Molecular mechanisms underlying the interactions between DNMTIs and RT will be investigated, including studies of H2AX phosphorylation, ATM/ATR and Chk1/Ch2 induction.
f. Involvement of the NO/cGMP/PKG signaling pathway in stimulating expression of the 8 IAPs (NAIP, cIAP-1, cIAP-2, XIAP, Ts-XIAP, LIVIN (ML-IAP), Apollon and Surivin) in prostate cancer cells will be determined.
g. Prostate cancer xenografts in athymic mice (*in vivo* model) with microMRI testing will be used to further determine the interactions of DNMTIs and RT as well as HDACIs, angiogenesis inhibitors and IAP inhibitors, and their potential synergistic ability to reduce tumor growth.

Findings as related to Statement of Work

a. Growth inhibition properties of DNMTIs alone and in combination with RT in prostate cancer cell lines.

One of the key aims of the here reported study was to evaluate the feasibility of utilizing several DNA methyl transferase inhibiting compounds as sensitizing agents during radiation treatment of prostate cancers. To that end, we have assessed the anti-proliferative properties of several DNA methyl transferase inhibiting compounds, either as single agent modalities or in combination with ionizing radiation. These studies were conducted in vitro, utilizing cultured prostate cancer cells, as well as in vivo, utilizing prostate cancer xenografts. The research methodology of both approaches is described in detail in the attached manuscript of Weterings et al. (Attachment I; 'Low dose 5-azacytidine radio-sensitizes prostate cancer cells by impairing DNA double-strand break repair.' by Eric Weterings, Pamela M. Dino, Yi Feng, Eugene F. Hayes, James Symanowski, Sunil Sharma, and Giuseppe Pizzorno.).

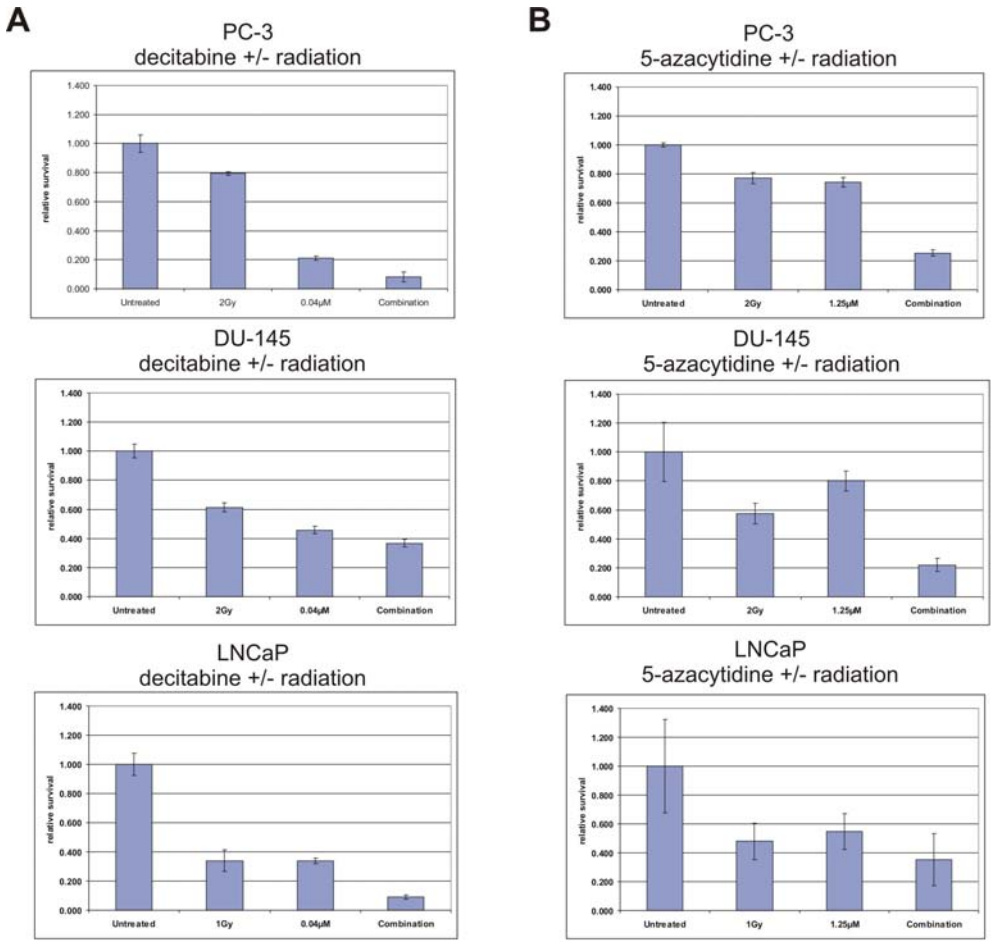

Figure 1. 5-azacytidine impairs DNA repair in prostate cancer cells

The in vitro component encompassed quantification of the effects of the cytidine analogue 5-azacytidine and its deoxy-derivative decitabine on the androgen-dependent LNCaP and the androgen-independent DU-145 and PC-3 prostate cancer cell lines. Clonogenic survival analysis demonstrated that both decitabine and 5-azacytidine as a single modality were capable of reducing cell survival (Figure 1). Interestingly, in androgen-insensitive PC-3 and DU-145 cells these effects were statistically significantly enhanced in a synergistic manner (Figure 1). These observations were solidified by ANOVA analysis and calculation of the synergy indexes as presented in Table 1. Taken together, these data serve as proof of principle that both 5-azacytidine and decitabine have a capability of serving as radiation potentiating compounds in vitro.

Table 1 Analysis of variance to assess synergistic potential of combination therapy

Drug	Cell Line	Survival Drug	Survival Radiation	Survival Comb.	Expected Survival[1]	Interaction p-value	Synergy Index
Decitabine	PC-3	21.1	79.4	8.1	16.7	0.007	0.48
Decitabine	DU-145	45.9	61.6	36.8	28.3	<0.001	1.30
Decitabine	LNCaP	33.8	33.9	9.3	11.5	<0.001	0.81
5-Azacyt	PC-3	74.1	77.2	25.3	57.2	<0.001	0.44
5-Azacyt	DU-145	80.0	57.4	22.1	46.0	0.513	NR
5-Azacyt	LNCaP	54.6	47.9	35.3	26.2	0.182	NR

1Expected survival for the combination if drug and radiation therapy were additive.
NR = not reported because interaction term was not significant indicating additivity.

The significant radiation sensitization of the DU-145 and PC-3 cell lines induced by 5-azacytidine and its deoxy-derivative lead us to speculate that these compounds may reduce the efficiency of DNA double-strand break (DSB) repair. In order to test this hypothesis, we measured the onset and disappearance of γ-H2AX foci at regular intervals after radiation, either in the absence or presence of 5-azacytidine or decitabine (Figure 2). This technique is one of the well-established methodologies available to quantify the presence of DSBs in cell nuclei.

As expected, we observed a temporary increase and a subsequent steady decrease in γ-H2AX foci in LNCaP, DU-145 and PC-3 prostate cancer cell lines after irradiation, indicating normal DSB repair (Figure 2). Interestingly, upon treatment of PC-3 and DU-145 cells with 5-azacytidine, a much less pronounced decrease of γ-H2AX foci numbers was observed. The difference in decreasing speed - reflecting the speed of DSB repair – was found to be highly statistically significant as further detailed in Table 2. We conclude from these findings that 5-

azacytidine treatment of the androgen-dependent cell lines DU-145 and PC-3 induced delay or impairment of DSB repair.

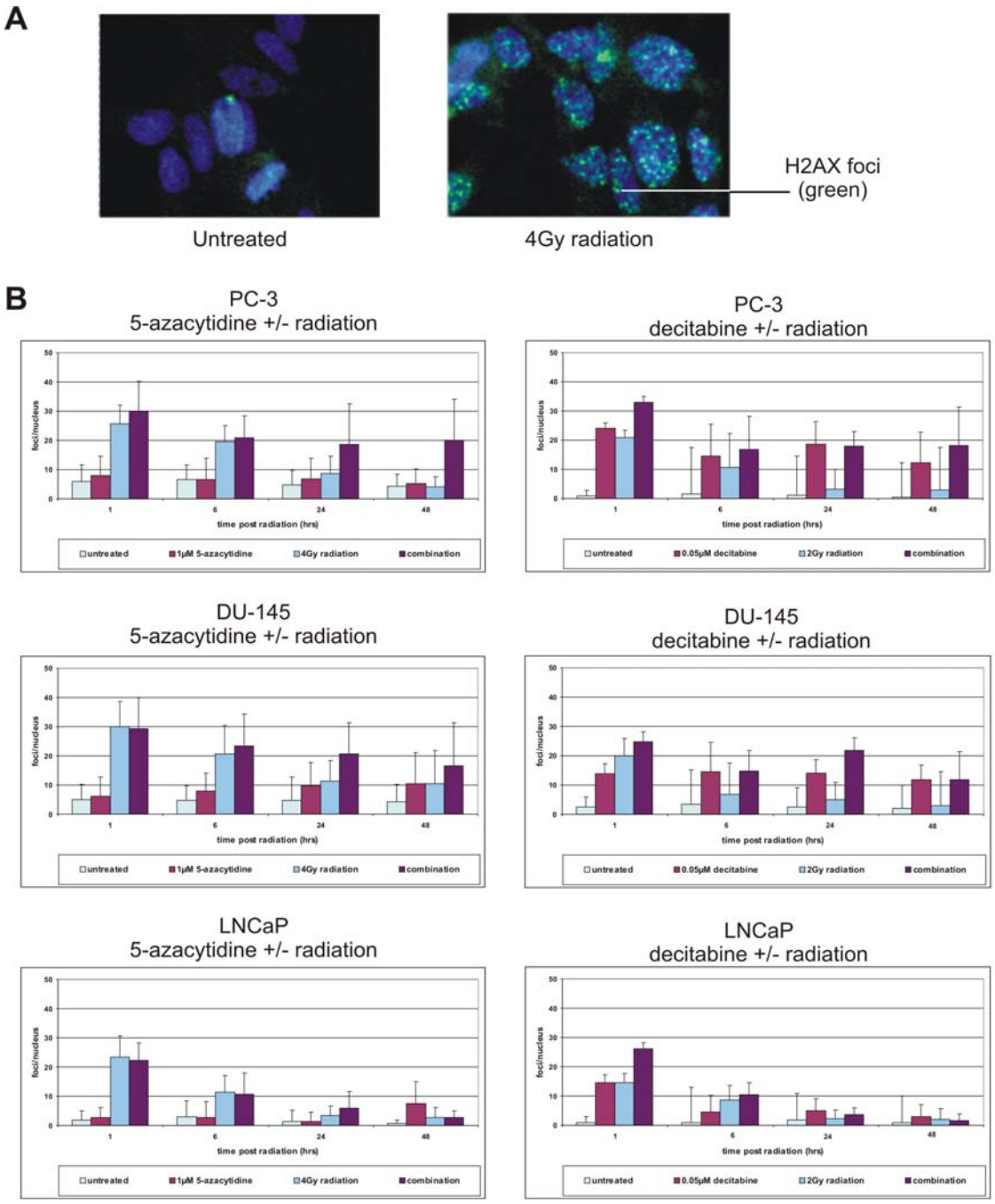

Figure 2. 5-Azacytidine impairs DNA repair in prostate cancer cells

Table 2. Analysis of time trends in gamma-H2AX foci decrease

		Time trend in radiation only groups		Time trend in combination groups		Comparison of trends	Comparison of trend ratios
Drug	**Cell Line**	**Decrease in foci per hrs**	**P-value**	**Decrease in foci per hour**	**P-value**	**P-value**	
5-Azacyt	PC-3	0.44	<0.001	0.15	<0.001	<0.001	2.9
5- Azacyt	DU-145	0.37	<0.001	0.23	<0.001	0.007	1.6
5- Azacyt	LNCaP	0.37	<0.001	0.34	<0.001	0.765	NR
Decitabine	PC-3	0.33	<0.001	0.19	<0.001	<0.001	1.7
Decitabine	DU-145	0.27	<0.001	0.18	<0.001	<0.001	1.5
Decitabine	LNCaP	0.24	<0.001	0.42	<0.001	0.080	NR

NR= not reported because difference in time trends was not significant

A similar effect was observed for decitabine (Figure 2). However, this observation was complicated by the fact that decitabine treatment as a single modality increased the number of γ-H2AX foci, indicating that decitabine, unlike 5-azacytidine, is capable of introducing DSB by itself. We theorize that this activity of decitabine is caused at least in part by the fact that this compound is exclusively incorporated into the DNA rather than the RNA, where it can cause DNA breaks by strand termination. From this observation we conclude that although decitabine and 5-azacytidine both radio-sensitize prostate cancer cells, the underlying mechanism of activity must be markedly different between both related compounds.

In order to further support our theory that 5-azacytidine radio-sensitizes DU-145 and PC-3 prostate cancer cells by impairing DSB repair, we performed a DSB repair efficiency assay which is based on transfection and subsequent repair of linearized plasmids (Figure 3). This methodology, as detailed in Attachment I, essentially utilizes linearized plasmids as mimic substrates for a DNA break. Repair of the plasmid by recipient cells can only occur through a direct joining process which is mediated by the non-homologous end-joining (NHEJ) mechanism. Quantification of DSB repair is done by performing a PCR reaction over the joint area of the 'repaired' plasmid, followed by measurement of the PCR product.

This line of investigation revealed that treatment with increasing concentrations of 5-azacytidine markedly reduced NHEJ efficiency in DU-145 and PC-3 cells, but not in LNCaP cells (Figure 3). These results were not obtained when 5-azacytidine was substituted with decitabine, once again demonstrating that 5-azacytidine and decitabine display different modes of activity with respect to radiation resistance mechanisms.

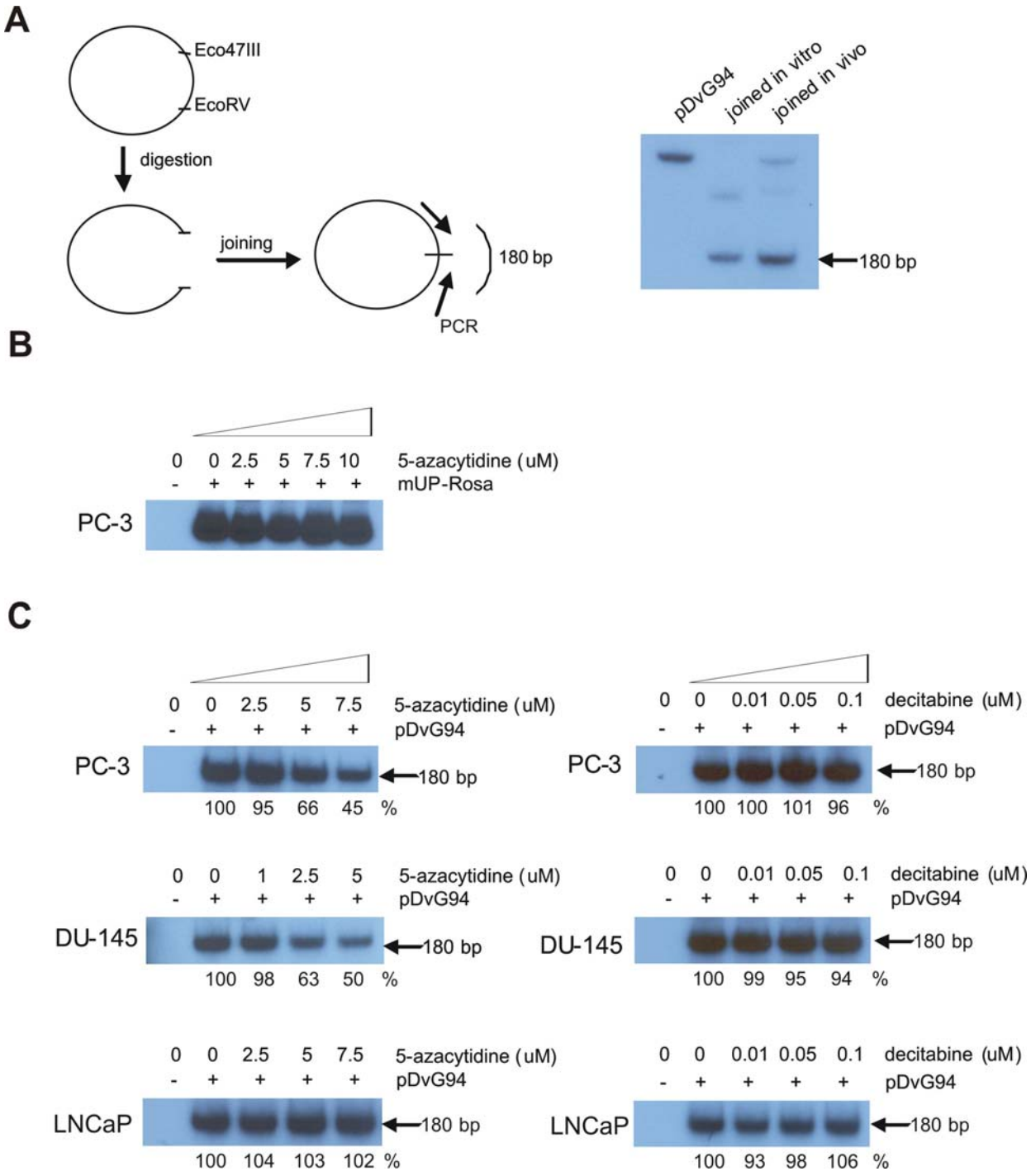

Figure 3. 5-Azacytidine reduces non-homologous end-joining efficiency

Taken all our observations together, we conclude that 5-azacytidine has a clear capability to increase radiation sensitivity of the commonly utilized androgen-insensitive prostate cancer cell lines DU-145 and PC-3. This potentiating activity is supported by the ability of this

compound to reduce the efficiency of DSB repair, which in turn is at least partially caused by delay or impairment of the NHEJ pathway. The deoxy-counterpart of 5-azacytidine, decitabine, has a similar radio-sensitizing effect, but the underlaying mechanism of activity is likely to be very dissimilar and less well understood than that of 5-azacytidine.

Based on our research, we propose that 5-azacytidine may be an interesting candidate for potentiation of radiation therapy during treatment of prostate cancers. We have further evaluated and confirmed the in vivo significance of these findings by examining the effects of 5-azacytidine on prostate cancer xenografts, the results of which we will discuss under point g.

A logical follow-up study of our research would be the evaluation of the influence of 5-azacytidine on expressional modulation of genes, RNA species, or proteins which are involved in DSB repair. In fact, we have at present started to engage in such a line of experimentation.

b. A novel technique pioneered by the Co-PI (Dr. Fiscus), utilizing the new technologies of capillary electrophoresis with laser-induced fluorescence detector (CE-LIF) and microchip electrophoresis (micro-CE), will be used to characterize and quantify levels of apoptotic DNA fragmentation in prostate cancer cell lines induced by the selected treatments.

A CE-LIF system (PA800 from Beckman Coulter, Inc.) was purchase as part of this DOD Award. For the micro-CE instruments, we tested two micro-CEs, the 2100 Bioanalyzer from Agilent and the LC3000 from Caliper, before purchasing, and found that both of these instruments could not provide adequate sensitivity (compared with a true CE-LIF system) for measuring apoptotic DNA fragmentation. In our search for an adequately-sensitive instrument, we found that a new type of CE, originally called a HDA-GT12 Genetic Analyzer from eGene, Inc. (Irvine, CA) (now called QIAxcel and marketed by Qiagen), which contains 12 capillaries and 12 light emitting diode (LED) detectors (which we call a 12-CE-LED-IF system), could provided sensitivity for DNA analysis that was nearly the sensitivity of a conventional CE-LIF system, but with much better throughput (because of the simultaneous use of 12 capillaries and shorter electrophoretic runs). This 12-CE-LED-IF system was purchased from eGene, Inc. as part of this DOD Award and was used in our experiments for apoptotic DNA fragmentation analysis in prostate cancer cells and other cancer cells, as related to the original objective (Statement of Work, b.) stated in the DOD Award (data shown below and in publications and manuscripts in the Appendix).

Initial experiments analyzing apoptotic DNA fragmentation analysis using both the single capillary CE-LIF system (PA800 system) and the 12-CE-LED-IF system (QIAxcel system) showed that human prostate cancer cell lines (PC-3, DU145 and LNCap) did not display clear apoptotic DNA fragmentation following exposure to chemotherapeutic agents, like we had

previously shown in mouse and rat cell lines. The reason for this difference is not clear, but may relate to different cellular mechanisms in the different species and in the initiation of the caspase-3-dependent activation of endonucleases that would result in apoptotic DNA fragmentation. Other studies from our lab as well as other labs have found clear differences in different species and cell lines concerning whether or not the cells show clear apoptotic DNA fragmentation during the development of apoptotic cell death. For example, in some cell lines exposed to chemotherapeutic agents and other toxins, secondary necrosis occurs, dumping the cellular contents into the media before apoptotic DNA fragmentation can occur, thus making it difficult to capture the apoptotic DNA fragments for analysis.

To utilize the CE-LIF and 12-CE-LED-IF instruments in our studies, we conducted experiments using the mouse N1E-115 neuroblastoma cell line and analyzed the induction of apoptotic DNA fragmentation by ODQ, an agent that blocks the activation of soluble guanylyl cyclase by endogenous nitric oxide (NO). Blocking the endogenous biosynthesis of cyclic GMP by using the ODQ caused a sizable increase in the levels of apoptotic DNA fragmentation in the N1E-115 cells, using the QIAxcel 12-CE-LED-IF system (shown in Figure 4).

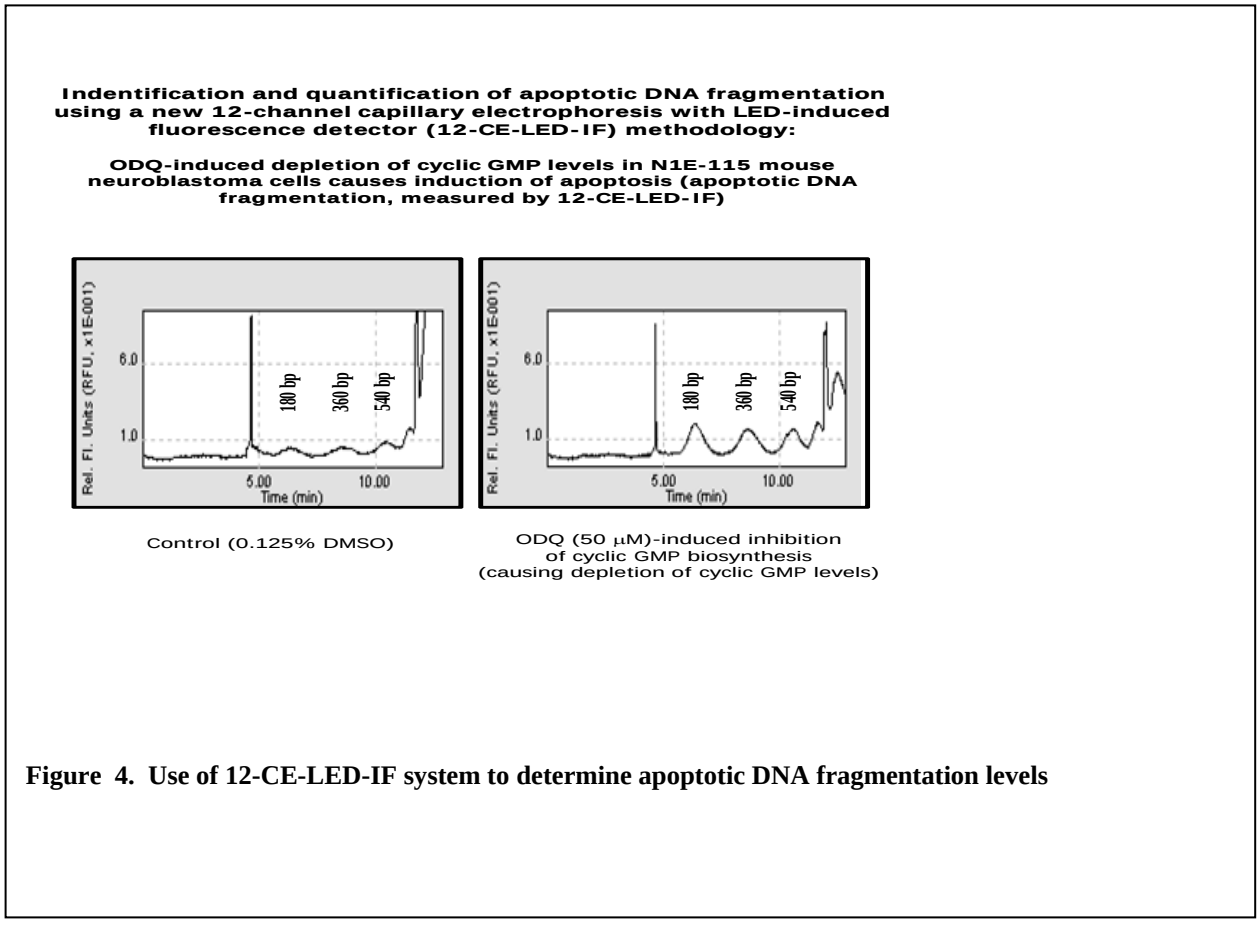

Figure 4. Use of 12-CE-LED-IF system to determine apoptotic DNA fragmentation levels

A published version of similar data are shown in Figure 5 on page 550 of the attached publication:

M.G. Johlfs and R.R. Fiscus, Protein kinase G type-Iα phosphorylates the apoptosis-regulating protein Bad at serine 155 and protects against apoptosis in N1E-115 cells, *Neurochem. Int.,* 56: 546-553, 2010.

Figure 5 illustrates another application for the QIAxcel 12-CE-LED-IF system, which we have developed during the last year of the DOD funded project, which was designed to provide a quantitative and accurate analyze of our mRNA samples. This new application involves multiplexed analysis of RT-PCR products, allowing us to use CE-based methodology to accurately measure the mRNA levels in biological samples. The advantage of this new methodology is that off-target DNA products or primer-dimers, which are often a problem when using conventional Real-time PCR methods, can be clearly visualized (and separated from the important data) when using the 12-CE-LED-IF system. The figure shows PCR products representing the two isoforms of PKG-I in a sample of SH-SY5Y human neuroblastoma cells, used as an example of the usefulness of this new methodology.

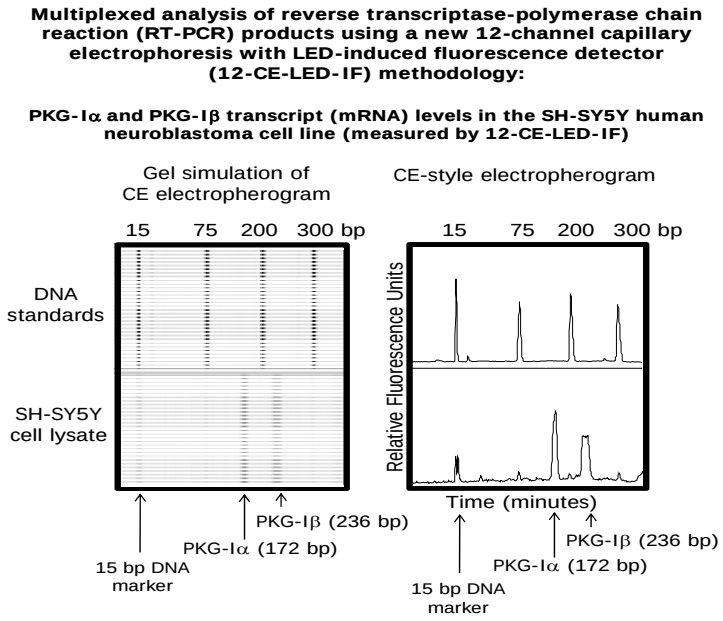

Figure 5. Use of the 12-CE-LED-IF system to analysis, in a multiplexed manned, RT-PCR products for the determination of mRNA levels in biological samples

Further studies using this new methodology were conducted on the prostate cancer cells described in the Statement of Work. Because of its superior ability to quantify mRNA expression levels, this new 12-CE-LED-IF system was used to accurately determine the level of gene knockdown caused by transfecting PC-3 cells with shRNA constructs designed to specifically silence the expression of PKG-Iα/β. The resulting data are shown in two attached manuscripts (in the Appendix):

R.R. Fiscus, M. Bathina, M.G. Johlfs, J.C. Wong, O.B. Goodman, Jr., S. Sharma, G. Pizzorno and N. J. Vogelzang. Involvement of the protein kinase G type-Iα signaling pathway in suppressing apoptotic cell death in prostate cancer cells. Manuscript prepared for submission to *Oncogene*. Figure 8, Panel a, showing dramatic downregulation of mRNA levels of the PKG-Iα transcripts following shRNA gene knockdown. This gene knockdown was then used to show that PKG-Iα plays an essential role in suppressing onset of apoptosis in prostate cancer cells (in partial fulfillment of the Statement of Work objective d., listed below).

R.R. Fiscus, M. Bathina, M.G. Johlfs, J.C. Wong, O.B. Goodman, Jr., S. Sharma, G. Pizzorno and N.J. Vogelzang. Basal cyclic GMP levels and protein kinase G type-Iα activity play an essential role in promoting cell proliferation in prostate cancer cells. Manuscript prepared for submission to *Cancer Res*. Figure 5, showing that two shRNA constructs decrease the PKG-Iα mRNA levels by 64% and 68%, thus showing successful gene knockdown. This knockdown was then used to show the essential role of PKG-Iα in promoting cell proliferation in prostate cancer cells.

c. <u>Apoptotic mechanisms of RT and DNMTIs will be determined using CE-LIF, micro-CE, caspase activity assays and PARP cleavage as well as analysis of pathways involving BCL-2, BAX, BID, IAP proteins and death receptors (DR4 and DR5).</u>

As discussed under point a., we have demonstrated during the course of the here described project that the DNMT inhibitor 5-azacytidine and its deoxy-derivative, decitabine, sensitize prostate cancer cells to ionizing radiation by inhibiting DSB break repair through the NHEJ mechanism. Because impairment of DNA damage repair is usually associated with delay or halting of the cell cycle and with the induction of apoptosis, we studied the effects of 5-azacytidine on expression of several apoptotic and cell cycle regulating factors.

First, we studied the induction of apoptosis in prostate cancer cells by examining expression of the apoptotic marker cleaved PARP (Figure 6). Treatment of androgen-dependent LNCaP or androgen-independent DU-145 and PC-3 prostate cancer cells with 5-Azacytidine resulted in clear and marked elevation of PARP cleavage, even in the absence of radiation (Figure 6). These results demonstrate the ability of 5-azacytidine to initiate apoptosis, and at

least in parts explains this drug's cytotoxic properties. The observed increase of apoptosis by 5-azacytidine can be either dependent or independent of the previously discussed impairment of DSB repair, but in any case this effect will strongly enhance the effectiveness of added cytotoxic stressors like ionizing radiation.

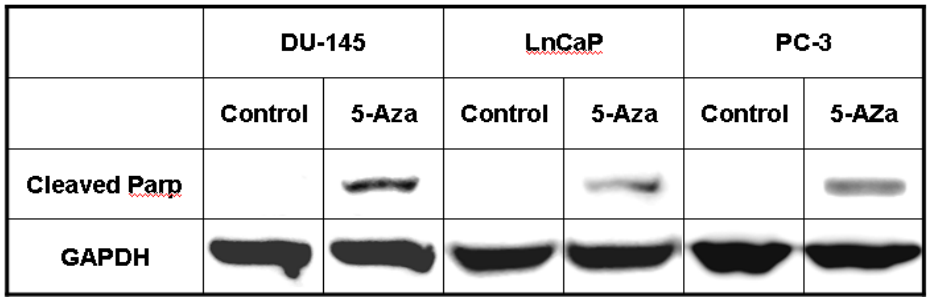

Figure 6. Induction of apoptotic PARP cleavage in prostate cancer cells by 5-azacytidine

Next, we studied in more detail the response of a panel of both apoptotic and cell cycle regulating factors to 5-azacytidine treatment in PC-3 prostate cancer cells (Figure 7). We observed that treatment with increasing doses of 5-azacytidine resulted in the down regulation of the X-linked inhibitor of apoptosis protein (XIAP) within 72 hours and an up regulation of the apotosis regulator Bcl-2 (Figure 7). In addition, we observed an increase in the expression levels of the cell cycle regulator and cellular senescence mediator p21 (Figure 7).

It was somewhat unexpected that we found an up regulation of the apoptosis inhibitor cIAP1 in response to 5-azacytidine treatment (Figure 7). This particular observation does not immediately fit the classical model of apoptotic activation and will need further evaluation before a fully comprehensive assessment can be made of the exact mechanism of 5-azacytidine induced apoptosis onset.

Finally, we investigated the influence of 5-azacytidine treatment on the functionality of apoptotic caspases (Figure 8). Therefore, we measured the specific activities of caspases 8, 9, and 3/7 in PC-3 prostate cancer cells after treatment with increasing doses of 5-azacytidine. For all the caspases we evaluated, a clear and marked increase (2-7 times the baseline levels) in activity was observed approximately 48 hours after administration of 5-azacytidine (Figure 8). These findings are highly consistent with our findings of PARP cleavage and up regulation of the apoptotic process in the presence of 5-azacytidine.

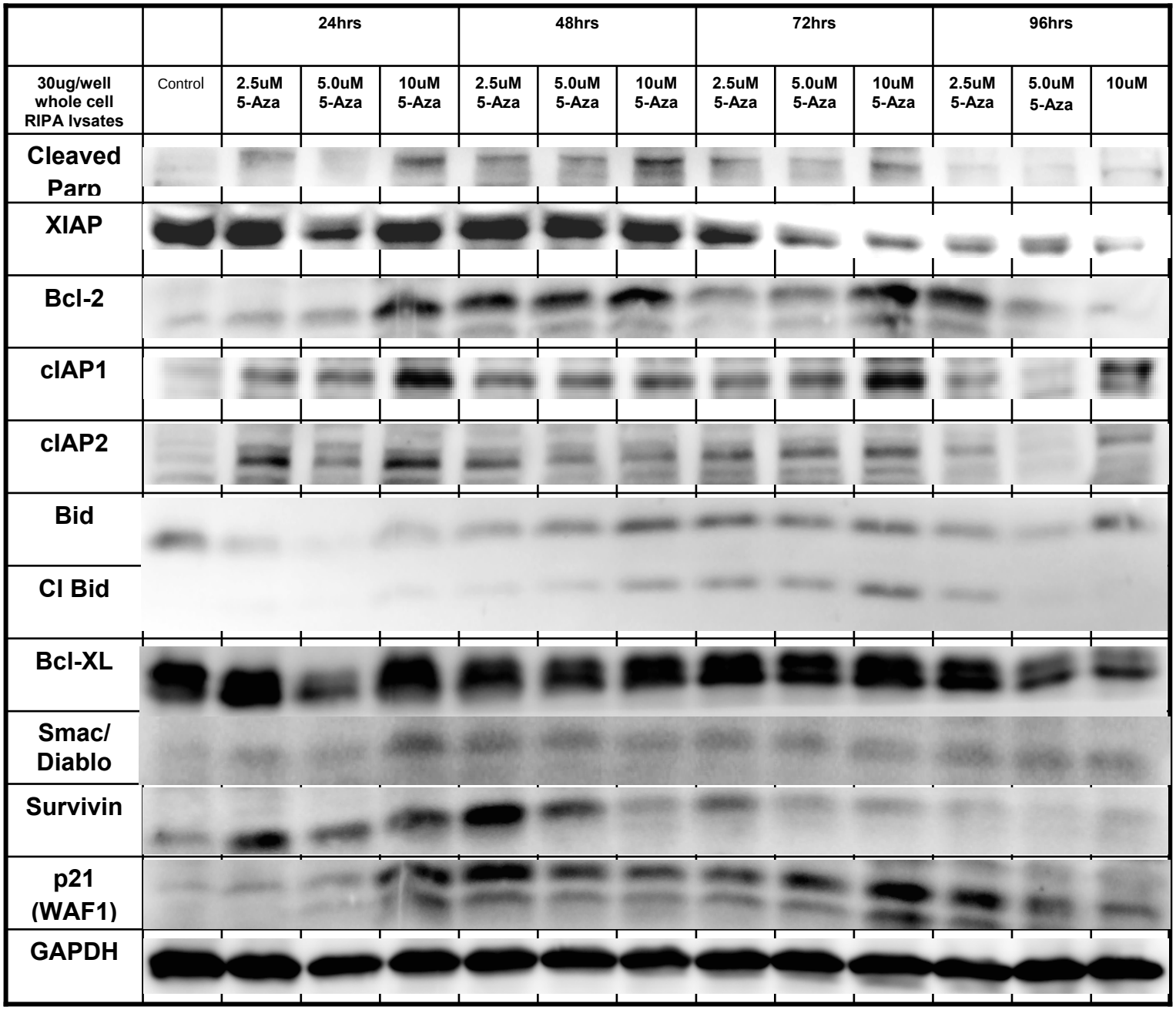

Figure 7. Regulation of apoptotic and cell cycle regulating factors in PC-3 prostate cancer cells in response to 5-azacytidine treatment

The down regulation of anti-apoptotic proteins and the up regulation of apoptosis regulators and cell cycle regulators is consistent with the onset of apoptosis induced by 5-azacytidine and further solidifies our observation that 5-azacytidine not only impairs DSB repair but stimulates apoptosis at the same time, possibly in a concentration-dependent manner. Stimulation of apoptosis during radiation-induced cell cycle arrest would significantly enhance the cytotoxic effects of radiation and we therefore conclude that the radiation sensitizing effects of 5-azacytidine can be attributed to the simultaneous events of repair inhibition and apoptosis enhancement.

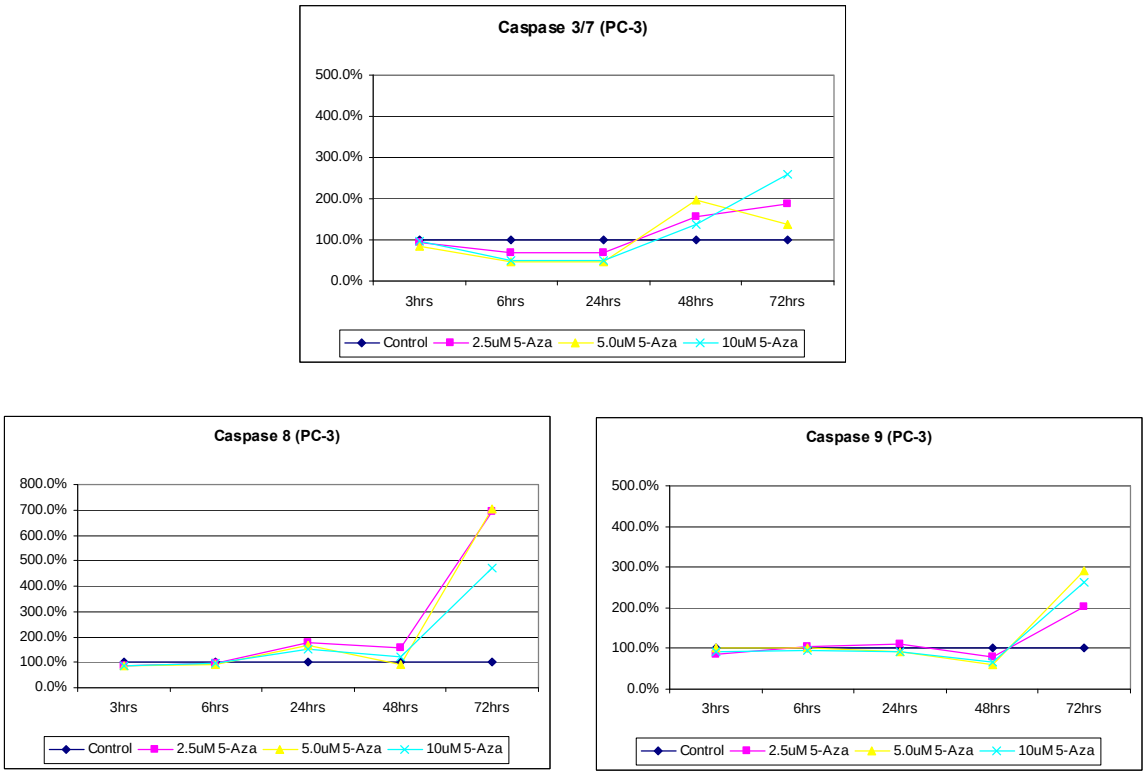

Figure 8. Regulation of activity of apoptotic caspases in PC-3 prostate cancer cells in response to 5-azacytidine treatment

d. Using specific inhibitors and siRNA gene knockdown of NOSs/PKGs, the involvement of the NO/cGMP/PKG signaling pathway in regulating the susceptibility of prostate cancer cells to induction of apoptosis in RT, DNMTIs and HDACIs, alone and in combination, will be determined.

As shown above in b., our studies have resulted in the development of a new methodology using capillary electrophoresis (specifically the 12-channel system, the 12-CE-

LED-IF system) for accurately quantifying the levels of siRNA- and shRNA-induced gene knockdown of PKG isoforms in prostate cancer cells. This was followed by showing that gene knockdown of PKG-Iα results in the induction of apoptosis (illustrating the need for continuous expression of PKG-Iα for preventing spontaneous apoptosis in prostate cancer cells) and in the inhibition of cell proliferation (illustrating the need for PKG-Iα for promoting cell proliferation) in the prostate cancer cell lines. Data is presented in the two manuscripts listed above.

Because prostate cancer cells did not show regulation of Inhibitor of Apoptosis Proteins (IAPs) by the NO/cGMP/PKG signaling pathway, as proposed to be tested in Statement of Work, f. (described below), further studies were conducted using types of cancer cells that also show chemoresistance and radioresistance. These further studies utilized lung cancer and mesothelioma cell line. The newly-developed 12-CE-LED-IF methodology was used to determine PKG knockdown in these other related cancer cells.

Attached in the Appendix is a manuscripts:

M.G. Johlfs and R.R. Fiscus. RNAi shows PKG type-I promotes integrin β1 expression, cell attachment and proliferation and prevents spontaneous apoptosis in pleural mesothelioma cells. Manuscript prepared for submission to *Journal of Biological Chemistry*.

Figure 4 of this manuscript and the supporting text show in detail the use of the new 12-CE-LED-IF methodology for accurately determining the levels of gene knockdown of PKG-Iα and PKG-Iβ caused by two shRNA constructs transfected into two mesothelioma cell lines, MSTO-211H cells and NCI-H2452 cells. Both cell lines express measurable amount of mRNA for both PKG-I isoforms. The shRNA contructs downregulate the mRNA expression of both PKG-I isoforms by 65 – 92%, showing successful gene knockdown. This knockdown of PKG-I results in suppressed PKG kinase activity, determined by measuring the phosphorylation of the target protein VASP, which occurred in both cell lines (see Figure 5 of manuscript). The knockdown of PKG-I expression also caused significant increases in apoptosis and decreases in cell proliferation, showing the essential role of PKG-I expression in promoting cell proliferation and suppressing spontaneous apoptosis, very similar to the resulted we had obtained with the prostate cancer cell lines (discussed above). Interestingly, cell attachment and colony formation in both mesothelioma cell lines were also dependent on PKG-I expression, determined using the same shRNA gene knockdown tools (shown in Figure 7 of the manuscript). Pharmacological inhibition of the PKG-I signaling pathway also demonstrates the essential role of PKG-I in promoting cell survival, cell proliferation and cell attachment in mesothelioma cells (see Figure 3 of manuscript).

Thus, mesothelioma cells, like we have shown with the three prostate cancer cell lines (PC-3, DU145 and LNCaP), are dependent on the continued expression and kinase activity of PKG-I in preventing spontaneous apoptosis and in promoting cell proliferation, which may contribute, at least in part, to the chemoresistance and radioresistance of mesothelioma cells.

Similar results were obtained in the non-small cell lung cancer cell line (NCI-H23), shown in the attached manuscript (in Appendix):

M.G. Johlfs and R.R. Fiscus, Direct serine-17 phosphorylation of Src by protein kinase G type-I as a cellular mechanism mediating anti-apoptotic and growth-stimulatory effects in malignant mesothelioma cells and non-small cell lung cancer cells, Manuscript prepared for submission to *Mol. Cancer*.

This manuscript shows that not only mesothelioma cells, but also non-small cell lung cancer cells (NCI-H23 cells), express both isoforms of PKG-I and that the PKG-I expression is essential for the survival and proliferation of these cells. This study makes the unique observation that PKG-I (either PKG-Iα or PKG-Iβ) can directly phosphorylate the oncogene protein c-Src (Src), which in turn causes activation of Src. Because of the importance of the Src signaling pathway in mediating cell survival and proliferation, the data of this manuscript suggest that a likely mechanism of PKG-I-induced promotion of cell survival and proliferation involves activation of the Src signaling pathway in mesothelioma and non-small cell lung cancer cells. Our further studies will determine if this novel interaction between the PKG-I signaling pathway and the Src signaling pathway also occurs in prostate cancer cells and if it is responsible to the resistance to radiation therapy and chemotherapy.

The further studies to determine the PKG and Src pathways in the resistance to therapy in prostate cancer cells had depended for cooperation with the lab of Dr. Sunil Sharma, the original Co-PI of this DOD Award. However, because of the early departure of Dr. Sharma, we were unable to complete this part of the proposed project. Nevertheless, solid progress has been made on the novel role of PKG-I and its interaction with Src (i.e. direct phosphorylation and activation of Src), which is likely involved in the chemoresistance and resistance to radiation therapy in the cell lines being studying. As shown above, this part of the DOD Award has resulting in two additional manuscripts, besides the two manuscripts dealing with prostate cancer cell survival and proliferation, described above in b.

e. Molecular mechanisms underlying the interactions between DNMTIs and RT will be investigated, including studies of H2AX phosphorylation, ATM/ATR and Chk1/Ch2 induction.

Progress on this sub-aim has been discussed under Statement of Work a.

f. Involvement of the NO/cGMP/PKG signaling pathway in stimulating expression of the 8 IAPs (NAIP, cIAP-1, cIAP-2, XIAP, Ts-XIAP, LIVIN (ML-IAP), Apollon and Survivin) in prostate cancer cells will be determined.

Our studied determined whether or not the NO/cGMP/PKG pathway was involved in regulating gene expression of the IAPs in prostate cancer cells. Unlike other cell types used in our previous studies, e.g. neuroblastoma cells (as outlined in the original grant proposal), the NO/cGMP/PKG signaling pathway in the prostate cancer cells (PC-3, DU145 and LNCaP cells) appeared to have no effect on the expression of the IAPs, as determined in experiments using both pharmacological inhibitors and siRNA/shRNA gene knockdown. Because of this lack of effect of PKG on the IAPs in prostate cancer cells, we determined if this was also the case for other human cancer cell lines. Thus, our further studies utilized a non-small cell lung cancer cell line, the NCI-H460, which, like the mesothelioma and NCI-H23 cells, have some properties in common with the prostate cancer cell lines.

In the NCI-H460 lung cancer cells, we found a clear dependency of expression for four of the IAPs, e.g. cIAP-1, LIVIN cIAP-2, and survivin, on the NO/cGMP/PKG-Iα signaling pathway. The dependency was determined using both pharmacological inhibitors (e.g. ODQ and the highly-selective PKG-Iα/β inhibitor DT-2) and gene knockdown using siRNA constructs specifically targeting PKG-Iα. Genetic silencing of PKG-Iα also resulted in a damatic decrease in the serine-133 phosphorylation (i.e. activation) of CREB (cAMP-response element binding protein) and in the expression of two anti-apoptotic proteins (Bcl-2 and Mcl-1), known to be dependent on the CREB phosphorylation and activation.

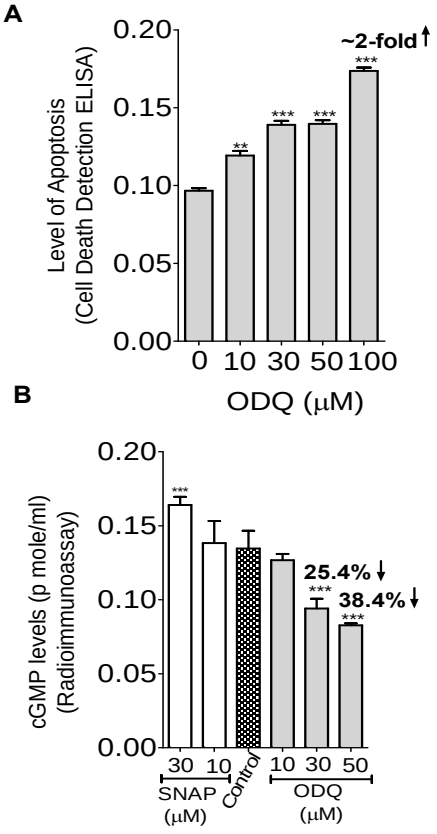

Figure 9. Inhibition of cGMP biosynthesis using ODQ induces apoptosis

Figure 9 shows the effects of ODQ on levels of apoptosis (Panel A) and cGMP (Panel B) in the NCI-H460 cells. The data show that inhibition of cGMP biosynthesis using ODQ causes significant, concentration-dependent decreases in cGMP levels, which correlate with induction of apoptosis, illustrating the need for continuous activation of the NO/cGMP/PKG signaling pathway in NCI-H460 cells for prevention of spontaneous apoptosis.

Figure 10 shows the effects of ODQ on colony formation and illustrate the need for continuous activation of the NO/cGMP/PKG pathway for the formation of NCI-H460 colonies.

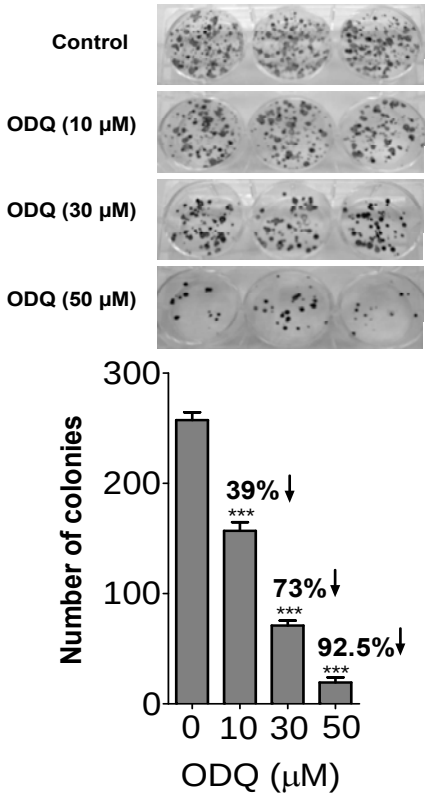

Figure 10. Inhibition of cGMP biosynthesis inhibition colony formation

Figure 11 shows the effects of ODQ on expression of the IAPs as well as on CREB phosphorylation and expression of the anti-apoptotic proteins, Bcl-2, Bcl-XL and Mcl-1. There appeared to be inhibition of cIAP-1, LIVIV and survivin by the ODQ treatment as well as suppression of CREB phosphorylation.

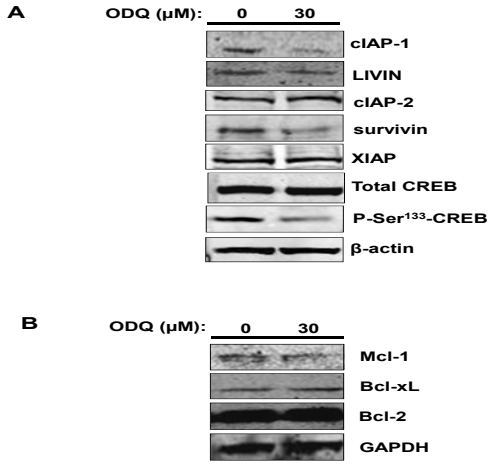

Figure 11. Inhibition of cGMP biosynthesis using ODQ suppresses expression to cIAP-1 and survivin

Figure 12 shows the expression of PKG-Iα in NCI-H460 cells (Panel A) as well as inhibition of colony formation (Panels B and C) and induction of apoptosis (Panel D) by treatment with the highly-selective inhibitor, DT-2.

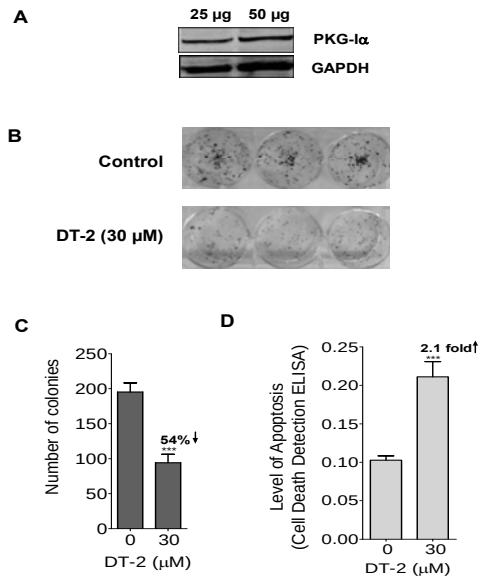

Figure 12. Direct inhibition of PKG-Iα using the specific inhibitor DT-2 suppresses colony formation

Figure 13 shows a dramatic inhibition of CREB phosphorylation at serine-133 (Panel A), a slight downregulation of cIAP-1 and LIVIN expression (Panel B), and increase in cleavage of caspase-3 (index of apoptosis) following the inhibition of PKG-Iα kinase activity with DT-2 in the NCI-H460 cells.

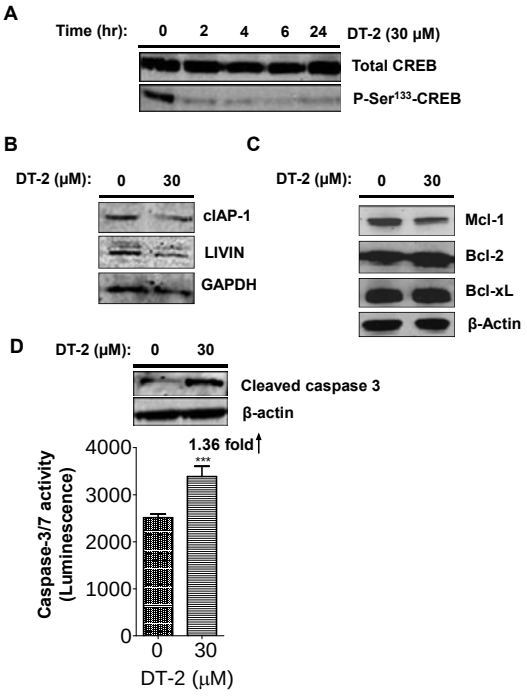

Figure 13. Inhibition of PKG-Iα kinase activity using DT-2 suppresses CREB phosphorylation at serine-133 and expression of cIAP-1 and LIVIN

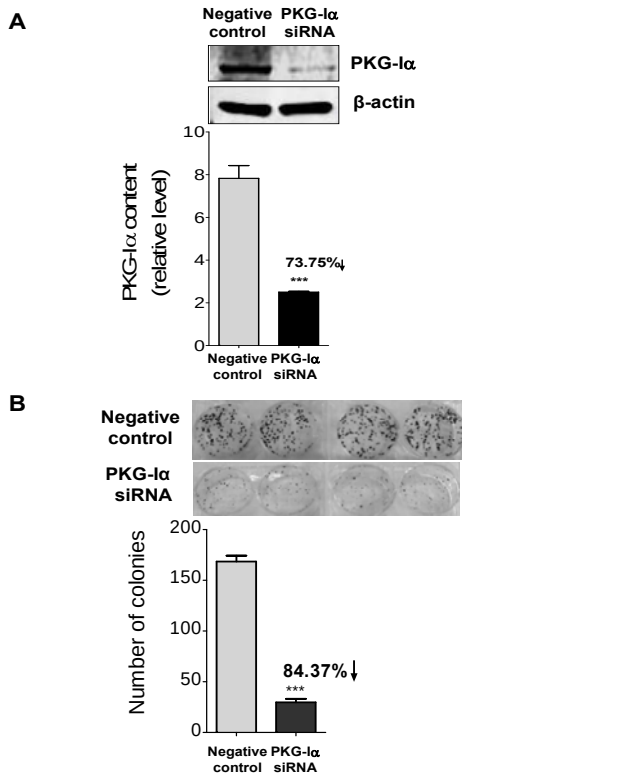

Figure 14. Gene knockdown of PKG-Iα using siRNA suppresses colony formation

Figure 14 shows the gene knockdown of PKG-Iα expression with the siRNA contruct and the resulting inhibition of colony formation.

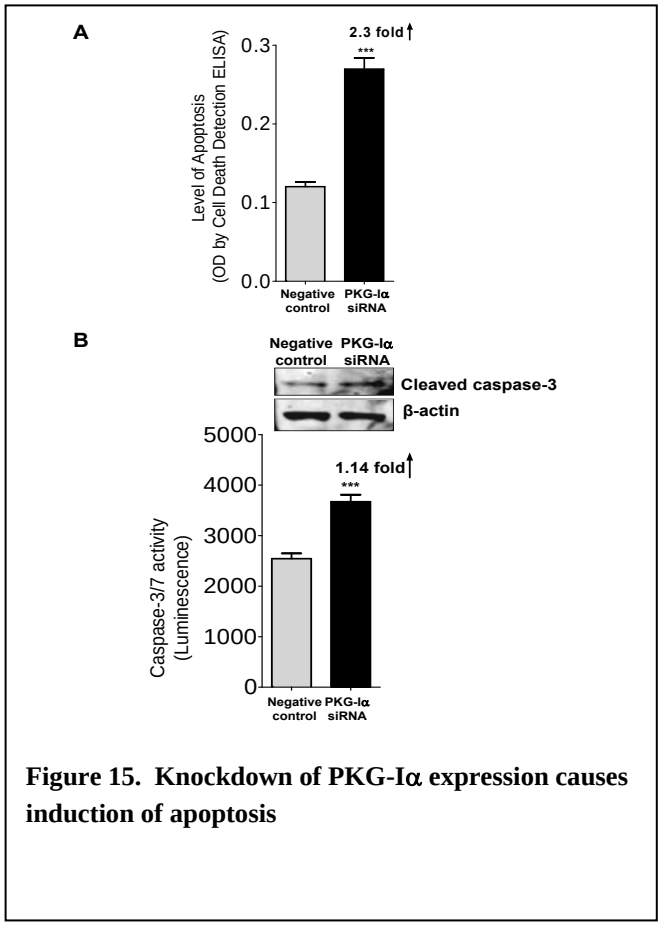

Figure 15. Knockdown of PKG-Iα expression causes induction of apoptosis

Figure 15 shows the induction of apoptosis caused by knocking down the expression of PKG-Iα.

Figure 16 shows the effects of knocking down the expression of PKG-Iα on the expression of the IAPs, Bcl-2, Bcl-XL and Mcl-1 as well as the phosphorylation of CREB. The expression of cIAP-1, LIVIN, cIAP-2 and survivin as well as Mcl-1 and Bcl-2 and the phosphorylation of CREB were all decreased by PKG-Iα knockdown.

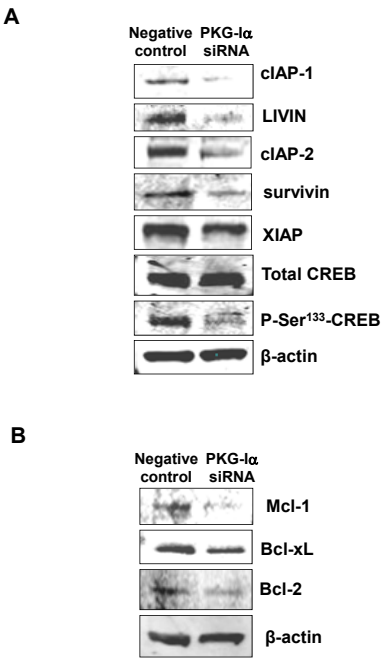

Figure 16. Knockdown of PKG-Iα suppresses expression of cIAP-1, LIVIN, cIAP-2, survivin, Mcl-1, Bcl-2 and phosphorylation of CREB

The data suggest that the NO/cGMP/PKG signaling pathway plays a important role in promoting the expression of several anti-apoptotic proteins, including cIAP-1, LIVIN, cIAP-2, survivin, Bcl-2 and Mcl-1, in the NCI-H460 lung cancer cell line. Because of the lack of effect in the prostate cancer cell lines, there appears to be a different role of the NO in these two types of cancer cells. The future studies will utilize the lung cancer cells to determine if inhibiting the NO/cGMP/PKG pathway can sensitize these cells to radiation therapy and chemotherapy. The data presented above are currently being prepared as a manuscript.

g. Prostate cancer xenografts in athymic mice .

In order to verify whether the in vitro radiation-sensitizing potential of 5-azacytidine as described under Statement of Work a. is reproducible under in vivo conditions, we designed and executed a set of preclinical experiments utilizing PC-3 based xenografts in mice. The research methodology of this approach is described in detail in the attached manuscript of Weterings et al. (Attachment I; 'Low dose 5-azacytidine radio-sensitizes prostate cancer cells by impairing DNA

double-strand break repair.' by Eric Weterings, Pamela M. Dino, Yi Feng, Eugene F. Hayes, James Symanowski, Sunil Sharma, and Giuseppe Pizzorno.).

Xenografts were created by implanting a suspension of PC-3 prostate cancer cells subcutaneously on the flanks of athymic nude mice, followed by a sufficient period of time to allow for the formation of an approximately 100 mm^3 starting tumor mass. 5-azacytidine was then administered at a 2.5 mg/kg/day dose and localized X-ray irradiation of the tumor was performed at different doses, as described in Attachment I. Tumor volumes were measured over time.

As expected, treatment of xenograft tumors with an initial and not sustained radiation dose resulted in retardation of tumor growth for a limited period of time, not exceeding 40 days in our study (Figure 9). However, inclusion of 5-azacytidine administration concurrent with the initial radiation treatment resulted in further delay of tumor progression for another approximately 20 days (Figure 17). This delay in tumor progression as introduced by 5-azacytidine treatment was highly significant and reproducible (Figure 17).

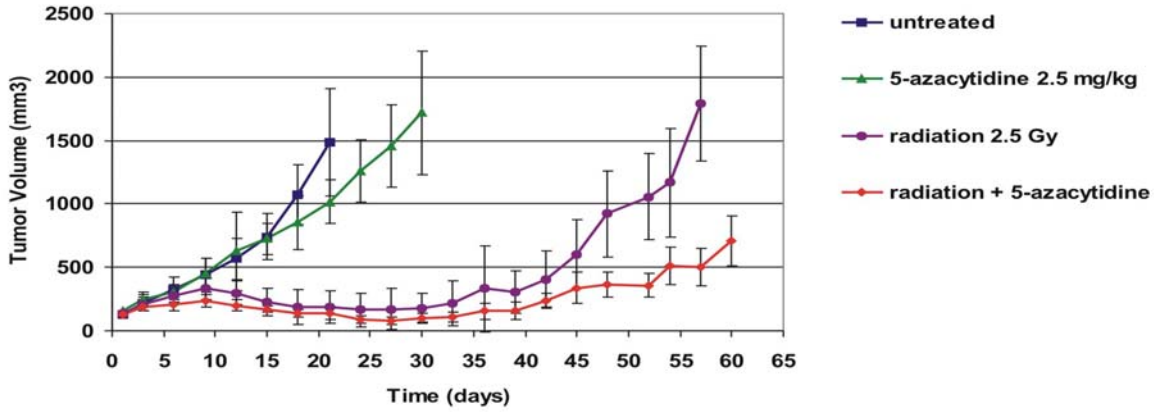

Figure 17. 5-Azacytidine impairs DNA repair in prostate cancer cells

We conclude from these results that 5-azacytidine is capable of markedly potentiating the effects of radiation therapy in prostate cancer xenografts. With this line of experimentation, we have demonstrated that 5-azacytidine does not only increase radiation sensitivity in cell cultures as described under point a., but is capable of displaying the same effect in a three-dimensional tumor generated in a living animal model. The success of this preclinical evaluation greatly increases the likelihood that 5-azacytidine will display a similar radiation-sensitization activity during future human clinical trial studies.

In addition to quantifying mere tumor progression in our xenograft animal models by measurement of tumor dimensions and mass, we have started initial evaluation of the possibility

of measuring changes in tissue spin relaxation (T2) as a means of following tumor responses to treatment. As shown in Figure 18, T2 values as obtained by the utilization of T2-weighted MRI imaging, are not tumor size dependent (Figure 18). Therefore the change in T2 might correlate to changes in tumor composition (vasculature and water contents) rather than size after treatment.

By normalizing the T2 values of tumors to muscle and then again to the **T2 SI** before treatment, we were able to demonstrate that T2 values are lower for tumors that received the highest radiation dose (Figure 19). Therefore, we conclude that changes in the T2 value may reflect changes in tumor composition and progression.

In order to further investigate this, we simultaneously followed the progression of tumor volumes and T2 values over a 24 day period (Figure 20). We observed a correlation between decreases in T2 values and decreases in actual tumor volume, as well as alterations in vasculature and water contents. We therefore conclude that T2 values do reflect changes in radiation-induced changes in the xenograft tumor mass. However, further experimentation in which tumor responses will be followed for a longer period and for more than one cycle of radiation treatment will be necessary to assess the practicality of this potentially interesting novel tumor monitoring technique.

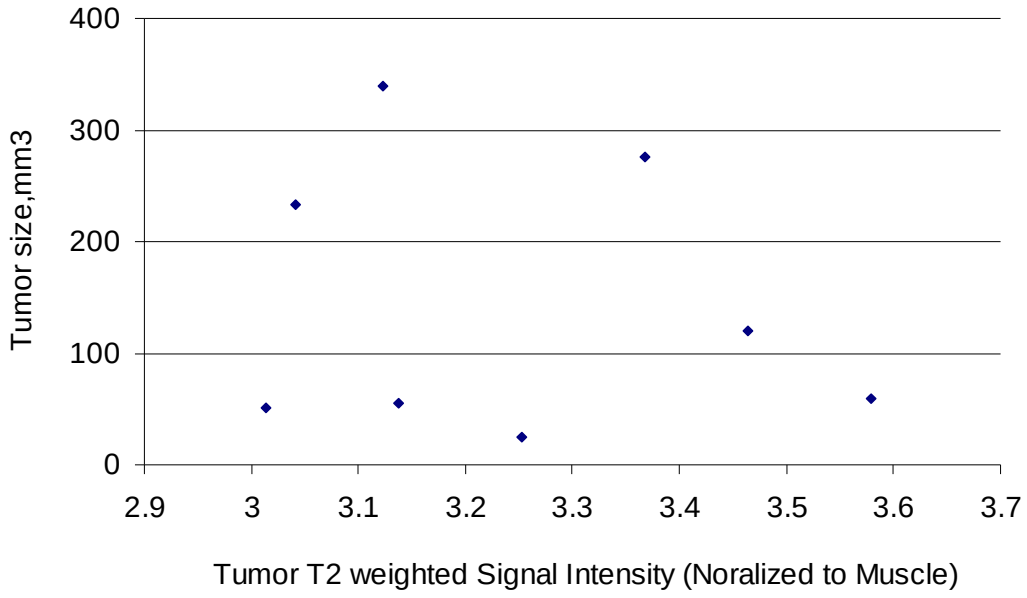

Figure 18. Tumor T2 values are not tumor size dependent

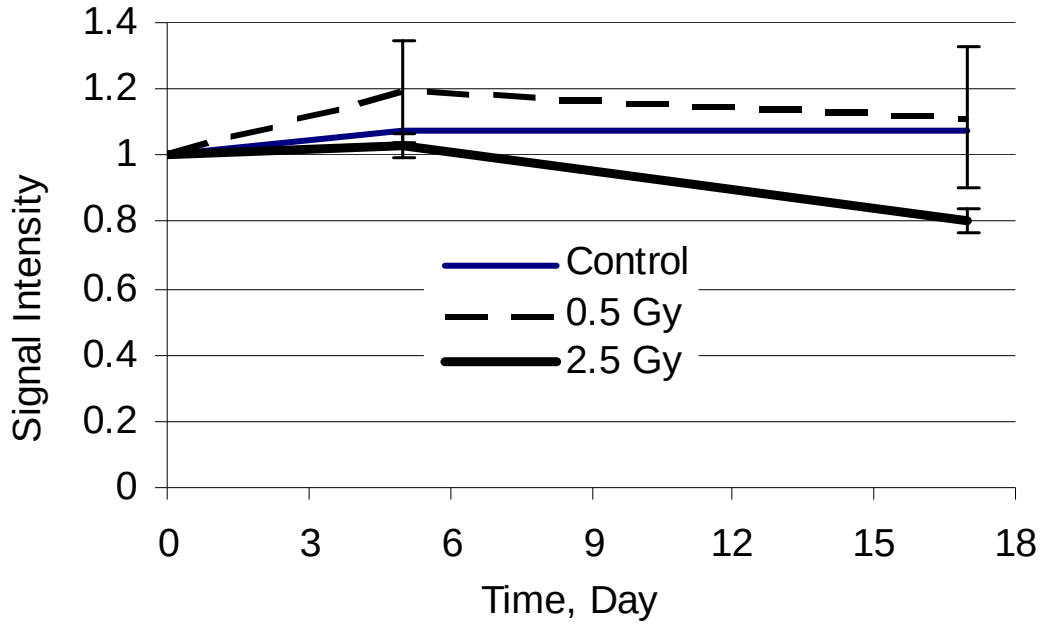

Figure 19. Tumor T2 values (first normalized to muscle, then normalized to T2 values before treatment) decrease as tumors respond to treatment (Rad 2.5 Gy group)

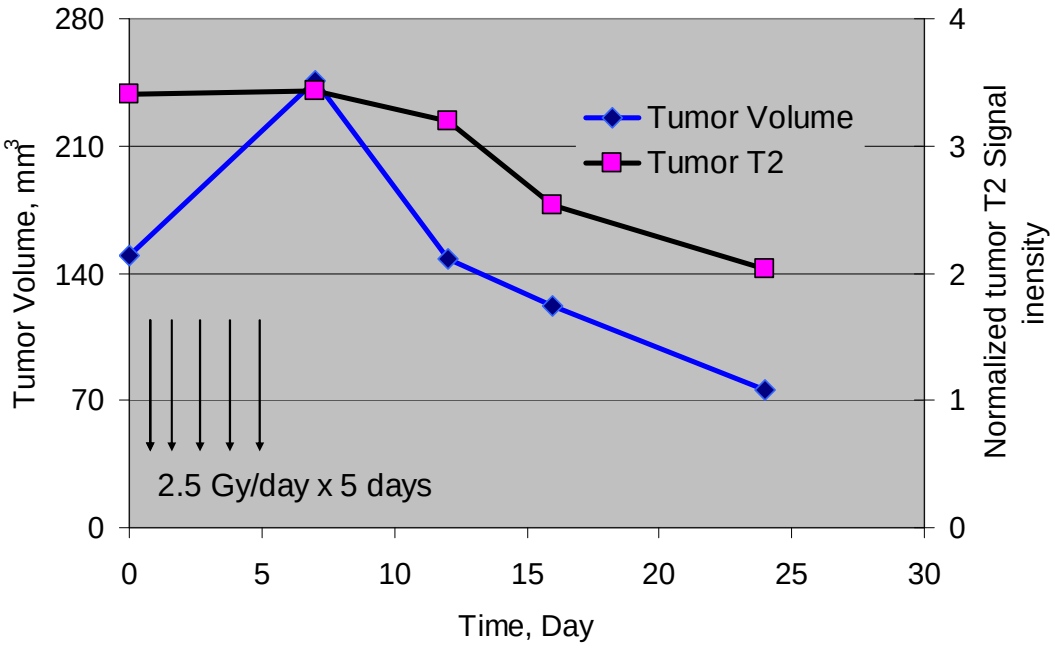

Figure 20. Tumor volume and MRI T2 values for a representative tumor treated by 2.5 Gy/day x 5 days

Key Research Accomplishments.

1. I*n vivo* and *in vitro* data indicate a significant additive and in the case of the PC-3 prostate cancer cells a synergistic effect on the reduction of prostate tumor growth when combining radiation treatment with administration of the DNMT inhibitor 5-azacytidine. Furthermore the deoxy derivative of 5-azacytidine, decitabine, when combined with low dose radiation resulted in a significant synergistic activity against the three prostate cancer cell lines we have utilized.

2. Combination of these therapies introduces a positive selection pressure for radiation resistant cells which eventually may counteract the additive effect. We are currently examining the underlying causes for selection of IR resistant cells and we hypothesize that resistant cells represent a growing subpopulation of stem cells.

3. 5-azacytidine treatment delays or impairs DNA double strand break repair, explaining the potential of this drug to radio-sensitize prostate cancer cells. In addition, 5-azacytidine treatment induces apoptosis, possibly due to its ability to hinder DNA damage repair and associated cell cycle progression.

4. Gene knockdown of PKG-Iα results in higher rates of spontaneous apoptosis and slower rates of cell proliferation in prostate cancer cells, indicating an essential role of this novel protein kinase in regulating prostate cancer apoptosis and proliferation.

5. Inhibition of endogenous NO-induced activation of the heme-soluable guanylyl cyclase causes dramatic sensitization of prostate cancer and mesothelioma cells to the toxic/pro-apoptotic effects of cisplatin. Similar sensitizing effects were observed with one of the five lung cancer cell lines, the one that was relatively insensitive to cisplatin alone.

6. The IAPs LIVIN and Survivin was not regulated by the NO/cGMP/PKG-Iα pathway in prostate cancer cells, but was regulated by this pathway in lung cancer cells.

Thus, there appears to be a cell-specific function of the NO/cGMP/PKG-Iα pathway in regulating LIVIN and Survivin expression levels in cancer cells.

7. Evidence is provided showing involvement of HSP90 in the anti-apoptotic effects of the NO/cGMP/PKG-Iα pathway. HSP90 is necessary for Akt-catalyzed phosphorylation (and activation) of eNOS, which drives the NO signaling in cancer cells of epithelial origin (lung and prostate cancer as well as mesothelioma).

8. PKG-Iα kinase activity in lung cancer cells is necessary for full expression of the two anti-apoptotic proteins, Bcl-2 and Mcl-1. The present data show that inhibition of endogenous PKG-Iα activity in lung cancer cells resulted in downregulation of Bcl-2 and Mcl-1 expression.

9. The overall data suggest that the NO/cGMP/PKG-Iα signaling pathway, because its essential role in promoting cell survival and proliferation in lung cancer, prostate cancer and mesothelioma, may provide a novel target for therapeutic intervention. Agents that inhibit this signaling pathway could be very useful in sensitizing cancer cells to the cancer-killing effects of traditional therapeutic agents.

Reportable Outcomes:

Abstracts:

Eric Weterings, Pamela M. Dino, Yi Feng, Sunil Sharma, Giuseppe Pizzorno. 5-azacytidine radio-sensitizes androgen-independent prostate cancer cells by impairing DNA double-strand break repair. Abstract # 189 Proceedings of the 101st Annual AACR Meeting 2010

Manuscripts/Publications:

Currently, there are 9 manuscripts, generated by this project, that have been published, submitted for review or in their final stage of preparation for submission for publication. Upon acceptance for publication, a copy of each manuscript will be sent to the DOD.

1) Low dose 5-azacytidine radio-sensitizes prostate cancer cells by impairing DNA double-strand break repair. Eric Weterings, Pamela M. Dino, Yi Feng, Eugene F. Hayes, James Symanowski, Sunil Sharma, and Giuseppe Pizzorno. Submitted to *Radiation Research* May 2010.

2) Protein kinase G type-Iα phosphorylates the apoptosis-regulating protein Bad at serine 155 and protects against apoptosis in N1E-115 cells. Johlfs, M.G. and R.R. Fiscus. *Neurochemistry International* 56: 546-553, 2010.

3) Protein kinase G type Iα activity in human ovarian cancer cells significantly contributes to enhanced Src activation and DNA synthesis/cell proliferation. Leung, E.L., Wong, J.C., Johlfs, M.G., Tsang, B.K., and R. R. Fiscus. *Molecular Cancer Research* 8(4): 578-591, 2010.

4) Protein kinase G activity prevents pathological-level nitric oxide-induced apoptosis and promotes DNA synthesis/cell proliferation in vascular smooth muscle cells. Wong, J.C. and R.R. Fiscus. *Cardiovascular Pathology*, In Press.

5) Nitric oxide (NO)/cGMP/protein kinase G type-1α (PKG-Iα) signaling pathway and the atrial natriuretic peptide (ANP)/cGMP/PKG-Iα autocrine loop play essential role in promoting proliferation and cell survival of OP9 bone marrow stromal cells, commonly used as a feeder layer to facilitate hematopoietic stem cell differentiation. Wong, J.C. and R.R. Fiscus. Submitted to *Journal of Biological Chemistry*, June 2010.

6) RNAi shows that PKG type-I promotes integrin β1 expression, cell attachment and proliferation and prevents spontaneous apoptosis in pleural mesothelioma cells. Johlfs, M.G. and R.R. Fiscus. Submitted to *Oncogene,* July 2010.

7) Involvement of the protein kinase G type-Iα signaling pathway in suppressing apoptotic cell death in prostate cancer cells. Fiscus, R.R., Bathina, M., Johlfs, M.G., Wong, J.C., Goodman, O.B., Jr., Sharma, S., Pizzorno, G. and N.J. Vogelzang. In preparation for submission to *Oncogene*.

8) Basal cyclic GMP levels and protein kinase G type-Iα activity play an essential role in promoting cell proliferation in prostate cancer cells. Fiscus, R.R., Bathina, M., Johlfs, M.G., Wong, J.C., Goodman, O.B., Jr., Sharma, S., Pizzorno, G. and N.J. Vogelzang. In preparation for submission to *Cancer Research*.

9) Direct serine-17 phosphorylation of Src by protein kinase G type-I as a cellular mechanism mediating anti-apoptotic and growth-stimulatory effects in malignant mesothelioma cells. Johlfs, M.G. and R.R. Fiscus. In preparation.

Conclusions:

Purpose: A significant portion of prostate cancer patients continue to develop locally advanced or metastatic disease. Neither surgery nor radiation therapy (RT) achieves long-term remission for many patients. New therapeutic approaches, in combination with RT, are needed.

Scope: The hypothesis to be tested is that growth inhibition and apoptosis induction by RT in prostate cancer cells may be synergistically enhanced by DNA-methylation inhibitors (DNMTIs), histone-deacetylase inhibitors (HDACIs) and anti-angiogenesis agents. Furthermore, prostate cancer cells may possess a novel signaling pathway involving nitric oxide (NO), cGMP and protein kinase G (PKG), which stimulates expression of Inhibitor of Apoptosis Proteins (IAPs), thereby altering susceptibility of these cells to RT-, DNMTI- and HDACI-induced apoptosis.

1. I*n vivo* and *in vitro* data indicate a significant additive effect and in some cases a synergistic effect on the inhibition of tumor growth in prostate cancer cells when combining radiation treatment with administration of the DNMT inhibitor 5-azacytidine. We are also currently testing the effect of adding anti-androgen agents to our dual

treatment to study the effect of epigenetic modulators in tumors refractory to hormonal therapy.

2. Combination of these therapies introduces a positive selection pressure for radiation resistant cells which eventually may counteract the additive effect. We are currently examining the underlying causes for selection of IR resistant cells and we hypothesize that resistant cells represent a growing subpopulation of stem cells.
3. 5-azacytidine treatment delays or impairs DNA double strand break repair, explaining the potential of this drug to radio-sensitize prostate cancer cells. In addition, 5-azacytidine treatment induces apoptosis, possibly due to its ability to hinder DNA damage repair and associated cell cycle progression.
4. PKG-Iα directly phosphorylates the apoptosis-regulating protein BAD at the serine-155 site, which can protect mammalian cells against the pro-apoptotic effects of BAD, explaining, in part, the anti-apoptotic mechanism of low-level nitric oxide (NO).
5. PKG-Iα interacts with Src in ovarian cancer cells in a way that leads to both enhanced Src tyrosine kinase activity and enhanced PKG-Iα serine/threonine kinase activity, which leads to enhanced DNA synthesis and cell proliferation in ovarian cancer cells.
6. PKG, likely the PKG-Iα isoform, plays an essential role in promoting DNA synthesis/cell proliferation in primary cultures of vascular smooth muscle cells (VSMCs), further establishing that PKG-Iα is important for promoting cell proliferation in many types of mammalian cells, both normal and transformed cells.
7. PKG-Iα is expressed in OP9 cells, a bone marrow stromal cell line commonly used as a feeder layer to facilitate hematopoietic stem cell differentiation, and, like in VSMCs and ovarian cancer cells; PKG-Iα plays an essential role in promoting cell survival and proliferation.
8. Using RNAi (shRNA gene knockdown) technique, PKG-I was identified as essential for promoting integrin β1 expression, cell attachment and cell proliferation in malignant mesothelioma cells.
9. PKG-Iα is also involved in suppressing apoptotic cell death in prostate cancer cells, contributing to the chemoresistance in these cells.
10. PKG-Iα in prostate cancer cells also plays an essential role in promoting DNA synthesis and cell proliferation.
11. Src, an oncogenic tyrosine kinase often overexpressed or hyperactivated in many types of cancer cells is directly phosphorylated by PKG-I at the serine-17 site of Src, resulting in enhanced autophosphorylation (i.e. phosphorylation at tyrosine- 419) and Src activation in malignant mesothelioma cells and non-small cell lung cancer cells.

The overall conclusion is that PKG-I, specifically the PKG-Iα splice variant, plays an essential role in promoting cell proliferation and protecting against onset of apoptosis in various types of cancer cells, including lung cancer, ovarian cancer and prostate cancer cells as well as mesothelioma cells, and normal cells, including VSMCs and OP9 bone marrow stromal cells. This represents a novel, previously unrecognized function for PKG-Iα in these cells. Part of the original hypothesis of this project had proposed that PKG may prevent apoptosis by promoting the induction of cIAP-2, one of the 8 known Inhibitor of Apoptosis Proteins (IAPs), based on our earlier studies with neuroblastoma cells. However, the studies of the current project showed that

cIAP-2 was not regulated by the PKG signaling pathway in lung and prostate cancer cells. Rather, the present study discovered that a novel mechanism involving Src interaction with PKG was involved as a major mechanism of the PKG-mediated stimulation of cell proliferation and prevention of apoptosis. Overall, the data show that the PKG/Src interaction is likely to play a major role in stimulating cancer cells proliferation and causing these cancer cells to be resistant to the pro-apoptotic effects of chemotherapy and radiation therapy. This valuable new information will allow us to develop new therapeutic agents that can specifically target the novel PKG/Src interaction, which should effectively counteract the chemoresistance and resistance to radiation therapy commonly observed in lung, ovarian and prostate cancer and mesothelioma.

List of Personnel that Received Salary

As we have previously mentioned Dr. Sunil Sharma has voluntarily terminated his employment with the Nevada Cancer Institute to move to the Huntsman Cancer Center in Salt Lake City, UT, and his part of the overall project has thus been transferred to Dr. Giuseppe Pizzorno, Director of the Drug Development Division and Vice President for Research at the Nevada Cancer Institute, who has continued as the Co-PI. A significant part of the data presented below has been generated in the laboratory of Dr. Pizzorno. Also, during the past year the original Principal Investigator Dr. Nicholas Vogelzang has left the Nevada Cancer Institute to join an Oncology private practice and Dr. Pizzorno has become the Principle Investigator responsible for this last year of no cost extension.

Balachandrasekaran, Arvind

Barnett, Tamara

Bathina, Madhavi

Dino, Pamela M.

Feng, Yi

Fiscus, Ronald

Gach, H Michael

Hayes, Eugene F.

Johlfs, Mary

McGregor, John

Pizzorno, Giuseppe

Roach, Joseph Dana Jr.

Symanowski, James

Weterings, Eric

Significance:

The data acquired during the project period will provide valuable new information on combining radiation therapy and DNMTIs and the effect of this combination on the DNA repair mechanism(s) that could be exploited not only for the treatment of prostate cancer but also in the therapeutic approach of other cancer know to be susceptible to the cell inhibitory effects of radiation. We have also elucidated the novel role of the NO/cGMP/PKG signaling pathway in regulating apoptotic susceptibility in prostate cancer cells and other types of cancer cells of epithelial origin, including lung cancer and mesothelioma cells. This new information will be used to develop new agents inhibiting the NO/cGMP/PKG signaling pathway and overall generating better therapeutic approaches for the treatment of epithelial cancers.

Low dose 5-azacytidine radio-sensitizes prostate cancer cells by impairing DNA double-strand break repair.

Eric Weterings PhD[1], Pamela M. Dino MSc[1], Yi Feng PhD[1], Eugene F. Hayes MSc[1], James Symanowski PhD[2], Sunil Sharma MD[3], and Giuseppe Pizzorno PhD[1]*

[1]Nevada Cancer Institute, Department of Drug Development, One Breakthrough Way, Las Vegas, Nevada, NV 89135.

[2]Nevada Cancer Institute, Department of Biostatistics, One Breakthrough Way, Las Vegas, Nevada, NV 89135.

[3]University of Utah, Huntsman Cancer Institute, Center for Investigational Therapeutics, 2000 Circle of Hope, Salt Lake City, Utah, UT 84112.

*Corresponding author, phone 702-822-5433, fax 702-944-2369, email gpizzorno@nvcancer.org

Running title

5-azacytidine impairs DNA repair in prostate cancer cells

Abstract

Weterings, E. et al. Low dose 5-azacytidine radio-sensitizes prostate cancer cells by impairing DNA double-strand break repair. *Radiat. Res*.

5-azacytidine is a cytidine analogue with cytotoxic and cytostatic activity, currently utilized for the treatment of myelodysplastic syndromes. The cytostatic activities of low-dose 5-azacytidine are attributed to its incorporation into the DNA and RNA of mammalian cells, which influences epigenetic regulation and protein expression. We here report that 5-azacytidine radio-sensitizes PC-3 and DU-145 prostate cancer cells, synergistically enhancing the overall efficiency of radiation treatment. Regrowth of PC-3 based xenograft tumors in mice was found to be markedly delayed after a combination treatment with 5-azacytidine and radiation. Furthermore, we found that exposure of PC-3 and DU-145 cells to 5-azacytidine impairs or delays the repair of radiation induced DNA double-strand breaks through the non-homologous end-joining pathway. This observation explains the radio-sensitizing potential of 5-azacytidine and constitutes the first conclusive evidence for a DNA repair defect introduced by this compound. We argue that 5-azacytidine could improve existing radiation protocols and that the combination of 5-azacytidine, androgen ablation therapy, and radiation may hold a marked therapeutic potential. Furthermore, our findings form a basis for future studies regarding the epigenetic, transcriptional, or translational regulation of DNA double strand break repair.

Introduction

5-azacytidine is a cytidine-based antimetabolite, currently marketed under the trade name Vidaza for the treatment of myelodysplastic syndromes (MDS). Mammalian metabolism of 5-azacytidine includes direct incorporation into RNA during transcription, as well as conversion to its deoxy derivative (decitabine) and subsequent incorporation into the genome during replication (*1*). The cytostatic activity of 5-azacytidine is often attributed to its ability to halt progression of DNA methyltransferases (DNMTs) along the DNA strand, thereby inducing genomic hypomethylation (*2, 3*) and possibly reversal of epigenetic silencing of tumor suppressor genes. (*4-6*). However, it must be noted that other activities of 5-azacytidine may play an equally or even more important role during induction of cytostasis.

Although these activities have been studied to a lesser extent, it has been suggested that incorporation of the 5-aza analogue into DNA can result in cell cycle delay, whereas incorporation into RNA has the potential to alter protein synthesis or gene expression regulation through miRNA (*1*). This latter pathway of 5-azacytidine metabolism, although recognized in the past, is only discussed to a limited extent in the literature. Nevertheless, incorporation of 5-azacytidine into RNA predominates DNA incorporation by as much as an order of magnitude and it is therefore likely that the cytotoxic properties of 5-azacytidine are at least in part attributable to RNA effects (*7, 8*).

Although 5-azacytidine was originally developed for the treatment of solid malignancies and leukemias, its severe hematopoietic toxicity at the utilized high doses limited its clinical use (*9, 10*). Therefore, research attention has shifted towards the utilization of 5-azacytidine at lower dosage in conjunction with other forms of antineoplastic therapy (*11, 12*). Such combination therapies aim to sensitize the tumor to the antineoplastic agent without introduction of the toxic effects of 5-azacytidine. Generally, these combination therapies are considered candidates for the treatment of high grade, chemo refractory cancers like estrogen receptor negative breast cancer (*13, 14*).

In the past two years it has become increasingly clear that 5-azacytidine displays an interesting potential to restore the androgen sensitivity of advanced prostate cancers (*15-17*). In addition, recent evidence suggests that prolonged androgen suppression may slow progression of the disease when combined with radiation treatment (*18, 19*). We here add a new dimension to these activities of 5-azacytidine by showing that this compound has the potential to increase the efficiency of radiation therapy *in vitro,* as well as *in vivo*. In this paper, we present evidence that treatments with radiation and either 5-azacytidine or its 2'-deoxy derivative (decitabine) are synergistic in several prostate cancer cell cultures and in a xenograft murine model. We argue that these findings open new therapeutic perspectives.

By using a substrate that mimics a radiation induced, non-complementary DNA double strand break (DSB), we were able to demonstrate that 5-azacytidine, but not decitabine, causes a delay in the repair of DSBs through the non-homologous end-joining (NHEJ) pathway (*20*). Importantly, this is the first time to our knowledge that a nucleotide analogue has been conclusively shown to induce a specific defect in DNA repair. The fact that 5-azacytidine induces impairment of NHEJ whereas its 2'-deoxy counterpart does not, leads us to infer that these compounds have a different mechanism of activity and that 5-azacytidine exerts its influence on DSB repair at least partially through its incorporation into the RNA.

Materials and Methods

Reagents

5-Azacytidine (>99% purity) was purchased from Sigma-Aldrich (St. Louis, MO, USA). Decitabine (>98% purity) was purchased from ChemSyn Laboratories (Harrisonville, MT, USA).

Cell culture

Prostate cancer cell lines (*21-23*) were purchased through American Type Culture Collection (ATCC). DU-145 (HTB-81), LNCaP (CRL-1740), PC-3 (CRL-1435) were maintained with Eagle's Minimum Essential Medium, RPMI-1640, and F-12K Medium, respectively. For full growth medium, the appropriate media was supplemented with 10% fetal bovine serum (PAA) and 1% penicillin streptomycin solution (Cellgro, Manassas, VA, USA). Cells were subcultured according to ATCC's recommendations in a 37ºC, 5% CO_2 humidified incubator and experiments were conducted at passages 2 through 10 at a confluence of approximately 20% prior to treatment.

X-ray treatment

Radiation therapy was conducted using an X-Rad 320 system (Precision X-ray Inc., North Branford, CT, USA). The dose rate was 100cGy/min at 50cm FSD, 320kV and 12.5mA using a 0.8mm Tin + 0.25mm Copper + 1.5mm Aluminum (HVL ≈ 3.7mm Cu) filter.

Cell survival assay

Cells were plated onto a 60 mm tissue culture dishes and allowed to attach overnight in a 37ºC, 5% CO_2, humidified incubator. Cells were treated daily with decitabine or 5-azacytidine at the indicated dose for 48 hrs. The medium was changed on a daily basis. On the third day, the cells were exposed to single dose X-ray treatment with concurrent 5-azacytidine or decitabine administration. Irradiated cells were allowed to recuperate for 6 hrs in growth medium, followed by trypsin treatment and cell counting. Subsequently, cells were plated in 60 mm dishes at a density of 10,000, 1,000, and 100 cells per plate and grown for 7-12 days until formation of

colonies became evident (>50 cells/colony). Cells were stained with a 0.1% crystal violet, 10% formaldehyde solution in PBS for 30 minutes, and washed with water until background staining was removed. Colonies containing more than 50 cells were counted and the survival percentage was determined by normalizing to the amount of colonies that formed in a mock-treated culture.

Animal studies

All utilized animal study protocols were IACUC approved and reviewed by our institutional committee. A total of $4x10^6$ PC-3 cells in a mixture of 50 µL complete medium and 50 µL Matrigel (Becton-Dickinson, Franklin Lakes, NJ) was implanted subcutaneously on the flank of 5 weeks old Athymic male NCr-nu/nu nude mice (NCI, Frederick, MD, USA). Tumors were allowed to develop for 3 weeks, yielding an approximately 100-125 mm^3 starting volume. 5-azacytidine was dissolved in PBS and a dose of 2.5 mg/kg/day was injected intra-peritoneal during a period of 5 days. Simultaneous X-ray treatment was delivered to the tumor at a 0.5 or 2.5 Gy/day dose during the same five day period. Lead shielding protected the surrounding tissue with a 1 cm margin. The tumor size was monitored every 3 days using a digital caliper and calculated using the ellipsoid volume formula: tumor volume = π/6 Ax Bx C, where A and B are the equatorial diameters and C is the polar diameter. Experiments were terminated when tumors reached a volume of 1800 mm^3.

γ-H2AX foci counting

Cells were plated onto 24 well tissue culture plates and allowed to attach overnight in a 37ºC, 5% CO_2 humidified incubator. Cells were treated with decitabine or 5-azacytidine at the indicated dose for 48 hrs and then exposed to single dose X-ray treatment with concurrent 5-azacytidine or decitabine administration. At 1, 6, 24, and 48 hrs post radiation, cells were fixed with 2% paraformaldehyde in PBS for 30 minutes and permeabilized with 0.2% Triton X-100 in PBS for 30 minutes. Wells were blocked with 0.05% Triton X-100 in PBS (PBST), containing 5% goat serum and 1% BSA for two hours. Cells were incubated overnight at 4ºC with 1:2000 γ-H2AX antibody (Cell Signaling Technology, Danvers, MA, USA) in PBST with 1% BSA. Alexa Fluor 488

(Invitrogen, Carlsbad, CA, USA) secondary antibody was diluted 1:2000 in PBST with 1% BSA and cells were incubated for 1 hr at room temperature. Cells were stained with DAPI at a 0.5µg/ml concentration for 15 minutes. γ-H2AX foci were visualized with the Opera Imaging System (Perkin Elmer, Waltham, MA, USA).

In vitro non-homologous end-joining assays

This assay was essentially performed as previously described (*24*). Briefly, the pDvG94 plasmid was digested with EcoRV and Eco47III in order to generate a linear plasmid. This plasmid was transfected to cell cultures (pretreated with 5-azacytidine or decitabine for 48 hrs) with the use of FuGene HD (Roche, Indianapolis, IN, USA). Rejoined plasmids were isolated from cell cultures 24 hrs post transfection as described by Hirt et al. (*25*). PCR input was corrected for total DNA concentration of the Hirt preparations, thereby correcting for differences in the total amount of cells present in the cultures at the time of harvest. PCR reactions were performed by amplification in cycles of 1 min 94°C, 1 min 55°C, and 2 min 55°C, using ^{32}P-labeled oligonucleotides DAR 5 and FM30 (*24*). The PCR reaction was performed under conditions excluding saturation, allowing the presence of unused primers at the completion of the reaction (typically after 26 cycles). PCR products were visualized by autoradiography.

PCR controls were performed by transfecting cell cultures with a circular vector (mUP-Rosa), followed by DNA isolation and PCR with primers mUP6503 and GFP5762 (sequence details available upon request) under identical conditions as used for the end-joining assay.

Quantification of 5-azacytidine incorporation into total RNA

RNA incorporation of 5-azacytidine in vivo was initiated by treating cell cultures with 1, 5, 10, and 15 µM 5-azacytidine for 72 hours. Subsequently, total RNA was extracted using the Total RNA Mini Kit (Omega Biotek, Norcross GA) according to manufacturer's instruction with DNase I digestion. Purified RNA was then digested with P1 nuclease (Sigma, St Louis MO) for 2 hours to obtain mono-nucleotides. Finally, the 5-azacytidine and cytidine contents of the mixture were separated and quantified using an API 3200 Tandem Mass Spectrometer with a Turbo V Ion

Source (Applied Biosystems, Foster City CA), connected to a SIL-HTc Autosampler/Controller, twin 20AD Pumps, and a CTO-20AC Column Heater (Shimadzu Scientific Instruments, Columbia, MD). Separation was achieved with a 2.1 by 100mm Diamond Hydride HPLC Column (MicroSolv Technology, Eatontown, NJ), using a 1ppt formic acid/acetonitrile gradient with a cycle time of 5 minutes. Retention times were as follows: 5-azacytidine 1.28, decitabine 1.15, cytidine 2.02 minutes.

Statistical analysis

Results from the cell survival assay (Figure 1) were analyzed with ANalysis Of VAriance (ANOVA) techniques after appropriate log-transformation. Sources of variation included drug (yes vs no), radiation (yes vs no) and the drug by radiation interaction. The interaction term was tested at the alpha = 0.05 significance level. Additivity between drug and radiation treatment was not excluded for cases where the interaction term was not statistically significant. The two treatment modalities were not considered additive in cases where the interaction term was statistically significant. In these situations the following calculation was made: $S_C = I \times S_D \times S_R$; where S_C, S_D, and S_R equals cell survival in the combination, drug, and radiation groups, respectively. I is the synergy index where values less than one indicate drug and radiation were working synergistically and values greater than one indicate drug and radiation were working together less than additive.

Results from the foci counting assay (Figure 3) were analyzed with Poisson regression. Sources of variation included treatment group (control, drug only, radiation therapy only, and the drug-radiation combination), hours post radiation (1, 6, 24, and 48), and the treatment by hour interaction. The standard error used for statistical testing was increased using the overdispersion parameter based on the residual deviance. For the radiation only and drug-radiation combination groups, linear treatment contrasts were evaluated to assess the significance and magnitude of decreasing trends in foci counts over time. Additionally, the radiation only linear trend was statistically compared to the combination group linear trend. To maintain an overall 0.05 Type I error rate, each time trend was tested at the alpha = 0.0167 (0.05/3) significance level. As a

supplemental analysis the drug, radiation, and combination groups were statistically compared to the control group at each time point separately. Additionally, the combination group was compared to both the drug and radiation groups. In order to maintain an overall 0.05 Type I error rate, these comparisons were each tested at the alpha = 0.01 significance level.

Results

5-azacytidine and decitabine radio-sensitize androgen-independent prostate cancer cells in vitro and in vivo.

We first evaluated whether prostate cancer cells could be radio-sensitized by treatment with 5-azacytidine and its 2'-deoxy derivative, decitabine. We therefore selected the androgen-independent PC-3 and DU-145 cell lines and the androgen-dependent LNCaP cell line (*21-23*). Cell cultures were pre-treated with either 5-azacytidine or decitabine for 48 hours, followed by single dosage X-ray exposure with concurrent 5-azacytidine or decitabine treatment. Subsequently, we performed a clonogenic survival assay.

All cell lines displayed sensitivity to both decitabine and 5-azacytidine, and to X-ray treatment alone (Figure 1 A and B panels). Simultaneous exposure of either the PC-3 or the LNCaP cell lines to decitabine and radiation yielded significant ANOVA interaction p-values, indicating that the combination therapy was not additive. Evaluation of survival in the combination group indicated that the combination therapy was synergistic in these cell lines (Figure 1A and Table 1). Combination of 5-azacytidine with radiation was found to be significantly synergistic in PC-3 cells and qualitatively synergistic (survival less than half the expected survival under additivity) in DU-145 cells (Figure 1B and Table 1). The most marked synergistic effect of both decitabine and 5-azacytidine was found in PC-3 cells (synergy index of 0.48 and 0.44, respectively).

Similar results were obtained by using different combinations of 5-azacytidine or radiation doses (data not shown), but effects were most evident at relatively low decitabine or 5-azacytidine doses (0.04 and 1.25 uM, respectively). We conclude that both 5-azacytidine and its 2'-deoxy derivative, decitabine, have a potential to radio-sensitize prostate tumor cells.

Next, we verified whether the radio-sensitizing effect of 5-azacytidine could be observed *in vivo* as well. We therefore implanted PC-3 prostate cancer cells in athymic nude mice. After

development of tumors at the inoculation site, 5-azacytidine was administered in conjunction with localized X-ray treatment of the tumors. Subsequently, changes in tumor volume were measured over time (Figure 2).

We initially tested a regiment of 2.5 mg/kg/day 5-azacytidine for 5 days, either combined with or preceding a 0.5 Gy/day radiation regiment for 5 days (Figure 2A). At these low radiation doses, we did not observe a beneficial effect of 5-azacytidine treatment, nor did we observe a difference in response between concurrent and sequential administration of 5-azacytidine and radiation (Figure 2A).

We then administered a higher dose of 2.5 Gy/day of X-rays in combination with a 2.5 mg/kg/day dose of 5-azacytidine during a 5 day period (Figure 2B). Treatment with 5-azacytidine alone had a moderate cytotoxic effect. X-ray treatment had a marked initial effect on tumor development, retarding tumor growth for approximately 40 days. After this initial delay, however, tumor volumes rapidly increased, presumably due to the absence of sustained radiation treatment (Figure 2B).

Interestingly, the combination of 5-azacytidine and radiation treatment resulted in a remarkably retarded tumor growth for up to 8 weeks with no associated host toxicity (Figure 2B). These findings clearly demonstrate that combination of 5-azacytidine treatment with radiation therapy has a beneficial effect on tumor growth, complementing our clonogenic survival studies in PC-3 cells (Figure 1).

5-azacytidine delays or impairs the repair of radiation induced DNA double-strand breaks.

In order to elucidate the radio-sensitizing activity of 5-azacytidine and decitabine we investigated whether these compounds had an adverse effect on the repair of radiation induced DSBs. Therefore, PC-3, DU-145, and LNCaP cell cultures were pre-treated with 5-azacytidine or decitabine for 48 hours, followed by single X-ray exposure with concurrent 5-azacytidine or decitabine treatment. Subsequently, cells were fixed at different time points post radiation and immuno-stained with an antibody generated against the phosphorylated form of the H2A histone

proteins (γ-H2AX), a generally recognized indicator of DSBs (*26*) (Figure 3A). We then established an average foci count per cell nucleus for each time point (Figure 3B).

For each cell line we observed a rise in the number of γ-H2AX foci 1 hr post radiation, indicating the presence of radiation induced DSBs (Figure 3B). In the absence of 5-azacytidine or decitabine these foci gradually disappeared in the 48 hr interval post radiation, demonstrating normal, efficient DSB repair in all cell lines tested (Figure 3B).

Interestingly, we found that 5-azacytidine treated PC-3 and DU-145 cells did not display such a marked decline in γ-H2AX foci (Figure 3B left panel). In order to quantify the γ-H2AX foci decline, we calculated a time trend which reflects the average decrease of foci per hour (Table 2). The difference in time trends between radiated cells and combination treated cells was strongly significant in PC-3 and DU-145 cells (Table 2). No significant difference was found in LNCaP cells. These findings suggests that 5-azacytidine possesses the capacity to delay or impair DSB repair in PC-3 and DU-145 lines, which fits our observation that 5-azacytidine and radiation have a synergistic effect on cell survival and tumor growth (Figure 1 and 2).

A similar but less pronounced effect was observed for decitabine combination treatment on PC-3 and DU-145 cells (Figure 3B right panel and Table 2). However, this observation was complicated by the fact that exposure of cells to decitabine without radiation increased the number of γ-H2AX foci in all three cell lines (Figure 3B right panel), suggesting that decitabine interacted with DNA in a fashion that was not observed with 5-azacytidine. Although the number of γ-H2AX foci remained high in PC-3 and DU-145 cells that were treated with both radiation and decitabine, this effect cannot be solely attributed to faulty DSB repair since decitabine by itself causes maintained elevation of the γ-H2AX foci count.

In order to further test the hypothesis that 5-azacytidine impairs DSB repair in PC-3 and DU-145 cells, we transfected 5-azacytidine or decitabine treated cell cultures with a linearized plasmid. This plasmid essentially mimics the presence of a DSB and recircularization of the plasmid indicates efficient DSB repair via the non-homologous end-joining (NHEJ) pathway. Based on methodology first described by Verkaik et al. (*24*), we quantified DSB rejoining by isolating

recircularized plasmids 24 hours post transfection, followed by PCR over the joint region of the plasmid (Figure 4A). Care was taken to ensure that the PCR reaction was not performed to saturation, allowing quantification of the signal. The occurrence of a false positive signal due to transfection with an incidental remnant of non-linearized plasmid was excluded due to a significant difference in size between the reaction products of recircularized and non-linearized plasmids (Figure 4A).

To ensure that 5-azacytidine did not have an aspecific effect on transfection efficiency, we transfected cells with an unrelated plasmid (mUP-Rosa) and performed a quantitative PCR on the isolated plasmid one day post transfection. As expected, no difference in signal was observed between untreated cells and cells treated with 5-azacytidine (Figure 4B).

Performing our end-joining assay with the linearized pDvG94 plasmid, we observed that treatment of the PC-3 and DU-145 cell lines with an increasing amount of 5-azacytidine resulted in a corresponding decrease of PCR product (Figure 4C left panel). These data indicate that NHEJ mediated DSB repair in PC-3 and DU-145 cells was impaired or delayed as a consequence of 5-azacytidine treatment.

We did not find any decrease in end-joining levels in the LNCaP cell line after treatment with 5-azacytidine (Figure 4C left panels). This correlates well with the observation that disappearance of γ-H2AX foci was not delayed in LNCaP cells (Figure 3) and that no obvious synergy was detectable between radiation and 5-azacytidine treatment in LNCap cells (Figure 1).

Next, we investigated whether the differences in response to 5-azacytidine between the three cell lines could be attributed to a differential RNA metabolism of 5-azacytidine. Therefore, we measured the incorporation of 5-azacytidine into the total RNA of all three cell lines at different 5-azacytidine concentrations (Figure 4D). This analysis revealed a clear correlation between 5-azacytidine concentration in the culture medium and 5-azacytidine RNA incorporation for all cell lines. Interestingly, PC-3 cells showed a steeper RNA incorporation pattern than DU-145 and LNCaP cells, which could explain why PC-3 cells are radio-sensitized more effectively than DU-145 cells. On the other hand, LNCaP cells displayed a 5-azacytidine incorporation rate that was intermediate to those of PC-3 and DU-145 cells. Therefore, the absence of a 5-azacytidine effect

on DNA repair in LNCaP cells can not be solely attributed to a lower 5-azacytidine incorporation rate and must be (co-)mediated by another characteristic that is inherent to LNCaP cells.

Treatment of PC-3, DU-145, and LNCaP cells with decitabine did not result in any detectable decrease in PCR product (Figure 4C right panels), demonstrating that decitabine does not interfere with DSB repair. These results further support our conclusion that although both decitabine and 5-azacytidine radio-sensitize prostate cancer cells, the mechanism by which these compounds exert their activity is distinctly different.

Discussion

In this paper we demonstrate that 5-azacytidine has a distinct potential to radio-sensitize prostate cancer cells by impairing DSB repair. Although Snyder and Lachmann (*27*) claimed an inhibitory effect of 5-azacytidine on DNA single-strand break repair in 1989, these authors used such high doses of 5-azacytidine and decitabine (100 and 500 μM, respectively) that their experimental design likely reflected apoptosis and cell death, rather than radiation-induced single-strand DNA breakage. In addition, differential effects on DNA breakage were only observed shortly after exposure to high radiation doses (16Gy).

The radio-sensitizing effect of the cytidine analog zebularine was previously reported and associated with increased levels of γ-H2AX, but a direct inhibition of DNA repair was never demonstrated (*28*). Dote et al. argue that increased levels of γ-H2AX could be caused by apoptosis, cell cycle arrest or impaired DNA repair. By using a DNA substrate that can only be repaired via the non-homologous end-joining pathway – the cell does not provide a homologous template, thereby excluding homologous recombination – we have demonstrated the involvement of a specific DNA repair mechanism in the radio-sensitizing activity of 5-azacytidine, rather than the involvement of apoptosis or cell cycle arrest.

Although decitabine does display a radio-sensitizing potential, our data demonstrates that decitabine, unlike 5-azacytidine, does not impair the NHEJ mechanism. We therefore infer that the mechanism of decitabine activity differs from that of 5-azacytidine. Our observation that decitabine treatment alone increases the number of γ-H2AX foci (Figure 3), suggests that incorporation of decitabine into the genome may induce DNA breakage and/or chain termination. Evidently, such an effect would enhance radiation efficiency.

Conversion of 5-azacytidine into decitabine followed by incorporation into the genome would partly explain the synergistic relationship between radiation and 5-azacytidine treatment. It would, however, not explain impairment of DSB repair because decitabine does not introduce the NHEJ defect. We therefore speculate that this latter effect is caused by incorporation of 5-azacyidine into the RNA, possibly influencing proper expression of certain protein factors involved

in DSB repair through the NHEJ pathway. This hypothesis is supported by the fact that 5-azacytidine, unlike decitabine, is not capable of inducing elevated levels of γ-H2AX foci, suggesting that the majority of 5-azacytidine molecules is incorporated directly into the RNA, rather than being converted to decitabine and incorporated into the genome. This explanation fits earlier observations, which have shown that up to 90% of the available 5-azacytidine molecules will be metabolized into RNA (*7*).

Our findings may provide some basis for future investigations into the regulatory mechanisms that control DSB break repair. Little information is currently available on the epigenetic or transcriptional/translational regulation of the HR and NHEJ repair pathways. Based on our experiments, it seems reasonable to assume that incorporation of 5-azacytidine into either mRNA or regulatory RNA may assert an influence on expression of repair genes. However, the fact that LNCaP cells do not show a detectable NHEJ impairment while they do incorporate 5-azacytidine into the RNA, demonstrates that RNA mediated effects are not the sole basis for repair regulation.

Despite the fact that the exact mechanism of 5-azacytidine action is still unclear, our findings open some new therapeutic vistas. Based upon the data we presented in this paper, we suggest further clinical investigation into the use of radiation and 5-azacytidine in prostate cancer patients, the initial goal being relief of the primary tumor burden. It lies within reason to expect that administration of 5-azacytidine would increase radiation efficiency, thereby decreasing the necessary dose and limiting exposure of surrounding tissue. Moreover, since incorporation of 5-azacytidine into the genome requires cell division, the drug is likely to be more effective in relatively fast dividing, cancerous tissue. This latter circumstance will help to reduce the radiation burden on healthy tissues which surround the tumor. Although this approach is not likely to prove curative, it may well improve existing radiation protocols.

The use of 5-azacytidine has so far only been FDA approved for treatment of myelodysplastic syndromes, but the data we here present suggest a chemotherapeutic potential beyond the treatment of myeloid disorders and argue for further investigation into the use of this drug for the treatment of solid malignancies; a recommendation echoed by a recent publication

on decitabine (*12*). Because we have no reason to assume that the effects of 5-azacytidine are tissue specific, we speculate that future experimentation can be relatively easily expanded to include other cancers for which radiation therapy is considered a first line of treatment. Clinical trials on lung cancers, pancreatic cancers, soft tissue sarcoma's and glioblastoma's, for example, could potentially reveal significant effects on tumor control within a relatively small test population.

Combining radiation therapy with long term androgen ablation has recently been proven to slow down the advance of castration resistant prostate cancers (*18, 19*). In addition, clinical trials have revealed that 5-azacytidine administration slowed progression of castration resistant prostate cancer by restoring responsiveness to standard androgen ablation therapy (*17*). It is theoretically conceivable that 5-azacytidine, having the dual potential to sensitize prostate tumors to androgen ablation and to radiation, may be a powerful therapeutic tool in combination with radiation of the primary tumor and long term androgen deprivation. Such a combined approach would not only increase efficiency of the early treatment, but might prolong the time necessary for disease progression. Further preclinical studies will be necessary in order to verify this hypothesis.

References

1. A. Cihak, Biological effects of 5-azacytidine in eukaryotes. *Oncology* **30**, 405-422 (1974).

2. M. Esteller, DNA methylation and cancer therapy: new developments and expectations. *Curr Opin Oncol* **17**, 55-60 (2005).

3. N. Yu and M. Wang, Anticancer drug discovery targeting DNA hypermethylation. *Curr Med Chem* **15**, 1350-1375 (2008).

4. S. B. Baylin, J. G. Herman, J. R. Graff, P. M. Vertino and J. P. Issa, Alterations in DNA methylation: a fundamental aspect of neoplasia. *Adv Cancer Res* **72**, 141-196 (1998).

5. P. A. Jones and P. W. Laird, Cancer epigenetics comes of age. *Nat Genet* **21**, 163-167 (1999).

6. P. M. Das and R. Singal, DNA methylation and cancer. *J Clin Oncol* **22**, 4632-4642 (2004).

7. L. H. Li, E. J. Olin, H. H. Buskirk and L. M. Reineke, Cytotoxicity and mode of action of 5-azacytidine on L1210 leukemia. *Cancer Res* **30**, 2760-2769 (1970).

8. T. Murakami, X. Li, J. Gong, U. Bhatia, F. Traganos and Z. Darzynkiewicz, Induction of apoptosis by 5-azacytidine: drug concentration-dependent differences in cell cycle specificity. *Cancer Res* **55**, 3093-3098 (1995).

9. R. L. Momparler, Epigenetic therapy of cancer with 5-aza-2'-deoxycytidine (decitabine). *Semin Oncol* **32**, 443-451 (2005).

10. V. Santini, H. M. Kantarjian and J. P. Issa, Changes in DNA methylation in neoplasia: pathophysiology and therapeutic implications. *Ann Intern Med* **134**, 573-586 (2001).

11. J. Lin, J. Gilbert, M. A. Rudek, J. A. Zwiebel, S. Gore, A. Jiemjit, M. Zhao, S. D. Baker, R. F. Ambinder, et al., A phase I dose-finding study of 5-azacytidine in combination with sodium phenylbutyrate in patients with refractory solid tumors. *Clin Cancer Res* **15**, 6241-6249 (2009).

12. H. J. Cho, S. Y. Kim, K. H. Kim, W. K. Kang, J. I. Kim, S. T. Oh, J. S. Kim and C. H. An, The combination effect of sodium butyrate and 5-Aza-2'-deoxycytidine on radiosensitivity in RKO colorectal cancer and MCF-7 breast cancer cell lines. *World J Surg Oncol* **7**, 49 (2009).

13. L. Fleury, M. Gerus, A. C. Lavigne, H. Richard-Foy and K. Bystricky, Eliminating epigenetic barriers induces transient hormone-regulated gene expression in estrogen receptor negative breast cancer cells. *Oncogene* **27**, 4075-4085 (2008).

14. J. Fan, W. J. Yin, J. S. Lu, L. Wang, J. Wu, F. Y. Wu, G. H. Di, Z. Z. Shen and Z. M. Shao, ER alpha negative breast cancer cells restore response to endocrine therapy by combination treatment with both HDAC inhibitor and DNMT inhibitor. *J Cancer Res Clin Oncol* **134**, 883-890 (2008).

15. G. L. Gravina, C. Festuccia, D. Millimaggi, V. Dolo, V. Tombolini, M. de Vito, C. Vicentini and M. Bologna, Chronic azacitidine treatment results in differentiating effects, sensitizes against bicalutamide in androgen-independent prostate cancer cells. *Prostate* **68**, 793-801 (2008).

16. G. Sonpavde, A. Aparicio, I. Guttierez, K. A. Boehm, T. E. Hutson, W. R. Berry, L. Asmar and D. D. von Hoff, Phase II study of azacitidine to restore responsiveness of prostate cancer to hormonal therapy. *Clin Genitourin Cancer* **5**, 457-459 (2007).

17. G. Sonpavde, A. M. Aparicio, F. Zhan, B. North, R. Delaune, L. E. Garbo, S. R. Rousey, R. E. Weinstein, L. Xiao, et al., Azacitidine favorably modulates PSA kinetics correlating with plasma DNA LINE-1 hypomethylation in men with chemonaive castration-resistant prostate cancer. *Urol Oncol* (2009).

18. M. Bolla, T. M. de Reijke, G. Van Tienhoven, A. C. Van den Bergh, J. Oddens, P. M. Poortmans, E. Gez, P. Kil, A. Akdas, et al., Duration of androgen suppression in the treatment of prostate cancer. *N Engl J Med* **360**, 2516-2527 (2009).

19. E. M. Horwitz, K. Bae, G. E. Hanks, A. Porter, D. J. Grignon, H. D. Brereton, V. Venkatesan, C. A. Lawton, S. A. Rosenthal, et al., Ten-year follow-up of radiation therapy oncology group protocol 92-02: a phase III trial of the duration of elective androgen deprivation in locally advanced prostate cancer. *J Clin Oncol* **26**, 2497-2504 (2008).

20. E. Weterings and D. J. Chen, The endless tale of non-homologous end-joining. *Cell Res* **18**, 114-124 (2008).

21. J. S. Horoszewicz, S. S. Leong, E. Kawinski, J. P. Karr, H. Rosenthal, T. M. Chu, E. A. Mirand and G. P. Murphy, LNCaP model of human prostatic carcinoma. *Cancer Res* **43**, 1809-1818 (1983).

22. M. E. Kaighn, K. S. Narayan, Y. Ohnuki, J. F. Lechner and L. W. Jones, Establishment and characterization of a human prostatic carcinoma cell line (PC-3). *Invest Urol* **17**, 16-23 (1979).

23. K. R. Stone, D. D. Mickey, H. Wunderli, G. H. Mickey and D. F. Paulson, Isolation of a human prostate carcinoma cell line (DU 145). *Int J Cancer* **21**, 274-281 (1978).

24. N. S. Verkaik, R. E. Esveldt-van Lange, D. van Heemst, H. T. Bruggenwirth, J. H. Hoeijmakers, M. Z. Zdzienicka and D. C. van Gent, Different types of V(D)J recombination and end-joining defects in DNA double-strand break repair mutant mammalian cells. *Eur J Immunol* **32**, 701-709 (2002).

25. B. Hirt, Selective extraction of polyoma DNA from infected mouse cell cultures. *J Mol Biol* **26**, 365-369 (1967).

26. E. P. Rogakou, D. R. Pilch, A. H. Orr, V. S. Ivanova and W. M. Bonner, DNA double-stranded breaks induce histone H2AX phosphorylation on serine 139. *J Biol Chem* **273**, 5858-5868 (1998).

27. R. D. Snyder and P. J. Lachmann, Differential effects of 5-azacytidine and 5-azadeoxycytidine on cytotoxicity, DNA-strand breaking and repair of X-ray-induced DNA damage in HeLa cells. *Mutat Res* **226**, 185-190 (1989).

28. H. Dote, D. Cerna, W. E. Burgan, D. J. Carter, M. A. Cerra, M. G. Hollingshead, K. Camphausen and P. J. Tofilon, Enhancement of in vitro and in vivo tumor cell radiosensitivity by the DNA methylation inhibitor zebularine. *Clin Cancer Res* **11**, 4571-4579 (2005).

Acknowledgements

The authors would like to thank Dr. Dik C. van Gent and Nicole S. Verkaik (Erasmus Medical Center, Department of Cell Biology and Genetics, Rotterdam, The Netherlands) for kindly providing the pDvG94 plasmid and for helpful technical advice. We would also like to thank Amy Ziemba (Nevada Cancer Institute, Department of Drug Development) for provision of the mUP-Rosa plasmid. Drs. Oscar Goodman and Tarmo Roosild (Nevada Cancer Institute) are acknowledged for their critical revision of the manuscript. This work was supported by the U.S. Department of Defense; award number W81XW8-07-1-0543.

Figure legends

Figure 1. Decitabine and 5-azacytidine radio-sensitize prostate cancer cells *in vitro*. (A) Clonogenic survivals of androgen-independent PC-3, DU-145, and androgen-dependent LNCaP cells after 48 hrs exposure to decitabine, followed by a single dose X-ray treatment. Cell survival percentages were normalized to the untreated control. **(B)** Clonogenic survivals of PC-3, DU-145, and LNCaP cells after 48 hrs exposure to 5-azacytidine, followed by a single dose X-ray treatment. Cell survival percentages were normalized to the untreated control. All data points are based on triplicate repeats. Error bars represent standard deviations.

Figure 2. 5-azacytidine delays regrowth of PC-3 tumors in athymic mice after radiation treatment. (A) Tumor volumes after a 5 day administration of 2.5 mg/kg/day 5-azacytidine in combination with a 0.5 Gy/day dose of X-rays. 5-azacytidine treatment was given either concurrently with radiation or preceding radiation. (B) Tumor volumes after a 5 day administration of 2.5 mg/kg/day 5-azacytidine in combination with a 2.5 Gy/day dose of X-rays. 5-azacytidine treatment was administered concurrently with radiation. A minimum of 6 mice, each bearing 2 tumors, was used per data point. Error bars represent standard deviations.

Figure 3. **5-azacytidine impairs or delays repair of DNA double strand breaks after radiation treatment. (A)** Example of γ-H2AX foci induced by X-rays, visualized by immuno-staining. **(B)** Quantitative representation of the average number of γ-H2AX foci/nucleus in 5-azacytidine treated (left panel) or decitabine treated (right panel) PC-3, DU-145, and LNCaP cells at 1, 6, 24, and 48 hours post radiation. A minimum of 50 nuclei was counted per data point. Error bars represent standard deviations.

Figure 4. **5-azacytidine reduces non-homologous end-joining efficiency. (A)** Left panel: flow scheme of the end-joining assay. Cells are transfected with the pDvG94 plasmid after linearization with the Eco47III and EcoRV restriction enzymes. Rejoined of the two resulting blunt

ends can only occur through non-homologous end-joining. Recircularized plasmid is isolated from the cells 24 hrs post transfection and quantified by PCR over the joined region. Right panel: only recircularized plasmid gives rise to the required 180 bp PCR product. First lane: uncut pDvG94, second lane: recircularized by T4 DNA ligase *in vitro*, third lane: recircularized in cells. **(B)** PCR control. Cells were transfected with a plasmid unrelated to pDvG94 (mUP-Rosa) after treatment with 5-azacytidine. No influence of 5-azacytidine on transfection efficiency, plasmid isolation or PCR yield was observed. Depicted are the results for PC-3 cells. DU-145 and LNCaP cells gave identical results. **(C)** PC-3, DU-145, and LNCaP cells were transfected with linearized pDvG94 plasmid after 5-azacytidine (left panel) or decitabine (right panel) treatment and the end-joining efficiency was measured by means of quantitative PCR. Percentages under the panels represent relative intensities of the PCR products. (D) Quantification of 5-azacytidine incorporation into total RNA as a function of 5-azacytidine concentration in the culture medium. Error bars represent standard deviations.

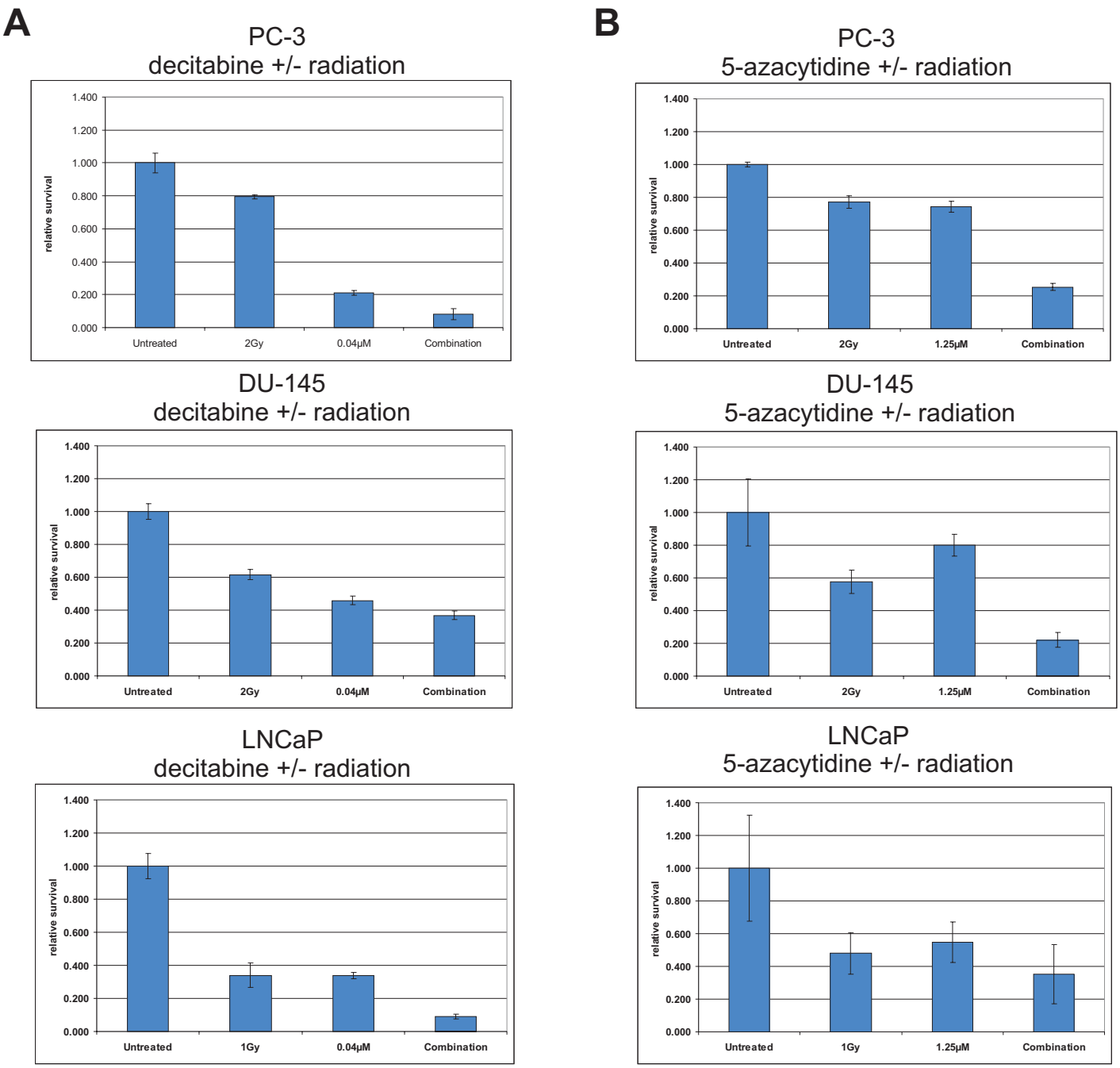

Figure 1 Weterings et al.

5-azacytidine impairs DNA repair in prostate cancer cells

A

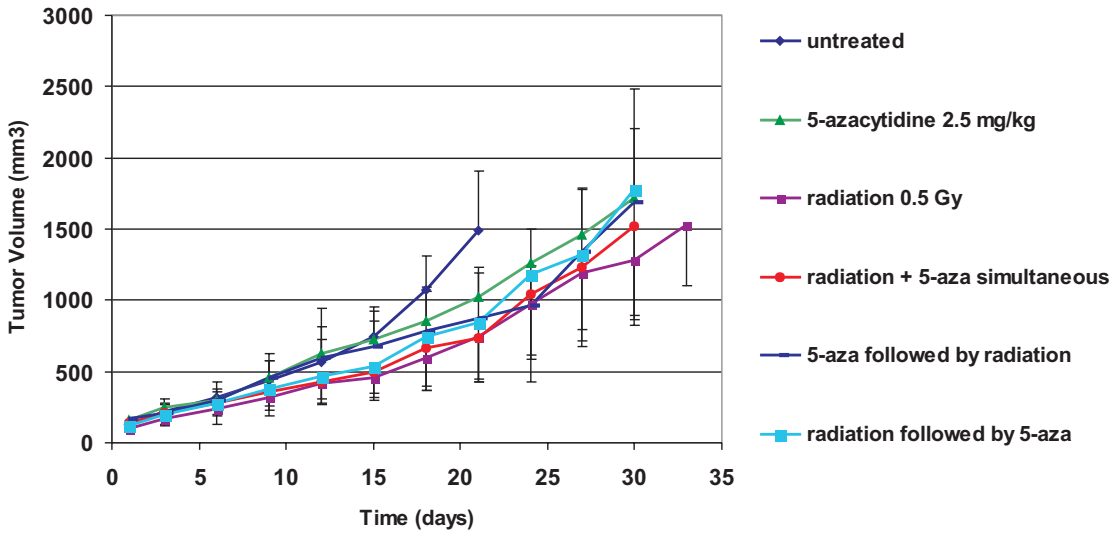

B

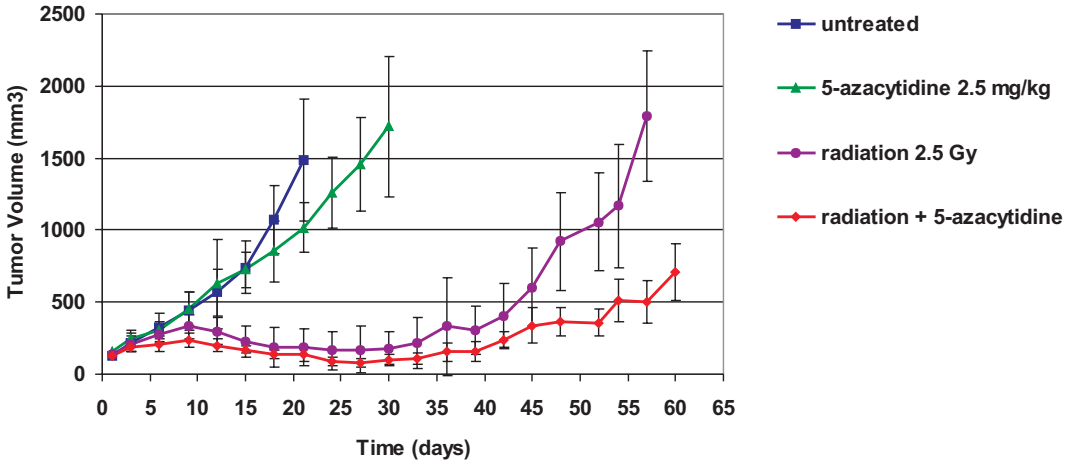

Figure 2 Weterings et al.

5-azacytidine impairs DNA repair in prostate cancer cells

A

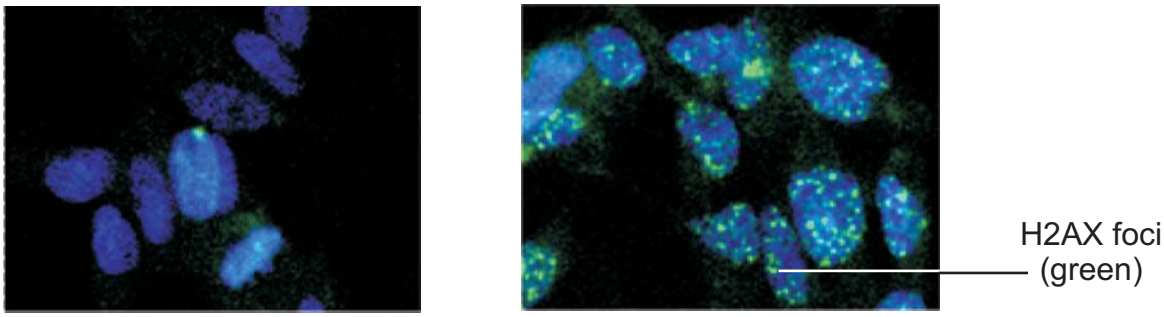

Untreated

4Gy radiation

B

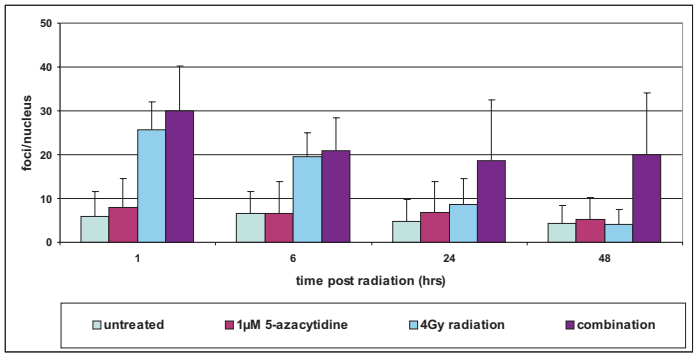

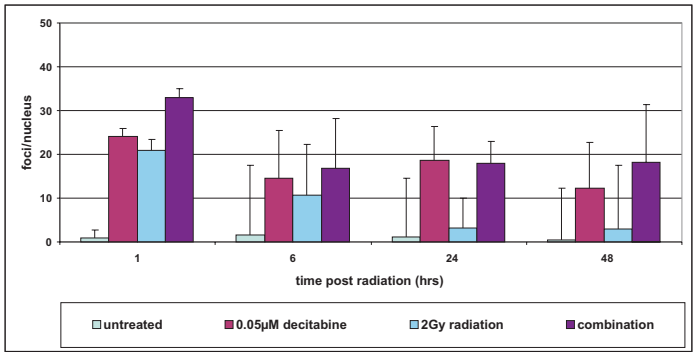

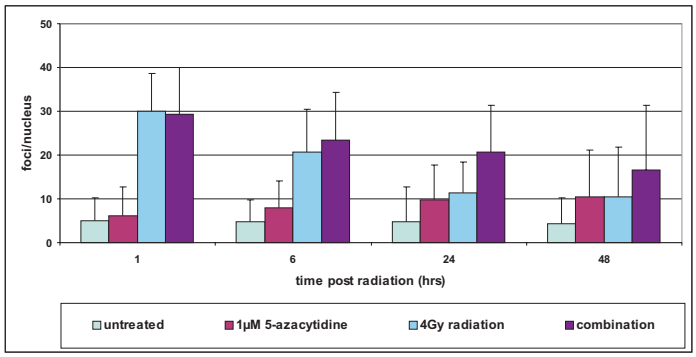

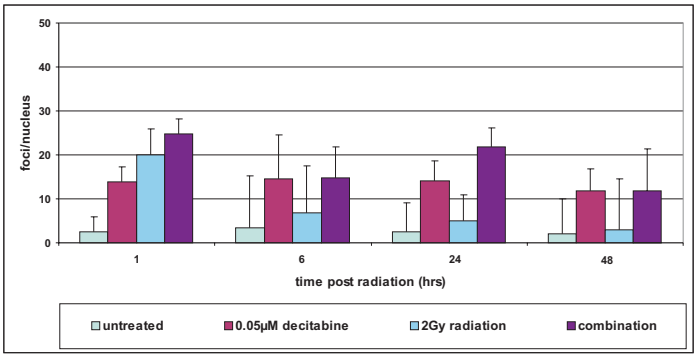

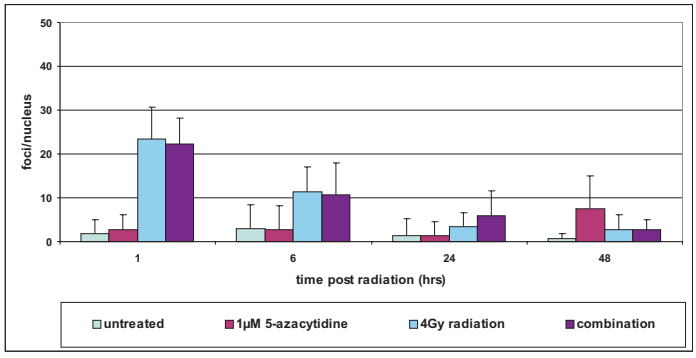

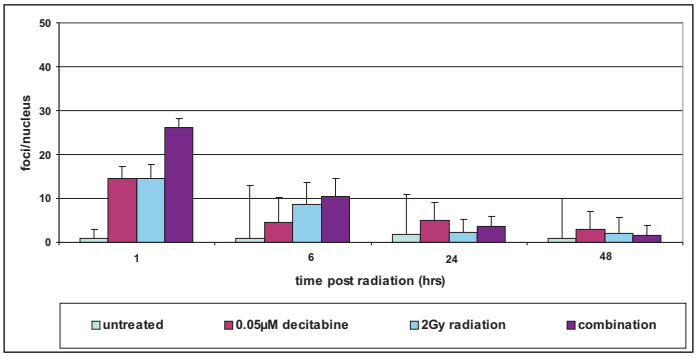

Figure 3 Weterings et al.

5-azacytidine impairs DNA repair in prostate cancer cells

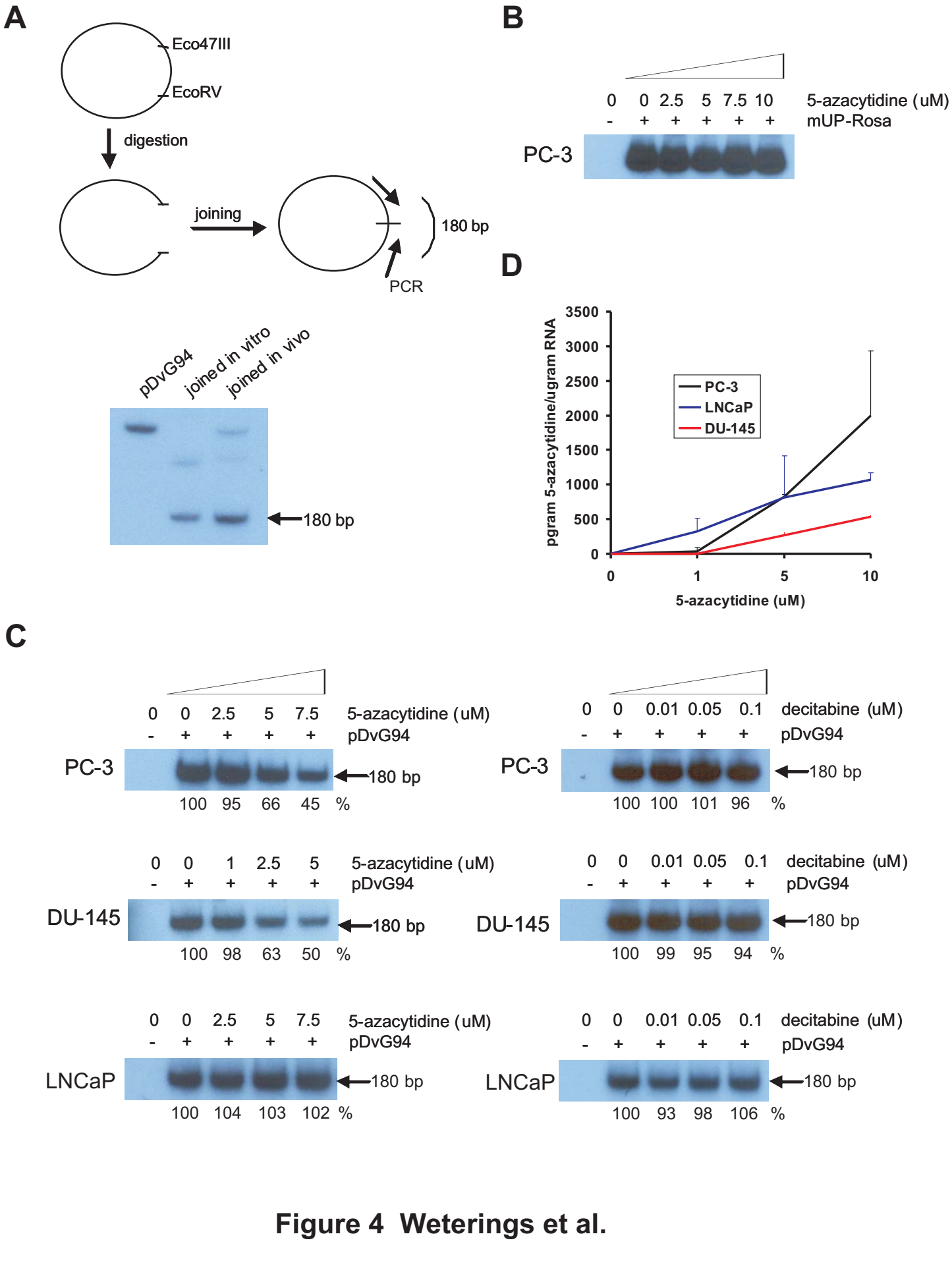

Figure 4 Weterings et al.

Table 1 Analysis of variance to assess synergistic potential of combination therapy (Figure 1).

Drug	Cell Line	Survival Drug	Survival Radiation	Survival Comb.	Expected Survival[1]	Interaction p-value	Synergy Index
decitabine	PC-3	21.1	79.4	8.1	16.7	0.007	0.48
decitabine	DU-145	45.9	61.6	36.8	28.3	<0.001	1.30
decitabine	LNCaP	33.8	33.9	9.3	11.5	<0.001	0.81
5-aza	PC-3	74.1	77.2	25.3	57.2	<0.001	0.44
5-aza	DU-145	80.0	57.4	22.1	46.0	0.513	NR
5-aza	LNCaP	54.6	47.9	35.3	26.2	0.182	NR

[1]Expected survival for the combination if drug and radiation therapy were additive.
NR = not reported because interaction term was not significant indicating additivity.

Table 2 Analysis of time trends in gamma-H2AX foci decrease (Figure 3)

		Time trend in radiation only groups		Time trend in combination groups		Comparison of trends	Comparison of trend ratios
Drug	Cell Line	Decrease in foci per hour	P-value	Decrease in foci per hour	P-value	P-value	
5-aza	PC-3	0.44	<0.001	0.15	<0.001	<0.001	2.9
5-aza	DU-145	0.37	<0.001	0.23	<0.001	0.007	1.6
5-aza	LNCaP	0.37	<0.001	0.34	<0.001	0.765	NR
decitabine	PC-3	0.33	<0.001	0.19	<0.001	<0.001	1.7
decitabine	DU-145	0.27	<0.001	0.18	<0.001	<0.001	1.5
decitabine	LNCaP	0.24	<0.001	0.42	<0.001	0.080	NR

NR= not reported because difference in time trends was not significant.

Neurochemistry International 56 (2010) 546–553

Contents lists available at ScienceDirect

Neurochemistry International

journal homepage: www.elsevier.com/locate/neuint

Protein kinase G type-Iα phosphorylates the apoptosis-regulating protein Bad at serine 155 and protects against apoptosis in N1E-115 cells

Mary G. Johlfs, Ronald R. Fiscus *

Cancer Molecular Biology Section, Nevada Cancer Institute, Las Vegas, NV 89135, USA

ARTICLE INFO

Article history:
Received 21 September 2009
Received in revised form 14 December 2009
Accepted 21 December 2009
Available online 4 January 2010

Keywords:
cGMP-dependent protein kinase
Bad phosphorylation
Apoptosis

ABSTRACT

Previous studies from our laboratory have shown that the cGMP/protein kinase G (PKG) signaling pathway plays an essential role in preventing spontaneous apoptosis in neural cells; however, the mechanism is not understood. A potential downstream target of PKG is the apoptosis-regulating protein Bad, which contains a sequence around its serine 155 (ser155 in mouse Bad, equivalent to ser118 in human Bad) predicted to be a consensus motif for PKG-catalyzed phosphorylation. Using both in vitro and cell-based experiments, we determined if PKG phosphorylates Bad at ser155 and if blocking/stimulating PKG-catalyzed Bad phosphorylation causes pro-apoptotic/anti-apoptotic responses. Recombinant PKG type-Iα (PKG-Iα) was found to directly phosphorylate recombinant Bad at ser155 in vitro. In N1E-115 mouse neural cells, which naturally express PKG-Iα as the predominant PKG isoform, addition of 8-Br-cGMP (0.1–1.0 mM), a cell-permeable direct PKG-Iα activator, increased ser155 phosphorylation of Bad. ODQ (50 μM), a soluble guanylyl cyclase inhibitor that lowers cGMP/PKG activity, decreased serum-induced ser155 phosphorylation of Bad and induced apoptosis in N1E-115 cells. Treatment with DT-2 and DT-3, selective PKG-Iα inhibitors, both decreased Bad ser155 phosphorylation and induced apoptosis. The data indicate that PKG-Iα directly phosphorylates Bad at ser155, which may participate in cGMP/PKG-induced anti-apoptotic/cytoprotective effects in neural cells.

1. Introduction

Exposure of neural cells to nitric oxide (NO) or atrial natriuretic peptide (ANP) stimulates the biosynthesis, intracellular accumulation and cellular efflux of cyclic GMP (cGMP), an important second messenger mediating a variety of biological functions in neural cells (Fiscus et al., 1987). One of the intracellular functions of cGMP is to activate cGMP-dependent protein kinase (protein kinase G, PKG), which results in neuroprotection (Chiueh et al., 2003; Ciani et al., 2002; Fiscus, 2002; Fiscus et al., 2002). Stimulation of the cGMP/PKG signaling pathway has been shown to protect primary hippocampal neurons against induction of cell death by glutamate toxicity and glucose deprivation (Barger et al., 1995), to prevent (or delay) the onset of serum-deprivation-induced apoptosis in PC12 cells (Fiscus et al., 2001b), to protect against the toxic/pro-apoptotic effects of high (pathological) levels of NO in NG108-15 neuroblastoma–glioma hybrid cells (Cheng Chew et al., 2003), and to protect against induction of apoptosis by reactive oxygen species, such as hydrogen peroxide, in chick retinal neurons (Mejia-Garcia and Paes-de-Carvalho, 2007). In contrast, the cGMP/PKG pathway has been reported to mediate cell death in certain neural cells, notably the photoreceptors in animal models of retinitis pigmentosa (Paquet-Durand et al., 2009). In this case, however, the toxic effects occurred because of a severe hyperactivation of the cGMP/PKG signaling pathway caused by a defect in cGMP degradation, characteristic of retinitis pigmentosa. In general, high levels of NO in the cell lead to toxic effects due to the formation of peroxynitrite (Beckman and Koppenol, 1996). In PC12 cells, it was shown that neural cell death in response to high levels of NO is mediated by a mechanism other than hyperactivation of the cGMP/PKG signaling pathway (Wada et al., 1996). At lower, physiological levels of activation of the cGMP/PKG pathway, such as that caused by the low (physiological) levels of NO within healthy mammalian brain and peripheral nerves, this signaling pathway is thought to provide continuous protection against neural cell death, limiting the loss of neural cells that may occur because of aging or exposure to stressful conditions, such as inflammation and ischemia (Chiueh et al., 2003; Ciani et al., 2002; Fiscus, 2002; Fiscus et al., 2002).

Abbreviations: Akt, protein kinase B; ANP, atrial natriuretic peptide; CREB, cAMP-response-element binding protein; NO, nitric oxide; ODQ, (1H-[1,2,4]Oxadiazolo[4,3-a]quinoxalin-1-one); PKA, protein kinase A or cAMP-dependent protein kinase; PKG, protein kinase G or cGMP-dependent protein kinase.

* Corresponding author. University of Southern Nevada, 11 Sunset Way, Henderson, NV 89014. Tel.: +1 702 968 5570.
E-mail address: rfiscus@usn.edu (R.R. Fiscus).

0197-0186/$ – see front matter © 2010 Elsevier Ltd. All rights reserved.
doi:10.1016/j.neuint.2009.12.017

Intracellular stimulation of PKG kinase activity by exposure to NO and ANP was first demonstrated in the vascular smooth muscle cells (VSMCs) of freshly isolated blood vessels (Fiscus, 1988; Fiscus and Murad, 1988; Fiscus et al., 1983, 1985). Interestingly, even the basal levels of NO tonically released from unstimulated endothelial cells lining the blood vessels were sufficient to significantly elevate the intracellular PKG kinase activity to approximately 30% of maximal activity in the underlying VSMCs, which provided a continuous biological action, in this case, protection against vasoconstriction (Fiscus et al., 1983). PKG is now recognized as a key downstream target of cGMP in the cellular signaling pathway that mediates ANP- and NO-induced vasodilations and the prevention against developing hypertension and other vascular diseases (Butt et al., 1993; Francis and Corbin, 1994; Hofmann et al., 2006; Lincoln et al., 2006).

The cGMP/PKG signaling pathway may participate in either pro-apoptotic or anti-apoptotic effects in mammalian cells, depending on the type of cells studied, the experimental conditions and the level of stimulation of the cGMP/PKG pathway (reviewed in Fiscus, 2002; Fiscus et al., 2002). Anti-apoptotic/cytoprotective effects of cGMP elevations and PKG activation are prominently observed in B lymphocytes (Kolb, 2000), leukemia cells (Flamigni et al., 2001), rat ovarian follicles (Chun et al., 1995), immortalized uterine epithelial cells (Chan and Fiscus, 2003) and many neural cells, including primary cultures of rat hippocampal neurons, dorsal root ganglion neurons and motor neurons, cerebellar granule cells and PC12 cells (reviewed in Fiscus, 2002), and in SH-SY5Y human neuroblastoma cells (Chiueh et al., 2003) as well as NG108-15 neuroblastoma–glioma hybrid cells and N1E-115 cells (Cheng Chew et al., 2003; Fiscus, 2002; Fiscus et al., 2002).

Even basal levels of cGMP and PKG activity appear sufficient, and necessary, to protect neural cells (e.g. N1E-115 and NG108-15) against spontaneous development of apoptosis during normal culturing conditions (Fiscus, 2002; Fiscus et al., 2002). The cGMP/PKG pathway, either at basal or slightly elevated activity, appears to inhibit a key step in the onset of apoptosis, thus helping to keep the pro-apoptotic pathway in check. Several potential downstream targets of PKG have been proposed, such as the transcription factor CREB (Jurado et al., 2004), and subsequent increased gene expression of cytoprotective proteins, such as Bcl-2 (Ciani et al., 2002; Fiscus, 2002), as well as induction of other proteins, including thioredoxin and manganese superoxide dismutase via the activation of unknown transcription factors (Chiueh et al., 2003). However, direct phosphorylation of other apoptosis-regulating proteins, such as members of the Bcl-2 protein family, by PKG has not yet been reported.

The present study determined if PKG phosphorylates Bad at its serine 155 residue, using both in vitro and intact-cell experiments. Bad is an important apoptosis-regulating Bcl-2 family member (Zha et al., 1997). Unphosphorylated Bad dimerizes with Bcl-xL, preventing the anti-apoptotic effects of Bcl-xL (i.e. inducing a pro-apoptotic effect). When phosphorylated at serine 112 and 136, Bad preferentially binds to 14-3-3 in the cytosol, preventing binding of Bad to Bcl-xL and thus blocking pro-apoptotic effects of Bad (Datta et al., 2000; Zha et al., 1997). Various extracellular survival factors increase phosphorylation at serine residues 112 and 136 of Bad, resulting in inhibition of apoptosis. Three kinases, Akt (protein kinase B), cAMP-dependent protein kinase (protein kinase A (PKA)) and RSK play prominent roles as mediators of Bad phosphorylation. For example, Akt directly phosphorylates serine 136 of Bad, whereas PKA directly phosphorylates serine residue 112. More recently, a third phosphorylation site on Bad, serine 155, which is in the BH3 domain necessary for dimerization, was identified and shown to be phosphorylated by PKA and RSK, but not Akt (Datta et al., 2000; Lizcano et al., 2000; Tan et al., 2000; Virdee et al., 2000; Zhou et al., 2000). When phosphorylated at serine 155, Bad is unable to bind to Bcl-xL. A number of cytoprotective factors appear to work via cAMP elevation, PKA activation and Bad phosphorylation at serine 155 (Datta et al., 2000; Lizcano et al., 2000; Tan et al., 2000; Virdee et al., 2000; Zhou et al., 2000).

We predicted that PKG may also directly phosphorylate serine 155 of Bad, based on the similarity of the sequence surrounding this phosphorylation site to that of the consensus motif for PKG-catalyzed phosphorylation. PKG is known to phosphorylate some of the same proteins as PKA, such as calcium-regulating proteins in smooth muscle cells (Butt et al., 1993; Fiscus, 1988; Francis and Corbin, 1994; Hofmann et al., 2006; Lincoln et al., 2006 and CREB in certain other cells, Ciani et al., 2002; Fiscus, 2002; Pilz and Casteel, 2003). The present study determined if PKG directly phosphorylates Bad at serine 155 using recombinant Bad and recombinant (cGMP-activated) PKG in in vitro kinase assays. Previous studies from our laboratory had suggested that neural cells, including the N1E-115 cell line, express predominantly the PKG-Iα isoform of PKG (Chan and Fiscus, 2003), and thus this PKG isoform was used in the in vitro experiments of the present study. N1E-115 cells were chosen as a model to determine if endogenous, naturally expressed PKG-Iα within neural cells could regulate the phosphorylation levels of endogenous Bad at serine 155 and whether this corresponds to protection against the onset of apoptosis.

2. Materials and methods

2.1. Materials

The materials used and their suppliers included recombinant Bad and recombinant PKG-Iα (Millipore, Billerica, MA, USA); DT-2 (Axorra, San Diego, CA, USA); DT-3 (Calbiochem, San Diego, CA, USA); cGMP, recombinant PKA (catalytic subunit), ODQ (1H-[1,2,4]Oxadiazolo[4,3-a]quinoxalin-1-one), Triton X-100 (Sigma, St. Louis, MO, USA); 8-Br-cGMP (BioMol, Plymouth Meeting, PA, USA); anti-PKG-Iα/β, anti-Bad (total), anti-phospho-Bad (Ser-155) antibodies (Cell Signaling Technology, Beverly, MA, USA); anti-rabbit-CW800 secondary antibody (LI-COR, Lincoln, NE, USA); DMEM (ATCC, Manassas, VA, USA); fetal bovine serum (Gemini Biosciences, Sacramento, CA, USA); 100 bp DNA ladder, 4–12% Bis–Tris NuPAGE gel system and EZQ protein Quantitation Kit (Invitrogen, Carlsbad, CA, USA); Caspase 3/7 Glo assay (Promega, Madison, WI, USA).

2.2. Cell cultures

The N1E-115 cells were purchased from ATCC. Cells were cultured in DMEM with 4.5 g/L glucose, 10% fetal bovine serum, penicillin (50 U/ml) and streptomycin (50 μg/ml) at 37 °C in a humidified atmosphere containing 5% CO_2, passaged twice weekly and used between passages 10 and 30. Cells were plated into 6-well plates and used 24 h later at a density of 80% confluency for in-cell phosphorylation assays. For DNA fragmentation studies and caspase assays, 10,000 cells were plated in a 48- and 96-well plate, respectively, and used 24 h later.

2.3. In vitro phosphorylation of recombinant Bad

Recombinant Bad (1.6 μM) was incubated in kinase reaction buffer (20 μl) with either recombinant PKG-Iα (0.33 μM) plus its allosteric activator cGMP (10 μM) or recombinant PKA (catalytic subunit) (0.33 μM) for 5 min at room temperature. Reaction buffer contained 20 mM Tris–HCl, pH 7.4, 1 mM ATP, 10 mM magnesium chloride, and 10 mM dithiothreitol. After 5 min, SDS gel loading buffer (5 μl) was added and the solution was heated at 95 °C for 10 min before the samples were applied to NuPAGE gels for Western blot analysis.

2.4. Cell lysis for determination of PKG protein expression and Bad phosphorylation

Cells were washed twice with PBS and suspended in lysis buffer (50 mM Tris–HCl pH 6.8, 100 mM DTT, 2% SDS, 10% glycerol), which had been pre-heated to 85 °C. The cell lysates were heated at 95 °C for 10 min, vortexed briefly to sheer DNA and centrifuged at 12,000 × *g* for 10 min at 4 °C. The amount of total cellular protein in the lysates was determined using EZQ Protein Quantitation Kit.

2.5. Determination of phosphorylation of Bad in N1E-115 cells

For determination of phosphorylation of Bad in the N1E-115 cells, the cells were treated with either 8-Br-cGMP (0.1 and 1.0 mM, 2 h) in the absence of serum (serum deprivation was for 2 h) or with NO/cGMP/PKG-Iα signaling inhibitors, ODQ (30–50 μM, 2 h) and DT-2/3 (1.0–10 μM, 24 h), in the presence of serum. Cells were then immediately lysed using the fore-mentioned lysis buffer and samples were assayed for phosphorylation levels via western blot analysis.

2.6. Traditional western blot analyses

For determination of in vitro phosphorylation of Bad, 20 μl of sample mixture was added to each well of a 4–12% Bis–Tris NuPAGE gel. For determination of PKG protein levels and Bad phosphorylation in cells, 30 μg of total protein in lysates was added to each well of the gel. Proteins were separated at 180 V for approximately 1 h and directly transferred onto nitrocellulose membranes (GE Healthcare) using a semi-wet transfer system. To block non-specific binding sites, the membranes were incubated in blocking buffer (LI-COR) for 1 h at room temperature. Anti-PKG-I, which recognizes both PKG-Iα and PKG-Iβ, was diluted 1:1000 and used as the primary antibody for detection of both PKG-Iα and PKG-Iβ. Other commercially available antibodies that are claimed to be specific for each of the two PKG-I isoforms were not used because of their lack of sufficient specificity. The identification of PKG-Iα versus PKG-Iβ in cell lysates was based on the differences in molecular weights of the two PKG isoforms, and by comparison with recombinant PKG-Iα and PKG-Iβ, which were used as standards in each western blot analysis. Antibodies for total Bad (1:1000) and p-Bad-Ser-155 (1:1000) were used as primary antibodies to determine Bad expression and phosphorylation. Antibodies were exposed to the blots overnight at 4 °C in the presence of 0.1% Tween-20 in blocking buffer. Blots were subsequently probed with infrared-fluorescent-labeled, species-specific secondary antibodies (1:20,000) and scanned using the Odyssey Infrared Imager from LI-COR.

2.7. In cell western blot analyses

For determination of in vitro phosphorylation of Bad, cells were seeded in a tissue culture plate and incubated overnight. The following day, the cells were treated with different concentrations of ODQ, followed by another overnight incubation. Cells were then fixed in 37% formaldehyde for 20 min at 4 °C, then washed with 0.1% Triton-X four times for 5 min each wash to permeate the cells. To block non-specific binding sites, the cells were incubated in blocking buffer (LI-COR) for 1 h at room temperature. An antibody for p-Bad-Ser-155 (1:100) was used as primary antibody to determine the level of Bad phosphorylation. The antibody, in the presence of 0.1% Tween-20 in blocking buffer, was exposed to the cells for 2 h. Cells were washed four times for 5 min each wash in TBS-T and subsequently probed with an infrared-fluorescent-labeled, species-specific secondary antibody (1:800) for 1 h and scanned using the Odyssey Infrared Imager from LI-COR.

2.8. Determination of apoptosis (apoptotic DNA fragmentation) using 12-channel capillary electrophoresis with light emitting diode-induced fluorescence detectors (12-CE-LED-IF)

Previously, our laboratory pioneered the use of capillary electrophoresis with laser-induced fluorescence detection (CE-LIF) as a highly quantitative, ultra-sensitive technique of measuring apoptotic (internucleosomal) DNA fragmentation in tissue and cell culture samples (Chan and Fiscus, 2003; Cheng Chew et al., 2003; Fiscus, 2002; Fiscus et al., 2001a,b, 2002). This technique represents greater than 1000-fold improvement in the sensitivity compared to the conventional agarose gel (slab gel) electrophoresis methodology for accessing apoptotic DNA fragmentation (often referred to as "DNA laddering"). A disadvantage of using CE-LIF, however, is the slow throughput, with each sample requiring approximately 30 min for analysis. Recently, our laboratory has begun using a new CE system with 12 capillaries in parallel, which possesses 12 light emitting diode-induced fluorescence detectors (12-CE-LED-IF) (originally called HDA-GT12 Genetic Analyzer by eGene, Inc. (Irvine, CA, USA), now marketed by QIAGEN, Inc. (Valencia, CA, USA) and called QIAxcel).

For 12-CE-LED-IF analysis, the NIE-115 cells were seeded at a density of 10,000 cells per well in 48-well plates and incubated overnight. The following day, the cells were treated with ODQ (50 μM) for 24 h. The cells were then collected and the DNA was purified using a QIAamp DNA Micro kit (QIAGEN, Inc.) and then analyzed on the QIAxcel instrument. Fragment sizes were extrapolated using a DNA ladder of known molecular weight.

3. Results

3.1. In vitro phosphorylation of recombinant Bad by recombinant PKG-Iα

Fig. 1 shows the general consensus motif of PKG-catalyzed phosphorylation of substrate proteins and the close match provided by the amino acid sequence around serine 155 residue (serine 155 in mouse Bad, corresponding to serine 118 in human Bad). Other known phosphorylation sites of Bad, such as serine 112 and serine 136 (discussed in Section 1) as well as more recently identified sites, serine 128 (Konishi et al., 2002) and serine 170 (Dramsi et al., 2002), do not have a sequence that matches the PKG consensus motif. Based on this, we predicted that PKG may phosphorylate the serine 155 site of Bad.

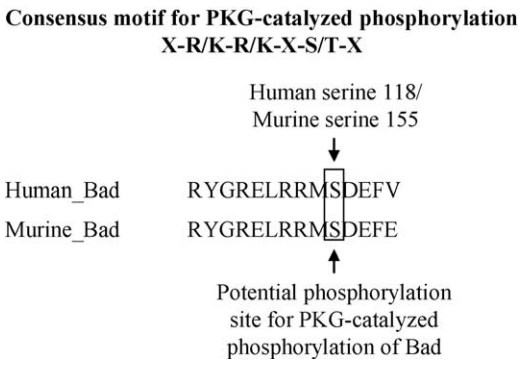

Fig. 1. Potential site for PKG-Iα-catalyzed phosphorylation of Bad. The common consensus motif for PKG-catalyzed phosphorylation, X-R/K-R/K-X-S/T-X, presents itself at serine 118 (human) and serine 155 (mouse) in the amino acid sequence of Bad. The sequence around this site is highly conserved in human and mouse Bad.

Fig. 2 (panel A) shows that PKA (used as a positive control) phosphorylated the recombinant Bad at serine 155. This confirmed that the kinase reaction conditions used in the present study were appropriate for showing in vitro phosphorylation of Bad at serine 155 by PKG-Iα. For the in vitro experiments with PKG, we selected the PKG-Iα isoform, because earlier studies from our laboratory had shown that PKG-Iα appears to be the predominant isoform of PKG expressed in neural cells such as N1E-115 and NG108-15 cells (Chan and Fiscus, 2003), both of which display the anti-apoptotic/cytoprotective effects mediated by basal cGMP/PKG activity (Fiscus, 2002; Fiscus et al., 2002). Fig. 2 (panel B) demonstrates that, under the same in vitro conditions as the PKA-catalyzed phosphorylation of serine 155 in Bad, recombinant PKG-Iα (activated by cGMP) caused a similar phosphorylation of Bad at serine 155.

3.2. The PKG-Iα isoform is predominantly expressed in N1E-115 cells

The present study used N1E-115 cells as a cell culture model to determine if endogenous, naturally expressed PKG can phosphorylate endogenous Bad in intact living cells. Our

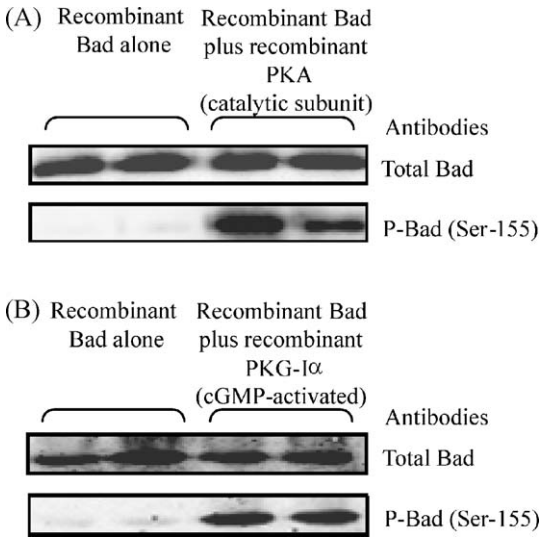

Fig. 2. Western blot analysis showing that PKG-Iα directly phosphorylates Bad at serine 155 (mouse sequence) using in vitro experimental conditions. (A) PKA, previously shown to phosphorylate Bad at serine 155, was used as a positive control to show that the in vitro kinase reaction conditions were appropriate for showing phosphorylation of Bad by PKG-Iα. (B) Recombinant human PKG-Iα, fully activated by the addition of 10 μM cGMP, effectively phosphorylated Bad at serine 155. Similar results were obtained in three other in vitro experiments.

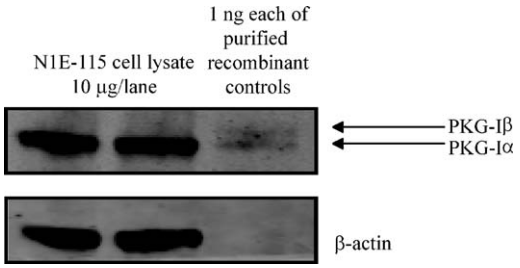

Fig. 3. Western blot analysis testing for expression of the two PKG-I splice variants, PKG-Iα and PKG-Iβ, in NIE-115 cells. Each lane represents 10 μg of total cellular protein. The analysis reveals that N1E-115 cells express relatively high levels of PKG-I, which was predominantly the PKG-Iα isoform. Similar results were obtained in three other experiments.

previous studies had suggested that N1E-115 cells express relatively high levels of PKG, likely the PKG-Iα isoform (Chan and Fiscus, 2003).

Fig. 3 shows that N1E-115 cells, grown under the culturing conditions of the present study, indeed expressed high levels of the PKG-Iα isoform of PKG, identified in Western blot analyses using an antibody specific for the C-terminal region of PKG-Iα/β (a region common to both of the PKG-I splice variants, PKG-Iα and PKG-Iβ). The two PKG-I isoforms were differentiated based on their different migration patterns in the Western blots. PKG-Iα corresponds to a molecular weight of 76.2 kDa, whereas PKG-Iβ corresponds to a molecular weight of 77.8 kDa.

3.3. A direct PKG-Iα activator, 8-Br-cGMP, stimulates increased levels of serine 155 phosphorylation of Bad in N1E-115 cells

To determine if intracellular activation of the endogenous naturally expressed PKG-Iα results in phosphorylation of endogenous Bad, N1E-115 cells were exposed to 8-Br-cGMP, a cell-permeable direct activator of PKG-Iα. Fig. 4 shows elevated levels of Bad phosphorylation at serine 155 following the exposure to 8-Br-cGMP for 2 h. For these experiments, the serum was removed prior to adding the 8-Br-cGMP, because serum, by itself, results in

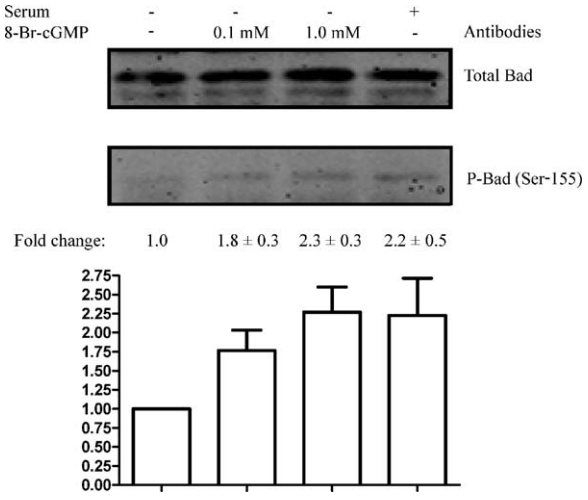

Fig. 4. Stimulation of PKG-Iα activity in N1E-115 cells by exposure to 8-Br-cGMP increases the phosphorylation of Bad at serine 155. After removing serum from the N1E-115 cells, the cells were exposed to 8-Br-cGMP (either 0.1 mM or 1 mM) for 2 h. 8-Br-cGMP is a cell-permeable analog of cGMP, which is a potent direct stimulator of PKG-Iα enzymatic activity. Each lane of the western blot represents 30 μg of total cellular protein. The 8-Br-cGMP treatment elevated serine 155 phosphorylation of Bad to levels equal to those induced by exposure to serum. Similar results were obtained in three other experiments.

elevated levels of serine 155 phosphorylation of Bad (see Figs. 4 and 6, panel A), which would mask the 8-Br-cGMP-stimulated response in the N1E-115 cells.

3.4. ODQ, an inhibitor of NO-induced activation of soluble guanylyl cyclase and cGMP synthesis, reduces the serum-induced phosphorylation of Bad at serine 155 and causes apoptosis in N1E-115 cells

To further test whether the cGMP/PKG signaling pathway is involved in intracellular phosphorylation of Bad at serine 155, the N1E-115 cells were exposed to ODQ, an agent that blocks NO-induced activation of soluble guanylyl cyclase (see Fig. 5, panel A), thus preventing the basal activation of the cGMP/PKG signaling pathway mediated by endogenous NO within mammalian cells (Fiscus, 2002; Fiscus et al., 2002). N1E-115 cells are known to express the neuronal form of NO synthase (nNOS) (Grant et al., 2002), which results in endogenous production of NO and elevated basal levels of cGMP (Forstermann et al., 1989; McKinney et al., 1990). Using a specialized microelectrode/biosensor technique that directly measures intracellular cGMP concentration, addition of ODQ to N1E-115 cells has been shown to dramatically reduce the basal concentration of intracellular cGMP (Trivedi and Kramer, 1998), which would lower basal activation of PKG-Iα.

In the present study, Fig. 5 (panel B) shows that ODQ, at 50 μM, increased the level of apoptotic DNA fragmentation in N1E-115 cells, suggesting that the cGMP/PKG-mediated phosphorylation of Bad at serine 155 is important for preventing spontaneous onset of apoptosis in these neural cells. Figs. 4 and 6 (panel A) show that the presence of serum elevated levels of serine 155 phosphorylation of Bad in N1E-115 cells. Fig. 6 (panel A) further shows that addition of ODQ (30–50 μM) blocked the serum-induced elevation of serine 155 phosphorylation of Bad in N1E-115 cells, assessed by Western blot analysis, suggesting that the endogenous NO and its downstream activation of the cGMP/PKG-Iα signaling pathway is involved in serum-induced phosphorylation of Bad at serine 155. Fig. 6 (panel B) shows that addition of ODQ (10–25 μM) blocked the serum-induced elevation of serine 155 phosphorylation of Bad in N1E-115 cells, assessed by in-cell Westerns, further suggesting that the endogenous PKG-Iα and its downstream activation of the cGMP/PKG-Iα signaling pathway contributes to serum-induced phosphorylation of Bad at serine 155.

3.5. Inhibition of PKG-Iα activity using the direct inhibitors, DT-2 and DT-3, also lowers serum-induced phosphorylation of Bad at serine 155 and causes apoptosis in N1E-115 cells

Fig. 7 (panel A) shows that inhibition of PKG-Iα, using two cell-permeable highly selective inhibitors of PKG-Iα, DT-2 and DT-3, reduced the serum-induced phosphorylation of Bad at serine 155. DT-2 and DT-3 are known to have 1300- and 20,000-fold specificity, respectively, for inhibiting PKG-Iα activity, as compared to inhibiting PKA activity, the most closely related protein kinase (Dostmann et al., 2000, 2002; Taylor et al., 2004). Thus, the present data suggest that the endogenous naturally expressed PKG-Iα in N1E-115 cells is directly responsible for contributing to the serum-induced phosphorylation of Bad at serine 155.

Fig. 7 (panel B) shows that DT-2 at 10 μM and DT-3 at 1.0 and 10 μM, the same concentrations of DT-2 and DT-3 that inhibit Bad serine 155 phosphorylation, significantly increased caspase 3/7 activity (index of apoptosis), suggesting that PKG-Iα-catalyzed phosphorylation of Bad at serine 155 may be needed for protecting N1E-115 cells against spontaneous induction of apoptosis.

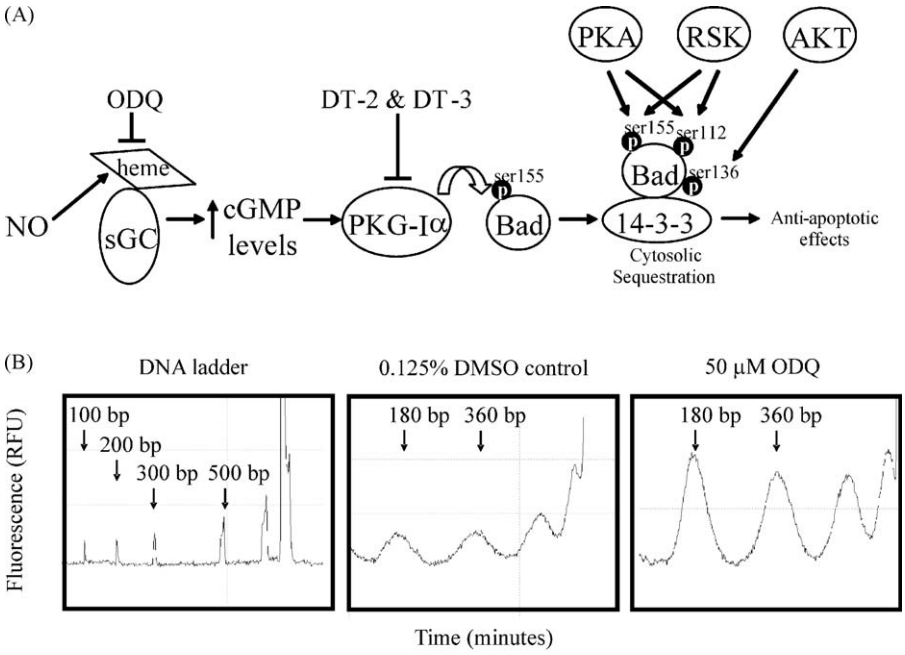

Relative difference in apoptotic fragment content

	0.125 % DMSO Control	50 μM ODQ
180bp	1.0	4.2
360bp	1.0	3.6

Fig. 5. (A) A model showing the proposed phosphorylation at serine 155 by PKG-Iα, in conjunction with phosphorylation at serines 112 and 136 by other important protein kinases (Akt, PKA and RSK) leads to cytosolic sequestration of Bad and subsequent anti-apoptotic effects. (B) ODQ, at 50 μM causes onset of apoptosis (approximately 4-fold increased level of fragmentation), indicated by the increase in apoptotic fragmentation of DNA in the N1E-115 cells. Total DNA was collected from cells following treatment with ODQ for 24 h, purified on mini-columns and analyzed in a 12-channel capillary electrophoresis apparatus with light emitting diode-induce fluorescence detectors (allowing ultra-sensitive analysis of apoptotic DNA fragmentation). Apoptotic fragments of DNA in multiples of approximately 180 base pairs were detected in the apoptotic cells. Fragment sizes were determined using a commercially available DNA ladder.

4. Discussion

Previously, PKA was shown to phosphorylate Bad at serine 155, both in vitro and in intact cells, and to prevent the pro-apoptotic effects of Bad in mammalian cells (Datta et al., 2000; Lizcano et al., 2000; Tan et al., 2000; Virdee et al., 2000; Zhou et al., 2000). The data of the present study show that PKG-Iα is also capable of effectively phosphorylating Bad at serine 155, using both in vitro experiments and intact-cell experiments that utilized cultured N1E-115 cells. The phosphorylation of serine 155 of Bad is known to prevent the interaction between Bad and Bcl-xL, thus promoting cell survival (Datta et al., 2000; Lizcano et al., 2000; Tan et al., 2000; Virdee et al., 2000; Zhou et al., 2000). The previous studies had shown that various growth/survival factors utilize the PKA pathway and the phosphorylation of Bad at serine 155 to induce anti-apoptotic/pro-survival effects (Datta et al., 2000; Lizcano et al., 2000; Tan et al., 2000; Virdee et al., 2000; Zhou et al., 2000). In light of the present data showing that serum-induced phosphorylation of Bad at serine 155 in N1E-115 cells is inhibited by ODQ, a blocker of NO-induced cGMP synthesis, and by DT-2/DT-3, inhibitors of PKG-Iα catalytic activity, it appears that the cGMP/PKG-Iα signaling pathway may also play a key role in growth/survival-factor-induced phosphorylation of Bad at serine 155 and the subsequent anti-apoptotic/cytoprotective effects in neural cells.

Although numerous previous studies have shown that the cGMP/PKG signaling pathway (at basal and moderately elevated levels) has anti-apoptotic/cytoprotective effects in certain types of mammalian cells, notably neural cells (Barger et al., 1995; Cheng Chew et al., 2003; Chiueh et al., 2003; Ciani et al., 2002; Fiscus, 2002; Fiscus et al., 2001b, 2002; Mejia-Garcia and Paes-de-Carvalho, 2007), epithelial cells (Chan and Fiscus, 2003) and leukocytes (Flamigni et al., 2001; Kolb, 2000), little is known about which proteins are the immediate downstream targets of PKG. Recently, three reports have suggested that activation of the cGMP/PKG pathway in leukemia cells (Flamigni et al., 2001), PC12 cells (Ha et al., 2003) and insulin-producing RINm5F cells (Tejedo et al., 2004) results in phosphorylation of Bad and subsequent anti-apoptotic effects. However, in all of these cases, the Bad phosphorylation (that was reported) occurred at serine 136 of Bad and appeared to be mediated via the cross-activation of the phosphatidylinositol 3-kinase/Akt pathway (not via direct PKG-catalyzed phosphorylation of Bad). Apparently, Bad phosphorylation at serine 155 was not measured in these previous reports (Flamigni et al., 2001; Ha et al., 2003; Tejedo et al., 2004).

Originally, PKG was thought to be expressed only in a limited number of cell types, such as smooth muscle cells of airways, blood vessels and intestines and only the Purkinje neurons of the brain (Butt et al., 1993; Fiscus, 2002; Francis and Corbin, 1994; Hofmann et al., 2006; Lincoln et al., 2006). However, other studies have suggested that PKG may be more widely distributed in many different types of mammalian cells, including hippocampal neurons of rat brain (Barger et al., 1995) and the cell lines C-6 glioma cells and NG108-15 neuroblastoma–glioma hybrid cells

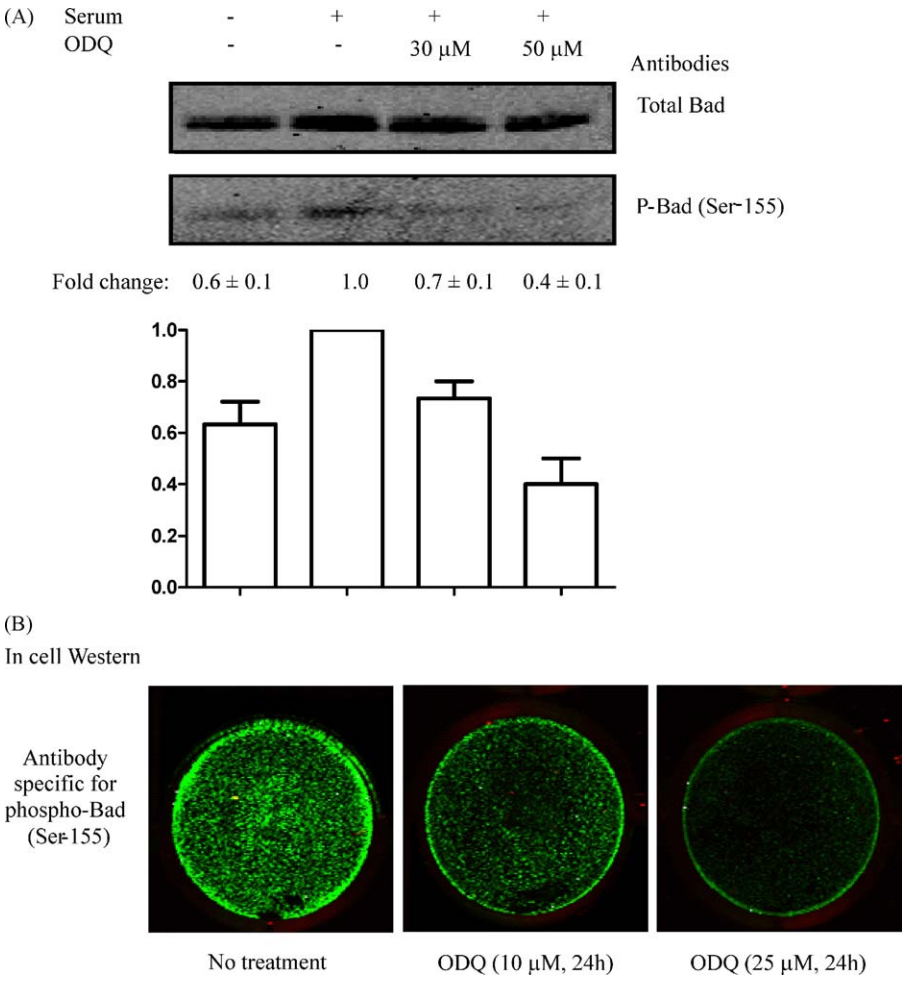

Fig. 6. (A) ODQ, an inhibitor of endogenous-NO-induced cGMP synthesis, blocks the serum-induced phosphorylation of Bad at serine 155 in N1E-115 cells. N1E-115 cells, cultured in the presence of serum, were treated for 2 h with ODQ. Each lane of the western blot represents 30 μg of total cellular protein. ODQ, in a concentration-dependent fashion, prevented serum-induced phosphorylation of Bad at serine 155. (B) N1E-115 cells, cultured in the presence of serum, were treated for 24 h with ODQ. Fixed and permeated cells were assessed by an in cell western technique (LI-COR). ODQ, in a concentration-dependent fashion, prevented serum-induced phosphorylation of Bad at serine 155. Similar results were obtained in three other experiments.

(Walter, 1981), although the isoform(s) of PKG expressed in these cells was not identified. Previous studies from our laboratory have shown that N1E-115 and NG108-15 cells possess functional activity of PKG that is essential for the survival (Fiscus et al., 2002; Fiscus, 2002) of these cells in culture and that both of these neural cell lines appear to express predominantly the PKG-Iα isoform.

The present study confirms our previous suggestion, showing that N1E-115 cells express almost exclusively the PKG-Iα isoform. Because basal intracellular concentrations of cGMP in N1E-115 cells are known to be between 0.1 and 1 μM (Trivedi and Kramer, 1998), which would cause a relatively high level of basal activation of PKG-Iα (K_{act} for PKG-Iα activation by cGMP is approximately 0.1 μM, Butt et al., 1993; Francis and Corbin, 1994; Hofmann et al., 2006; Lincoln et al., 2006), it is likely that the PKG-Iα in N1E-115 cells, even under normal culturing conditions, would be capable of continually phosphorylating Bad at serine 155 and mediating the anti-apoptotic/cytoprotective effects of basal cGMP in N1E-115 cells.

By using in vitro kinase experiments utilizing human recombinant PKG-Iα and recombinant Bad, the present study shows that PKG-Iα directly phosphorylates Bad at serine 155. Furthermore, using intact N1E-115 cells, the present study suggests that naturally expressed PKG-Iα also phosphorylates Bad at serine 155. This was shown in experiments using 8-Br-cGMP, a cell-permeable analog of cGMP that directly activates PKG-Iα, which elevates the level of phosphorylation of Bad at serine 155. Furthermore, inhibition of cGMP synthesis with ODQ, which is known to dramatically lower cGMP levels in N1E-115 cells (Trivedi and Kramer, 1998), decreases serum-induced phosphorylation of Bad at serine 155 and causes onset of apoptosis. Likewise, inhibition of PKG-Iα catalytic activity, using the PKG-I-selective inhibitors DT-2 and DT-3, decreases serum-induced phosphorylation of Bad at serine 155 and causes apoptosis in N1E-115 cells. Thus, the present data suggest that growth/survival factors present within serum require the endogenous catalytic activity of PKG-Iα for phosphorylation of Bad at serine 155 and for continuous protection against spontaneous onset of apoptosis.

In summary, we demonstrate that PKG-Iα is capable of directly phosphorylating Bad at serine 155, similar to the phosphorylation induced by the established Bad serine 155 phosphorylating kinase, PKA. N1E-115 cells express predominantly the PKG-Iα isoform of PKG-I. Activation of this PKG-Iα, using the cell-permeable cGMP analog 8-Br-cGMP, elevates serine 155 phosphorylation of Bad in N1E-115 cells, whereas inhibition of NO-sensitive soluble guanylyl cyclase with ODQ, which causes cGMP depletion, or direct inhibition of PKG-Iα with the highly selective PKG-I inhibitors DT-2 and DT-3 causes dramatic reductions in the levels of Bad phosphorylation at serine 155. In fact, both ODQ and DT-2/DT-3 decreased the levels of serine 155 phosphorylation in serum-treated cells to the levels

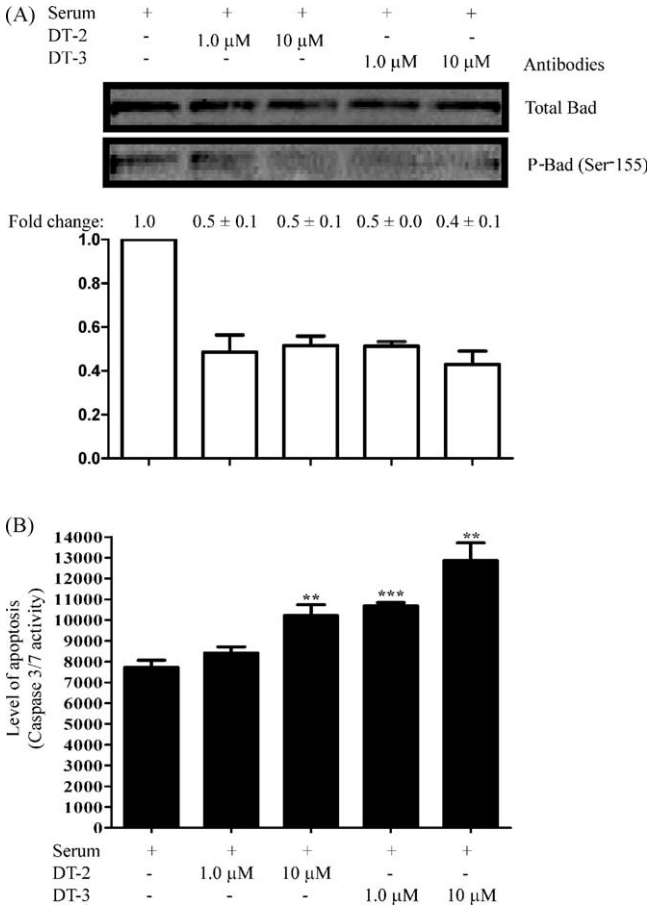

Fig. 7. DT-2 and DT-3, two highly selective inhibitors of PKG-Iα, both decrease the serum-induced phosphorylation of Bad at serine 155 and induce onset of apoptosis in N1E-115 cells. (A) N1E-115 cells were treated with either DT-2 or DT-3 (each at 1.0 and 10 μM) for 24 h. Each lane of the western blots represents 30 μg of total cellular protein. The western blots show that the inhibition of endogenous PKG-Iα enzymatic activity in N1E-115 cells reduces the serum-induced phosphorylation of Bad at serine 155, suggesting dependence on PKG-Iα activity. (B) DT-2 and DT-3 (at the same concentration) also increase the levels of apoptosis (indicated by increased levels of caspase 3/7 activity) in N1E-115 cells. The effects of DT-2 and DT-3 on induction of apoptosis were concentration-dependent and corresponded with the decreases in Bad phosphorylation at serine 155 following the inhibition of PKG-Iα activity ($n = 4$). Similar results were obtained in three other experiments.

observed in serum-deprived cells, suggesting an important role of the cGMP/PKG-Iα signaling pathway in mediating the serum-induced phosphorylation of Bad at serine 155. The ODQ- and DT-2/DT-3-induced inhibition of Bad phosphorylation at serine 155 was accompanied by induction of apoptosis in the N1E-115 cells. The data of the present study suggest that Bad is likely to be an important downstream substrate of PKG-Iα in neural cells, and that the PKG-Iα-catalyzed phosphorylation of Bad at serine 155 may contribute to the anti-apoptotic/pro-survival effects mediated by the basal cGMP/PKG-Iα activity in neural cells.

Acknowledgement

This study was supported by a grant from the Department of Defense (grant # W81XWH-07-1-0543) and Nevada Cancer Institute Start-up Funding awarded to RRF.

References

Barger, S.W., Fiscus, R.R., Ruth, P., Hofmann, F., Mattson, M.P., 1995. Role of cyclic GMP in the regulation of neuronal calcium and survival by secreted forms of beta-amyloid precursor. J. Neurochem. 64, 2087–2096.

Beckman, J.S., Koppenol, W.H., 1996. Nitric oxide, superoxide, and peroxynitrite: the good, the bad, and ugly. Am. J. Physiol. 271, C1424–C1437.

Butt, E., Geiger, J., Jarchau, T., Lohmann, S.M., Walter, U., 1993. The cGMP-dependent protein kinase—gene, protein, and function. Neurochem. Res. 18, 27–42.

Chan, S.L., Fiscus, R.R., 2003. Guanylyl cyclase inhibitors NS2028 and ODQ and protein kinase G (PKG) inhibitor KT5823 trigger apoptotic DNA fragmentation in immortalized uterine epithelial cells: anti-apoptotic effects of basal cGMP/PKG. Mol. Hum. Reprod. 9, 775–783.

Cheng Chew, S.B., Leung, P.Y., Fiscus, R.R., 2003. Preincubation with atrial natriuretic peptide protects NG108-15 cells against the toxic/proapoptotic effects of the nitric oxide donor S-nitroso-N-acetylpenicillamine. Histochem. Cell Biol. 120, 163–171.

Chiueh, C., Lee, S., Andoh, T., Murphy, D., 2003. Induction of antioxidative and antiapoptotic thioredoxin supports neuroprotective hypothesis of estrogen. Endocrine 21, 27–31.

Chun, S.Y., Eisenhauer, K.M., Kubo, M., Hsueh, A.J., 1995. Interleukin-1 beta suppresses apoptosis in rat ovarian follicles by increasing nitric oxide production. Endocrinology 136, 3120–3127.

Ciani, E., Guidi, S., Bartesaghi, R., Contestabile, A., 2002. Nitric oxide regulates cGMP-dependent cAMP-responsive element binding protein phosphorylation and Bcl-2 expression in cerebellar neurons: implication for a survival role of nitric oxide. J. Neurochem. 82, 1282–1289.

Datta, S.R., Katsov, A., Hu, L., Petros, A., Fesik, S.W., Yaffe, M.B., Greenberg, M.E., 2000. 14-3-3 proteins and survival kinases cooperate to inactivate BAD by BH3 domain phosphorylation. Mol. Cell 6, 41–51.

Dostmann, W.R., Taylor, M.S., Nickl, C.K., Brayden, J.E., Frank, R., Tegge, W.J., 2000. Highly specific, membrane-permeant peptide blockers of cGMP-dependent protein kinase Ialpha inhibit NO-induced cerebral dilation. Proc. Natl. Acad. Sci. U.S.A. 97, 14772–14777.

Dostmann, W.R., Tegge, W., Frank, R., Nickl, C.K., Taylor, M.S., Brayden, J.E., 2002. Exploring the mechanisms of vascular smooth muscle tone with highly specific, membrane-permeable inhibitors of cyclic GMP-dependent protein kinase Ialpha. Pharmacol. Ther. 93, 203–215.

Dramsi, S., Scheid, M.P., Maiti, A., Hojabrpour, P., Chen, X., Schubert, K., Goodlett, D.R., Aebersold, R., Duronio, V., 2002. Identification of a novel phosphorylation site, Ser-170, as a regulator of bad pro-apoptotic activity. J. Biol. Chem. 277, 6399–6405.

Fiscus, R.R., 1988. Molecular mechanisms of endothelium-mediated vasodilation. Semin. Thromb. Hemost. 14 (Suppl), 12–22.

Fiscus, R.R., 2002. Involvement of cyclic GMP and protein kinase G in the regulation of apoptosis and survival in neural cells. Neurosignals 11, 175–190.

Fiscus, R.R., Murad, F., 1988. cGMP-dependent protein kinase activation in intact tissues. Methods Enzymol. 159, 150–159.

Fiscus, R.R., Rapoport, R.M., Murad, F., 1983. Endothelium-dependent and nitrovasodilator-induced activation of cyclic GMP-dependent protein kinase in rat aorta. J. Cyclic Nucleotide Protein Phosphor. Res. 9, 415–425.

Fiscus, R.R., Rapoport, R.M., Waldman, S.A., Murad, F., 1985. Atriopeptin II elevates cyclic GMP, activates cyclic GMP-dependent protein kinase and causes relaxation in rat thoracic aorta. Biochim. Biophys. Acta 846, 179–184.

Fiscus, R.R., Robles, B.T., Waldman, S.A., Murad, F., 1987. Atrial natriuretic factors stimulate accumulation and efflux of cyclic GMP in C6-2B rat glioma and PC12 rat pheochromocytoma cell cultures. J. Neurochem. 48, 522–528.

Fiscus, R.R., Leung, C.P., Yuen, J.P., Chan, H.C., 2001a. Quantification of apoptotic DNA fragmentation in a transformed uterine epithelial cell line, HRE-H9, using capillary electrophoresis with laser-induced fluorescence detector (CE-LIF). Cell Biol. Int. 25, 1007–1011.

Fiscus, R.R., Tu, A.W., Chew, S.B., 2001b. Natriuretic peptides inhibit apoptosis and prolong the survival of serum-deprived PC12 cells. Neuroreport 12, 185–189.

Fiscus, R.R., Yuen, J.P., Chan, S.L., Kwong, J.H., Chew, S.B., 2002. Nitric oxide and cyclic GMP as pro- and anti-apoptotic agents. J. Card. Surg. 17, 336–339.

Flamigni, F., Facchini, A., Stanic, I., Tantini, B., Bonavita, F., Stefanelli, C., 2001. Control of survival of proliferating L1210 cells by soluble guanylate cyclase and p44/42 mitogen-activated protein kinase modulators. Biochem. Pharmacol. 62, 319–328.

Forstermann, U., Ishii, K., Gorsky, L.D., Murad, F., 1989. The cytosol of N1E-115 neuroblastoma cells synthesizes an EDRF-like substance that relaxes rabbit aorta. Naunyn Schmiedebergs Arch. Pharmacol. 340, 771–774.

Francis, S.H., Corbin, J.D., 1994. Progress in understanding the mechanism and function of cyclic GMP-dependent protein kinase. Adv. Pharmacol. 26, 115–170.

Grant, M.K., Cuadra, A.E., El-Fakahany, E.E., 2002. Endogenous expression of nNOS protein in several neuronal cell lines. Life Sci. 71, 813–817.

Ha, K.S., Kim, K.M., Kwon, Y.G., et al., 2003. Nitric oxide prevents 6-hydroxydopamine-induced apoptosis in PC12 cells through cGMP-dependent PI3 kinase/Akt activation. FASEB J. 17, 1036–1047.

Hofmann, F., Feil, R., Kleppisch, T., Schlossmann, J., 2006. Function of cGMP-dependent protein kinases as revealed by gene deletion. Physiol. Rev. 86, 1–23.

Jurado, S., Sanchez-Prieto, J., Torres, M., 2004. Elements of the nitric oxide/cGMP pathway expressed in cerebellar granule cells: biochemical and functional characterisation. Neurochem. Int. 45, 833–843.

Kolb, J.P., 2000. Mechanisms involved in the pro- and anti-apoptotic role of NO in human leukemia. Leukemia 14, 1685–1694.

Konishi, Y., Lehtinen, M., Donovan, N., Bonni, A., 2002. Cdc2 phosphorylation of BAD links the cell cycle to the cell death machinery. Mol. Cell 9, 1005–1016.

Lincoln, T.M., Wu, X., Sellak, H., Dey, N., Choi, C.S., 2006. Regulation of vascular smooth muscle cell phenotype by cyclic GMP and cyclic GMP-dependent protein kinase. Front. Biosci. 11, 356–367.

Lizcano, J.M., Morrice, N., Cohen, P., 2000. Regulation of BAD by cAMP-dependent protein kinase is mediated via phosphorylation of a novel site, Ser155. Biochem. J. 349, 547–557.

McKinney, M., Bolden, C., Smith, C., Johnson, A., Richelson, E., 1990. Selective blockade of receptor-mediated cyclic GMP formation in N1E-115 neuroblastoma cells by an inhibitor of nitric oxide synthesis. Eur. J. Pharmacol. 178, 139–140.

Mejia-Garcia, T.A., Paes-de-Carvalho, R., 2007. Nitric oxide regulates cell survival in purified cultures of avian retinal neurons: involvement of multiple transduction pathways. J. Neurochem. 100, 382–394.

Paquet-Durand, F., Hauck, S.M., van Veen, T., Ueffing, M., Ekstrom, P., 2009. PKG activity causes photoreceptor cell death in two retinitis pigmentosa models. J. Neurochem. 108, 796–810.

Pilz, R.B., Casteel, D.E., 2003. Regulation of gene expression by cyclic GMP. Circ. Res. 93, 1034–1046.

Tan, Y., Demeter, M.R., Ruan, H., Comb, M.J., 2000. BAD Ser-155 phosphorylation regulates BAD/Bcl-XL interaction and cell survival. J. Biol. Chem. 275, 25865–25869.

Taylor, M.S., Okwuchukwuasanya, C., Nickl, C.K., Tegge, W., Brayden, J.E., Dostmann, W.R., 2004. Inhibition of cGMP-dependent protein kinase by the cell-permeable peptide DT-2 reveals a novel mechanism of vasoregulation. Mol. Pharmacol. 65, 1111–1119.

Tejedo, J.R., Cahuana, G.M., Ramirez, R., Esbert, M., Jimenez, J., Sobrino, F., Bedoya, F.J., 2004. Nitric oxide triggers the phosphatidylinositol 3-kinase/Akt survival pathway in insulin-producing RINm5F cells by arousing Src to activate insulin receptor substrate-1. Endocrinology 145, 2319–2327.

Trivedi, B., Kramer, R.H., 1998. Real-time patch-cram detection of intracellular cGMP reveals long-term suppression of responses to NO and muscarinic agonists. Neuron 21, 895–906.

Virdee, K., Parone, P.A., Tolkovsky, A.M., 2000. Phosphorylation of the pro-apoptotic protein BAD on serine 155, a novel site, contributes to cell survival. Curr. Biol. 10, 1151–1154.

Wada, K., Okada, N., Yamamura, T., Koizumi, S., 1996. Nerve growth factor induces resistance of PC12 cells to nitric oxide cytotoxicity. Neurochem. Int. 29, 461–467.

Walter, U., 1981. Distribution of cyclic-GMP-dependent protein kinase in various rat tissues and cell lines determined by a sensitive and specific radioimmunoassay. Eur. J. Biochem. 118, 339–346.

Zha, J., Harada, H., Osipov, K., Jockel, J., Waksman, G., Korsmeyer, S.J., 1997. BH3 domain of BAD is required for heterodimerization with BCL-XL and pro-apoptotic activity. J. Biol. Chem. 272, 24101–24104.

Zhou, X.M., Liu, Y., Payne, G., Lutz, R.J., Chittenden, T., 2000. Growth factors inactivate the cell death promoter BAD by phosphorylation of its BH3 domain on Ser155. J. Biol. Chem. 275, 25046–25051.

Published Online First on April 6, 2010

Signaling and Regulation

Molecular Cancer Research

Protein Kinase G Type Iα Activity in Human Ovarian Cancer Cells Significantly Contributes to Enhanced Src Activation and DNA Synthesis/Cell Proliferation

Elaine L. Leung[1,3], Janica C. Wong[1,2], Mary G. Johlfs[1], Benjamin K. Tsang[4,5,6], and Ronald R. Fiscus[1,2,3,7]

Abstract

Previously, we showed that basal activity of nitric oxide (NO)/cyclic GMP (cGMP)/protein kinase G (PKG) signaling pathway protects against spontaneous apoptosis and confers resistance to cisplatin-induced apoptosis in human ovarian cancer cells. The present study determines whether basal PKG kinase activity regulates Src family kinase (SFK) activity and proliferation in these cells. PKG-Iα was identified as predominant isoform in both OV2008 (cisplatin-sensitive, wild-type p53) and A2780cp (cisplatin-resistant, mutated p53) ovarian cancer cells. In both cell lines, ODQ (inhibitor of endogenous NO-induced cGMP biosynthesis), DT-2 (highly specific inhibitor of PKG-Iα kinase activity), and PKG-Iα knockdown (using small interfering RNA) caused concentration-dependent inhibition of DNA synthesis (assessed by bromodeoxyuridine incorporation), indicating an important role of basal cGMP/PKG-Iα kinase activity in promoting cell proliferation. DNA synthesis in OV2008 cells was dependent on SFK activity, determined using highly selective SFK inhibitor, 4-(4′-phenoxyanilino)-6,7-dimethoxyquinazoline (SKI-1). Studies using DT-2 and PKG-Iα small interfering RNA revealed that SFK activity was dependent on PKG-Iα kinase activity. Furthermore, SFK activity contributed to endogenous tyrosine phosphorylation of PKG-Iα in OV2008 and A2780cp cells. *In vitro* coincubation of recombinant human c-Src and PKG-Iα resulted in c-Src–mediated tyrosine phosphorylation of PKG-Iα and enhanced c-Src autophosphorylation/activation, suggesting that human c-Src directly tyrosine phosphorylates PKG-Iα and the c-Src/PKG-Iα interaction enhances Src kinase activity. Epidermal growth factor–induced stimulation of SFK activity in OV2008 cells increased PKG-Iα kinase activity (indicated by Ser^{239} phosphorylation of the PKG substrate vasodilator-stimulated phosphoprotein), which was blocked by both SKI-1 and SU6656. The data suggest an important role of Src/PKG-Iα interaction in promoting DNA synthesis/cell proliferation in human ovarian cancer cells. The NO/cGMP/PKG-Iα signaling pathway may provide a novel therapeutic target for disrupting ovarian cancer cell proliferation. *Mol Cancer Res; 8(4); 578–91. ©2010 AACR.*

Introduction

Cyclic GMP (cGMP)–dependent protein kinase [protein kinase G (PKG)], a widely expressed serine/threonine kinase in mammalian cells, is recognized as the key downstream protein kinase mediating many of the biological effects of nitric oxide (NO) and natriuretic peptides in the cardiovascular system (1-4). Early studies using isolated arteries had shown that endogenous kinase activity of PKG in vascular smooth muscle cells was significantly stimulated by basal endogenously generated NO, synthesized by nearby endothelial cells, as well as by exogenous NO generated by certain cardiovascular therapeutic agents, such as sodium nitroprusside (5). Furthermore, PKG activity in vascular smooth muscle cells was found to be stimulated by atrial natriuretic peptide (also called atriopeptin), a heart-derived hormone important for regulating blood pressure and kidney function (6).

More recent studies from our laboratory have shown the cGMP/PKG signaling pathway plays another important biological role as an antiapoptotic mechanism that promotes cell survival in many types of mammalian cells, including hippocampal neurons (7), PC12 pheochromocytoma cells (8), neuroblastoma and neuroblastoma-glioma hybrid cells (9-11), immortalized uterine epithelial cells (12), and

Authors' Affiliations: [1]Cancer Molecular Biology Section, Nevada Cancer Institute; [2]Department of Chemistry, University of Nevada, Las Vegas, Nevada; [3]Department of Physiology (Faculty of Medicine), Centre for Gerontology and Geriatrics, and Epithelial Cell Biology Research Centre, The Chinese University of Hong Kong, Shatin, New Territories, Hong Kong; [4]Reproductive Biology Unit and Division of Gynecological Oncology, Department of Obstetrics and Gynecology and Molecular Medicine, University of Ottawa; [5]Chronic Disease Program, Ottawa Hospital Research Institute, Ottawa, Ontario, Canada; [6]WCU Biomodulation Major, Department of Agricultural Biotechnology, Seoul National University, Seoul, Korea; and [7]College of Pharmacy, University of Southern Nevada, Henderson, Nevada

Note: E.L. Leung and J.C. Wong contributed equally to this work.

Corresponding Author: Ronald R. Fiscus, University of Southern Nevada, 11 Sunset Way, Henderson, NV 89014. Phone: 702-968-5570; Fax: 702-968-5573. E-mail: rfiscus@usn.edu

doi: 10.1158/1541-7786.MCR-09-0178

ovarian cancer cells (13, 14). We identified PKG-Iα as the predominant PKG isoform expressed in the neuroblastoma and neuroblastoma-glioma hybrid cells, suggesting that PKG-Iα represents the key isoform of PKG mediating the cGMP-stimulated antiapoptotic effects in these cells (10-12).

In human ovarian cancer cells, we have found that the basal activity of the cGMP/PKG pathway is essential for preventing spontaneous apoptosis (13) and that endogenously produced NO, generated by two NO synthases (NOS), endothelial NOS (also called NOS-3) and neuronal NOS (also called NOS-1), contribute significantly to the cisplatin resistance phenotype in chemoresistant ovarian cancer cells (14). Interestingly, the chemoresistant ovarian cancer cells could be dramatically sensitized to cisplatin by inhibiting endogenous NO synthesis. These data suggest that the NO/cGMP/PKG signaling pathway plays a key role in protecting human ovarian cancer cells against both spontaneous and cisplatin-induced apoptosis. However, it was not clear whether the NO/cGMP/PKG pathway also regulates other biological functions, such as cell proliferation, in human ovarian cancer cells.

In vascular smooth muscle cells, our laboratory has shown that basal kinase activity of PKG (likely involving selectively the PKG-Iα isoform) plays a critically important role in promoting the DNA synthesis and cell proliferation that occurs under typical culturing conditions (i.e., cells stimulated by the mitogenic effects of fetal serum growth factors; ref. 15). This growth-promoting effect of PKG is in stark contrast to the previously proposed antiproliferative effect of PKG, which was based on earlier studies that had shown a growth-inhibitory role of PKG in various types of cells, including vascular smooth muscle cells (16), cardiac fibroblasts (17), T-cell lymphocytes (18), and colon cancer cells (19). However, in all of these cells, the growth-inhibitory responses were initiated by either overexpression of PKG (especially the PKG-Iβ isoform) or the elevation of PKG activity (not by basal PKG activity) and seemed, in all cases, to involve the PKG-Iβ isoform. Thus, there is growing evidence that the different isoforms of PKG may be regulating cell proliferation in very different ways, with PKG-Iα kinase activity (especially at basal levels) promoting cell proliferation, whereas PKG-Iβ kinase activity (when hyperactivated or when PKG-Iβ is overexpressed) inhibiting cell proliferation (15). The present study determines if and how the basal kinase activity of PKG (specifically PKG-Iα) regulates DNA synthesis/cell proliferation in human ovarian cancer cells.

Src (or c-Src) and other members of the Src family kinases (SFK) of nonreceptor tyrosine kinases are thought to play an important role in growth factor–induced DNA synthesis and cell proliferation in both normal and transformed mammalian cells, including the mitogenic responses stimulated by epidermal growth factor (EGF; refs. 20-22). Src is overexpressed and/or aberrantly activated in a variety of cancer cells, including human ovarian cancer cells (22). Src overexpression is especially noticeable in late-stage human ovarian cancer, suggesting that Src kinase activity may contribute to ovarian cancer progression (23). In lung cancer cells, Src, via its tyrosine kinase activity, is known to catalyze the tyrosine phosphorylation of the EGF receptor (EGFR), thereby enhancing EGFR downstream mitotic signaling, including mitogen-activated protein kinase signaling, resulting in enhanced cell proliferation (21, 24).

In the present study, we have determined if basal PKG kinase activity regulates DNA synthesis in human ovarian cancer cells and if an interaction between PKG and Src plays a role in this response. To assess endogenous PKG activity in the ovarian cancer cells, phosphorylation of vasodilator-stimulated phosphoprotein (VASP) at Ser^{239} was used. VASP, an actin-binding protein involved in focal adhesion, is a PKG downstream substrate that is directly phosphorylated at Ser^{239} by PKG in mammalian cells, providing a useful indicator of endogenous PKG kinase activity (25-27). The present study shows that OV2008 (chemosensitive, with wild-type p53) and A2780cp (chemoresistant, with mutated p53) human ovarian cancer cells express predominantly the PKG-Iα isoform and that PKG-Iα kinase activity contributes significantly to promoting DNA synthesis in both cell lines. Our findings also suggest that PKG-Iα interacts with Src (or related SFK) in a way that enhances both SFK activity (assessed by autophosphorylation) and PKG-Iα kinase activity (assessed by VASP phosphorylation at Ser^{239}) and that both contribute to enhanced DNA synthesis in ovarian cancer cells. We also found that EGF-induced stimulation of SFK activity and DNA synthesis is dependent on PKG-Iα kinase activity in these cells. Thus, the data suggest that PKG-Iα plays an important role in promoting SFK activity and DNA synthesis in human ovarian cancer cells.

Materials and Methods

Culture of Ovarian Cancer Cells

Two established human epithelial ovarian cancer cell lines, OV2008 and A2780cp, were used in this study (provided by the laboratory of Dr. Benjamin Tsang). OV2008 cells are cisplatin sensitive and A2780cp cells are cisplatin resistant (13, 14, 28). Both cell lines were derived from ovarian cystoadenocarcinoma patients without prior chemotherapy; the OV2008 cells have wild-type *TP53*, whereas the A2780cp cells harbor a *TP53* mutation, as determined by direct sequencing (28). The cell lines were cultured at 37°C in an atmosphere of 5% CO_2/95% air. OV2008 cells were maintained in RPMI 1640, whereas A2780cp cells were maintained in DMEM. All media were supplemented with fetal bovine serum (10%), streptomycin (50 μg/mL), penicillin (50 units/mL), and nonessential amino acids (1%; Life Technologies). Cells were plated for 16 to 18 h before experimental treatments at a density of $5 \times 10^4/cm^2$ in six-well plates and kept at <85% confluent at the time of treatment with human recombinant EGF (Invitrogen) and/or the pharmacologic inhibitors.

Pharmacologic Inhibitors and Small Interfering RNA Gene Knockdown

ODQ (1*H*-[1,2,4]oxadiazolo[4,3-*a*]quinoxalin-1-one) and Src kinase inhibitor I (SKI-1; 4-(4′-phenoxyanilino)-6,7-dimethoxyquinazoline) were purchased from

Calbiochem. DT-2 was purchased from Biolog. SU6656 was purchased from Sigma.

For small interfering RNA (siRNA)–mediated silencing of gene expression, cells were transfected with 50 and 100 nmol/L of Stealth RNAi (siRNA, 5′-GAGGAAGACUUUGCCAAGAUUCUCA-3′) for specifically targeting the expression of PKG-Iα (Invitrogen). Transfection of the human ovarian cancer cells was conducted using RNAiMAX (Invitrogen). Nonsilencing siRNA (Invitrogen) was used as the negative control. At 72 h after transfection, the culture medium was changed and fresh medium was supplied. The cells were used in experiments 16 h later.

Determination of Cell Proliferation Rates

DNA synthesis/cell proliferation rates were determined by measuring the rate of bromodeoxyuridine incorporation into DNA over a 3-h incubation using an ELISA kit (Roche). Most experiments were conducted using 10% fetal bovine serum to stimulate basal cell proliferation. For the EGF stimulation experiments, cells were first starved in serum-free medium for 24 h. The extraction and assay procedures were as recommended by the manufacturer.

Determination of Cellular SFK Activity

Relative levels of SFK phosphorylation at the autophosphorylation/activation site (equivalent to Tyr^{416} phosphorylation in v-Src) were determined by ELISA (Roche) and Western blot analysis. In both types of analysis, the antibody that was used recognizes the phosphorylated form of Tyr^{416} of activated v-Src as well as the equivalent autophosphorylation/activation sites in activated c-Src and other activated SFKs. The ELISA technique used a cell-based ELISA that directly measures protein phosphorylation in cultured cells. The kits included anti-Src and anti–phospho-Tyr^{416}-Src antibodies for colorimetric quantification, and the amount of phospho-Src protein was normalized against the amount of total Src protein. Western blot analysis of $SrcTyr^{416}$ phosphorylation is described below. In some experiments, human EGF (Invitrogen) at 10 and 50 ng/mL was added to the cells for 30 min to stimulate autophosphorylation of Src/SFKs.

Protein Extraction and Western Blotting Using IR Imaging

Cells were lysed in 85°C hot 1× SDS lysis buffer [50 mmol/L Tris-HCl (pH 6.8), 2% SDS, 10 mmol/L DTT, and 10% glycerol]. The supernatant fractions were collected by centrifugation (15,000 × *g*; 10 min). The total amount of protein in the lysates was calculated from the fluorescence-based protein quantitation kit EZQ (Molecular Probes). The amount of total protein loaded on the gels for PKG-Iα/PKG-Iβ determination was 20 μg for mouse aorta and MSTO-211H mesothelioma cells and 80 μg for ovarian cancer cells. For the determination of other proteins, 50 μg of total protein were used. Proteins were separated on 4% to 12% polyacrylamide NuPage gels (Invitrogen) and then transferred to nitrocellulose membranes. Membranes were blocked (room temperature, 1 h) with blocking buffer (Rockland Immunochemicals) and then incubated at 4°C overnight with primary anti-bodies [PKG-Iα/β (1:1,000), phospho-Tyr^{416}-Src (1:1,000), total Src (1:2,000), anti-tyrosine phosphorylation antibody (PY20; 1:1,000), phospho-Tyr^{845}-EGFR (1:1,000), total EGFR (1:1,000), phospho-Ser^{239}-VASP (1:500), total VASP (1:1,000; all from Cell Signaling Technology), and glyceraldehyde-3-phosphate dehydrogenase (1:2,500; Santa Cruz Biotechnology)] and subsequently with secondary antibodies labeled with IR dyes (1:25,000 in blocking buffer; room temperature for 1 h; LI-COR Biosciences). The membranes were scanned on the Odyssey IR imaging system (LI-COR Biosciences).

Immunoprecipitation of PKG in Ovarian Cancer Cells

Cells were lysed in 0.5 mL ice-cold radioimmunoprecipitation assay buffer [with freshly added protease and phosphatase inhibitors, phenylmethylsulfonyl fluoride (1 mmol/L), aprotonin (10 g/L), and Na_3VO_4 (1 mmol/L)] for 10 min on ice followed by centrifugation at 10,000 × *g* for 10 min. Supernatant fractions were transferred to new tubes. Primary anti–PKG-Iα/β antibody (1:100; Cell Signaling Technology) was added to the cell lysates with gentle shaking overnight at 4°C. Protein G–Sepharose (40 μL; Invitrogen) was then added and suspensions were incubated overnight at 4°C. Immunoprecipitates were collected by centrifugation at ~1,000 × *g* for 5 min, and pellets were washed thrice with 0.5 mL radioimmunoprecipitation assay buffer. Pellets were resuspended in 1× SDS buffer and analyzed by Western blot using anti-tyrosine phosphorylation antibody (PY20) and anti–PKG-Iα/β antibody (Cell Signaling Technology).

***In vitro* Phosphorylation Reaction of Recombinant Human PKG-Iα and Recombinant Human c-Src**

Interactions between recombinant human PKG-Iα and recombinant human c-Src (both from Calbiochem) were determined using *in vitro* experiments. The recombinant PKG-Iα (75 ng) was incubated with the recombinant c-Src (10 ng) in a kinase reaction buffer containing Tris buffer (50 mmol/L), $MgCl_2$ (0.1 mol/L), bovine serum albumin (10 mg/mL), and ATP (1 mmol/L) at 30°C for 10 min. The recombinant PKG-Iα alone group and the recombinant c-Src alone group were done in the same way. To show dephosphorylation of PKG-Iα, protein tyrosine phosphatases (Millipore) were also included as a group. The samples were analyzed by Western blot analysis using the anti-tyrosine phosphorylation (PY20) antibody (Cell Signaling Technology). A similar *in vitro* procedure was used for determining if the autophosphorylation/activation of recombinant human c-Src is affected by coincubation with recombinant human PKG-Iα. The samples were analyzed by Western blot using anti–phospho-Tyr^{416}-Src antibody and anti–total Src antibody (Cell Signaling Technology).

Statistical Analysis

Results are expressed as the mean ± SE of at least four independent experiments. Statistical analysis was done by one- or two-way ANOVA using GraphPad (Prism Software). Bartlett's tests were used to establish the homogeneity of variance on the basis of the differences among SDs. Differences between experimental groups were determined by the

Bonferroni multiple comparison test. A value of $P < 0.05$ was considered to be significant.

Results

Inhibition of cGMP Biosynthesis Using ODQ Decreases Both DNA Synthesis and Endogenous Kinase Activity of PKG (Phosphorylation of VASP at Ser^{239}) in Both Chemosensitive (OV2008) and Chemoresistant (A2780cp) Human Ovarian Cancer Cells

Previous studies from our laboratory have shown that ODQ, an agent that selectively inhibits endogenous NO-induced activation of soluble guanylyl cyclase (sGC), significantly reduces the basal cGMP levels in human ovarian cancer cells to approximately two third, one third, and one forth of control levels when ODQ is used at 10, 50, and 100 μmol/L, respectively, and this results in concentration-dependent increases in both p53 protein levels and apoptosis (13). Coadministration of a cell-permeable analogue of cGMP (8-bromo-cGMP, a direct activator of PKG) prevented the ODQ-induced p53 elevation and apoptosis, suggesting that ODQ-induced elevation of p53 and apoptosis in ovarian cancer cells was a consequence of the decrease in basal PKG kinase activity. These findings highlighted an important biological role of basal PKG kinase activity in preventing apoptosis in ovarian cancer cells.

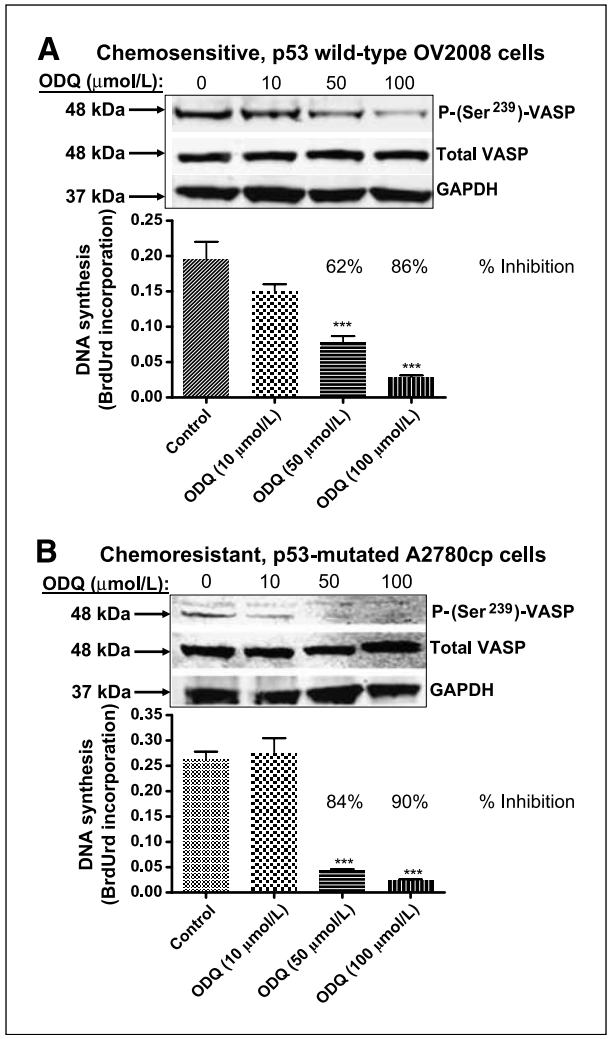

FIGURE 1. ODQ-induced inhibition of endogenous NO-stimulated sGC activity lowers endogenous PKG kinase activity (Ser^{239} phosphorylation of VASP) and DNA synthesis in both OV2008 and A2780cp cells. Both OV2008 cells (A), possessing wild-type p53, and A2780cp cells (B), possessing mutated p53, show dramatic reduction in the DNA synthesis rate and VASP phosphorylation at Ser^{239} (Western blot analysis) following exposure to ODQ, a selective inhibitor of the endogenous NO-stimulated sGC. The Western blots are representative of four experiments. Columns, mean of data from four experiments; bars, SEM. ***, $P < 0.001$, compared with the control. BrdUrd, bromodeoxyuridine.

In Fig. 1 of the present study, we have determined if ODQ-induced inhibition of cGMP biosynthesis affects the endogenous PKG kinase activity (assessed by VASP phosphorylation at Ser^{239}) and the rate of DNA synthesis/cell proliferation in two ovarian cancer cell lines, OV2008 and A2780cp cells. OV2008 cells are sensitive to cisplatin-induced apoptosis and possess wild-type p53, whereas A2780cp cells are resistant to cisplatin-induced apoptosis and possess mutated p53 (13, 14, 28). In Fig. 1A, we show that ODQ caused concentration-dependent reduction in the rate of DNA synthesis in OV2008 cells, with significant decreases noted at 50 and 100 μmol/L ODQ. Western blot analysis showed that VASP phosphorylation at Ser^{239} was also decreased in response to ODQ at 50 and 100 μmol/L, suggesting that there was substantial downregulation of the basal PKG kinase activity caused by treatment with ODQ. This inhibition of basal PKG kinase activity by ODQ corresponded, in a concentration-dependent manner, to the decreases in DNA synthesis. Figure 1B shows that inhibition of cGMP biosynthesis with ODQ resulted in similar responses in the p53-mutated, chemoresistant A2780cp cells, suggesting that the ability of ODQ to inhibit both PKG kinase activity and DNA synthesis in the ovarian cancer cells is independent of p53 mutation.

OV2008 and A2780cp Human Ovarian Cancer Cells Express Predominantly the PKG-Iα Isoform and the Inhibition of the Endogenous PKG-Iα Kinase Activity Decreases DNA Synthesis

Figure 2A shows the results of Western blot analysis determining the expression of the PKG-I isoforms in OV2008 and A2780cp cells. For positive controls, mouse aorta (expressing predominately PKG-Iα) and the MSTO-211H mesothelioma cell line (expressing both PKG-Iα and PKG-Iβ) were included. Recombinant human PKG-Iα and PKG-Iβ were also used as positive controls. The primary antibody recognized the COOH-terminal region of PKG-I, which is common for both of the PKG-I splice variants PKG-Iα and PKG-Iβ. A single band, corresponding to PKG-Iα, was observed for both ovarian cancer cell lines, whereas two bands, corresponding to PKG-Iα and PKG-Iβ, were observed for MSTO-211H cells. To our knowledge,

this represents the first report of PKG expression in these three cancer cell lines.

Figure 2B shows the effects of inhibiting PKG-Iα kinase activity (using DT-2) on the DNA synthesis in OV2008 cells. DT-2 is a peptide inhibitor of PKG-Iα kinase activity that is cell permeable in mammalian cells (because of the inclusion of a membrane translocation sequence), has exceptionally high specificity (1,300-fold specificity for PKG-Iα/β over a closely related protein kinase, protein kinase A), and has high potency (IC_{50} value of 12.5 nmol/L for inhibiting the kinase activity of purified PKG-Iα under *in vitro* conditions; refs. 29-31). However, when used in intact mammalian cells, DT-2 has a considerably higher IC_{50} value of 3.7 μmol/L for inhibiting endogenous (intracellular) PKG kinase activity, with the PKG kinase-inhibitory effects beginning at a threshold concentration of 2 μmol/L and reaching maximal inhibitory effects at 10 μmol/L DT-2 when used in vascular smooth muscle cells (31). In the present study, Fig. 2B shows that DT-2 caused a concentration-dependent inhibition of DNA synthesis and VASP Ser^{239} phosphorylation in OV2008 cells (with inhibitory effects occurring at concentrations of DT-2 similar to those found to be effective in vascular smooth muscle cells). The data suggest a key role of basal PKG-Iα kinase activity in promoting DNA synthesis in the chemosensitive ovarian cancer cell line.

Figure 3 shows that DT-2 also inhibits the DNA synthesis and endogenous VASP Ser^{239} phosphorylation in the chemoresistant, p53-mutated A2780cp cells. The data suggest that the effects of basal PKG-Iα kinase activity on promoting DNA synthesis in human ovarian cancer cells may be independent of p53 mutational status and whether the cells are resistant to cisplatin.

Both Basal and EGF-Induced Stimulation of SFK Activity Are Dependent on PKG-Iα Kinase Activity in OV2008 Cells

Figure 4A shows that inhibition of endogenous basal PKG-Iα kinase activity using DT-2 significantly lowers the SFK activity in OV2008 cells, assessed by the autophosphorylation

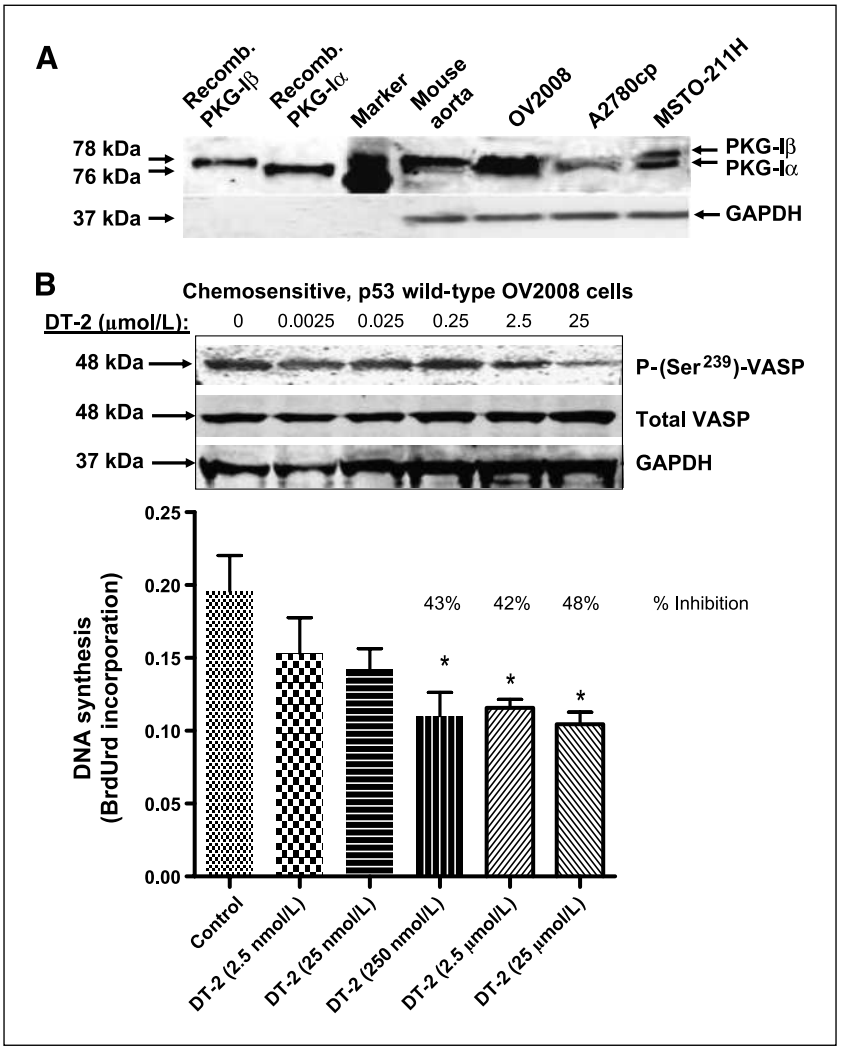

FIGURE 2. Both OV2008 and A2780cp cells express predominantly the PKG-Iα isoform and the inhibition of the PKG-Iα kinase activity reduces VASP Ser^{239} phosphorylation and DNA synthesis rate in OV2008 cells. A, Western blot analysis showing predominant expression of the PKG-Iα isoform in the two human ovarian cancer cell lines (OV2008 and A2780cp cells). The MSTO-211H mesothelioma cells, which express high levels of both PKG-Iα and PKG-Iβ, were used as a positive control. Mouse aorta, which expresses predominantly PKG-Iα, was also used as a positive control. Recombinant PKG-Iα (molecular weight = 76.2 kDa) and PKG-Iβ (molecular weight = 77.8 kDa) were also loaded as positive controls/molecular weight markers. The Western blot conditions were optimized for effectively separating the two isoforms of PKG-I. B, inhibition of basal PKG-Iα kinase activity, using the highly selective inhibitor DT-2, reduced VASP phosphorylation (Western blot) and the DNA synthesis rate (graph) in OV2008 cells. The Western blots in A and B are representative of four experiments. Columns, mean of data from four experiments; bars, SEM. *, $P < 0.05$, compared with the control.

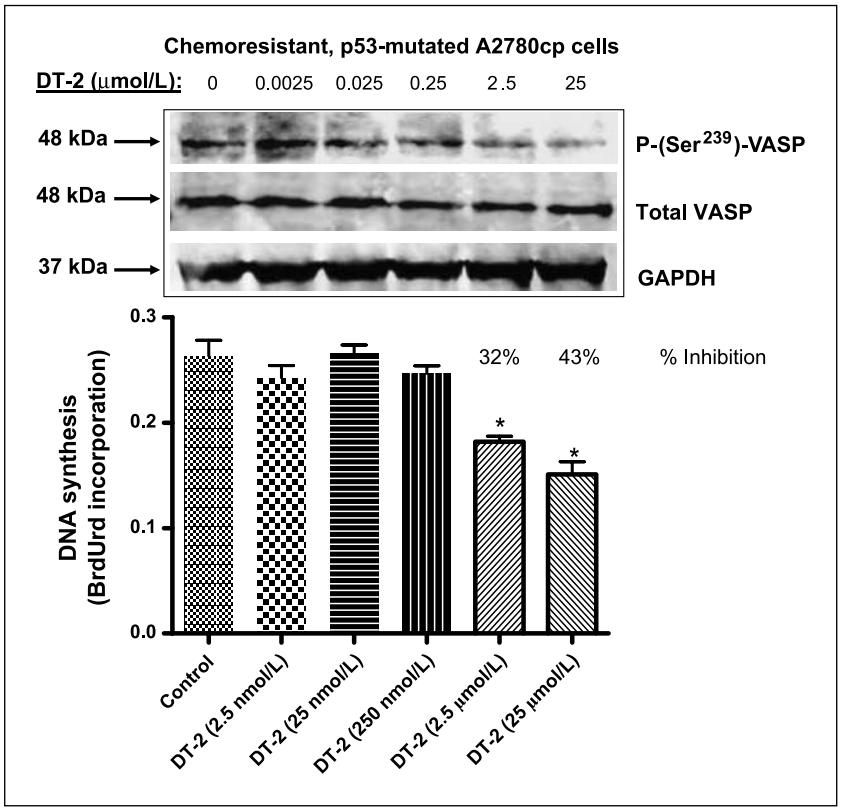

FIGURE 3. Inhibition of basal PKG-Iα kinase activity in A2780cp cells using DT-2 lowers VASP Ser^{239} phosphorylation (indicator of endogenous kinase activity of PKG-Iα) and DNA synthesis. The Western blot is representative of four experiments. Columns, mean of data from four experiments; bars, SEM. *, $P < 0.05$, compared with the control.

of the activation site (the SFK equivalent of Tyr^{416} in v-Src) using both Western blot analysis and ELISA (graph). The data suggest that basal PKG-Iα kinase activity, under normal growing conditions of ovarian cancer cells, promotes SFK activity. Figure 4B further shows that the DT-2–induced inhibition of SFK activity corresponds to the inhibition of basal PKG-Iα kinase activity (assessed by phosphorylation of VASP at Ser^{239}) and that EGF-induced stimulation of SFK activity is also dramatically inhibited by DT-2. Furthermore, EGF-induced stimulation of DNA synthesis in the OV2008 cells was completely inhibited by DT-2. The data suggest that the stimulatory effects of EGF on SFK activity and cell proliferation in ovarian cancer cells are dependent on PKG-Iα kinase activity.

Gene Knockdown of PKG-Iα Expression Using siRNA Decreases Both SFK Activity and DNA Synthesis in Both OV2008 and A2780cp Human Ovarian Cancer Cells

Figure 5 shows the effects of silencing the expression of PKG-Iα by transfecting the cells with PKG-Iα–specific siRNA in OV2008 cells (Fig. 4A) and A2780cp cells (Fig. 4B). Western blot analysis shows that PKG-Iα expression (at the protein level) was partially and almost completely knocked down when using PKG-Iα siRNA constructs at 50 and 100 nmol/L, respectively. The knockdown of PKG-Iα expression corresponded to decreases in both SFK activity (autophosphorylation of SFKs at the equivalent of Tyr^{416}) and DNA synthesis rate in both ovarian cancer cell lines. Thus, these data, using a gene knockdown approach, confirm the data using pharmacologic inhibitors (ODQ and DT-2) shown above, indicating that basal PKG-Iα plays an important role in promoting SFK activity and DNA synthesis in human ovarian cancer cells.

SKI-1 Inhibits Basal and EGF-Stimulated SFK Activity, PKG-Iα Kinase Activity (VASP Ser^{239} Phosphorylation), and DNA Synthesis in OV2008 Human Ovarian Cancer Cells

EGF, via activation of EGFR, is thought to play an important role in stimulating ovarian cancer cell proliferation (32, 33). The activation of EGFR by EGF is known to stimulate the SFK signaling pathway, leading to enhanced cell proliferation in various types of cancer cells (21, 22). To assess the effects of EGF on SFK activity in the ovarian cancer cells of the present study, we determined the time course and concentration-response relationship of EGF-induced stimulation of SFK activity (autophosphorylation of SFKs at the equivalent of Tyr^{416}) in OV2008 cells. Figure 6 shows the results of these experiments, confirming that EGF causes both time-dependent (Fig. 6A) and concentration-dependent (Fig. 6B) stimulation of SFK activity in these cells. Figure 6B also shows that EGF stimulates Ser^{239} phosphorylation of VASP, which indicates that EGF not only stimulates SFK activity but also

enhances the endogenous kinase activity of PKG-Iα in the ovarian cancer cells.

Figure 6C shows the effects of SU6656, a selective SFK inhibitor, on the EGF-induced stimulation of SFK and PKG-Iα activities in OV2008 cells. SU6656, an ATP-competitive inhibitor of SFKs, has been shown to inhibit SFK activity in murine embryonic stem cells when used at 4 and 8 μmol/L (34). In the present study, preincubation with SU6656 at 1 and 5 μmol/L suppressed the stimulatory effects of EGF on SFK activity (autophosphorylation at site equivalent to Tyr^{416}) and Tyr^{845} phosphorylation of EGFR (site phosphorylated by activated Src) in the OV2008 cells. Interestingly, SU6656 also prevented the EGF-induced stimulation of VASP phosphorylation at Ser^{239}, indicating that the stimulation of PKG-Iα activity by EGF in ovarian cancer cells requires the presence of SFK activity.

Figure 7 shows the effects of SKI-1, a recently developed highly selective SFK inhibitor, on basal and EGF-stimulated SFK activities and DNA synthesis in OV2008 human ovarian cancer cells. SKI-1 derives its superior selectivity by being able to block both the ATP-binding site and the peptide/protein substrate–binding site of Src and several closely related SFKs (35). The specificity of SKI-1 as an inhibitor of Src kinase activity in mammalian cells has been validated in experiments using specific Src siRNA gene knockdown (21). Conventional Src/SFK inhibitors, such as dasatinib and PP1, typically block only the ATP-binding site of Src/SFKs and consequently have nonspecific inhibitory effects, resulting in the inhibition of various other protein kinases, such as EGFR, platelet-derived growth factor receptor, Kit, and Abl (35, 36). The IC_{50} value of SKI-1 was reported to be 44 nmol/L under *in vitro* condition using purified Src (35). However, when using SKI-1 to inhibit endogenous Src kinase activity in intact mammalian cells, considerably higher concentrations are needed. For example, the successful inhibition of endogenous (intracellular) Src kinase activity required using SKI-1 in a concentration

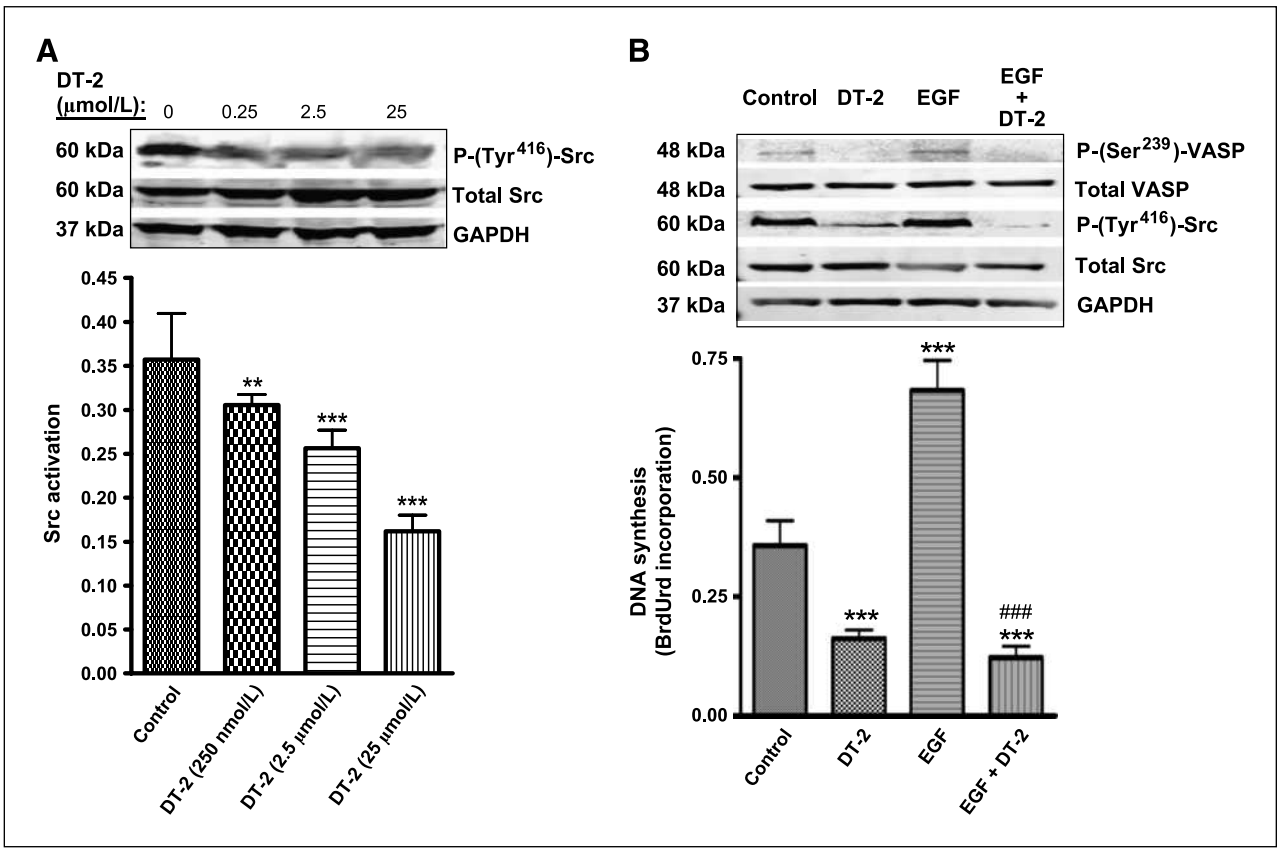

FIGURE 4. Inhibition of endogenous basal PKG-Iα activity using DT-2 in OV2008 ovarian cancer cells reduces the basal level of autophosphorylation of endogenous SFKs and completely inhibits EGF-induced stimulation of SFK autophosphorylation and DNA synthesis. A, the PKG-Iα kinase inhibitor DT-2 dramatically lowered the basal SFK autophosphorylation level, assessed by both Western blot analysis determining autophosphorylation (the equivalent of Tyr^{416}; top image) and ELISA measuring Tyr^{416} autophosphorylation versus total Src (graph). B, EGF (10 ng/mL) elevated VASP Ser^{239} phosphorylation and Src Tyr^{416} phosphorylation in OV2008 cells, assessed by Western blot analysis, and elevated DNA synthesis in OV2008 cells, assessed by bromodeoxyuridine incorporation. Pretreatment with DT-2 (2.5 μmol/L) for 2 h completely inhibited the EGF-stimulated increases in VASP phosphorylation, Src/SFK autophosphorylation, and DNA synthesis. The Western blots shown in A and B are representative of four experiments. Columns, mean of four experiments; bars, SEM. **, $P < 0.01$; ***, $P < 0.001$, compared with the control; ###, $P < 0.001$, compared with EGF alone.

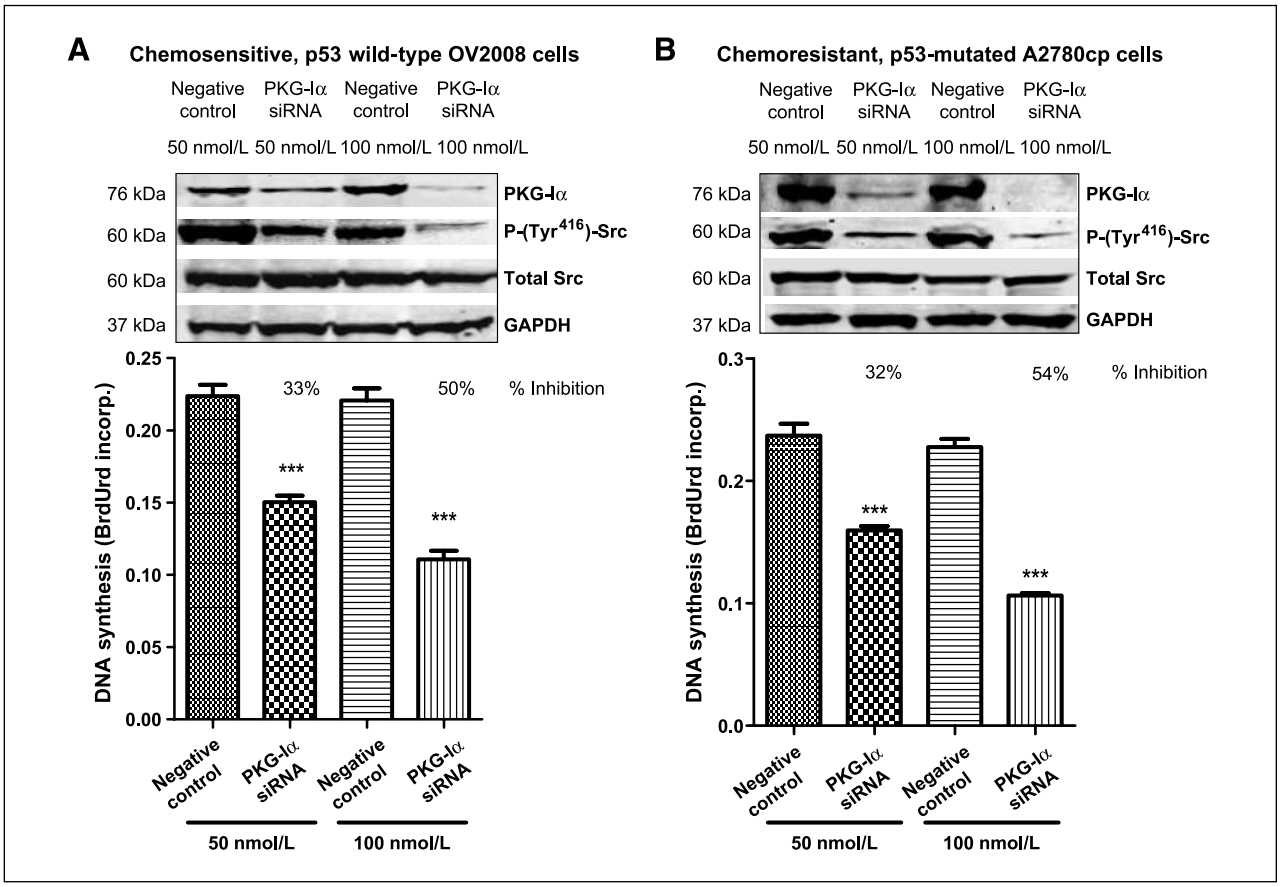

FIGURE 5. Gene knockdown using PKG-Iα–specific siRNA lowers basal Src Tyr^{416} autophosphorylation and DNA synthesis in both OV2008 cells (A) and A2780cp cells (B). The Western blots shown are representative of four experiments. Columns, mean from four experiments; bars, SEM. ***, $P < 0.001$, compared with the negative control.

range of 0.5 to 2.5 μmol/L in lung cancer cells (21) and 5 to 20 μmol/L in murine embryonic stem cells (34).

Figure 7 shows that both basal and EGF-stimulated SFK activity (A and B) and DNA synthesis (C) in OV2008 cells are inhibited by SKI-1 at 0.5 and 1 μmol/L. In addition, Fig. 7A shows that SKI-1 inhibits the phosphorylation of EGFR at Tyr^{845} (site phosphorylated by Src), confirming that SKI-1, at these concentrations, inhibits endogenous Src kinase activity in the ovarian cancer cells. Like SU6656 (shown in Fig. 6C), SKI-1 also inhibited the EGF-stimulated phosphorylation of VASP at Ser^{239}, further indicating that the increased PKG-Iα kinase activity stimulated by EGF (shown in Figs. 4 and 6) is dependent on SFK activity. Interestingly, in the case of the SKI-1–inhibitory experiments, even basal activity of PKG-Iα (i.e. basal phosphorylation of VASP at Ser^{239}) in the OV2008 ovarian cancer cells was highly dependent on SFK activity (Fig. 7A). Thus, Src or a closely related SFK seems to interact with PKG-Iα in both an upstream and downstream role, with SFK activity enhancing the serine/threonine kinase activity of PKG-Iα (Fig. 7) and PKG-Iα kinase activity enhancing the tyrosine kinase activity of Src/SFKs (Figs. 4 and 5).

In vitro and *In vivo* Cross talk of PKG-Iα and Src

A previous study, using *in vitro* phosphorylation experiments, had shown that the viral form of Src (v-Src) is capable of phosphorylating PKG-Iα on a tyrosine residue, which dramatically enhanced both basal activity and cGMP activatibility of PKG-Iα (37). Because of the similarities between v-Src and the cellular form of Src (c-Src) found in mammalian cells, we had hypothesized that c-Src may interact with PKG-Iα in human ovarian cancer cells, resulting in c-Src–catalyzed tyrosine phosphorylation of PKG-Iα. Predictably, this would result in enhanced basal PKG kinase activity as well as enhanced cGMP-stimulated PKG kinase activity (i.e., intracellular cGMP at basal levels would become more effective as an endogenous activator of PKG-Iα).

To test whether human c-Src directly phosphorylates human PKG-Iα on a tyrosine residue *in vitro*, we used recombinant human PKG-Iα and recombinant human c-Src, which were incubated in a kinase reaction buffer containing the necessary ATP and Mg^{2+}. Tyrosine phosphorylation of the proteins was determined by Western blot analysis using the anti-phosphotyrosine antibody PY20, which recognizes general tyrosine phosphorylation.

Figure 8A shows the results of a representative *in vitro* experiment. Lane 4 contains a band at 60 kDa, representing the autophosphorylated form of human c-Src. When both human c-Src and PKG-Iα were present together (lane 1), a second band appeared at a molecular weight of ~76 kDa (corresponding to PKG-Iα), indicating that recombinant human PKG-Iα was phosphorylated on a tyrosine residue by the recombinant human c-Src. Addition of protein tyrosine phosphatases to the reaction mixture reduced the tyrosine phosphorylation of PKG-Iα (lane 2). The data indicate that human c-Src, like v-Src, is capable of directly phosphorylating PKG-Iα on a tyrosine residue.

Figure 8B shows the results of an experiment using intact ovarian cancer cells, both OV2008 and A2780cp cells, determining whether endogenous SFK activity is capable of phosphorylating PKG-Iα on a tyrosine residue. The cells were exposed to SKI-1 to inhibit the endogenous SFK activity, and the levels of tyrosine phosphorylation of immunoprecipitated PKG-Iα were determined by Western blot analysis. The data show that SKI-1 substantially reduced the level of tyrosine phosphorylation of PKG-Iα in both ovarian cancer cell lines, suggesting that endogenous SFK activity contributes to the tyrosine phosphorylation of PKG-Iα in intact ovarian cancer cells.

The data shown in Figs. 2 to 5 above had suggested that Src (or a closely related SFK) may be serving not only as an upstream stimulator of PKG-Iα but also as a downstream target of PKG-Iα, which was indicated by the decrease in SFK activity caused by the pharmacologic inhibition of PKG-Iα activity and by the siRNA gene knockdown of PKG-Iα expression. To test the possibility that PKG-Iα may directly stimulate c-Src kinase activity, we conducted additional *in vitro* experiments using recombinant human c-Src and PKG-Iα. Figure 8C shows the results of these experiments. In this case, the Western blots were probed using an antibody that specifically recognized the tyrosine-phosphorylated form of the autophosphorylation/activation site of Src (and other SFKs; equivalent to Tyr^{416} site of

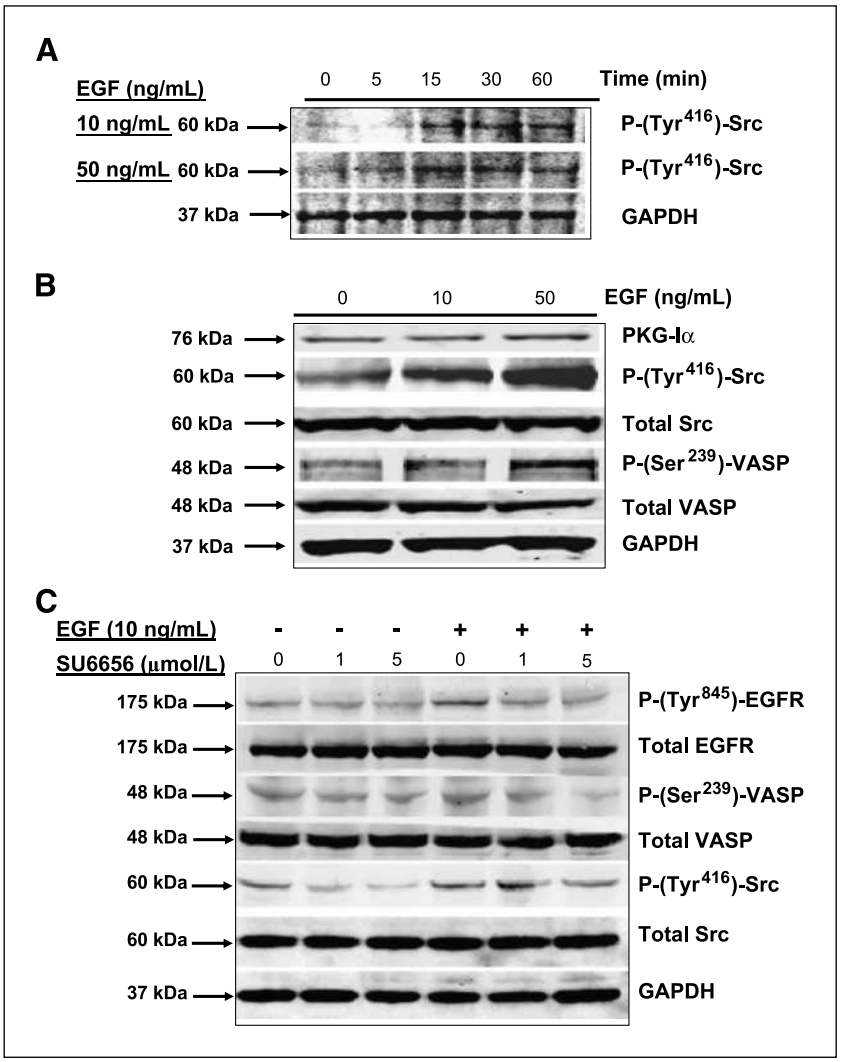

FIGURE 6. EGF stimulates both Src/SFK autophosphorylation and PKG-Iα kinase activity (VASP Ser^{239} phosphorylation) in OV2008 ovarian cancer cells and these responses are inhibited by SU6656, a SFK-selective tyrosine kinase inhibitor. A, Western blot showing that EGF (10 and 50 ng/mL) increases Src/SFK autophosphorylation (equivalent of Tyr^{416}) in OV2008 cells in a time-dependent manner, with the phosphorylation reaching a peak at 15 to 30 min. B, Western blot showing that EGF (10 and 50 ng/mL) increases both Src/SFK activity (autophosphorylation) and PKG-Iα kinase activity (assessed by downstream phosphorylation of the PKG-Iα substrate, VASP at Ser^{239}) in OV2008 cells in a concentration-dependent manner. C, SU6656 (1 and 5 μmol/L) inhibited the EGF-induced stimulation of the EGFR phosphorylation at Tyr^{845} (site phosphorylated by Src), the Ser^{239} phosphorylation of VASP (PKG-Iα substrate), and the autophosphorylation of Src/SFK. The Western blots shown are representative of four experiments.

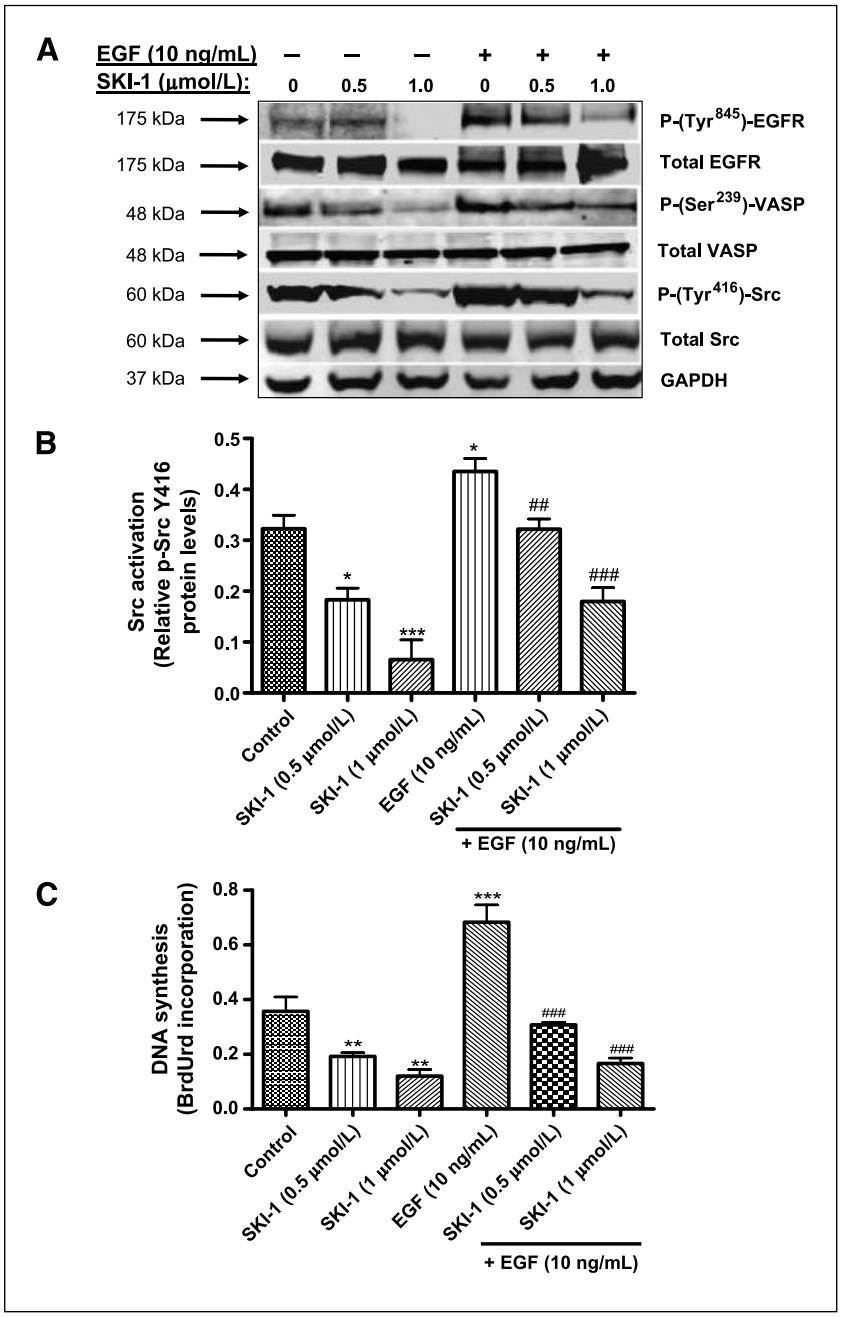

FIGURE 7. Endogenous SFK activity plays an important role in phosphorylating EGFR, enhancing the endogenous serine/threonine kinase activity of PKG-Iα, and promoting DNA synthesis under both basal condition (normal plus serum growing condition) and EGF-stimulated condition in OV2008 cells. A, SKI-1 (0.5 and 1 μmol/L), a potent and highly selective SFK tyrosine kinase inhibitor, reduces both basal and EGF-stimulated phosphorylation of EGFR, Src/SFK autophosphorylation, and VASP phosphorylation at Ser^{239} (Western blot analysis). B, the inhibition of SFK activity by SKI-1 was also determined using an ELISA, measuring autophosphorylation of Src (equivalent of Tyr^{416} phosphorylation) versus total Src. As with the Western blots, SKI-1 (0.5 and 1 μmol/L) dramatically lowered both basal and EGF-stimulated Src autophosphorylation/activation in the OV2008 cells. C, at the same concentrations used in A and B (0.5 and 1 μmol/L), SKI-1 also inhibited both basal (plus serum growing condition) and EGF-stimulated DNA synthesis in OV2008 cells. The Western blots in A are representative of four experiments. B and C, columns, mean of data from four experiments; bars, SEM. *, $P < 0.05$; **, $P < 0.01$; and ***, $P < 0.001$, compared with the control; ##, $P < 0.01$ and ###, $P < 0.001$, compared with EGF alone.

v-Src). Figure 8C shows that the copresence of PKG-Iα does indeed enhance the autophosphorylation of c-Src, confirming that PKG-Iα interacts with c-Src in a way that elevates Src kinase activity. At present, it is unclear how PKG-Iα is able to enhance the Src kinase activity. However, the experiments shown in Fig. 4, which used DT-2 to inhibit the endogenous kinase activity of PKG-Iα in ovarian cancer cells, suggest that the stimulatory effect of PKG-Iα on Src/SFK activity may involve the serine/threonine kinase activity of PKG-Iα and potentially the phosphorylation of a serine or threonine residue in Src/SFK, which could potentially enhance Src/SFK autophosphorylation and activation. Further experiments, beyond the scope of the present study, will be needed to confirm this idea.

Figure 8D shows a model, based on the data of the present study, illustrating the proposed role of the NO/cGMP/PKG-Iα signaling pathway and its interaction with Src in promoting DNA synthesis and cell proliferation in ovarian cancer cells. Previous studies from our lab have shown that both endothelial NOS and neuronal NOS are expressed in

ovarian cancer cells and, via their ability to generate endogenous NO, play an important role in contributing to chemoresistance (14). Furthermore, our previous studies have shown that endogenous NO, via its ability to bind and activate the heme moiety of sGC, enhances the generation of cGMP in ovarian cancer cells, which in turn protects these cells against the development of spontaneous apoptosis (13). The present study, using both pharmacologic inhibitors (ODQ, DT-2, and SKI-1) and gene knockdown technique (siRNA), shows that PKG-Iα kinase activity and the interactions between PKG-Iα and Src play a key role in promoting DNA synthesis in ovarian cancer cells.

Discussion

The present study showed that basal PKG-Iα kinase activity plays an important role in enhancing the DNA synthesis rate in two human ovarian cancer cell lines: OV2008 cells (wild-type p53 and cisplatin sensitive) and A2780cp cells (mutated p53 and cisplatin resistant). Thus, the ability of PKG-Iα to promote cell proliferation in human ovarian cancer cells seems to be independent of the p53 mutation status and whether the cancer cells are sensitive to cisplatin. Inhibition of either the basal PKG-Iα serine/threonine kinase activity or the basal Src/SFK

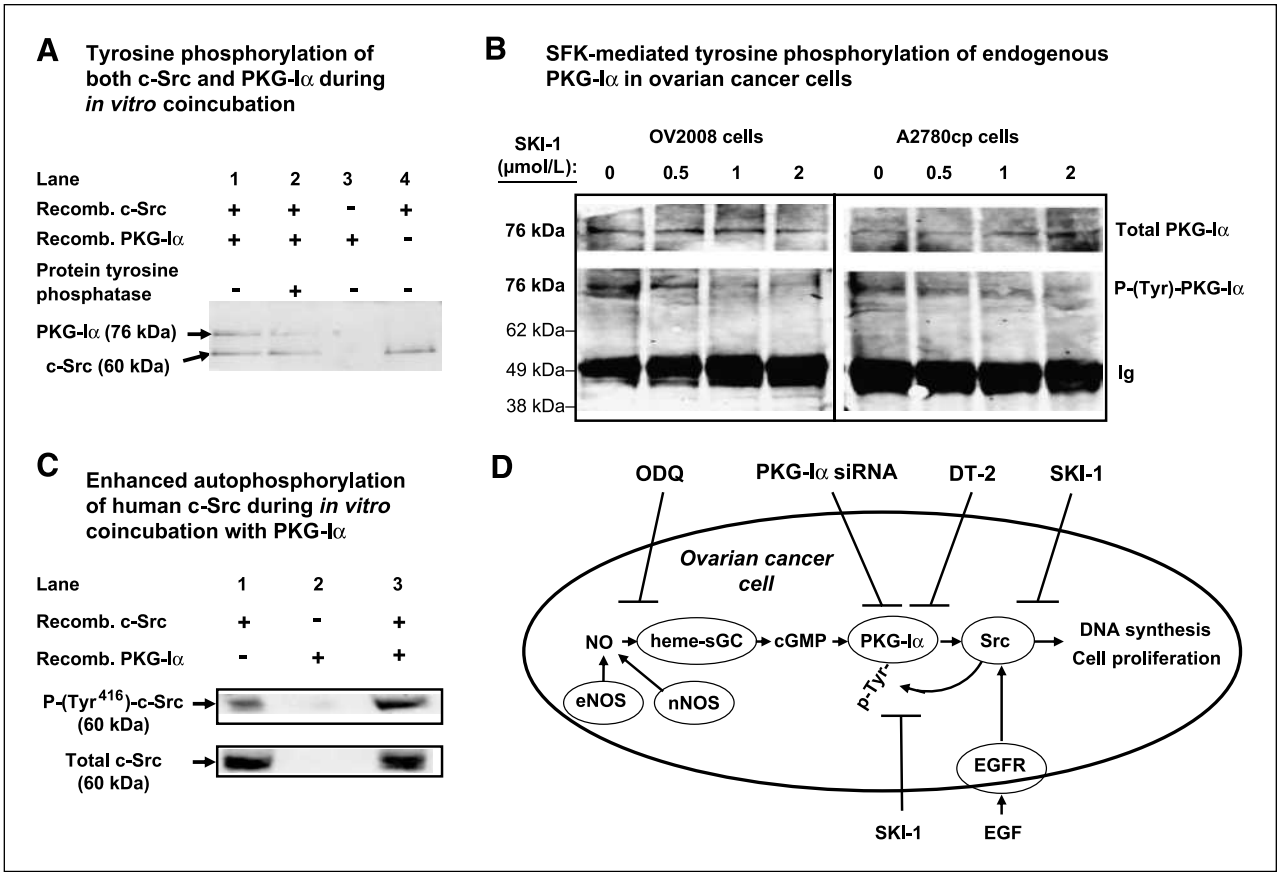

FIGURE 8. In both *in vitro* and *in vivo* (intact cell) experiments, Src seems to directly tyrosine phosphorylate PKG-Iα and the interaction of PKG-Iα with Src enhances the activation of Src. A, Western blot showing general tyrosine phosphorylation of human recombinant c-Src and PKG-Iα following coincubation in an *in vitro* experiment. The PY20 antibody, which recognizes phosphorylation on all phosphorylated tyrosine residues, was used. The coincubation of c-Src and PKG-Iα caused tyrosine phosphorylation of PKG-Iα. B, experiments using intact OV2008 cells with immunoprecipitation of PKG-Iα show that the endogenous tyrosine phosphorylation of PKG-Iα in these cancer cells is dependent on endogenous Src kinase/SFK activity. SKI-1 at 0.5, 1, and 2 μmol/L dramatically reduced that level of tyrosine phosphorylation of the immunoprecipitated PKG-Iα, assessed by Western blot analysis. C, Western blot showing the effect of recombinant human PKG-Iα on the autophosphorylation of recombinant human c-Src using an antibody that specifically recognizes the autophosphorylation site of Src. The presence of PKG-Iα increased the level of autophosphorylation of Src, indicating that PKG-Iα and Src interact in a way that enhances Src kinase activity. The Western blots in A, B, and C are representative of four experiments, all showing similar results. D, model showing the role of the NO/sGC/cGMP/PKG-Iα signaling pathway in promoting Src kinase activity and DNA synthesis/cell proliferation in ovarian cancer cells. ODQ inhibits the heme moiety of sGC (heme-sGC), which blocks the ability of endogenous NO to activate sGC and stimulate cGMP synthesis. The data of the present study, using pharmacologic inhibitors (ODQ, DT-2, and SKI-1) and PKG-Iα siRNA gene knockdown, show that this signaling pathway plays an important role in enhancing Src kinase activation and promoting DNA synthesis in human ovarian cancer cells. eNOS, endothelial NOS; nNOS, neuronal NOS.

tyrosine kinase activity decreases DNA synthesis in these cells. Both *in vitro* and *in vivo* experiments suggest that PKG-Iα and Src interact in a way that results in the enhancement of both PKG-Iα serine/threonine kinase activity and Src tyrosine kinase activity, both of which seem to be important for the enhanced DNA synthesis in human ovarian cancer cells.

Several previous studies have suggested that PKG can participate in either the inhibition of cell proliferation or the stimulation of cell proliferation, apparently depending on the types of cells studied and/or the conditions of the experimental procedures. For example, stimulation of endogenous PKG kinase activity in vascular smooth muscle cells (16), cardiac fibroblasts (17), T-cell lymphocytes (18), and human colon cancer cells (19) all resulted in a decrease in cell proliferation rate. In contrast, stimulation of endogenous PKG kinase activity in human umbilical vein endothelial cells (HUVEC) resulted in enhanced rate of cell proliferation (38). In the HUVECs, vascular endothelial growth factor, a proangiogenic factor important in tumor angiogenesis, was shown to stimulate the proliferation of these cells via a cellular mechanism involving vascular endothelial growth factor–induced/Akt-mediated phosphorylation (and stimulation) of endothelial NOS, enhanced production of endogenous NO, elevation of cGMP levels, and stimulation of PKG kinase activity (38).

The reason for the opposite effects of PKG on cell proliferation in the different cell types/experimental conditions is currently unclear. However, it is important to note that the previous reports showing PKG-mediated inhibition of cell proliferation in vascular smooth muscle cells, cardiac fibroblasts, T-cell lymphocytes, and human colon cancer cells were all linked to activation of the PKG-Iβ isoform of PKG (16-19), suggesting that the antiproliferative effects of PKG activation may be mediated selectively by the PKG-Iβ isoform. Although the PKG isoform mediating the growth-promoting effects in HUVECs was not identified in the previous report (38), recent studies in our laboratory have shown that PKG-Iα is the predominant isoform expressed in HUVECs and that PKG-Iα participates in promoting HUVEC cell proliferation.[8] Likewise, we have recently shown that the basal kinase activity of endogenous PKG-Iα in vascular smooth muscle cells is critically important for promoting the cell proliferation of these cells when grown in culture (15). Thus, the different effects of PKG on cell proliferation may depend on which isoform of PKG-I is expressed and activated [i.e., PKG-Iα (at basal activity) mediating increased cell proliferation, whereas PKG-Iβ (when highly activated or overexpressed) mediating decreased cell proliferation]. The data of the present study are consistent with this concept, showing that human ovarian cancer cells, which express predominantly the PKG-Iα isoform, exhibit enhanced cell proliferation promoted by the basal kinase activity of PKG-Iα. To our knowledge, this is the first report of the involvement of endogenous PKG in the regulation of cell proliferation in human ovarian cancer cells.

Previous data from our laboratory had shown that basal activity of the NO/sGC/cGMP/PKG signaling pathway in chemosensitive human ovarian cancer cells results in a continuous suppression of p53 accumulation and protection against spontaneous onset of apoptosis (13). Because p53, in addition to regulating apoptosis, is also involved in regulating cell cycle progression (39), the present study determined if basal activity of the PKG pathway may also provide a continuous control over the proliferation rate of human ovarian cancer cells in a way that may be dependent on the mutational status of p53. Using two human ovarian cancer cell lines with different p53 status, we show in the present study that blocking the endogenous NO-induced activation of sGC (using ODQ) or the inhibition of endogenous PKG-Iα kinase activity (using DT-2–selective or PKG-Iα–selective siRNA) significantly reduces the rate of DNA synthesis in both OV2008 cells (with wild-type p53) and A2780cp cells (with mutated p53). Although the level of inhibition of DNA synthesis by DT-2 seemed to be somewhat smaller in the A2780 cells compared with the OV2008 cells (Figs. 2 and 3), the data obtained with PKG-Iα siRNA gene knockdown (Fig. 5) show that PKG-Iα contributes similarly to promoting cell proliferation in both cell lines. Thus, the data suggest that PKG-Iα kinase activity in human ovarian cancer cells plays an important role in promoting cell proliferation and that the mechanism seems to be independent of the p53 mutational status.

The present study also shows that both OV2008 and A2780cp ovarian cancer cells express PKG, predominately the PKG-Iα isoform. This observation is in contrast to a previous report showing that, although PKG was highly expressed in normal surface epithelial cells of the ovary, the expression of PKG seemed to be "absent" in various ovarian cancer cells (40). The difference may be related to the use of different ovarian cancer cell lines in the two studies or to differences in sensitivity for detecting PKG expression. Nevertheless, the present study shows that at least two human ovarian cancer cell lines do indeed express PKG-Iα and that the expression levels are sufficient to play an important role in promoting SFK activity and cell proliferation.

Src is overexpressed and/or aberrantly activated in late-stage human ovarian cancer cells (23). Via its tyrosine kinase activity, which phosphorylates EGFR and other growth-promoting proteins on tyrosine residues, and via its ability to inhibit the actions of the tumor suppressor p53, Src is known to promote cell proliferation in a variety of cells (20, 22). The present study shows that there is another potential site of action of Src within mammalian cells (i.e., Src-mediated tyrosine phosphorylation of PKG-Iα), which may result in enhanced serine/threonine kinase activity of PKG-Iα (indicated in the present study by the enhanced Ser^{239} phosphorylation of VASP). Previously, the

[8] R.R. Fiscus, unpublished observations.

viral homologue of c-Src, v-Src, was shown to be capable of phosphorylating PKG-Iα on a tyrosine residue during *in vitro* coincubation (37). The tyrosine phosphorylation of PKG-Iα leads to elevated basal activity as well as substantial enhancement in the ability of cGMP to stimulate PKG-Iα kinase activity, shifting the K_{act} for cGMP from 109 nmol/L (in PKG-Iα without tyrosine phosphorylation) to 39 nmol/L (in PKG-Iα with tyrosine phosphorylation). However, to our knowledge, the phosphorylating effect of a mammalian form of Src (mammalian c-Src) on PKG-Iα has not been reported previously. We predicted, based on the similarity between v-Src and c-Src, that endogenous c-Src in human ovarian cancer cells may phosphorylate endogenous PKG-Iα, greatly enhancing its ability to be stimulated by the basal cGMP levels within these cells. Because ovarian cancer cells often overexpress Src or posses a higher level of Src kinase activity, it is further hypothesized that PKG-Iα would be activated to a relatively high level (i.e., hyperactivated) in these cancer cells and this may contribute to enhanced proliferation rate.

The present study, using both *in vitro* and *in vivo* (intact cell) experiments, suggest that the human form of c-Src is indeed capable of tyrosine phosphorylating PKG-Iα (illustrated in Fig. 8). Using the highly selective Src/SFK tyrosine kinase inhibitor SKI-1, we showed that both OV2008 and A2780cp ovarian cancer cells have tyrosine phosphorylation of the endogenous PKG-Iα under normal culturing conditions that is dependent on endogenous Src/SFK tyrosine kinase activity (Fig. 8B). Thus, the data of the present study suggest that the overexpressed/hyperactivated Src within ovarian cancer cells may be continually phosphorylating PKG-Iα on a tyrosine residue (likely the same tyrosine residue phosphorylated by v-Src used in the previous *in vitro* study; ref. 37), resulting in high-level activation of PKG-Iα in ovarian cancer cells. The data presented in Figs. 1 to 3 of the present study further suggest that the endogenous PKG-Iα kinase activity (indicated by VASP Ser^{239} phosphorylation) is at a high basal level in both OV2008 and A2780cp cells, which is consistent with the idea that PKG-Iα kinase activity is continually enhanced by the high-level Src tyrosine kinase activity within these cells.

The mitogenic effect of EGF observed in the present study is relatively small, likely because basal SFK activity and EGFR kinase activity are already partially activated in the absence of exogenous EGF. This is suggested by the data in Figs. 6 and 7, which show that inhibition of SFK activity with SU6656 or SKI-1 causes substantial lowering of both SFK autophosphorylation and EGFR phosphorylation at Tyr^{845}. Elevations of basal EGFR/Src kinase activity are frequently reported in cancer cells due to the overexpression of ligand and/or mutation(s) of EGFR (41). We do not rule out the possibilities that the ovarian cancer cells of the present study may harbor such kinds of abnormalities.

To our knowledge, the present study represents the first report showing direct cross talk between PKG and c-Src/SFKs in intact mammalian cells resulting in the regulation of cell proliferation. Two previous reports, showing that c-Src is involved in the antiapoptotic effects of NO in RINm5F insulin-producing cells, have proposed that Src and PKG may interact to mediate the NO-induced antiapoptotic effects; however, a direct interaction between PKG and c-Src was not established (42, 43). The data of the present study suggest that Src and possibly other SFKs serve both upstream and downstream of PKG-Iα in human ovarian cancer cells and that these interactions promote DNA synthesis. Src is a close associator with EGFR, and they mutually activate each other at Tyr^{845} of EGFR and Tyr^{416} of Src. PKG-Iα may exert its mitogenic effect in ovarian cancer cells via the enhanced activation of the EGFR/Src signaling pathway, which includes downstream effectors such as Akt, signal transducer and activator of transcription 3/5, and mitogen-activated protein kinase (24), as well as other promitogenic mechanism mediated by activated Src.

In conclusion, the present study provides the first report showing the direct cross talk between PKG-Iα and Src in human ovarian cancer cells. Both basal PKG-Iα serine/threonine kinase activity and Src/SFK tyrosine kinase activity were found to be important for promoting DNA synthesis in human ovarian cancer cells. Furthermore, EGF stimulation of SFK activity and the resulting enhanced DNA synthesis seemed to be dependent on PKG-Iα kinase activity. Overall, the present data suggest the presence of a novel signaling cross talk between Src and the NO/cGMP/PKG-Iα signaling pathway that is important for promoting DNA synthesis and cell proliferation in human ovarian cancer cells. Therapeutic agents that target the NO/cGMP/PKG-Iα signaling pathway or the novel Src/PKG-Iα cross talk may represent a new approach for effectively controlling the proliferation of human ovarian cancer cells in the treatment of ovarian cancer.

Disclosure of Potential Conflicts of Interest

No potential conflicts of interest were disclosed.

Grant Support

All experiments involving Western blot analysis and siRNA gene knockdown using ovarian cancer cells as well as some of the experiments measuring DNA synthesis in cancer cells were conducted in the Cancer Molecular Biology Section of the Nevada Cancer Institute and were funded by U.S. Department of Defense grant W81XWH-07-1-0543 (R.R. Fiscus) and Nevada Cancer Institute startup funding (R.R. Fiscus). Other parts of the study, conducted at the Chinese University of Hong Kong (CUHK), were supported by Research Grants Council of Hong Kong grant CUHK4169/02M (R.R. Fiscus), Direct Grant for Research from the Medicine Panel of CUHK (R.R. Fiscus), Operating Grant from the Canadian Institutes of Health Research grant MOP-15691 (B.K. Tsang), the World Class University (WCU) Program (R31-10056) through the National Research Foundation of Korea, funded by the Ministry of Education, Science and Technology, Korea (B.K. Tsang), and funding for graduate student projects from the Department of Physiology, Faculty of Medicine, CUHK (E.L. Leung).

The costs of publication of this article were defrayed in part by the payment of page charges. This article must therefore be hereby marked *advertisement* in accordance with 18 U.S.C. Section 1734 solely to indicate this fact.

Received 05/01/2009; revised 02/19/2010; accepted 02/22/2010; published OnlineFirst 04/06/2010.

References

1. Fiscus RR. Molecular mechanisms of endothelium-mediated vasodilation. Semin Thromb Hemost 1988;14 Suppl:12–22.
2. Fiscus RR, Murad F. cGMP-dependent protein kinase activation in intact tissues. Methods Enzymol 1988;159:150–9.
3. Hofmann F, Feil R, Kleppisch T, Schlossmann J. Function of cGMP-dependent protein kinases as revealed by gene deletion. Physiol Rev 2006;86:1–23.
4. Lincoln TM, Wu X, Sellak H, Dey N, Choi CS. Regulation of vascular smooth muscle cell phenotype by cyclic GMP and cyclic GMP-dependent protein kinase. Front Biosci 2006;11:356–67.
5. Fiscus RR, Rapoport RM, Murad F. Endothelium-dependent and nitrovasodilator-induced activation of cyclic GMP-dependent protein kinase in rat aorta. J Cyclic Nucleotide Protein Phosphor Res 1983;9:415–25.
6. Fiscus RR, Rapoport RM, Waldman SA, Murad F. Atriopeptin II elevates cyclic GMP, activates cyclic GMP-dependent protein kinase and causes relaxation in rat thoracic aorta. Biochim Biophys Acta 1985;846:179–84.
7. Barger SW, Fiscus RR, Ruth P, Hofmann F, Mattson MP. Role of cyclic GMP in the regulation of neuronal calcium and survival by secreted forms of β-amyloid precursor. J Neurochem 1995;64:2087–96.
8. Fiscus RR, Tu AW, Chew SB. Natriuretic peptides inhibit apoptosis and prolong the survival of serum-deprived PC12 cells. Neuroreport 2001;12:185–9.
9. Cheng Chew SB, Leung PY, Fiscus RR. Preincubation with atrial natriuretic peptide protects NG108-15 cells against the toxic/proapoptotic effects of the nitric oxide donor *S*-nitroso-*N*-acetylpenicillamine. Histochem Cell Biol 2003;120:163–71.
10. Fiscus RR. Involvement of cyclic GMP and protein kinase G in the regulation of apoptosis and survival in neural cells. Neurosignals 2002;11:175–90.
11. Fiscus RR, Yuen JP, Chan SL, Kwong JH, Chew SB. Nitric oxide and cyclic GMP as pro- and anti-apoptotic agents. J Card Surg 2002;17:336–9.
12. Chan SL, Fiscus RR. Guanylyl cyclase inhibitors NS2028 and ODQ and protein kinase G (PKG) inhibitor KT5823 trigger apoptotic DNA fragmentation in immortalized uterine epithelial cells: anti-apoptotic effects of basal cGMP/PKG. Mol Hum Reprod 2003;9:775–83.
13. Fraser M, Chan SL, Chan SS, Fiscus RR, Tsang BK. Regulation of p53 and suppression of apoptosis by the soluble guanylyl cyclase/cGMP pathway in human ovarian cancer cells. Oncogene 2006;25:2203–12.
14. Leung EL, Fraser M, Fiscus RR, Tsang BK. Cisplatin alters nitric oxide synthase levels in human ovarian cancer cells: involvement in p53 regulation and cisplatin resistance. Br J Cancer 2008;98:1803–9.
15. Wong JC, Fiscus RR. Protein kinase G activity prevents pathological-level nitric oxide-induced apoptosis and promotes DNA synthesis/cell proliferation in vascular smooth muscle cells. Cardiovasc Pathol. In press 2010.
16. Chiche JD, Schlutsmeyer SM, Bloch DB, et al. Adenovirus-mediated gene transfer of cGMP-dependent protein kinase increases the sensitivity of cultured vascular smooth muscle cells to the antiproliferative and pro-apoptotic effects of nitric oxide/cGMP. J Biol Chem 1998;273:34263–71.
17. Smolenski A, Schultess J, Danielewski O, et al. Quantitative analysis of the cardiac fibroblast transcriptome—implications for NO/cGMP signaling. Genomics 2004;83:577–87.
18. Fischer TA, Palmetshofer A, Gambaryan S, et al. Activation of cGMP-dependent protein kinase Iβ inhibits interleukin 2 release and proliferation of T cell receptor-stimulated human peripheral T cells. J Biol Chem 2001;276:5967–74.
19. Deguchi A, Thompson WJ, Weinstein IB. Activation of protein kinase G is sufficient to induce apoptosis and inhibit cell migration in colon cancer cells. Cancer Res 2004;64:3966–73.
20. Bromann PA, Korkaya H, Courtneidge SA. The interplay between Src family kinases and receptor tyrosine kinases. Oncogene 2004;23:7957–68.
21. Leung EL, Tam IY, Tin VP, et al. Src promotes survival and invasion of lung cancers with epidermal growth factor receptor abnormalities and is a potential candidate for molecular-targeted therapy. Mol Cancer Res 2009;7:923–32.
22. Summy JM, Gallick GE. Src family kinases in tumor progression and metastasis. Cancer Metastasis Rev 2003;22:337–58.
23. Wiener JR, Windham TC, Estrella VC, et al. Activated SRC protein tyrosine kinase is overexpressed in late-stage human ovarian cancers. Gynecol Oncol 2003;88:73–9.
24. Sordella R, Bell DW, Haber DA, Settleman J. Gefitinib-sensitizing EGFR mutations in lung cancer activate anti-apoptotic pathways. Science 2004;305:1163–7.
25. Butt E, Abel K, Krieger M, et al. cAMP- and cGMP-dependent protein kinase phosphorylation sites of the focal adhesion vasodilator-stimulated phosphoprotein (VASP) *in vitro* and in intact human platelets. J Biol Chem 1994;269:14509–17.
26. Chen H, Levine YC, Golan DE, Michel T, Lin AJ. Atrial natriuretic peptide-initiated cGMP pathways regulate vasodilator-stimulated phosphoprotein phosphorylation and angiogenesis in vascular endothelium. J Biol Chem 2008;283:4439–47.
27. Isenberg JS, Romeo MJ, Yu C, et al. Thrombospondin-1 stimulates platelet aggregation by blocking the antithrombotic activity of nitric oxide/cGMP signaling. Blood 2008;111:613–23.
28. Fraser M, Bai T, Tsang BK. Akt promotes cisplatin resistance in human ovarian cancer cells through inhibition of p53 phosphorylation and nuclear function. Int J Cancer 2008;122:534–46.
29. Dostmann WR, Taylor MS, Nickl CK, Brayden JE, Frank R, Tegge WJ. Highly specific, membrane-permeant peptide blockers of cGMP-dependent protein kinase Iα inhibit NO-induced cerebral dilation. Proc Natl Acad Sci U S A 2000;97:14772–7.
30. Dostmann WR, Tegge W, Frank R, Nickl CK, Taylor MS, Brayden JE. Exploring the mechanisms of vascular smooth muscle tone with highly specific, membrane-permeable inhibitors of cyclic GMP-dependent protein kinase Iα. Pharmacol Ther 2002;93:203–15.
31. Taylor MS, Okwuchukwuasanya C, Nickl CK, Tegge W, Brayden JE, Dostmann WR. Inhibition of cGMP-dependent protein kinase by the cell-permeable peptide DT-2 reveals a novel mechanism of vasoregulation. Mol Pharmacol 2004;65:1111–9.
32. Alper O, De Santis ML, Stromberg K, Hacker NF, Cho-Chung YS, Salomon DS. Anti-sense suppression of epidermal growth factor receptor expression alters cellular proliferation, cell-adhesion and tumorigenicity in ovarian cancer cells. Int J Cancer 2000;88:566–74.
33. Porcile C, Bajetto A, Barbieri F, et al. Stromal cell-derived factor-1α (SDF-1α/CXCL12) stimulates ovarian cancer cell growth through the EGF receptor transactivation. Exp Cell Res 2005;308:241–53.
34. Meyn MA 3rd, Schreiner SJ, Dumitrescu TP, Nau GJ, Smithgall TE. SRC family kinase activity is required for murine embryonic stem cell growth and differentiation. Mol Pharmacol 2005;68:1320–30.
35. Tian G, Cory M, Smith AA, Knight WB. Structural determinants for potent, selective dual site inhibition of human pp60c-src by 4-anilinoquinazolines. Biochemistry 2001;40:7084–91.
36. Force T, Krause DS, Van Etten RA. Molecular mechanisms of cardiotoxicity of tyrosine kinase inhibition. Nat Rev Cancer 2007;7:332–44.
37. LaFevre-Bernt M, Corbin JD, Francis SH, Miller WT. Phosphorylation and activation of cGMP-dependent protein kinase by Src. Biochim Biophys Acta 1998;1386:97–105.
38. Hood J, Granger HJ. Protein kinase G mediates vascular endothelial growth factor-induced Raf-1 activation and proliferation in human endothelial cells. J Biol Chem 1998;273:23504–8.
39. Zeimet AG, Riha K, Berger J, et al. New insights into p53 regulation and gene therapy for cancer. Biochem Pharmacol 2000;60:1153–63.
40. Wong AS, Kim SO, Leung PC, Auersperg N, Pelech SL. Profiling of protein kinases in the neoplastic transformation of human ovarian surface epithelium. Gynecol Oncol 2001;82:305–11.
41. Jorissen RN, Walker F, Pouliot N, Garrett TP, Ward CW, Burgess AW. Epidermal growth factor receptor: mechanisms of activation and signalling. Exp Cell Res 2003;284:31–53.
42. Tejedo JR, Cahuana GM, Ramirez R, et al. Nitric oxide triggers the phosphatidylinositol 3-kinase/Akt survival pathway in insulin-producing RINm5F cells by arousing Src to activate insulin receptor substrate-1. Endocrinology 2004;145:2319–27.
43. Tejedo JR, Ramirez R, Cahuana GM, Rincon P, Sobrino F, Bedoya FJ. Evidence for involvement of c-Src in the anti-apoptotic action of nitric oxide in serum-deprived RINm5F cells. Cell Signal 2001;13:809–17.

ELSEVIER

Cardiovascular Pathology 19 (2010) e221 – e231

CARDIOVASCULAR PATHOLOGY

Original Article

Protein kinase G activity prevents pathological-level nitric oxide-induced apoptosis and promotes DNA synthesis/cell proliferation in vascular smooth muscle cells

Janica C. Wong[a,b,c], Ronald R. Fiscus[a,b,c,d,*]

[a]*Cancer Molecular Biology Section, Nevada Cancer Institute, Las Vegas, NV 89135, USA*
[b]*Department of Chemistry, University of Nevada Las Vegas, Las Vegas, NV 89154, USA*
[c]*Cardiovascular Research Group, Department of Physiology, Faculty of Medicine, and Molecular Gerontology, Centre for Gerontology and Geriatrics, The Chinese University of Hong Kong, Shatin, New Territories, Hong Kong*
[d]*College of Pharmacy, University of Southern Nevada, Henderson, NV 89014, USA*

Received 24 May 2009; received in revised form 26 August 2009; accepted 2 November 2009

Abstract

Background: Protein kinase G (PKG), a recognized downstream mediator of nitric oxide, is a key regulator of cardiovascular physiology and pathology. High-level stimulation of cyclic guanosine monophosphate/PKG signaling using high concentrations of nitric oxide donors, mimicking pathological conditions, induces apoptosis in vascular smooth muscle cells. In contrast, we have found that PKG at basal and moderately elevated activity prevents both spontaneous and toxin-induced apoptosis in many other cells. We hypothesized that PKG's apoptosis-regulatory role in vascular smooth muscle cells depends on PKG activation levels [low/basal-level activation prevents apoptosis, whereas high-level activation (hyperactivation) causes apoptosis]. Furthermore, we hypothesized that, although PKG hyperactivation inhibits vascular smooth muscle cell proliferation (potentially causing anti-atherogenic effects), basal PKG activity may promote vascular smooth muscle cell proliferation/atherogenesis. **Methods:** Involvement of PKG in apoptosis and proliferation was determined in unpassaged vascular smooth muscle cells from mouse aorta. Western blot analysis was used to determine PKG expression, and activators/inhibitors of PKG activity were used to determine involvement in apoptosis (Hoechst staining and DNA-fragmentation ELISAs) and proliferation (cell count, MTT assay, and BrdU incorporation). **Results:** Both PKG-Iα and PKG-Iβ isoforms were expressed. Lower-level stimulation of PKG using the nitric oxide donor *S*-nitroso-acetylpenacillamine (10, 50 μM) significantly ($P<.05$) lowered spontaneous apoptosis, whereas *S*-nitroso-acetylpenacillamine at higher concentrations (500, 1000 μM) elevated apoptosis. Twenty-four-hour pretreatment with atrial natriuretic peptide, a PKG activator, completely prevented high-concentration, nitric oxide-induced apoptosis. Inhibition of basal PKG activity using highly selective PKG inhibitors, DT-2 and DT-3, significantly ($P<.001$) increased apoptosis and inhibited DNA synthesis/proliferation. **Conclusion:** The data suggest that basal/moderately elevated PKG activity protects against high/pathological-level nitric oxide-induced apoptosis and promotes DNA synthesis/proliferation in vascular smooth muscle cells, potentially important for atherogenesis.

Keywords: Protein kinase G; Nitric oxide; Apoptosis; DNA synthesis; Vascular smooth muscle cells; Proliferation

1. Introduction

Cyclic guanosine monophosphate (cGMP)-dependent protein kinase [protein kinase G (PKG)] is recognized as the key protein kinase mediating some biological effects (e.g., vasodilation) of nitric oxide (NO) and is an important regulator of cardiovascular physiology and pathology [1,2]. Aberrant expression of NO-synthesizing enzymes, both endothelial NO synthase and inducible NO synthase, was found in vascular smooth muscle cells (VSMCs) of

This study was supported by the Research Grants Council of Hong Kong (Grant #CUHK4169/02M) and a Direct Grant for Research, Medicine Panel of the Chinese University of Hong Kong (CUHK), to R.R.F., and by funding for graduate student projects from the Department of Physiology, Faculty of Medicine, CUHK, to J.C.W. This project was also supported in part by a grant from the U.S. Department of Defense (# W81XWH-07-1-0543), awarded to R.R.F. at the Nevada Cancer Institute.

* Corresponding author. Director of Research, University of Southern Nevada, Henderson, NV 89014, USA. Tel.: +1 702 968 5570; fax: +1 702 968 5573.

E-mail address: rfiscus@usn.edu (R.R. Fiscus).

1054-8807/09/$ – see front matter
doi:10.1016/j.carpath.2009.11.001

atherosclerotic human aortae, suggesting involvement of NO and possibly downstream PKG in the vascular dysfunction and abnormal vascular tissue growth associated with atherosclerosis [3].

Early studies had shown that exposure of blood vessels to either therapeutically important NO donors (e.g., sodium nitroprusside) or endogenously produced NO, released from acetylcholine-stimulated endothelial cells, significantly increases intracellular activation of PKG in VSMCs [4]. The data suggested that PKG was the key protein kinase mediating the vasodilatory and antihypertensive effects of therapeutic NO donors as well as endogenous hormones and local hormones that utilize the endothelium-dependent mechanism [5]. Even basal release of NO in unstimulated aorta (possessing healthy endothelium) significantly elevates the intracellular PKG activation in VSMCs, and this elevated PKG activity tonically suppresses the vascular effects of many vasoconstrictors [4–6]. Other early studies showed that exposure of aorta, with or without endothelium, to atrial natriuretic peptide (ANP), a cardiac hormone with vasodilatory effects, causes similar increases in intracellular PKG activation in the VSMCs [7]. Thus, these early studies helped to establish PKG as a major regulator of vascular tone and an important protein in preventing the development of hypertension.

More recent studies from our laboratory have identified PKG as a key mediator of cell survival in certain types of mammalian cells. For example, PKG activity, either basal or moderately elevated, was found to be essential for the survival of certain neural cells, including primary hippocampal neurons [8] and a number of established neural cell lines, including PC12, N1E-115, and NG108-15 cells [9–11]. Basal activation of PKG protects these cells against both spontaneous apoptosis and toxin-induced apoptosis. Our laboratory has also shown that basal PKG activity plays a similar cytoprotective role in preventing spontaneous apoptosis in immortalized uterine epithelial cells and human ovarian cancer cells [12–14].

In contrast, other laboratories have reported that high-level stimulation of PKG causes the induction of apoptosis. For example, high concentrations of NO donors or phosphodiesterase inhibitors, mimicking the effects of pathological levels of endogenous NO, were found to induce pro-apoptotic effects in several other types of mammalian cells, including VSMCs [15,16], cardiomyocytes [17], the pancreatic β-cell line HIT-T15 [18], and colon cancer cells [19]. Although initially it was thought that these opposite effects of PKG on apoptosis were due to cell-type differences [10], other causes, such as differences in the levels of PKG activation, may have been responsible. The present study hypothesizes that PKG plays a dual role in regulating apoptosis in VSMCs, i.e., basal/moderately elevated levels of PKG activation suppress the onset of apoptosis, whereas high levels of activation (i.e., hyperactivation) of PKG cause induction of apoptosis. Until now, only the pro-apoptotic effects of PKG hyperactivation in VSMCs have been reported [15,16]. The present study determined whether basal activation of PKG has anti-apoptotic effects and whether prior moderate stimulation of PKG can protect against the apoptosis in VSMCs induced by high/pathological levels of NO.

VSMCs can change from a contractile phenotype to a "synthetic" noncontractile (fibro-proliferative) phenotype, a process known as phenotypic modulation, which occurs during vascular injury and, in some cases, in vitro culturing [20–22]. PKG is thought to play an important role in the phenotypic modulation [1,23]. For example, when rat VSMCs begin to change their phenotype during culturing, PKG expression levels were reported to dramatically decrease to "undetectable levels" [24]. Serum-derived growth factors, such as platelet-derived growth factor (PDGF), are known to reduce PKG expression [25], which likely contributed to the apparent loss of PKG expression during in vitro culturing [1,26,27]. Interestingly, Lincoln et al. [1,23,28] have shown that this decrease of PKG expression during repeated passaging of VSMCs in culture may be an important step in the phenotypic modulation process.

In the present study, only unpassaged VSMCs were used for studying the involvement of PKG activity in regulating apoptosis, cell proliferation, and DNA synthesis. To determine the role of basal PKG activity in regulating the rates of apoptosis, DNA synthesis, and proliferation, the PKG inhibitors DT-2 and DT-3 were used. DT-2 and DT-3 are unique among the various PKG inhibitors because of their high-level selectivity for PKG and the capability to inhibit not only stimulated PKG activity but also basal PKG activity [29–31].

2. Materials and methods

2.1. Materials

Materials were purchased as follows: Dulbecco's Modified Eagle's Medium (DMEM), fetal bovine serum (FBS), penicillin–streptomycin phosphate-buffered saline, Trypsin-EDTA (0.5%) 10×, and fungizone were from Gibco BRL (Gaithersburg, MD, USA). Hyaluronidase, 8-Br-cGMP, and Hoechst 33258 stain were from Sigma (St. Louis, MO, USA). Collagenase A and Cell Death Detection ELISA^{PLUS} kit, MTT assay, and BrdU-(5′bromo-2-deoxyuridine) ELISA colorimetric assays were from Roche Diagnostics (Mannheim, Germany). ANP was from Phoenix Pharmaceuticals (Burlingame, CA, USA). cGMP ELISA was from Assay Designs (Ann Arbor, MI, USA). Bradford reagent was from Bio-Rad (Hercules, CA, USA). DT-2 was from Biolog (Bremen, Germany). KT-5823, DT-3, and anti-PKG-Iα/β antibody (product no. 539729) were from Calbiochem-Novabiochem (San Diego, CA, USA). The anti-β-actin antibody was from Santa Cruz Biotechnologies (Santa Cruz, CA, USA) and the anti-phospho-VASP (serine 239) antibody was from Cell Signaling Technologies (Danvers, MA, USA).

2.2. Animals

Mice of 8 to 10 weeks old were obtained from the Laboratory Animal Services Centre of the Chinese University of Hong Kong. The treatment of laboratory animals and the experimental procedures of the study adhered to established international guidelines, including the NIH Guidelines for Animal Care, and were approved by the Animal Experimentation Ethics Committee of the Chinese University of Hong Kong.

2.3. Cell culture

VSMCs were isolated from mouse aortas using an enzymatic dissociation method as described previously and cultured with 15% FBS (for optimal cell survival and proliferation) [32]. To avoid potential loss of PKG because of culturing conditions, the present study used only primary cultures of unpassaged VSMCs for studies of apoptosis and proliferation. Most previous studies of VSMC apoptosis and proliferation have used VSMC cultures that were repeatedly passaged (typically more than three passages), which may have caused phenotypic modulation and changes in the expression levels and function of PKG. All experiments studying apoptosis and proliferation used primary cultures of VSMCs within the first 2 days after isolation (before passaging). Previous studies from our laboratory have shown that the VSMCs remain phenotypically normal during this 2-day period of primary culturing [32]. Immunocytochemical staining showed that >95% of cells stained for smooth muscle-type α-actin.

2.4. Protein extraction and Western blot analysis of PKG expression and VASP phosphorylation at serine 239

Cells were lysed for 20 min on ice in 50 μl RIPA with 1× protease inhibitor cocktail (Roche) and 3 mM DTT. Similarly, freshly isolated aortas were homogenized in RIPA using tissue grinder. Samples were centrifuged at 10,000×*g* at 4°C and supernatant fractions used for Western blot analysis. Cellular protein was measured by Bradford analysis. The proteins were resolved by electrophoresis in 8% SDS-polyacrylamide gels and transferred to PVDF membranes. The blots were blocked in 5% nonfat milk and probed with anti-PKG-Iα/β antibody (#539729, Calbiochem) (1:5000), which recognizes the C-terminal (common region) of both PKG-Iα and PKG-Iβ, or anti-phospho-VASP (serine 239) antibody. The level of phosphorylation of VASP at serine 239 is a measure of intracellular PKG activity [33].

2.5. Measurement of cell proliferation by counting cell number

Cells were seeded in 24-well plates in DMEM with 15% FBS and incubated at 37°C in 5% CO_2 for 24 h. DT-2 or DT-3 was added once per day for 3 days. Trypsinized cells were counted by a hemocytometer. Increase in the number of cells was calculated by subtracting initial cell number from cell number after treatments.

2.6. Measurement of cell proliferation by MTT assay

Proliferation of VSMCs was also measured by MTT assay (Roche), following the protocol of the manufacturer. Cells were seeded in 96-well microplates (2×10^4 cells per well) in DMEM with 15% FBS and incubated at 37°C in 5% CO_2 for 24 h. DT-2 or DT-3 was added once per day for 3 days. The data are presented as increases in number of cells, with data converted from absorbance units in MTT assay into number of cells using standard curves of cell number vs. absorbance units.

2.7. Measurement of de novo DNA synthesis by BrdU-(5′ bromo-2-deoxyuridine) ELISA colorimetric assay

The rate of DNA synthesis of VSMCs was measured by BrdU ELISA assay (Roche), following the protocol of the manufacturer. Cells were seeded in 96-well microplates (5×10^3 cells per well) in DMEM with 15% FBS and incubated at 37°C in 5% CO_2 for 24 h. DT-2 or DT-3 was added for 24 h, followed by BrdU for 4 h.

2.8. Measurement of apoptosis by Cell Death Detection ELISA^{PLUS}

The Cell Death Detection ELISA^{PLUS} assay (Roche), based on quantitative sandwich-enzyme-immunoassay principle with monoclonal antibodies directed against apoptotic-fragmented DNA and histones, were used to quantify apoptotic levels. Procedures followed the manufacturer's protocol, with the following exception. A longer centrifugation time (i.e., 30 min, instead of the recommended 10 min), after cell permeation for releasing apoptotic fragments of DNA, was used in order to obtain a cleaner separation of apoptotic DNA fragments from genomic DNA in cell nuclei. This modification dramatically lowered background interference caused by contaminating genomic DNA and thus allowed better quantification of apoptotic responses.

2.9. Assessment of apoptosis by Hoechst 33258 staining

Cells were handled and stained with Hoechst 33258 as described in our previous publications [13,14]. Apoptotic cells were identified as those cells with highly condensed nuclei or fragmented nuclei.

2.10. Measurements of cGMP levels by enzyme-linked immunoassay

Levels of cGMP were measured by an enzyme-linked immunoassay (Assay Design) as described previously [13].

Unpassaged VSMCs in six-well plates were incubated with ANP for 4 min.

2.11. Statistical analysis

All experiments were repeated at least three times, representing an *N* value of at least 4 for each study. The results are expressed as mean±S.E.M. Statistical analysis was carried out by ANOVA (PRISM software, version 3.0; GraphPad, San Diego, CA, USA), followed by Dunnett's post hoc test. Statistical significance was inferred at $P<.05$.

3. Results

3.1. Both PKG-Iα and PKG-Iβ isoforms are expressed in unpassaged and early-passaged mouse aortic VSMCs

Previous studies have reported that rat aortic VSMCs possess dramatically reduced expression levels of PKG after repeated passaging of the cells, which resulted in an apparent loss of PKG as the cells became phenotypically modulated [1,24,28]. However, it was not clear from these earlier studies which isoform of PKG-I was diminished during passaging.

The present study determined expression levels of the two different PKG-I isoforms in mouse aortic VSMCs in Passage 0 (unpassaged), Passage 1, and Passage 2 as well as in freshly isolated aorta, assessed by Western blot analysis (Fig. 1). NG108-15 cells were used as a positive control for PKG-Iα expression. Previous studies from our laboratory had shown that NG108-15 cells express predominately PKG-Iα and that basal activation of this protein kinase is essential for protection against both spontaneous and toxin-induced apoptosis [9,10,12]. Also, recombinant PKG-Iα (approximate molecular weight=76.2 kDa) and PKG-Iβ (approximate molecular weight=77.8 kDa) were used as standards. Electrophoretic conditions were optimized to separate and identify the two PKG-I isoforms.

Fig. 1 shows that both PKG-Iα and PKG-Iβ are expressed at high levels in freshly isolated aorta, thus confirming a previous report showing PKG-I isoforms expression in various mouse tissues [34]. Levels of both PKG-Iα and PKG-Iβ were diminished (but clearly *not* lost) in cultured VSMCs, compared to freshly isolated aorta, beginning as early as Passage 0. This reduction in PKG expression likely resulted from exposure to serum factors known to decrease PKG expression [25]. However, it is important to emphasize that cultured unpassaged VSMCs still expressed both isoforms of PKG-I, which could potentially mediate functional activity (e.g., regulation of apoptosis and proliferation).

3.2. At lower/physiological concentrations, NO has anti-apoptotic effects, whereas at higher/pathological concentrations, NO has pro-apoptotic effects in unpassaged VSMCs

Fig. 2 shows the effects of the NO donor *S*-nitroso-acetylpenacillamine (SNAP), in a wide concentration range from 10 to 1000 μM (representing physiological to pathological concentrations of NO) on apoptosis in unpassaged VSMCs. SNAP is known to release NO at a slow rate, generating NO at a concentration that is 0.1% [35] to 0.3% [36] of the original SNAP concentration. Thus, SNAP at 10 μM would generate NO at 10–30 nM (physiological levels), whereas SNAP at 1000 μM would generate NO at 1–3 μM (pathological levels). The physiological levels of NO that are generated by healthy endothelial cells during normal regulation of vascular tone are 1–30 nM, whereas the pathological levels of NO generated by activated macrophages during severe inflammation are 1–4 μM [37,38].

Panel A of Fig. 2 shows a concentration-dependent increase in intracellular PKG activity in VSMCs exposed to SNAP (10–1000 μM), indicated by increased levels of phosphorylation of VASP at serine 239 (a site selective for PKG) [33]. Panel B shows the effects of SNAP on apoptosis

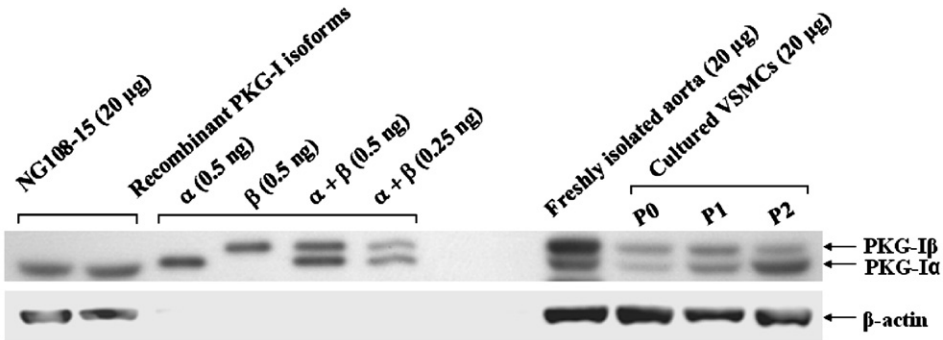

Fig. 1. Western blot analysis showing protein expression levels of the PKG isoforms in cultured VSMCs from mouse aorta. Both PKG-I isoforms, PKG-Iα and PKG-Iβ, are expressed in freshly isolated aorta as well as in cultured VSMCs at Passage 0 (P0) (i.e., unpassaged), Passage 1 (P1), and Passage 2 (P2). Although expression levels of both isoforms are diminished during culturing, compared to freshly isolated aorta, both PKG-Iα and PKG-Iβ continue to be expressed at detectable levels in unpassaged primary cultures and passaged cultures of the VSMCs. As a positive control for PKG-Iα expression, cell lysates of NG108-15 neuroblastoma-glioma hybrid cells were included. β-Actin was used as the loading control. Similar results were obtained in three additional experiments.

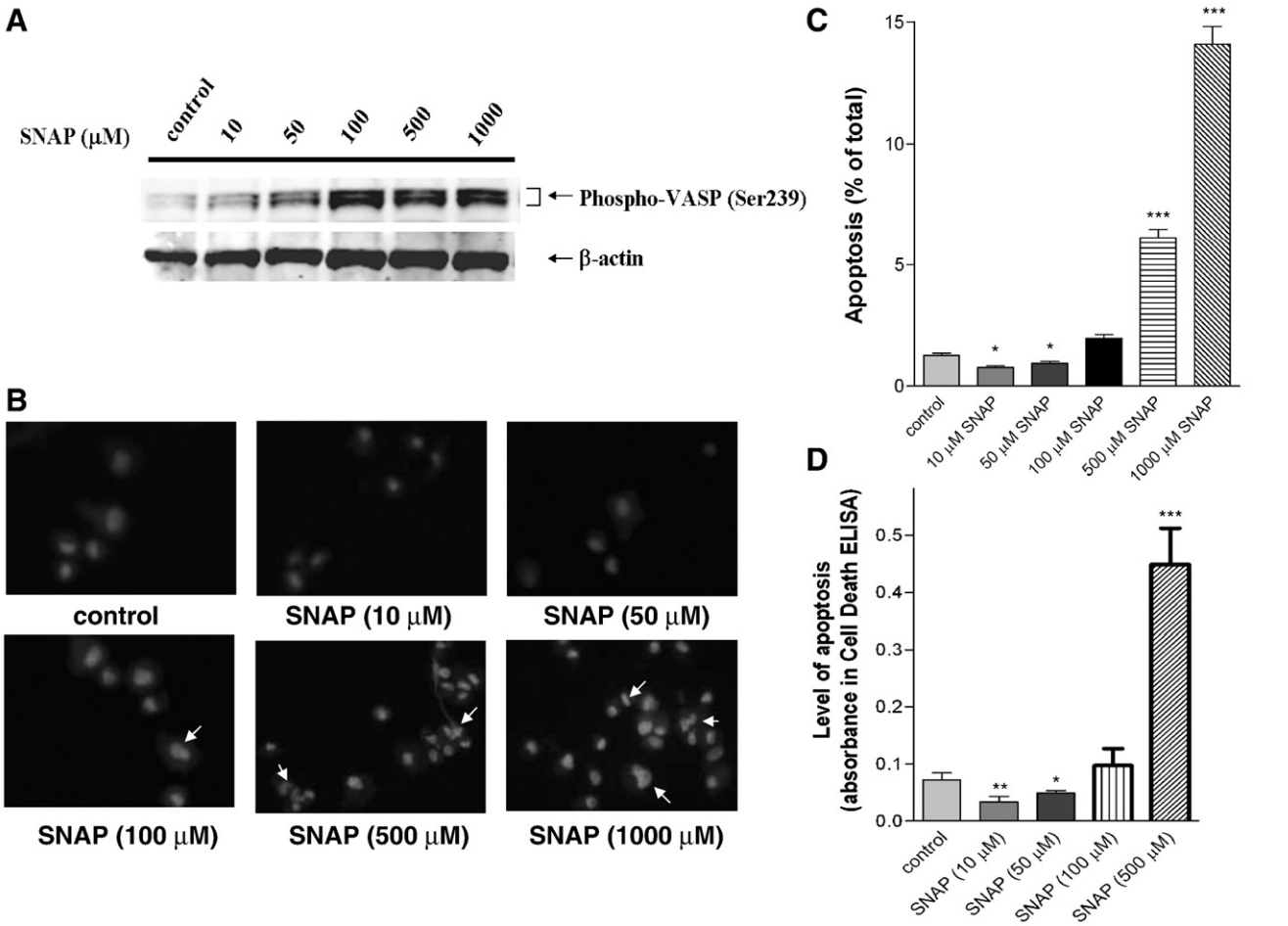

Fig. 2. The NO donor SNAP at lower concentrations (10 and 50 μM) significantly reduces, whereas at higher concentrations (500 and 1000 μM) significantly elevates, the levels of apoptosis in unpassaged VSMCs. (A) SNAP at 10–1000 μM (10 min) caused concentration-dependent elevations of phosphorylation of the PKG-substrate protein VASP, indicating that endogenous PKG in the VSMCs is activated by SNAP throughout the concentration range used for testing the effects on apoptosis. This Western blot used an antibody that specifically recognizes the phosphorylation of VASP at serine 239, the site selectively phosphorylated by PKG. Similar effects were observed in three other Western blots. (B) Biphasic effects on apoptosis (decreased apoptosis at lower concentrations and increased apoptosis at higher concentrations) in the unpassaged mouse aortic VSMCs exposed to increasing concentrations of SNAP, assessed by Hoechst 33258 staining. Similar results were obtained in three additional experiments. (C) Graph showing the percent of cells that were apoptotic in the experiments using Hoechst 33258 staining from Panel B. N=4 for each treatment group. (D) Levels of apoptosis in the VSMCs exposed to increasing concentrations of SNAP, quantified by measuring levels of apoptotic DNA fragmentation using the Cell Death Detection ELISA. Cells were incubated under serum-free conditions for 72 h with or without additional SNAP. The data represent the mean±S.E.M. from four experiments. *P<.05, **P<.01, ***P<.001.

in the VSMCs, indicated by morphological changes in the nuclei of Hoechst-stained cells. SNAP at the higher concentrations (500 and 1000 μM) induced apoptosis, like shown before in passaged VSMCs [16]. At the lower concentrations (10 and 50 μM), however, SNAP caused the opposite effect, i.e., a decrease in the number of apoptotic cells. Panel C shows a graph indicating the % of cells that were apoptotic (by Hoechst staining, same cells as in Panel B). SNAP at 10 and 50 μM significantly decreased the levels of apoptosis, whereas SNAP at 500 and 1000 μM significantly increased the levels of apoptosis. Panel D shows the results of an additional study in which apoptosis was measured by DNA-fragmentation ELISA (Cell Death Detection ELISA) technique. SNAP at lower concentrations, 10 μM (P<.01) and 50 μM (P<.05), significantly decreased apoptotic levels and at a higher concentration, 500 μM (P<.001), caused an elevation in the levels of apoptosis. The data are consistent with the concept that low-level activation of PKG by lower (physiological) levels of NO protects against apoptosis, whereas high-level activation of PKG by higher (pathological) levels of NO promotes the onset of apoptosis.

3.3. Prior stimulation of PKG activity in unpassaged VSMCs by pretreatment with ANP or 8-Br-cGMP protects these cells against high-level, NO-induced apoptosis

To test whether prior activation of PKG has cytoprotective effects, two agents were used: 8-bromo-cGMP (8-Br-cGMP), which is a cell-permeable cGMP analog that directly activates PKG [10,39], and ANP, a cardiac hormone that indirectly activates PKG. ANP is known to stimulate cell-

surface ANP receptors that possess particulate guanylyl cyclase activity on the intracellular side, resulting in elevated levels of cGMP and downstream enhanced activation of PKG in mammalian cells [6,7].

Panel A of Fig. 3 shows that pretreatment of VSMCs with 8-Br-cGMP for 24 h before the induction of apoptosis with high-level SNAP (1 mM) causes significant ($P<.01$) protection against the induction of apoptosis. Because 8-Br-cGMP is metabolized by many phosphodiesterases, which can shorten and diminish 8-Br-cGMP's ability to activate PKG in VSMCs [40], relatively high concentrations of this cGMP analog were needed to show significant cytoprotective effects.

To avoid the problem of transient PKG stimulation, further studies used preincubations with ANP. The natriuretic peptides, including ANP and a related peptide, B-type (brain) natriuretic peptide, are known to cause prolonged stimulation of the cGMP/PKG pathway in mammalian cells [11,41]. Panel B of Fig. 3 shows that preincubation with ANP causes complete protection against high-level, SNAP-induced apoptosis, even when ANP was used at a concentration as low as 10 nM ($*P<.05$). Panel C of Fig. 3 shows that these cells possess functional ANP receptors and respond to ANP exposure with increases in cGMP levels.

3.4. Basal PKG activity in unpassaged VSMCs protects against induction of apoptosis by serum removal

To further investigate pro-apoptotic/anti-apoptotic effects of cGMP/PKG pathway, the effects on apoptosis of PKG inhibitors were studied. DT-2 and DT-3 are two recently developed highly selective inhibitors of PKG-I activity [29–31]. Unlike other PKG inhibitors that are commercially available, DT-2 and DT-3 effectively inhibit not only stimulated PKG activity but also basal PKG activity [29,30].

Fig. 4 shows the effects of these PKG inhibitors on apoptotic levels in unpassaged VSMCs, both in the presence (+S) and absence (−S) of serum over 72 h. The PKG inhibitors had no significant effect on apoptotic levels in the presence of serum. However, in the absence of serum, DT-2 (250 nM) and DT-3 (250 nM) significantly ($P<.001$) enhanced the pro-apoptotic effects of serum removal by twofold and threefold, respectively, suggesting that basal PKG activity in unpassaged VSMCs is providing an anti-apoptotic/pro-survival signal that protected these cells against the induction of apoptosis caused by the loss of serum survival factors.

A previous study had shown that pretreatment of rabbit aortic VSMCs (in Passages 5 to 9) with the PKG inhibitor Rp-8-pCPT-cGMPS caused complete inhibition of SNAP (0.5 mM)-induced apoptosis, suggesting that PKG activation was involved in mediating the pro-apoptotic effects of high-level NO [16]. In the present study, we performed similar experiments, but used unpassaged mouse aortic VSMCs and the highly selective PKG inhibitor DT-2. Panel B of Fig. 4 shows that DT-2 (250 nM), when added before SNAP (1 mM), was not capable of inhibiting the pro-apoptotic effects of SNAP. Rather, DT-2 and SNAP (high concentration) had additive effects in causing induction of apoptosis in unpassaged mouse aortic VSMCs. Thus, unlike in the multiply passaged rabbit aortic VSMCs, the high-concentration, SNAP-induced apoptosis in the unpassaged mouse aortic VSMCs of the present study appears not to involve activation of PKG.

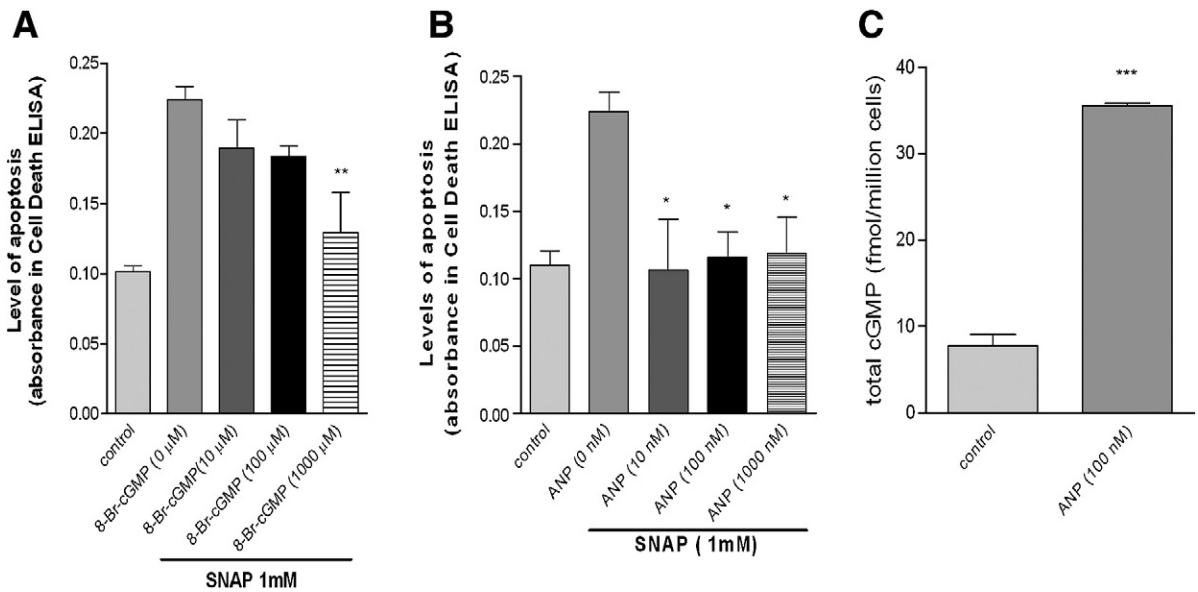

Fig. 3. Prior stimulation of intracellular PKG activity in unpassaged VSMCs by pretreatment for 24 h with 8-Br-cGMP (A) or atrial natriuretic peptide (ANP) (B) protects against high-level, NO-induced apoptosis. (C) ANP (100 nM) significantly elevates intracellular cGMP levels in the unpassaged VSMCs, indicating the presence of ANP receptors with particulate guanylyl cyclase activity in these cells. The data represent the mean±S.E.M. from four experiments. $*P<.05$; $**P<.01$, $***P<.001$.

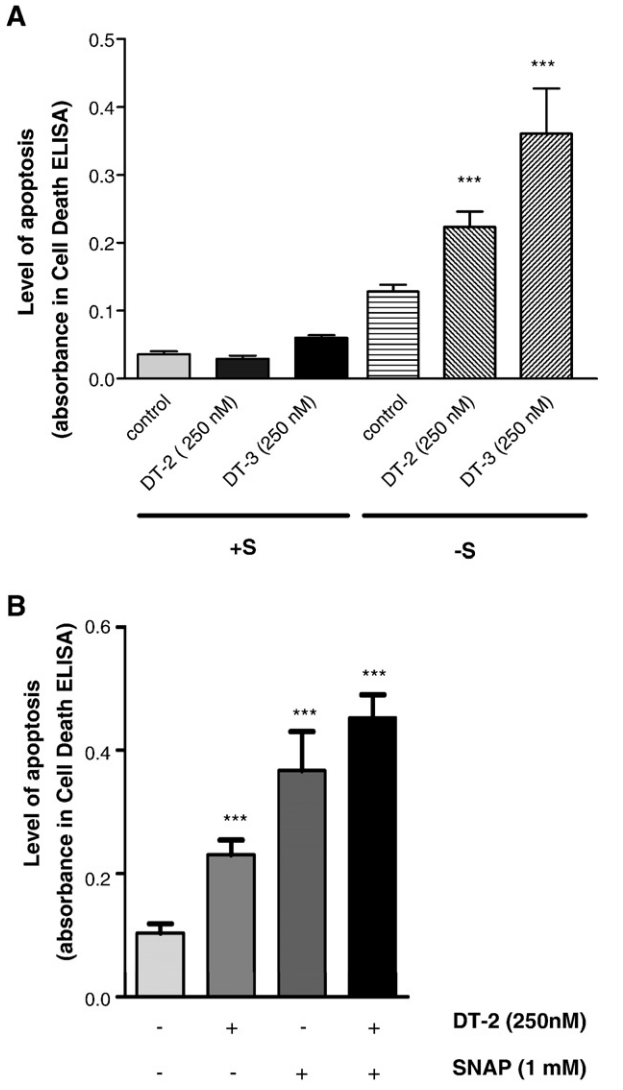

Fig. 4. (A) Inhibition of basal PKG activity in unpassaged VSMCs, using the highly selective PKG inhibitors DT-2 and DT-3, significantly enhances the apoptosis induced by serum removal (−S) over 72 h, quantified by Cell Death Detection ELISA. In the presence of serum (+S), DT-2 and DT-3 had no effect on apoptotic levels. (B) When used in combination with SNAP (1 mM, in serum-deprived unpassaged VSMCs), DT-2 (250 nM) was not able to block the induction of apoptosis caused by SNAP. The data represent the mean±S.E.M. of four experiments. ***P<.001.

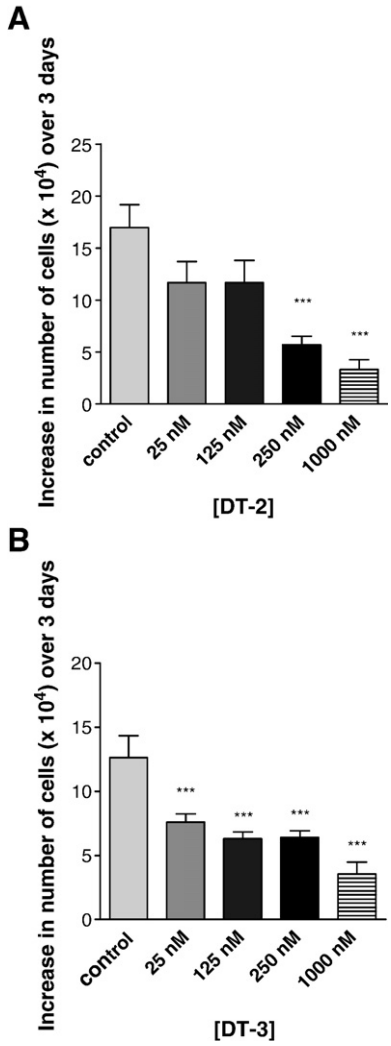

Fig. 5. Inhibition of basal PKG activity in unpassaged VSMCs, using the highly selective PKG inhibitors DT-2 (A) and DT-3 (B), dramatically and significantly reduces the cell proliferation rate, assessed by measuring the increase in number of cells over 3 days. The data represent the mean±S.E.M. of six experiments. ***P<.001.

3.5. Basal PKG activity promotes cell proliferation and de novo DNA synthesis in unpassaged VSMCs

Fig. 5 shows the effects of the PKG inhibitors DT-2 and DT-3 on serum-induced proliferation of unpassaged VSMCs, assessed by measuring increases in cell number over 3 days in primary culture. DT-2 at 250 nM and 1000 nM (72 h) significantly (P<.001) decreased proliferation by 65% and 82%, respectively. DT-3 significantly lowered the rate of cell proliferation at all concentrations between 25 and 1000 nM.

Fig. 6 shows the results of other experiments using MTT assay to measure cell proliferation (A) and BrdU incorporation to measure de novo synthesis of DNA (B). Panel A shows that inhibition of basal PKG activity with DT-2 (250 and 1000 nM) significantly (P<.001) decreased the rate of cell proliferation by 43% and 53%, respectively. Similar results were obtained using DT-3. Panel B shows that DT-2 at 125 nM (P<.001), 250 nM (P<.001), and 1000 nM (P<.05) significantly decreased the rate of DNA synthesis. Similar inhibition of DNA synthesis was obtained with DT-3.

4. Discussion

Hyperstimulation of the cGMP/PKG signaling pathway in VSMCs, caused by exposure to high concentrations of NO mimicking pathological conditions, is reported to cause apoptosis [15,16]. However, NO is also known to have anti-apoptotic/cytoprotective effects in many other types of cells, including vascular endothelial cells [42], uterine epithelial

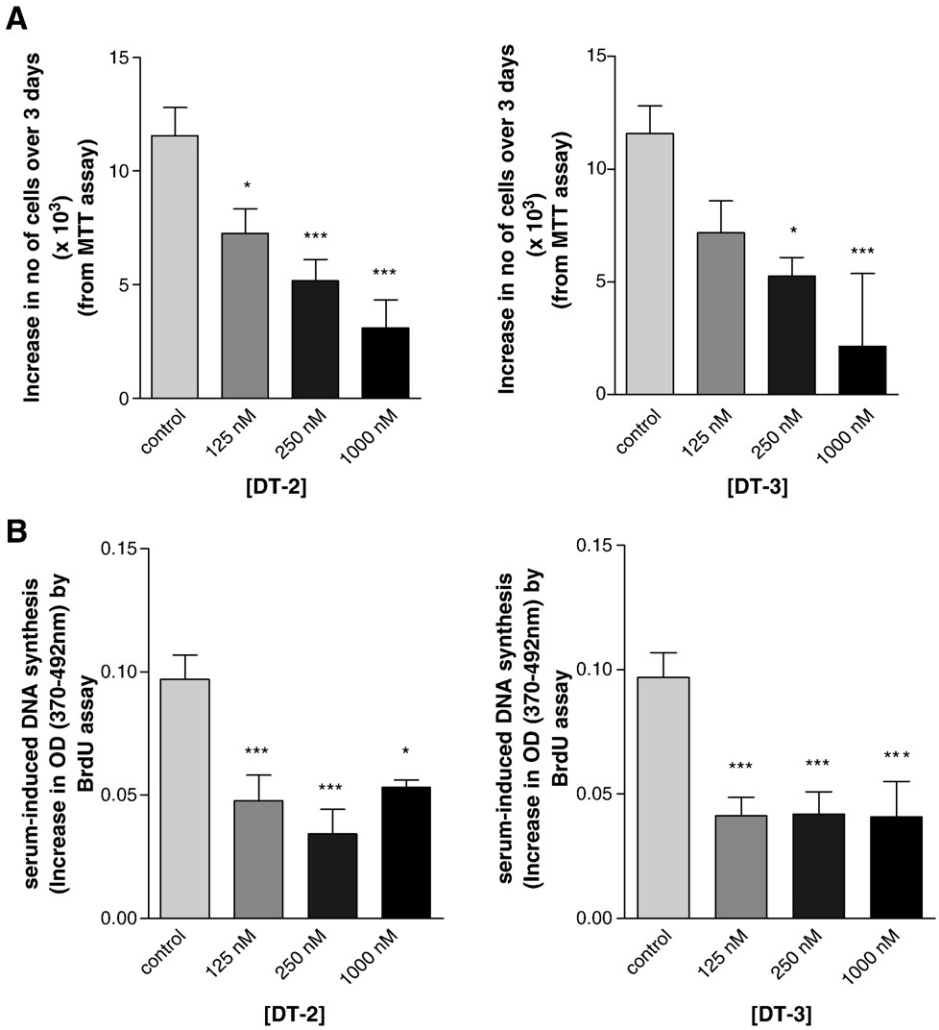

Fig. 6. Inhibition of basal PKG activity in unpassaged VSMCs, using DT-2 and DT-3, significantly lowers the cell proliferation rate, assessed by MTT assay (A), and the rate of de novo DNA synthesis, assessed by BrdU incorporation (B). The data represent the mean±S.E.M. of four experiments . *P<.05, ***P<.001.

cells [12], human ovarian cancer cells [13,14], and many types of neural cells [9–11]. In the case of the neural, uterine epithelial, and ovarian cancer cells, the anti-apoptotic effects of NO are thought to involve basal or low-level activation of PKG. The differences in the effects of NO on apoptosis may depend on differences in cell type and/or levels of activation of the cGMP/PKG pathway. In VSMCs, PKG activation may have a dual role, i.e., mediating pro-apoptotic effects at high/pathological levels of activation and anti-apoptotic effects at lower/basal levels of activation. Another issue complicating interpretation of PKG's role in regulating apoptosis in VSMCs is the previous widespread use of repeatedly passaged (phenotypically modulated) VSMCs, rather than primary unpassaged VSMCs. A goal of the present study was to clarify whether PKG, at basal or moderately elevated levels of activation, contributes to the regulation of apoptosis in unpassaged VSMCs.

Early studies of VSMC proliferation showed that high-level stimulation of the cGMP/PKG pathway, using high/pathological concentrations of NO donors or natriuretic peptides, causes anti-proliferative effects [1,43,44]. However, other data suggest that this NO/cGMP-mediated inhibition of proliferation in VSMCs may instead involve cross-activation of cAMP-dependent protein kinase [1]. Also, recent studies using knockout mice deficient in the expression of PKG in the VSMCs suggest that the PKG expressed in wild-type VSMCs tends to promote, rather than inhibit, proliferation [2,43,44]. Thus, the role of PKG in regulating VSMC proliferation appears contradictory. However, as with apoptosis regulation, the differences in proliferative responses mediated by PKG may have resulted from differences in PKG activation levels (i.e., basal activation vs. hyperactivation).

The present study shows that cultures of mouse aortic VSMCs in primary cultures have noticeably reduced protein expression levels of PKG, compared with freshly isolated aorta, but clearly do not lose the PKG expression. Both PKG-Iα and PKG-Iβ isoforms continue to be expressed in these VSMCs during culturing. The decrease in PKG protein levels is likely due to exposure to serum factors, such as

PDGF, known to reduce PKG expression [25]. Even though the expression levels of PKG are reduced in the cultured unpassaged VSMCs, as compared to freshly isolated uncultured VSMCs, the lower-level expression of PKG in the cultured unpassaged VSMC plays an important role in protecting these cells against the induction of apoptosis by toxic levels of NO and in promoting cell proliferation stimulated by serum factors, indicated by the data of the present study.

The present study used the NO donor SNAP in a wide concentration range to mimic exposures to low levels (physiological levels) and high levels (pathological levels) of NO. At lower concentrations of SNAP (10–50 μM), representing physiological concentrations (10–150 nM) of NO, apoptotic levels were significantly reduced in the unpassaged VSMCs, consistent with a cytoprotective role of NO when present at physiological concentrations. In contrast, at higher concentrations of SNAP (500–1000 μM), representing pathological concentrations (0.5–3 μM) of NO, SNAP increased the levels of apoptosis in the unpassaged VSMCs, similar to results shown in a previous study [16].

At the lower physiological concentrations, NO is known to stimulate soluble guanylyl cyclase, causing modest increases in cGMP levels and PKG activation in mammalian cells [1,2,4–6,10,39]. This was confirmed in the present study using unpassaged VSMCs by showing that SNAP, at concentrations as low as 10 μM (representing NO concentrations of 10–30 nM), increases the level of phosphorylation of VASP, an intracellular substrate of PKG (shown in Panel A of Fig. 2). This intracellular activation of PKG by the low-level NO corresponds to the cytoprotective/anti-apoptotic effects in VSMCs (shown in Panels B–D of Fig. 2). The present data suggest that the NO/cGMP/PKG signaling pathway, at basal or moderately elevated activity, serves a cytoprotective/anti-apoptotic role in the unpassaged VSMCs.

Healthy endothelium lining the arteries, even without exposure to acetylcholine or other vasodilatory agents, is known to continually release low levels of NO capable of causing moderate stimulation of intracellular PKG activity (to levels approximately 30% of maximal activity) within VSMCs, which provides a continual vasodilatory effect that counteracts the effects of vasoconstrictors [4–6]. The data of the present study suggest that this moderate PKG activation by endothelium-derived NO in healthy blood vessels may serve an additional physiological function, i.e., providing a continual cytoprotective/anti-apoptotic effect in VSMCs, protecting against spontaneous or toxin-induced apoptosis. This low/moderate activation of the cGMP/PKG signaling pathway in VSMCs may become diminished during certain conditions, such as aging and diabetes mellitus, which are associated with reduced bioavailability of NO [10,45]. Predictably, VSMCs may be at higher risk of apoptotic cell death during aging and diabetes mellitus because of the diminished NO/cGMP/PKG-mediated cytoprotective effects, potentially contributing to the development of cardiovascular pathologies.

The present study also shows that prior stimulation of PKG by 24-h pretreatment with ANP (an activator of PKG) completely protects VSMCs against the pro-apoptotic/cytotoxic effects of high-level NO. Previous studies from our laboratory have shown that ANP at these same concentrations is capable of moderately stimulating PKG activity in VSMCs [6,7]. Thus, prior moderate stimulation of PKG in VSMCs, by both circulating natriuretic peptides and low-level NO continually released from the endothelium, may play an important physiological role to protect against the induction of apoptosis that could occur because of exposure of VSMCs to high/toxic levels of NO, as, for example, during severe inflammation.

The present study also shows that inhibition of basal PKG activity using the highly selective PKG inhibitors DT-2 and DT-3 significantly enhances the induction of apoptosis caused by serum removal (see Fig. 4). Thus, basal PKG activity appears to play an important role in protecting against the onset of apoptosis during the stressful condition of serum depletion. When DT-2 was added before SNAP (1 mM), the induction of apoptosis caused by the high concentration of NO was enhanced. This is in contrast to the complete inhibition of SNAP-induced apoptosis caused by PKG inhibition with Rp-8-pCPT-cGMPS in multiply passaged rabbit aorta VSMCs [16], which had suggested that apoptosis induced by high-level NO involved hyperactivation of PKG. In the present study, using unpassaged mouse aortic VSMCs, it appears that the predominant role of PKG is to prevent the onset of apoptosis. Another reason for the opposite effects of PKG inhibition in our study vs. the study by Pollman et al. [16] may be related to the difference in the two PKG inhibitors used. For example, Rp-8-pCPT-cGMPS inhibits only stimulated PKG activity (and does not inhibit basal PKG activity), whereas DT-2 inhibits both stimulated and basal PKG activity [29]. Additionally, Rp-8-pCPT-cGMPS can actually stimulate PKG activity under basal conditions (i.e., in the absence of elevated cGMP levels), opposite to the strong inhibitory effects of DT-2 [29].

Previous studies had suggested that NO/cGMP/PKG pathway mediates antiproliferative effects in VSMCs, which may be responsible for the anti-atherogenic effects of NO. For example, NO (at high/pathological levels) was shown to inhibit VSMC growth in vitro and this response, at least originally, was thought to involve elevation of cGMP levels and stimulation of PKG activity [1,43,44]. However, in other studies, stimulation of PKG activity in primary VSMCs by adding cGMP analogs or NO at low/physiological concentrations was shown to enhance, not inhibit, DNA synthesis and proliferation rates induced by certain growth factors, such as fibroblast growth factor-2 [46,47] or PDGF [44]. Interestingly, the ability of cGMP analogs and low-level NO to enhance PDGF-induced DNA synthesis and proliferation was lacking in VSMCs that had genetic deletion of PKG, suggesting that PKG may be responsible for promoting PDGF-induced mitogenesis [44]. Also, a recent study has shown that low (physiological) concentrations of NO, when

added to VSMCs grown in 2% FBS, have stimulatory effects on cell proliferation and DNA synthesis [48]. Higher concentrations of NO tended to counteract this stimulatory effect on proliferation/DNA synthesis. These previous studies, however, did not report whether basal activation of PKG (i.e., PKG activation in the absence of added cGMP analogs or NO) was involved in promoting VSMC proliferation. The data of the present study, using two highly selective PKG inhibitors, DT-2 and DT-3, have now shown that basal PKG activation plays a significant role in promoting cell proliferation and DNA synthesis in VSMCs.

Presently, the downstream cellular mechanisms mediating these anti-apoptotic and growth-promoting effects of basal PKG activity in VSMCs are not clear. A possible mechanism may be activation of the MAP kinases, ERK1/2 and JNK. For example, pharmacological stimulation of PKG activity in phenotypically normal VSMCs has been shown to activate both ERK1/2 and JNK [49]. Further studies will be needed to determine whether activation of ERK1/2 and/or JNK is involved in the enhanced cell proliferation and DNA synthesis in VSMCs caused by the basal PKG activity.

In conclusion, the present data suggest that PKG activity, at basal and moderately elevated levels, plays a key role in preventing the apoptosis induced by high/pathological levels of NO in VSMCs. Hyperactivation of PKG may not be the primary mechanism mediating the pro-apoptotic effects of high-level NO in the unpassaged VSMCs, because this apoptosis was not reduced by PKG inhibition with DT-2. Rather, the toxic/pro-apoptotic effects of high-level NO in these cells are more likely mediated by other toxic mechanisms, such as nitration and the formation of peroxynitrite [35,37,38]. The data of the present study further suggest that, unlike hyperactivation of PKG, which causes inhibition of VSMC proliferation, the basal PKG activation promotes DNA synthesis and cell proliferation in VSMCs. These findings suggest that basal and moderately elevated levels of PKG activity in VSMCs, although capable of suppressing the development of hypertension because of the vasodilatory effects, may also play an important role in promoting the abnormal growth of vascular tissue associated with the development of atherosclerosis.

References

[1] Lincoln TM, Dey N, Sellak H. Invited review: cGMP-dependent protein kinase signaling mechanisms in smooth muscle: from the regulation of tone to gene expression. J Appl Physiol 2001;91:1421–30.

[2] Hofmann F, Feil R, Kleppisch T, Schlossmann J. Function of cGMP-dependent protein kinases as revealed by gene deletion. Physiol Rev 2006;86:1–23.

[3] Perrotta I, Brunelli E, Sciangula A, Zuccala V, Donato G, Tripepi S, et al. Inducible and endothelial nitric oxide synthase expression in human atherogenesis: an immunohistochemical and ultrastructural study. Cardiovasc Pathol 2009;18:361–8.

[4] Fiscus RR, Rapoport RM, Murad F. Endothelium-dependent and nitrovasodilator-induced activation of cyclic GMP-dependent protein kinase in rat aorta. J Cyclic Nucleotide Protein Phosphor Res 1983;9:415–25.

[5] Fiscus RR. Molecular mechanisms of endothelium-mediated vasodilation. Semin Thromb Hemost 1988;14(Suppl):12–22.

[6] Fiscus RR, Murad F. cGMP-dependent protein kinase activation in intact tissues. Methods Enzymol 1988;159:150–9.

[7] Fiscus RR, Rapoport RM, Waldman SA, Murad F. Atriopeptin II elevates cyclic GMP, activates cyclic GMP-dependent protein kinase and causes relaxation in rat thoracic aorta. Biochim Biophys Acta 1985;846:179–84.

[8] Barger SW, Fiscus RR, Ruth P, Hofmann F, Mattson MP. Role of cyclic GMP in the regulation of neuronal calcium and survival by secreted forms of beta-amyloid precursor. J Neurochem 1995;64:2087–96.

[9] Cheng Chew SB, Leung PY, Fiscus RR. Preincubation with atrial natriuretic peptide protects NG108-15 cells against the toxic/proapoptotic effects of the nitric oxide donor *S*-nitroso-*N*-acetylpenicillamine. Histochem Cell Biol 2003;120:163–71.

[10] Fiscus RR, Yuen JP, Chan SL, Kwong JH, Chew SB. Nitric oxide and cyclic GMP as pro- and anti-apoptotic agents. J Card Surg 2002;17:336–9.

[11] Fiscus RR, Tu AW, Chew SB. Natriuretic peptides inhibit apoptosis and prolong the survival of serum-deprived PC12 cells. Neuroreport 2001;12:185–9.

[12] Chan SL, Fiscus RR. Guanylyl cyclase inhibitors NS2028 and ODQ and protein kinase G (PKG) inhibitor KT5823 trigger apoptotic DNA fragmentation in immortalized uterine epithelial cells: anti-apoptotic effects of basal cGMP/PKG. Mol Hum Reprod 2003;9:775–83.

[13] Fraser M, Chan SL, Chan SS, Fiscus RR, Tsang BK. Regulation of p53 and suppression of apoptosis by the soluble guanylyl cyclase/cGMP pathway in human ovarian cancer cells. Oncogene 2006;25:2203–12.

[14] Leung EL, Fraser M, Fiscus RR, Tsang BK. Cisplatin alters nitric oxide synthase levels in human ovarian cancer cells: involvement in p53 regulation and cisplatin resistance. Br J Cancer 2008;98:1803–9.

[15] Chiche JD, Schlutsmeyer SM, Bloch DB, de la Monte SM, Roberts Jr JD, Filippov G, et al. Adenovirus-mediated gene transfer of cGMP-dependent protein kinase increases the sensitivity of cultured vascular smooth muscle cells to the antiproliferative and pro-apoptotic effects of nitric oxide/cGMP. J Biol Chem 1998;273:34263–71.

[16] Pollman MJ, Yamada T, Horiuchi M, Gibbons GH. Vasoactive substances regulate vascular smooth muscle cell apoptosis. Countervailing influences of nitric oxide and angiotensin II. Circ Res 1996;79:748–56.

[17] Shimojo T, Hiroe M, Ishiyama S, Ito H, Nishikawa T, Marumo F. Nitric oxide induces apoptotic death of cardiomyocytes via a cyclic-GMP-dependent pathway. Exp Cell Res 1999;247:38–47.

[18] Loweth AC, Williams GT, Scarpello JH, Morgan NG. Evidence for the involvement of cGMP and protein kinase G in nitric oxide-induced apoptosis in the pancreatic B-cell line, HIT-T15. FEBS Lett 1997;400:285–8.

[19] Deguchi A, Thompson WJ, Weinstein IB. Activation of protein kinase G is sufficient to induce apoptosis and inhibit cell migration in colon cancer cells. Cancer Res 2004;64:3966–73.

[20] Campbell GR, Campbell JH. Smooth muscle phenotypic changes in arterial wall homeostasis: implications for the pathogenesis of atherosclerosis. Exp Mol Pathol 1985;42:139–62.

[21] Chamley-Campbell JH, Campbell GR, Ross R. Phenotype-dependent response of cultured aortic smooth muscle to serum mitogens. J Cell Biol 1981;89:379–83.

[22] Majesky MW, Giachelli CM, Reidy MA, Schwartz SM. Rat carotid neointimal smooth muscle cells reexpress a developmentally regulated mRNA phenotype during repair of arterial injury. Circ Res 1992;71:759–68.

[23] Lincoln TM, Wu X, Sellak H, Dey N, Choi CS. Regulation of vascular smooth muscle cell phenotype by cyclic GMP and cyclic GMP-dependent protein kinase. Front Biosci 2006;11:356–67.

[24] Cornwell TL, Soff GA, Traynor AE, Lincoln TM. Regulation of the expression of cyclic GMP-dependent protein kinase by cell density in vascular smooth muscle cells. J Vasc Res 1994;31:330–7.

[25] Tamura N, Itoh H, Ogawa Y, Nakagawa O, Harada M, Chun TH, et al. cDNA cloning and gene expression of human type Ialpha cGMP-dependent protein kinase. Hypertension 1996;27:552–7.
[26] Sellak H, Choi C, Browner N, Lincoln TM. Upstream stimulatory factors (USF-1/USF-2) regulate human cGMP-dependent protein kinase I gene expression in vascular smooth muscle cells. J Biol Chem 2005;280:18425–33.
[27] Browner NC, Sellak H, Lincoln TM. Downregulation of cGMP-dependent protein kinase expression by inflammatory cytokines in vascular smooth muscle cells. Am J Physiol Cell Physiol 2004;287: C88–C96.
[28] Brophy CM, Woodrum DA, Pollock J, Dickinson M, Komalavilas P, Cornwell TL, et al. cGMP-dependent protein kinase expression restores contractile function in cultured vascular smooth muscle cells. J Vasc Res 2002;39:95–103.
[29] Taylor MS, Okwuchukwuasanya C, Nickl CK, Tegge W, Brayden JE, Dostmann WR. Inhibition of cGMP-dependent protein kinase by the cell-permeable peptide DT-2 reveals a novel mechanism of vasoregulation. Mol Pharmacol 2004;65:1111–9.
[30] Dostmann WR, Tegge W, Frank R, Nickl CK, Taylor MS, Brayden JE. Exploring the mechanisms of vascular smooth muscle tone with highly specific, membrane-permeable inhibitors of cyclic GMP-dependent protein kinase Ialpha. Pharmacol Ther 2002;93:203–15.
[31] Dostmann WR, Taylor MS, Nickl CK, Brayden JE, Frank R, Tegge WJ. Highly specific, membrane-permeant peptide blockers of cGMP-dependent protein kinase Ialpha inhibit NO-induced cerebral dilation. Proc Natl Acad Sci U S A 2000;97:14772–7.
[32] Lu LF, Fiscus RR. Nitric oxide donors enhance calcitonin gene-related peptide-induced elevations of cyclic AMP in vascular smooth muscle cells. Eur J Pharmacol 1999;376:307–14.
[33] Isenberg JS, Romeo MJ, Yu C, Yu CK, Nghiem K, Monsale J, et al. Thrombospondin-1 stimulates platelet aggregation by blocking the antithrombotic activity of nitric oxide/cGMP signaling. Blood 2008; 111:613–23.
[34] Geiselhoringer A, Gaisa M, Hofmann F, Schlossmann J. Distribution of IRAG and cGKI-isoforms in murine tissues. FEBS Lett 2004;575: 19–22.
[35] Crow JP, Beckman JS. Reactions between nitric oxide, superoxide, and peroxynitrite: footprints of peroxynitrite in vivo. Adv Pharmacol 1995; 34:17–43.
[36] Hirota Y, Ishida H, Genka C, Obama R, Matsuyama S, Nakazawa H. Physiological concentration of nitric oxide induces positive inotropic effects through cGMP pathway in isolated rat ventricular myocytes. Jpn J Physiol 2001;51:455–61.
[37] Beckman JS, Koppenol WH. Nitric oxide, superoxide, and peroxynitrite: the good, the bad, and ugly. Am J Physiol 1996;271:C1424–1437.
[38] Thomas DD, Ridnour LA, Isenberg JS, Flores-Santana W, Switzer CH, Donzelli S, et al. The chemical biology of nitric oxide: implications in cellular signaling. Free Radic Biol Med 2008;45:18–31.
[39] Fiscus RR. Involvement of cyclic GMP and protein kinase G in the regulation of apoptosis and survival in neural cells. Neurosignals 2002; 11:175–90.
[40] Zimmerman AL, Yamanaka G, Eckstein F, Baylor DA, Stryer L. Interaction of hydrolysis-resistant analogs of cyclic GMP with the phosphodiesterase and light-sensitive channel of retinal rod outer segments. Proc Natl Acad Sci U S A 1985;82:8813–7.
[41] Zhou HL, Fiscus RR. Brain natriuretic peptide (BNP) causes endothelium-independent relaxation and elevation of cyclic GMP in rat thoracic aorta. Neuropeptides 1989;14:161–9.
[42] Dimmeler S, Haendeler J, Nehls M, Zeiher AM. Suppression of apoptosis by nitric oxide via inhibition of interleukin-1beta-converting enzyme (ICE)-like and cysteine protease protein (CPP)-32-like proteases. J Exp Med 1997;185:601–7.
[43] Feil R, Feil S, Hofmann F. A heretical view on the role of NO and cGMP in vascular proliferative diseases. Trends Mol Med 2005;11:71–5.
[44] Wolfsgruber W, Feil S, Brummer S, Kuppinger O, Hofmann F, Feil R. A proatherogenic role for cGMP-dependent protein kinase in vascular smooth muscle cells. Proc Natl Acad Sci U S A 2003;100:13519–24.
[45] Chan GH, Fiscus RR. Severe impairment of CGRP-induced hypotension in vivo and vasorelaxation in vitro in elderly rats. Eur J Pharmacol 2002;434:133–9.
[46] Hassid A, Arabshahi H, Bourcier T, Dhaunsi GS, Matthews C. Nitric oxide selectively amplifies FGF-2-induced mitogenesis in primary rat aortic smooth muscle cells. Am J Physiol 1994;267:H1040–1048.
[47] Dhaunsi GS, Hassid A. Atrial and C-type natriuretic peptides amplify growth factor activity in primary aortic smooth muscle cells. Cardiovasc Res 1996;31:37–47.
[48] Isenberg JS, Wink DA, Roberts DD. Thrombospondin-1 antagonizes nitric oxide-stimulated vascular smooth muscle cell responses. Cardiovasc Res 2006;71:785–93.
[49] Komalavilas P, Shah PK, Jo H, Lincoln TM. Activation of mitogen-activated protein kinase pathways by cyclic GMP and cyclic GMP-dependent protein kinase in contractile vascular smooth muscle cells. J Biol Chem 1999;274:34301–9.

ARTICLE
Journal of Cellular Biochemistry 112:829–839 (2011)

Journal of Cellular Biochemistry

Essential Roles of the Nitric Oxide (NO)/cGMP/Protein Kinase G type-Iα (PKG-Iα) Signaling Pathway and the Atrial Natriuretic Peptide (ANP)/cGMP/PKG-Iα Autocrine Loop in Promoting Proliferation and Cell Survival of OP9 Bone Marrow Stromal Cells

Janica C. Wong[1,2] and Ronald R. Fiscus[1,2,3*]

[1]*Cancer Molecular Biology Section, Nevada Cancer Institute, Las Vegas, Nevada 89135*

[2]*Department of Chemistry, University of Nevada Las Vegas, Las Vegas, Nevada 89154*

[3]*College of Pharmacy, University of Southern Nevada, Henderson, Nevada 89014*

ABSTRACT

Inappropriate signaling conditions within bone marrow stromal cells (BMSCs) can lead to loss of BMSC survival, contributing to the loss of a proper micro-environmental niche for hematopoietic stem cells (HSCs), ultimately causing bone marrow failure. In the present study, we investigated the novel role of endogenous atrial natriuretic peptide (ANP) and the nitric oxide (NO)/cGMP/protein kinase G type-Iα (PKG-Iα) signaling pathway in regulating BMSC survival and proliferation, using the OP9 BMSC cell line commonly used for facilitating the differentiation of HSCs. Using an ANP-receptor blocker, endogenously produced ANP was found to promote cell proliferation and prevent apoptosis. NO donor SNAP (S-nitroso-*N*-acetylpenicillamine) at low concentrations (10 and 50 μM), which would moderately stimulate PKG activity, protected these BMSCs against spontaneous apoptosis. YC-1, a soluble guanylyl cyclase (sGC) activator, decreased the levels of apoptosis, similar to the cytoprotective effects of low-level NO. ODQ (1H-[1,2,4]oxadiazolo[4,3,-a]quinoxalin-1-one), which blocks endogenous NO-induced activation of sGC and thus lowers endogenous cGMP/PKG activity, significantly elevated apoptotic levels by 2.5- and three-fold. Pre-incubation with 8-Bromo-cGMP or ANP, which bypass the ODQ block, almost completely prevented the ODQ-induced apoptosis. A highly-specific PKG inhibitor, DT-3, at 20, and 30 μM, caused 1.5- and two-fold increases in apoptosis, respectively. ODQ and DT-3 also decreased BMSCs proliferation and colony formation. Small Interfering RNA gene knockdown of PKG-Iα increased apoptosis and decreased proliferation in BMSCs. The data suggest that basal NO/cGMP/PKG-Iα activity and autocrine ANP/cGMP/PKG-Iα are necessary for preserving OP9 cell survival and promoting cell proliferation and migration. J. Cell. Biochem. 112: 829–839, 2011.

KEY WORDS: PROTEIN KINASE G; BONE MARROW STROMAL CELLS; PROLIFERATION; APOPTOSIS

Bone marrow stromal cells (BMSCs) have been implicated in a wide range of clinical applications and regenerative medicine, such as tissue repair [Kitada and Dezawa, 2009], myocardial infarction [Psaltis et al., 2008] and neurodegenerative diseases [Sadan et al., 2009]. BMSCs were first characterized by Friedenstein et al. [1968] as an adherent, fibroblast-like population in the adult bone marrow. Multipotent BMSCs are capable of differentiating along the mesenchymal lineage to form bone, fat, and cartilage [Caplan, 1991; Hassan and El-Sheemy, 2004] and potentially could be used to regenerate other tissues. Also, BMSCs provide a proper micro-environmental niche for the growth/cultivation of hematopoietic stem cells (HSCs) [Wilson and Trumpp, 2006]. The proper environment for HSCs in the bone marrow requires several specific groups of cells, including endothelial cells and BMSCs and, along with the extracellular matrix elements, interact with HSCs to promote/inhibit their self renewal, differentiation and migration.

Our early studies had identified cGMP-dependent protein kinase (protein kinase G, PKG) as a key protein kinase mediating the vasodilatory effects of nitric oxide (NO) and atrial natriuretic peptide (ANP, ANF, atriopeptin) in blood vessels, specifically by relaxing the vascular smooth muscle cells (VSMCs) within the walls

Grant sponsor: The US Department of Defense; Grant number: W81XWH-07-1-0543.

*Correspondence to: Ronald R. Fiscus, College of Pharmacy, University of Southern Nevada, 11 Sunset Way, Henderson, NV 89014. E-mail: rfiscus@usn.edu

Received 12 August 2010; Accepted 22 November 2010 • DOI 10.1002/jcb.22981 • © 2010 Wiley-Liss, Inc.
Published online 28 December 2010 in Wiley Online Library (wileyonlinelibrary.com).

of these vessels [Fiscus et al., 1983, 1985; Fiscus, 1988; Fiscus and Murad, 1988]. More recent studies from our laboratory have shown that basal or moderately elevated PKG activity is essential for the survival of certain neural cell lines, including PC12, N1E-115 and NG108-15 cells [Fiscus et al., 2001, 2002; Fiscus, 2002; Cheng Chew et al., 2003; Johlfs and Fiscus, 2010]. Our laboratory has also shown that basal PKG activity plays a similar cytoprotective role in preventing spontaneous apoptosis in primary murine VSMCs, immortalized uterine epithelial cells, and human ovarian cancer cells [Chan and Fiscus, 2003; Fraser et al., 2006; Leung et al., 2008, 2010; Wong and Fiscus, 2010].

Although research on stem cells has increased drastically in recent years, there are very few studies on the role of the NO/cGMP/PKG pathway in stem cells [Krumenacker et al., 2006]. Expression of mRNA and protein levels of the three NOSs and sGC has been reported in mouse embryonic stem (ES) cells and the expression of PKG in ES cell-derived cardiomyocytes is known to increase during differentiation [Krumenacker and Murad, 2006]. Very recently, the NO/cGMP/PKG signaling pathway has been proposed to promote stem cell-like characteristics in glioma cells in the tumor perivascular niche of medulloglioma [Charles et al., 2010].

In the present study, the BMSC cell line OP9 was used to investigate the role of endogenous ANP/cGMP/PKG and NO/cGMP/PKG signaling pathways in BMSCs. These cells are mouse BMSCs lacking the expression of macrophage-colony stimulating factor, making them especially useful as a feeder layer for hematopoietic differentiation down a lineage other than monocytes. OP9 cells are reported to augment the survival of hematopoietic precursors and progenitors [Ji et al., 2008], and can be used in a coculture system with mouse ES cells and induced pluripotent stem (iPS) cells to induce the differentiation of ES cells into endothelial cells [Kelly and Hirschi, 2009] and blood cells of erythroid, myeloid, and B cell lineages [Nakano et al., 1994; Nakano, 1995; Kitajima et al., 2003; Ji et al., 2008], and iPS into hematopoietic cell lineages [Niwa et al., 2009].

MATERIALS AND METHODS

CELL CULTURE AND TISSUE

OP9 mouse BMSCs were purchased from American Type Culture Collection (ATCC). BMSCs were cultured in α-Minimum Eagle's Medium (α MEM), supplemented with fetal bovine serum (20%),streptomycin (50 μg/ml), and penicillin (50 units/ml) (all from Lonza), and cultured at 37°C in an atmosphere of 5% CO_2/95% air.

The aortas were isolated from mice as previous described [Wong and Fiscus, 2010]. The mice were obtained from Jackson Laboratories. The treatment of laboratory animals and the experimental procedures of the present study adhered to the NIH Guidelines for Animal Care, and were approved by IACUC at the Nevada Cancer Institute.

PROTEIN EXTRACTION AND WESTERN BLOTTING USING INFRARED IMAGING

For protein extraction, the cells were lysed using 85°C hot 1× sodium dodecyl sulfate (SDS) lysis buffer (50 mmol/L Tris–HCL, pH 6.8, 2% SDS, 10 mmol/L dithiolthreitol, and 10% glycerol). The supernatant fractions were collected by centrifugation (15,000*g*; 10 min). The total amount of protein in the lysates was calculated from the fluorescence-based protein quantitation kit EZQ (Molecular Probes). Proteins were separated on 4–12% polyacrylamide NuPage gels (Invitrogen) and then transferred to nitrocellulose membranes. Membranes were blocked (room temperature, 1 h) with blocking buffer (Rockland Immunochemicals), then incubated at 4°C overnight with primary antibodies [PKG-Iα/β (1:1,000), p-(ser-239)-vasodilator-stimulated phosphoprotein (VASP; 1:500), total VASP (1:1,000), eNOS (1:1,000), p-(ser-1,177)-eNOS (1:1,000), total PARP (1:1,000), and cleaved PARP (1:1,000) (all from Cell Signaling Technology), KLF4 (1:1,000) (Chemicon), NPR-A (1:500), ANP (1:1,000), β-actin (1:1,000) (Santa Cruz Biotechnology)] and subsequently with secondary antibodies labeled with infrared dyes (LI-COR Biosciences) (1:25,000 in blocking buffer; room temperature for 1 h). The membranes were scanned on the Odyssey infrared imaging system (LI-COR Biosciences).

CLONOGENIC CELL SURVIVAL ASSAY

Clonogenic assays were used to assess the cell survival in cells after treatment with sGC inhibitor ODQ, sGC activator YC-1, and selective PKG-Iα inhibitor DT-3 (Calbiochem). Around 500 cells per well were plated in six-well plates, treated with ODQ (10, 40, and 100 μM), YC-1 (5, 10, 20, 40, and 100 μM) and DT-3 (10, 20 and 30 μM) for 24 h. After the incubation period the cells were washed with 1× PBS (Lonza) twice and once with fresh media. Fresh media was added and cells were incubated for 7–10 days to form colonies (or until control wells attain confluency), followed by staining with crystal violet (5 mg/ml crystal violet in 95% ethanol). The number of colonies in the controls and treatments were counted and compared. Acetic acid (10%) was used to dissolve the crystal violet, and the amount of color was quantified with a spectrophotometer at absorbance 570 nm.

ASSESSMENT OF CELL PROLIFERATION BY MTT ASSAY

Proliferation of BMSCs was measured by MTT assay (Roche Applied Science), following the protocol of the manufacturer.

ASSESSMENT OF DE NOVO DNA SYNTHESIS BY BrdU-(5′Bromo-2-deoxyuridine) ELISA COLORIMETRIC ASSAY

The rate of DNA synthesis of BMSCs was measured by BrdU ELISA assay (Roche Applied Science), following protocol of the manufacturer. Cells were seeded in 96-well microplates (1×10^3 cells per well) and incubated at 37°C in 5% CO_2 for 24 h, followed by treatment for 72 h with BrdU label.

ASSESSMENT OF APOPTOSIS BY CELL DEATH DETECTION ELISA PLUS

The Cell Death Detection ELISA^{PLUS} assay (Roche Applied Science), based on quantitative sandwich-enzyme-immunoassay-principle with monoclonal antibodies directed against DNA and histones, were used to quantify apoptotic levels in BMSCs treated with ODQ, SNAP, YC-1, and DT-3 (Calbiochem), 8-Br-cGMP (Sigma) and ANP (Phoenix Pharmaceuticals). Procedures followed the manufacturer's protocol, with the following exception. A longer centrifugation time (i.e., 30 min, instead of the recommended 10 min), after cell permeation for releasing apoptotic fragments of DNA, was used in

order to obtain a cleaner separation of apoptotic DNA fragments from genomic DNA in cell nuclei. This modification dramatically lowered background interference caused by contaminating genomic DNA and thus allowed better quantification of apoptotic responses.

MEASUREMENTS OF cGMP LEVELS BY ENZYME-LINKED-IMMUNOASSAY

Levels of cGMP were measured by an enzyme-linked immunoassay (Assay Designs) as described previously [Wong and Fiscus, 2010].

SMALL INTERFERING RNA (siRNA) GENE KNOCKDOWN

For siRNA-mediated silencing of gene expression, cells were transfected with 50 nmol/L and 100 nmol/L Stealth^{TM} RNAi (siRNA, 5'-GAGGAAGACUUUGCCAAGAUUCUCA-3') for specifically targeting the expression of PKG-Iα (Invitrogen). Transfection of BMSCs was conducted using RNAiMAX (Invitrogen). Non-silencing siRNA (Invitrogen) was used as the negative control. At 72 h after transfection, the culture medium was changed and fresh medium was supplied. The cells were used in experiments 16 h later.

IN VITRO CELL MIGRATION (INVASION) ASSAY

Migration of cells was assessed using transwells (Corning) containing inserts with polycarbonated filter of 8 μM pore size. The inserts were coated with growth factor-reduced matrigel (BD Bioscience) at 37°C for 30 min. The upper chamber contained 4×10^4 cells in 0.1 ml complete medium mixed with inhibitors or DMSO (control). The lower chamber contained 0.6 ml of complete medium with the same concentration of the inhibitors or DMSO. Migration through the membrane was determined after 24 h of incubation at 37°C. Cells remaining on the topside of the transwell membrane were removed using a cotton swab. The membrane was washed with ice-cold PBS. Cells that had migrated to bottom side were stained with 0.5% crystal violet.

STATISTICAL ANALYSIS

Results are expressed as the mean ± standard error of at least four independent experiments. Statistical analysis was performed by one- or two-way ANOVA using GraphPad (PRISM software). Bartlett's tests were used to establish the homogeneity of variance on the basis of the differences among standard deviations. Differences between experimental groups were determined by the Dunnett's test. A value of $P < 0.05$ was considered to be significant.

RESULTS

To investigate the role of endogenous ANP and the NO/cGMP/PKG-Iα signaling pathway in regulating BMSC survival and proliferation, inhibitors and activators of the signaling pathway as well as gene knockdown, utilizing siRNA, were used in the present study, as illustrated in Figure 1.

OP9 CELLS PREDOMINANTLY EXPRESS THE PKG-Iα ISOFORM AND EXPRESS ENDOGENOUS eNOS AND KLF4

Both PKG-Iα (~76 kDa) and PKG-Iβ (~78 kDa) are highly expressed in freshly isolated aorta, as showed by our recent study [Wong and Fiscus, 2010], and another report [Geiselhoringer et al., 2004] on PKG isoforms in mouse tissues. Figure 2A of the present study shows that OP9 cells express predominantly the PKG-Iα isoform. Freshly isolated mouse aorta was used as a positive control. BMSCs also express eNOS and have basal eNOS phosphorylation at serine 1,177, suggesting that endogenous eNOS in BMSCs may provide endogenous NO for downstream activation of the sGC/cGMP/PKG-Iαsignaling pathway for protection against spontaneous apoptosis. BMSCs also express the Kruppel-like factor 4 (KLF4), necessary for survival and proliferation of stem cells, which has previously been shown to bind to the Sp1 promoter of the PKG-Iα gene for regulation of PKG-Iα expression in VSMCs [Zeng et al., 2006].

THE ANP AUTOCRINE LOOP FOR BOTH PROTECTION AGAINST SPONTANEOUS APOPTOSIS AS WELL AS STIMULATION OF CELL PROLIFERATION

Figure 2A shows that OP9 BMSCs express both ANP and the ANP receptor NPR-A, and Figure 2B shows the effects on apoptotic levels of blocking the NPR-A receptors on the surface of BMSCs with the specific ANP antagonist, A71915, which caused significantly higher levels of spontaneous apoptosis. A71915, when used in combination with sGC inhibitor ODQ (which blocks the cytoprotective effects contributed by endogenous NO), causes an even larger increase in apoptosis. Blocking the NPR-A receptors also significantly inhibits proliferation and DNA synthesis (Fig. 2C,D). The data suggest that BMSCs endogenously produce the natriuretic peptide ANP, which in turn causes downstream activation of the cGMP/PKG-Iα pathway. BMSCs may utilize the

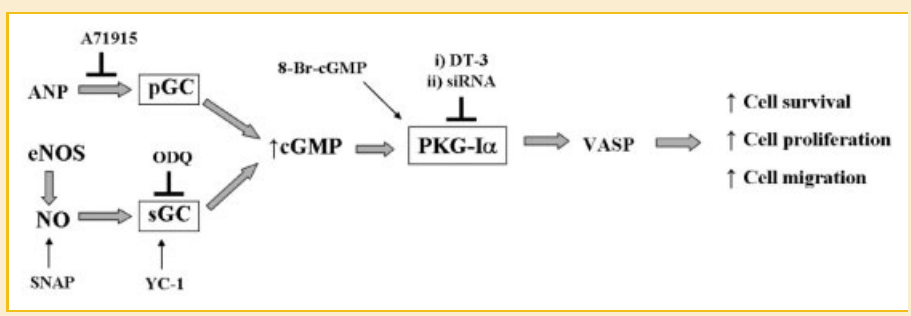

Fig. 1. The NO/sGC/cGMP/PKG-Iα and ANP/pGC(NPR-A)/cGMP/PKG-Iαsignaling pathway are shown, along with the inhibitors and activators used in the present study.

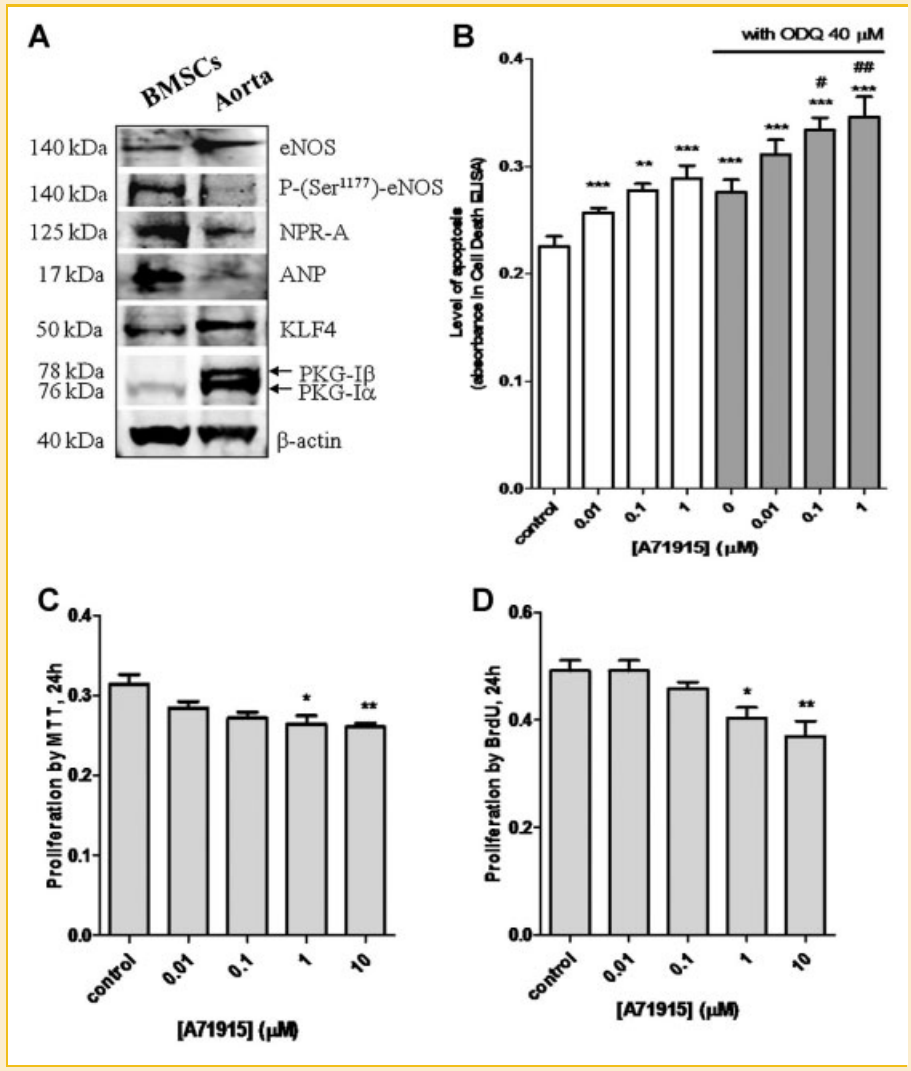

Fig. 2. A: Western blot analysis of the expression of eNOS, phosphorylation of eNOS at Ser-1177, and the expression of NPR-A, ANP precursor, KLF4, and PKG-Iα and PKG-Iβ in OP9 BMSCs and freshly isolated mouse aorta. Total protein (60 μg) was loaded for BMSCs and 20 μg of total protein for the aorta. β-actin was used for normalization. B: Effects on apoptotic levels of blocking the NPR-A receptors with the ANP antagonist A71915 and in combinations with ODQ. *Treatment groups compared with control ($^{*}P<0.05$, $^{**}P<0.01$, $^{***}P<0.001$). #Treatment groups of A71915 used with ODQ compared to the corresponding concentration of A71915 without ODQ ($^{\#}P<0.05$, $^{\#\#}P<0.01$). C and D: Effects on proliferation and DNA synthesis observed from blocking the NPR-A receptors with A71915. Proliferation rates of BMSCs were significantly decreased by A71915 at 1 μM ($^{*}P<0.05$) and 10 μM ($^{**}P<0.01$). The data represent the mean ± SEM of four observations per treatment group.

ANP autocrine loop for both protection against spontaneous apoptosis as well as stimulation of cell proliferation.

BASAL NO/cGMP LEVELS PROTECT BMSCs AGAINST SPONTANEOUS APOPTOSIS

Figure 3A–C shows the effects of a soluble guanylyl cyclase (sGC) inhibitor, ODQ, the NO donor SNAP and the sGC activator YC-1 on the levels of cGMP in OP9 cells. Figure 3D shows a biphasic apoptotic curve in response to increasing concentrations of SNAP. ODQ causes concentration-dependent depletion of basal cGMP levels (Fig. 3A) and apoptosis (Fig. 3D). SNAP is known to release NO at a slow rate, generating NO at a concentration at 0.1% [Crow and Beckman, 1995] to 0.3% [Hirota et al., 2001] of the original SNAP concentration. SNAP at 10 and 50 μM generate NO at 10–50 nM (physiological levels), significantly decreasing the levels of apoptosis, whereas SNAP at 500 and 1,000 μM would generate NO at pathological levels, significantly increasing the levels of apoptosis. YC-1, a sGC activator, at 10 μM to 40 μM, causes ~1.5- to 2-fold increases in cGMP levels and significantly protects BMSCs against spontaneous apoptosis (Fig. 3E). Figure 3F shows ODQ-induced inhibition of endogenous NO-stimulated sGC activity lowers endogenous PKG kinase activity, indicated by Ser239 phosphorylation of VASP. The level of VASP-serine239 phosphorylation was known to be a representation of intracellular PKG activity. Cleaved PARP indicated apoptosis, which confirmed the results from Cell Death ELISA. The data suggest that the basal activation of the NO/cGMP/PKG-Iα signaling pathway in BMSCs is important for protecting against spontaneous onset of apoptosis.

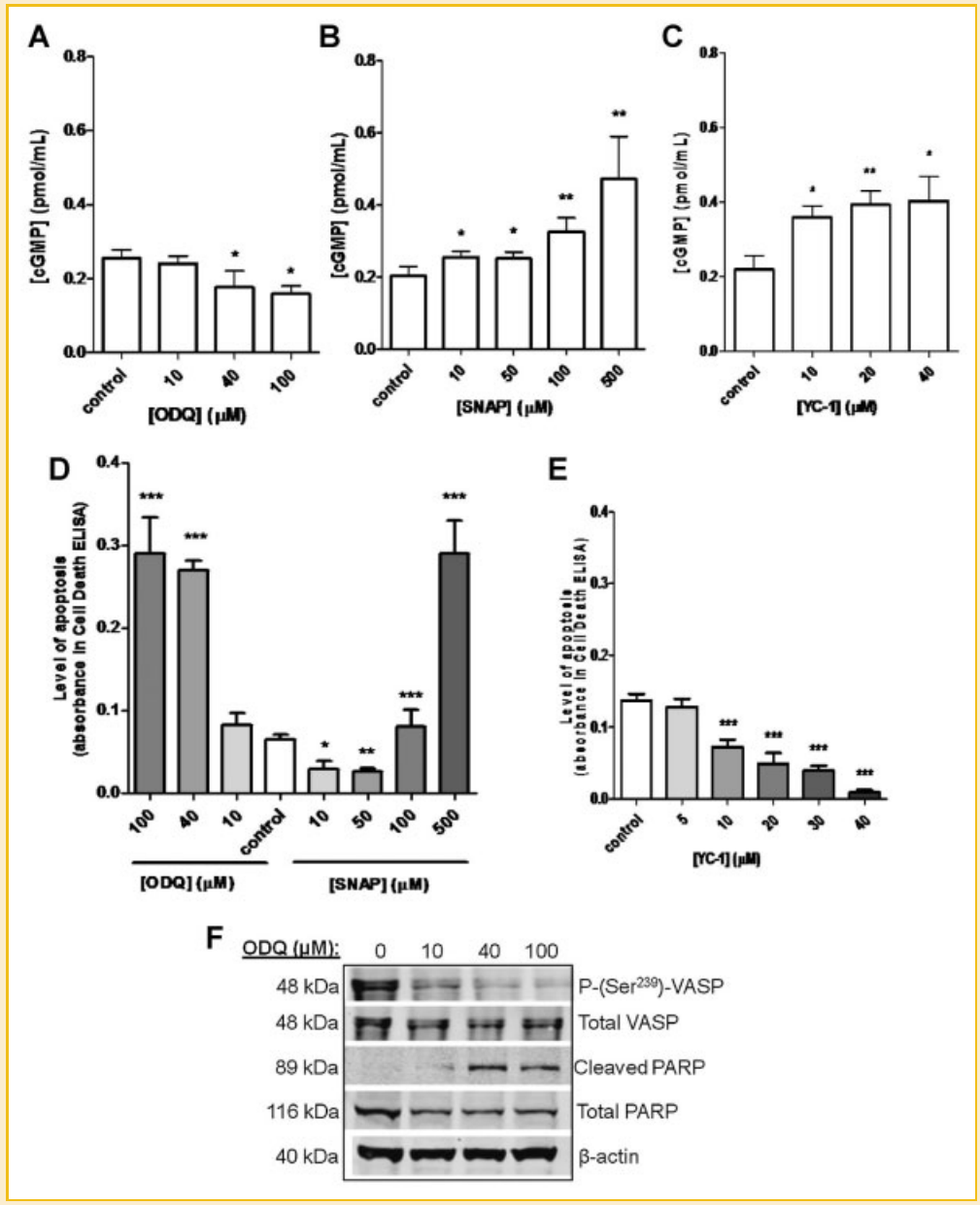

Fig. 3. A: ODQ significantly decreased cGMP levels at 40 and 100 μM ($^{*}P < 0.05$) in BMSCs. B and C: SNAP and YC-1 significantly elevated cGMP levels in BMSCs in a concentration-dependent manner. D: Biphasic apoptotic curve in BMSCs treated with ODQ and SNAP. ODQ, a sGC inhibitor, depleted basal cGMP levels and caused apoptosis at 40 μM ($^{***}P < 0.001$) and 100 μM ($^{***}P < 0.001$), respectively. SNAP, a NO donor, protected cells from apoptosis at 10 μM ($^{*}P < 0.05$) and 50 μM ($^{**}P < 0.01$) and caused apoptosis at 500 μM ($^{***}P < 0.001$). E: YC-1, a sGC activator, protects cells from apoptosis dose dependently from 10 μM to 40 μM ($^{***}P < 0.001$). The data represent the mean ± SEM of six observations per treatment group. F: Western blot analysis showing decreased VASP-phosphorylation at serine239 and increased PARP cleavage in BMSCs treated with ODQ. $^{*}P < 0.05$, $^{**}P < 0.01$, $^{***}P < 0.001$.

These results are consistent with our data in VSMCs [Wong and Fiscus, 2010].

BASAL cGMP LEVELS STIMULATE CELL PROLIFERATION/COLONY FORMATION/MIGRATION

Figure 4A shows that depletion of cGMP by the sGC inhibitor ODQ decreased cell proliferation in MTT assay at 10, 40, 100 μM ($^{***}P < 0.001$). ODQ also inhibits cell migration (Fig. 4C) and colony formation (Fig. 4E,G), suggesting that endogenous PKG-Iα kinase activity (Ser239 phosphorylation of VASP) may play a role in cell migration. The sGC activator YC-1 also inhibited cell proliferation (Fig. 4B), migration (Fig. 4D), and colony formation (Fig. 4F,H), likely via effects unrelated to cGMP (see Discussion).

PRETREATMENT WITH ANP OR 8-Br-cGMP, WHICH BYPASS THE ODQ BLOCK, REVERSES THE ODQ-INDUCED INCREASE IN APOPTOSIS IN BMSCs

The role of PKG-Iα as an important part of the anti-apoptotic/cytoprotective mechanism was confirmed by Figure 5A, showing

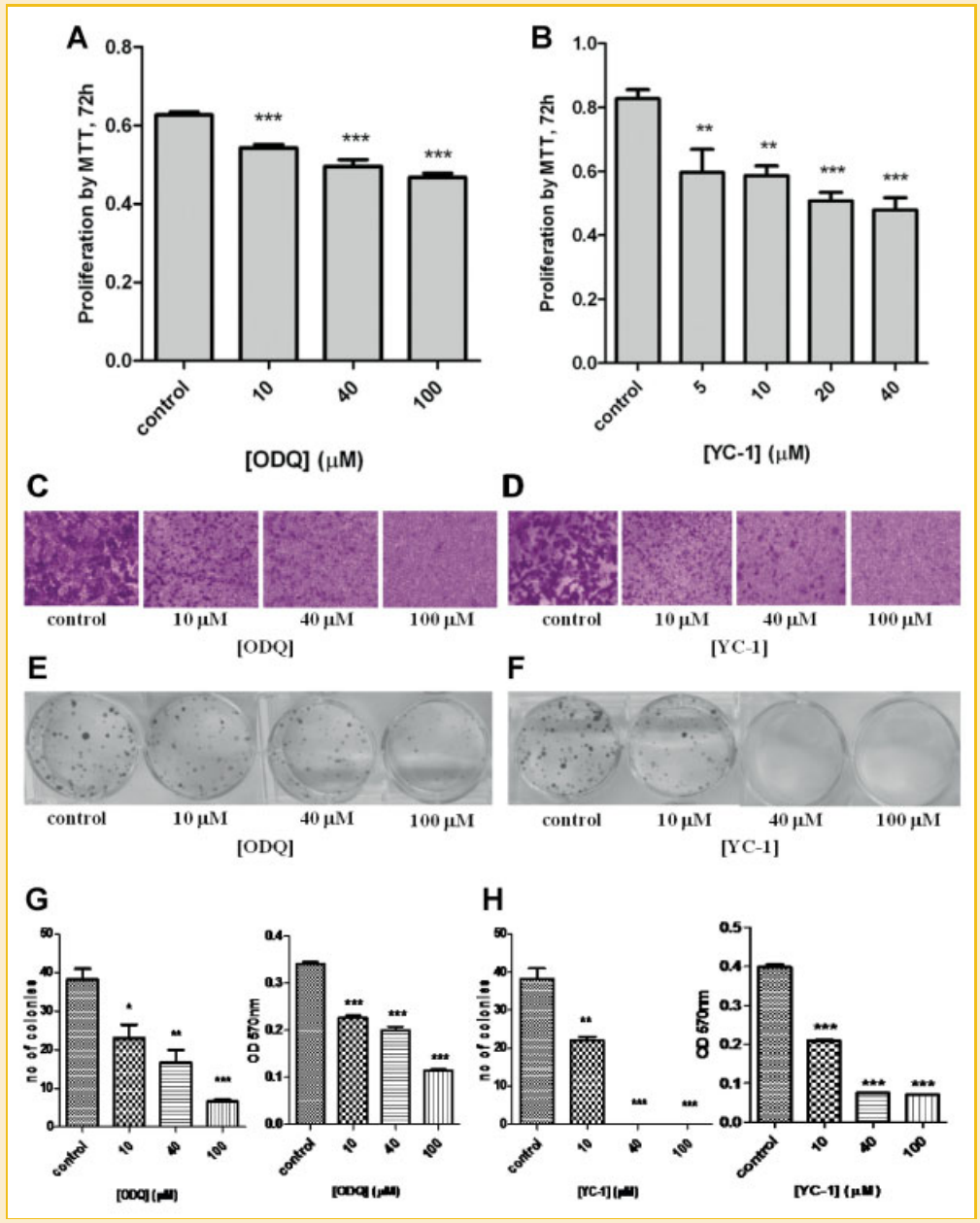

Fig. 4. Cell proliferation, migration, and colony formation were decreased in BMSCs by ODQ and YC-1. A: ODQ inhibits cell proliferation in MTT assay at 10 μM ($^{***}P < 0.001$), 40 μM ($^{***}P < 0.001$), and 100 μM ($^{***}P < 0.001$). B: YC-1 inhibits cell proliferation in MTT assay at 5 μM ($^{**}P < 0.01$), 10 μM ($^{**}P < 0.01$), 20 μM ($^{***}P < 0.001$), and 40 μM ($^{***}P < 0.001$). C and D: Pictures of the cells that have migrated to the bottom of transwell inserts, using staining with crystal violet. The data show inhibition of cell migration by treatment with ODQ and YC-1. E and F: Pictures of colonies formed in six-well plates follows the staining with crystal violet. G and H: Left panel, number of colonies counted (only colonies larger than 500 cells were counted); Right panel, quantification of the crystal violet dye dissolved with 10% acetic acid at 570 nm. The data represent the mean ± SEM of eight observations per treatment group. $^{*}P < 0.05$, $^{**}P < 0.01$, $^{***}P < 0.001$.

that simultaneous addition by 8-bromo-cGMP, a cell-permeable direct activator of PKG-Iα, could almost completely reverse the pro-apoptotic effects of ODQ. Figure 5B shows that exposure of the BMSCs to the natriuretic peptide ANP also causes nearly complete reversal of the ODQ-induced apoptosis. The data further confirm that ANP-induced activation of the NPR-A/cGMP/PKG-Iα signaling pathway can protect (almost completely) the BMSCs from the pro-apoptotic effects of ODQ. The data suggest that BMSCs utilize both sGC, which is stimulated by endogenously-produced NO, and NPR-A (a particulate guanylyl cyclase), which is stimulated by endogenously-produced ANP, to protect against spontaneous onset of apoptosis.

BASAL PKG-Iα ACTIVITY IN BMSCs PROTECTS AGAINST INDUCTION OF APOPTOSIS

To further investigate the anti-apoptotic role of PKG-Iα in BMSCs, a specific PKG-Iαinhibitor, DT-3, was used. DT-3 can effectively inhibit not only stimulated PKG activity, but also basal PKG activity

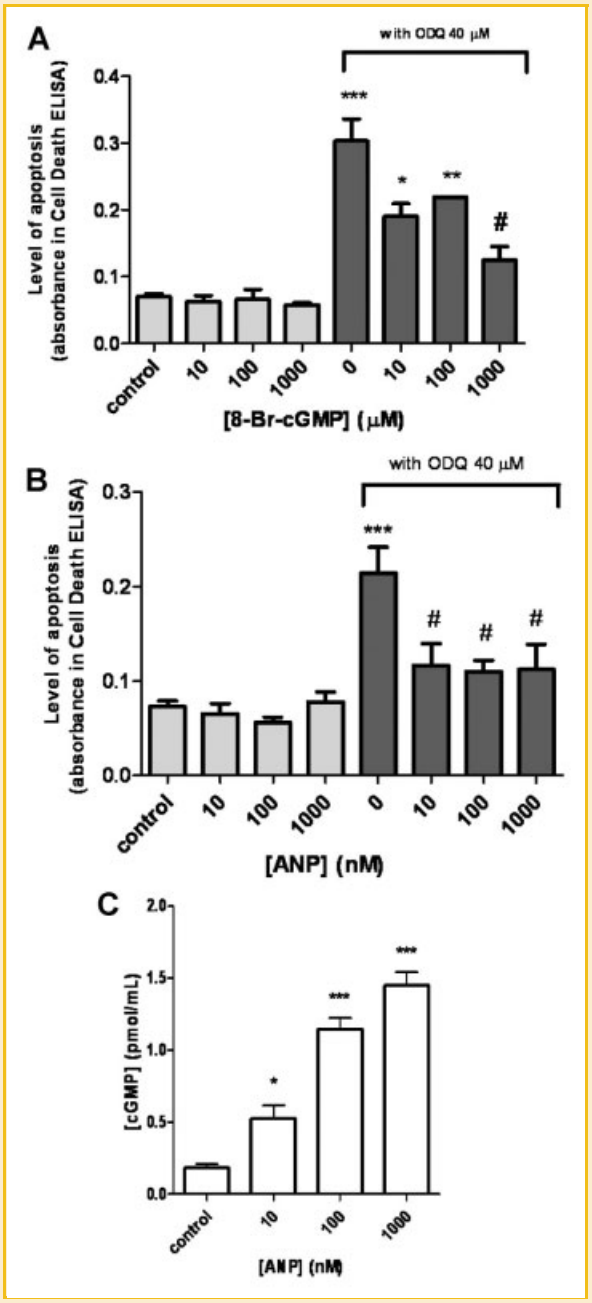

Fig. 5. A: 8-Br-cGMP reverses the ODQ-induced increase in apoptosis in BMSCs. 8-Br-cGMP, at 1,000 μM ($^{\#}P < 0.05$), a direct activator of PKG, prevented apoptosis caused by depletion of cGMP by ODQ (40 μM). B: ANP completely abolished the ODQ-induced apoptosis in BMSCs. ANP at 10 nM ($^{\#}P < 0.05$), 100 nM ($^{\#}P < 0.05$) and 1,000 nM ($^{\#}P < 0.05$), a particulate guanylyl cyclase activator, completely prevented ODQ-induced apoptosis. C: ANP elevated cGMP levels in BMSCs in a concentration-dependent manner. The data represent the mean ± SEM of four observations per treatment group. *Treatment groups compared with control ($^{*}P < 0.05$, $^{**}P < 0.01$, $^{***}P < 0.001$). #Treatment groups compared with ODQ (40 μM) alone.

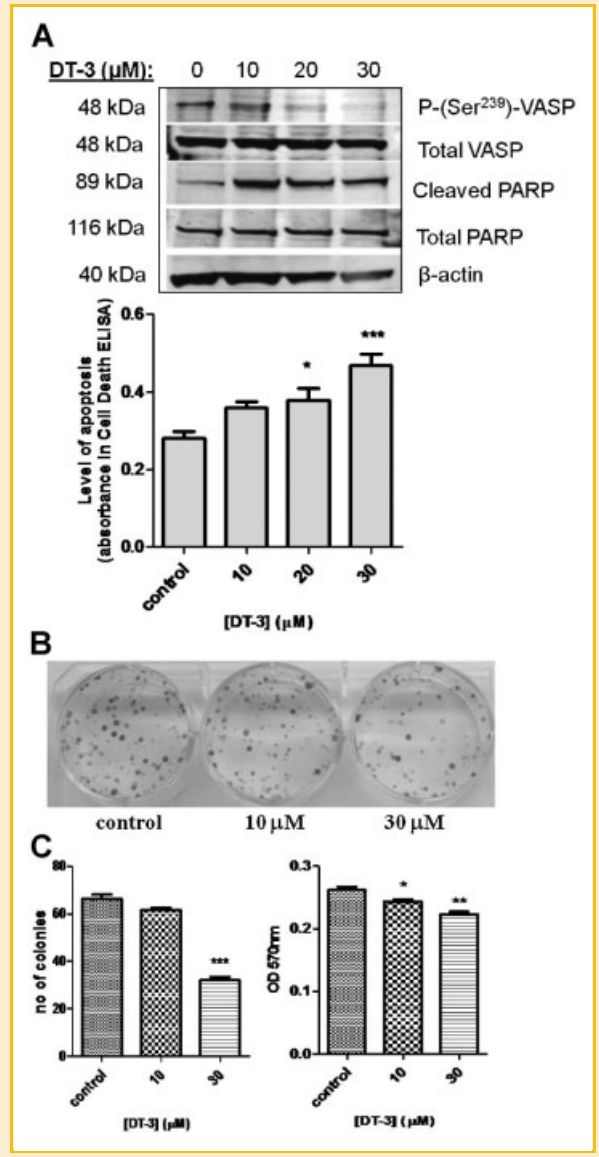

Fig. 6. Inhibition of endogenous PKG activity caused induction of apoptosis, inhibition of cell proliferation and colony formation in BMSCs. A: Upper panel, Western blot analysis showing decreased VASP-phosphorylation at serine239 and increased PARP cleavage in BMSCs treated with DT-3, a PKG-Iα inhibitor; Lower panel, DT-3 significantly induced apoptosis (determined by Cell Death Detection ELISA) at 20 μM ($^{*}P < 0.05$) and 30 μM ($^{***}P < 0.001$). B: Pictures showing DT-3 decreased colony formation in BMSCs. C, Left, number of colonies counted (only colonies larger than 500 cells were counted); Right, quantification of the crystal violet dye dissolved with 10% acetic acid at 570 nm. The data represent the mean ± SEM of four observations per treatment group. $^{*}P < 0.05$, $^{**}P < 0.01$, $^{***}P < 0.001$.

[Dostmann et al., 2002; Taylor et al., 2004]. Western blot analysis in Figure 6 shows DT-3 effectively decreased VASP-phosphorylation at serine239, an indication of intracellular PKG kinase activity. DT-3 also significantly induced apoptosis at 20 μM ($^{*}P < 0.05$) and 30 μM ($^{***}P < 0.001$), apoptosis results confirmed by increased PARP cleavage (Fig. 6A). PKG-Iα-siRNA at 100 nM increased apoptosis (Fig. 7B). Apoptosis results were confirmed by increased PARP cleavage (Fig. 7D). PKG-Iα-siRNA at 50 nM and 100 nM cause approximately 40% and 60% knockdown of PKG expression, as shown by Western blot analysis (Fig. 7C). PKG-Iα-siRNA at 50 nM and 100 nM both effectively decreased intracellular PKG kinase activity (VASP-phosphorylation at serine239) (Fig. 7D).

BASAL PKG ACTIVITY IN BMSCs STIMULATES CELL PROLIFERATION, COLONY FORMATION, AND CELL MIGRATION

Figure 6B,C show that DT-3 decreased colony formation in BMSCs. The result is further confirmed by PKG-Iα knockdown in Figure 7A. PKG-Iα-siRNA at 50 nM and 100 nM also decreased cell migration (Fig. 7E). PKG-Iα knockdown with PKG-Iα-siRNA (100 nM) decreased de novo DNA synthesis (Fig. 7F) and proliferation (Fig. 7G) at 24, 48, and 72 h, respectively. The data suggest that basal PKG activity in BMSCs is essential for stimulating cell proliferation and cell migration.

DISCUSSION

BMSCs are adherent, fibroblast-like cells in the adult bone marrow [Friedenstein et al., 1968]. BMSCs are multipotent stem cells, and are capable of differentiating along the mesenchymal lineage to form bone, fat, and cartilage. Hence, over recent years, the potential for the use of BMSCs in stem cell therapy for replacing damaged bone, cartilage, and muscle, especially, for example, cardiac muscle after heart attack, have been implicated [Psaltis et al., 2008]. The BMSC line OP9 has been used in coculture systems as a feeder layer with mouse ES cells and iPS cells to induce the differentiation of ES cells and iPS cells along hematopoietic lineages [Nakano et al., 1994; Nakano, 1995; Kitajima et al., 2003; Ji et al., 2008]. OP9 cells can also be differentiated into adipocytes and used as a model for adipogenesis [Wolins et al., 2006].

Our early studies were the first to show that NO, both therapeutically-administered NO and endogenous endothelium-derived NO, stimulates the intracellular activity of PKG in VSMCs [Fiscus et al., 1983], and that ANP stimulates intracellular PKG in VSMCs [Fiscus et al., 1985]. These studies led to later establishment of PKG as the key protein kinase mediating the biological effects (e.g., vasodilation and anti-hypertensive effects) of NO and the natriuretic peptides [Fiscus, 1988, 2002; Fiscus and Murad, 1988; Lincoln et al., 2001; Fung et al., 2005]. Recently, our laboratory has shown that many mammalian cells, including epithelial cells, neural cells, and various cancer cells (e.g., breast cancer, lung cancer, mesothelioma, ovarian cancer, prostate cancer, and VSMCs), all express at least one or both of the two PKG-I isoforms, PKG-Iα and PKG-Iβ, and that the PKG-Iα isoform is essential for the survival and proliferation of these cells [Fiscus et al., 2001, 2002; Fiscus, 2002; Chan and Fiscus, 2003; Cheng Chew et al., 2003; Fung et al., 2005; Fraser et al., 2006; Leung et al., 2008, 2010; Johlfs and Fiscus, 2010; Wong and Fiscus, 2010].

The present study shows that phosphorylation of VASP at serine 239 serves as a useful indicator of endogenous PKG activity in the BMSCs. VASP is a PKG downstream substrate that is directly phosphorylated at Ser239 by PKG in a number of mammalian cells [Butt et al., 1994; Chen et al., 2008; Isenberg et al., 2008], but the present study shows PKG-mediated phosphorylation of VASP in BMSCs for the first time. VASP is an actin-binding protein involved in focal adhesion [Butt et al., 1994], and VASP phosphorylation at ser239 by PKG was shown to cause redistribution of VASP to the plasma membrane, and thereby may promote cell attachment and migration, potentially also promoting cell survival and proliferation [Harbeck et al., 2000; Li Calzi et al., 2008].

Human BMSCs have been reported to synthesize and release endogenous brain (B-type) natriuretic peptide (BNP) and the released BNP was proposed to mediate the neuroprotective effects of BMSCs in animal model of stroke [Song et al., 2004]. The present study using OP9 BMSCs shows that these cells produce detectable levels of ANP precursor [Noyan-Ashraf et al., 2009] (Fig. 2A), suggesting that these cells likely synthesize and release ANP, similar to the data of a previous study showing endogenous production of another natriuretic peptide, BNP, in human BMSCs [Song et al., 2004], and that released ANP activates the NPR-A receptors to stimulate cell proliferation and survival of the OP9 cells. This mechanism may provide an autocrine loop that protects BMSCs from spontaneous apoptosis and stimulates cell proliferation.

The present study suggests that basal activation of the NO/cGMP/PKG-Iα signaling pathway in BMSCs is important for cell proliferation, colony formation and migration. However, the sGC activator YC-1 also inhibited cell proliferation (Fig. 4B), migration (Fig. 4D), and colony formation (Fig. 4F,H). These anti-proliferative, anti-colony formation, and anti-migration effects are likely to be mediated by other effects of YC-1 (which are independent of cGMP) [Pan et al., 2005]. In another example, YC-1 has been shown to have anti-proliferative effects in hepatocellular carcinoma cells by a mechanism that is independent of its effects on the cGMP signaling pathway and instead involves YC-1-induced up-regulation of $p21^{CIP1/wap1}$ [Wang et al., 2005].

Figure 8 shows a cellular model illustrating the findings of the present study. Also included in the model are the phosphorylation of other downstream target proteins, BAD [Johlfs and Fiscus, 2010], CREB [Fiscus, 2002], and Src [Leung et al., 2010], previously reported by our laboratory as intracellular proteins that are directly phosphorylated by PKG-Iα promoting cell proliferation and survival. The data from the present study suggest that BMSCs utilize both the NO/sGC/cGMP/PKG-Iα pathway and the ANP/NPR-A/cGMP/PKG-Iα pathway, in an autocrine loop fashion, to protect the cells from spontaneous onset of apoptosis and to stimulate cell proliferation. Furthermore, the present study shows that these signaling pathways promote migration of the OP9 BMSCs, shown in the model of Figure 8. In the bone marrow micro-environmental niche, endothelial cells, which are in close proximity to BMSCs,

Fig. 7. Gene knockdown of PKG-Iα expression using PKG-Iα-siRNA increased apoptosis and decreased proliferation in BMSCs. A: PKG-Iα knockdown decreased BMSC colony formation. B: Gene knockdown by PKG-Iα-siRNA (100 nM) significantly ($^{**}P < 0.01$) increased spontaneous apoptosis compared to negative control. C: Western blot analysis showing decreased PKG-Iα expression after treatment with PKG-Iα-siRNA. The relative intensity of the bands in the western blots were quantified, showing about 40% and 60% knockdown at 50 nM and 100 nM, respectively. D: Western blot analysis showing decreased VASP-phosphorylation at serine239 and increased PARP cleavage in BMSCs after gene knockdown of PKG-Iα. E: PKG-Iα knockdown decreased cell migration. F and G, PKG-Iα knockdown decreased de novo DNA synthesis at 48 h ($^{*}P < 0.05$) and 72 h ($^{**}P < 0.01$) in cultures treated with PKG-Iα-siRNA (100 nM). Similar results obtained by MTT assay. PKG-Iα knockdown decreased proliferation at 24 h ($^{***}P < 0.001$), 48 h ($^{***}P < 0.001$), and 72 h ($^{***}P < 0.001$). The data represent the mean ± SEM of six observations per treatment group.

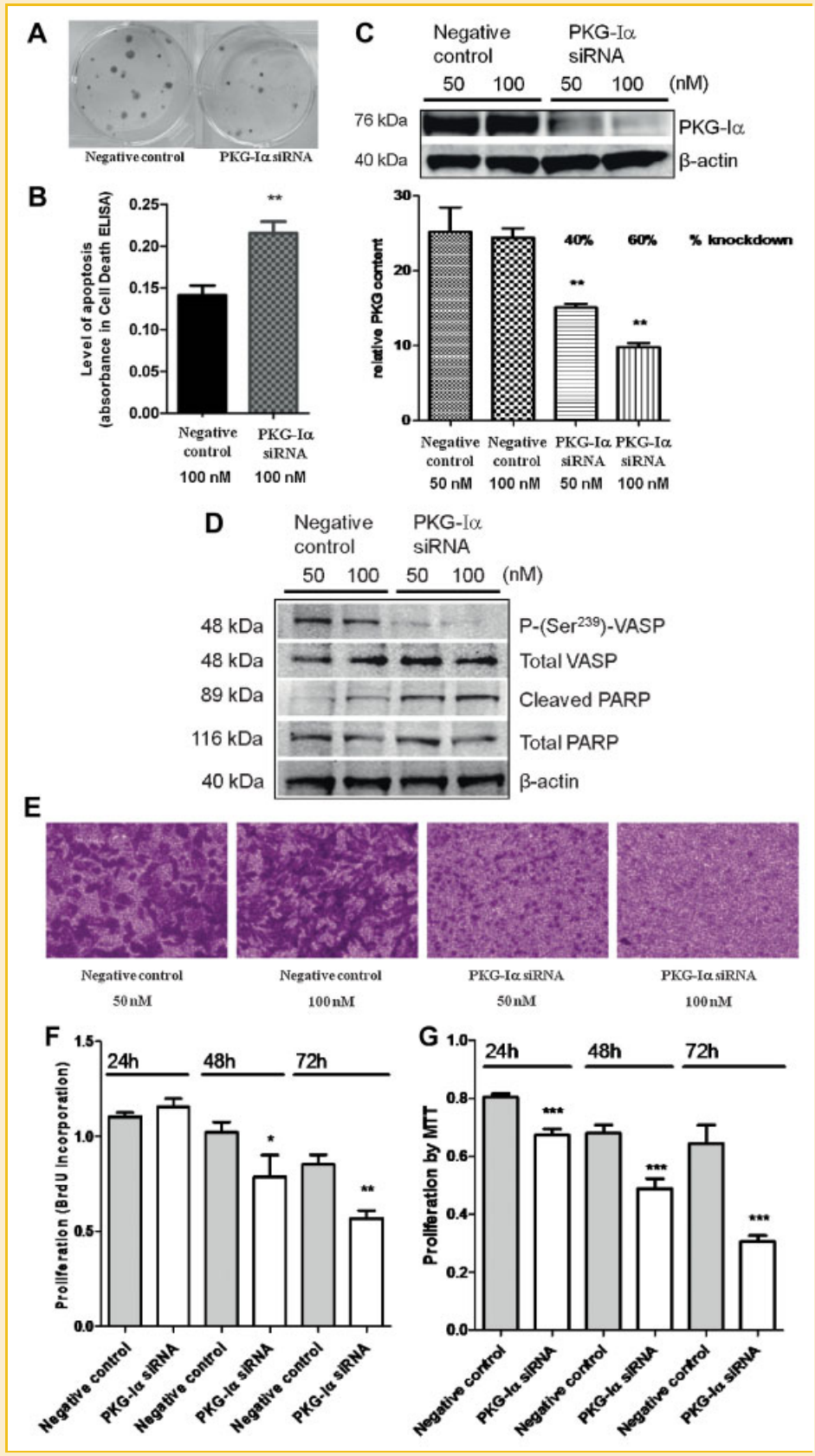
A
Negative control
PKG-Iα siRNA
B
Level of apoptosis (absorbance in Cell Death ELISA)
0.25
0.20
0.15
0.10
0.05
0.00
**
Negative control
PKG-Iα siRNA
100 nM
100 nM
C
Negative control
PKG-Iα siRNA
50
100
50
100
(nM)
76 kDa
40 kDa
PKG-Iα
β-actin
relative PKG content
30
20
10
0
40%
60%
% knockdown
**
**
Negative control
Negative control
PKG-Iα siRNA
PKG-Iα siRNA
50 nM
100 nM
50 nM
100 nM
D
Negative control
PKG-Iα siRNA
50
100
50
100
(nM)
48 kDa
48 kDa
89 kDa
116 kDa
40 kDa
P-(Ser239)-VASP
Total VASP
Cleaved PARP
Total PARP
β-actin
E
Negative control
50 nM
Negative control
100 nM
PKG-Iα siRNA
50 nM
PKG-Iα siRNA
100 nM
F
Proliferation (BrdU incorporation)
1.5
1.0
0.5
0.0
24h
48h
72h
*
**
Negative control
PKG-Iα siRNA
Negative control
PKG-Iα siRNA
Negative control
PKG-Iα siRNA
G
Proliferation by MTT
1.0
0.8
0.6
0.4
0.2
0.0
24h
48h
72h
***
***
***
Negative control
PKG-Iα siRNA
Negative control
PKG-Iα siRNA
Negative control
PKG-Iα siRNA

Fig. 7.

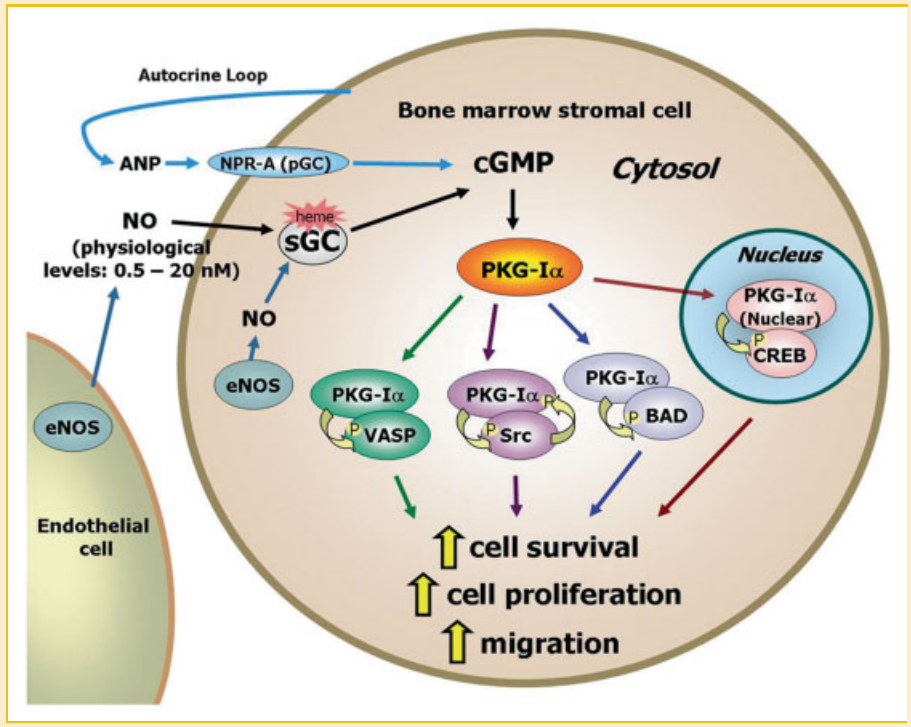

Fig. 8. The overall model illustrating the findings of the present study. BMSCs utilize the NO/sGC/cGMP/PKG-Iα signaling pathway as well as the ANP/pGC(NPR-A)/cGMP/PKG-Iα signaling pathway to stimulate cell proliferation and inhibit spontaneous onset of apoptosis. ANP released from BMSCs may participate in a novel autocrine loop mechanism for regulating BMSC survival and proliferation. Also, natriuretic peptides and NO, released from nearby endothelial cells in the bone marrow stroma, may also participate as a paracrine mechanism regulating BMSC survival and proliferation.

provide another source of endogenous NO. Also, endothelial cells are reported to synthesize and release all three natriuretic peptides, ANP, BNP, and CNP [Bordenave et al., 2002], which may also potentially stimulate BMSC survival and proliferation via a paracrine mechanism. Therefore, the cytoprotective and growth-promoting mechanism involving the NO/sGC/cGMP/PKG-Iα and ANP/NPR-A/cGMP/PKG-Iα pathways may play an important role within the bone marrow to provide a healthy micro-environmental niche for the survival, growth, and differentiation of HSCs. Furthermore, the data of the present study provide a unique insight into a key cell signaling pathway in OP9 cells that could be used to develop new strategies for improving ex vivo survival and expansion of these cells or similar cells.

REFERENCES

Bordenave L, Georges A, Bareille R, Conrad V, Villars F, Amedee J. 2002. Human bone marrow endothelial cells: A new identified source of B-type natriuretic peptide. Peptides 23:935–940.

Butt E, Abel K, Krieger M, Palm D, Hoppe V, Hoppe J, Walter U. 1994. cAMP- and cGMP-dependent protein kinase phosphorylation sites of the focal adhesion vasodilator-stimulated phosphoprotein (VASP) in vitro and in intact human platelets. J Biol Chem 269:14509–14517.

Caplan AI. 1991. Mesenchymal stem cells. J Orthop Res 9:641–650.

Chan SL, Fiscus RR. 2003. Guanylyl cyclase inhibitors NS2028 and ODQ and protein kinase G (PKG) inhibitor KT5823 trigger apoptotic DNA fragmentation in immortalized uterine epithelial cells: Anti-apoptotic effects of basal cGMP/PKG. Mol Hum Reprod 9:775–783.

Charles N, Ozawa T, Squatrito M, Bleau AM, Brennan CW, Hambardzumyan D, Holland EC. 2010. Perivascular nitric oxide activates notch signaling and promotes stem-like character in PDGF-induced glioma cells. Cell Stem Cell 6:141–152.

Chen H, Levine YC, Golan DE, Michel T, Lin AJ. 2008. Atrial natriuretic peptide-initiated cGMP pathways regulate vasodilator-stimulated phosphoprotein phosphorylation and angiogenesis in vascular endothelium. J Biol Chem 283:4439–4447.

Cheng Chew SB, Leung PY, Fiscus RR. 2003. Preincubation with atrial natriuretic peptide protects NG 108–15 cells against the toxic/proapoptotic effects of the nitric oxide donor S-nitroso- N-acetylpenicillamine. Histochem Cell Biol 120:163–171.

Crow JP, Beckman JS. 1995. Reactions between nitric oxide, superoxide, and peroxynitrite: Footprints of peroxynitrite in vivo. Adv Pharmacol 34:17–43.

Dostmann WR, Tegge W, Frank R, Nickl CK, Taylor MS, Brayden JE. 2002. Exploring the mechanisms of vascular smooth muscle tone with highly specific, membrane-permeable inhibitors of cyclic GMP-dependent protein kinase Ialpha. Pharmacol Ther 93:203–215.

Fiscus RR. 1988. Molecular mechanisms of endothelium-mediated vasodilation. Semin Thromb Hemost 14(Suppl.):12–22.

Fiscus RR. 2002. Involvement of cyclic GMP and protein kinase G in the regulation of apoptosis and survival in neural cells. Neurosignals 11:175–190.

Fiscus RR, Murad F. 1988. cGMP-dependent protein kinase activation in intact tissues. Methods Enzymol 159:150–159.

Fiscus RR, Rapoport RM, Murad F. 1983. Endothelium-dependent and nitrovasodilator-induced activation of cyclic GMP-dependent protein kinase in rat aorta. J Cyclic Nucleotide Protein Phosphor Res 9:415–425.

Fiscus RR, Rapoport RM, Waldman SA, Murad F. 1985. Atriopeptin II elevates cyclic GMP, activates cyclic GMP-dependent protein kinase and causes relaxation in rat thoracic aorta. Biochim Biophys Acta 846:179–184.

Fiscus RR, Tu AW, Chew SB. 2001. Natriuretic peptides inhibit apoptosis and prolong the survival of serum-deprived PC12 cells. Neuroreport 12:185–189.

Fiscus RR, Yuen JP, Chan SL, Kwong JH, Chew SB. 2002. Nitric oxide and cyclic GMP as pro- and anti-apoptotic agents. J Card Surg 17:336–339.

Fraser M, Chan SL, Chan SS, Fiscus RR, Tsang BK. 2006. Regulation of p53 and suppression of apoptosis by the soluble guanylyl cyclase/cGMP pathway in human ovarian cancer cells. Oncogene 25:2203–2212.

Friedenstein AJ, Petrakova KV, Kurolesova AI, Frolova GP. 1968. Heterotopic of bone marrow. Analysis of precursor cells for osteogenic and hematopoietic tissues. Transplantation 6:230–247.

Fung E, Fiscus RR, Yim AP, Angelini GD, Arifi AA. 2005. The potential use of type-5 phosphodiesterase inhibitors in coronary artery bypass graft surgery. Chest 128:3065–3073.

Geiselhoringer A, Gaisa M, Hofmann F, Schlossmann J. 2004. Distribution of IRAG and cGKI-isoforms in murine tissues. FEBS Lett 575:19–22.

Harbeck B, Huttelmaier S, Schluter K, Jockusch BM, Illenberger S. 2000. Phosphorylation of the vasodilator-stimulated phosphoprotein regulates its interaction with actin. J Biol Chem 275:30817–30825.

Hassan HT, El-Sheemy M. 2004. Adult bone-marrow stem cells and their potential in medicine. J R Soc Med 97:465–471.

Hirota Y, Ishida H, Genka C, Obama R, Matsuyama S, Nakazawa H. 2001. Physiological concentration of nitric oxide induces positive inotropic effects through cGMP pathway in isolated rat ventricular myocytes. Jpn J Physiol 51:455–461.

Isenberg JS, Romeo MJ, Yu C, Yu CK, Nghiem K, Monsale J, Rick ME, Wink DA, Frazier WA, Roberts DD. 2008. Thrombospondin-1 stimulates platelet aggregation by blocking the antithrombotic activity of nitric oxide/cGMP signaling. Blood 111:613–623.

Ji J, Vijayaragavan K, Bosse M, Menendez P, Weisel K, Bhatia M. 2008. OP9 stroma augments survival of hematopoietic precursors and progenitors during hematopoietic differentiation from human embryonic stem cells. Stem Cells 26:2485–2495.

Johlfs MG, Fiscus RR. 2010. Protein kinase G type-Ialpha phosphorylates the apoptosis-regulating protein Bad at serine 155 and protects against apoptosis in N1E-115 cells. Neurochem Int 56:546–553.

Kelly MA, Hirschi KK. 2009. Signaling hierarchy regulating human endothelial cell development. Arterioscler Thromb Vasc Biol 29:718–724.

Kitada M, Dezawa M. 2009. Induction system of neural and muscle lineage cells from bone marrow stromal cells; a new strategy for tissue reconstruction in degenerative diseases. Histol Histopathol 24:631–642.

Kitajima K, Tanaka M, Zheng J, Sakai-Ogawa E, Nakano T. 2003. In vitro differentiation of mouse embryonic stem cells to hematopoietic cells on an OP9 stromal cell monolayer. Methods Enzymol 365:72–83.

Krumenacker JS, Murad F. 2006. NO-cGMP signaling in development and stem cells. Mol Genet Metab 87:311–314.

Krumenacker JS, Katsuki S, Kots A, Murad F. 2006. Differential expression of genes involved in cGMP-dependent nitric oxide signaling in murine embryonic stem (ES) cells and ES cell-derived cardiomyocytes. Nitric Oxide 14:1–11.

Leung EL, Fraser M, Fiscus RR, Tsang BK. 2008. Cisplatin alters nitric oxide synthase levels in human ovarian cancer cells: Involvement in p53 regulation and cisplatin resistance. Br J Cancer 98:1803–1809.

Leung EL, Wong JC, Johlfs MG, Tsang BK, Fiscus RR. 2010. Protein kinase G type Ialpha activity in human ovarian cancer cells significantly contributes to enhanced Src activation and DNA synthesis/cell proliferation. Mol Cancer Res 8:578–591.

Li Calzi S, Purich DL, Chang KH, Afzal A, Nakagawa T, Busik JV, Agarwal A, Segal MS, Grant MB. 2008. Carbon monoxide and nitric oxide mediate cytoskeletal reorganization in microvascular cells via vasodilator-stimulated phosphoprotein phosphorylation: Evidence for blunted responsiveness in diabetes. Diabetes 57:2488–2494.

Lincoln TM, Dey N, Sellak H. 2001. Invited review: cGMP-dependent protein kinase signaling mechanisms in smooth muscle: From the regulation of tone to gene expression. J Appl Physiol 91:1421–1430.

Nakano T. 1995. Lymphohematopoietic development from embryonic stem cells in vitro. Semin Immunol 7:197–203.

Nakano T, Kodama H, Honjo T. 1994. Generation of lymphohematopoietic cells from embryonic stem cells in culture. Science 265:1098–1101.

Niwa A, Umeda K, Chang H, Saito M, Okita K, Takahashi K, Nakagawa M, Yamanaka S, Nakahata T, Heike T. 2009. Orderly hematopoietic development of induced pluripotent stem cells via Flk-1(+) hemoangiogenic progenitors. J Cell Physiol 221:367–377.

Noyan-Ashraf MH, Momen MA, Ban K, Sadi AM, Zhou YQ, Riazi AM, Baggio LL, Henkelman RM, Husain M, Drucker DJ. 2009. GLP-1R agonist liraglutide activates cytoprotective pathways and improves outcomes after experimental myocardial infarction in mice. Diabetes 58:975–983.

Pan SL, Guh JH, Peng CY, Wang SW, Chang YL, Cheng FC, Chang JH, Kuo SC, Lee FY, Teng CM. 2005. YC-1 [3-(5'-hydroxymethyl-2'-furyl)-1-benzyl indazole] inhibits endothelial cell functions induced by angiogenic factors in vitro and angiogenesis in vivo models. J Pharmacol Exp Ther 314:35–42.

Psaltis PJ, Zannettino AC, Worthley SG, Gronthos S. 2008. Concise review: Mesenchymal stromal cells: Potential for cardiovascular repair. Stem Cells 26:2201–2210.

Sadan O, Melamed E, Offen D. 2009. Bone-marrow-derived mesenchymal stem cell therapy for neurodegenerative diseases. Expert Opin Biol Ther 9:1487–1497.

Song S, Kamath S, Mosquera D, Zigova T, Sanberg P, Vesely DL, Sanchez-Ramos J. 2004. Expression of brain natriuretic peptide by human bone marrow stromal cells. Exp Neurol 185:191–197.

Taylor MS, Okwuchukwuasanya C, Nickl CK, Tegge W, Brayden JE, Dostmann WR. 2004. Inhibition of cGMP-dependent protein kinase by the cell-permeable peptide DT-2 reveals a novel mechanism of vasoregulation. Mol Pharmacol 65:1111–1119.

Wang SW, Pan SL, Guh JH, Chen HL, Huang DM, Chang YL, Kuo SC, Lee FY, Teng CM. 2005. YC-1 [3-(5'-hydroxymethyl-2'-furyl)-1-benzyl Indazole] exhibits a novel antiproliferative effect and arrests the cell cycle in G0-G1 in human hepatocellular carcinoma cells. J Pharmacol Exp Ther 312:917–925.

Wilson A, Trumpp A. 2006. Bone-marrow haematopoietic-stem-cell niches. Nat Rev Immunol 6:93–106.

Wolins NE, Quaynor BK, Skinner JR, Tzekov A, Park C, Choi K, Bickel PE. 2006. OP9 mouse stromal cells rapidly differentiate into adipocytes: Characterization of a useful new model of adipogenesis. J Lipid Res 47:450–460.

Wong JC, Fiscus RR. 2010. Protein kinase G activity prevents pathological-level nitric oxide-induced apoptosis and promotes DNA synthesis/cell proliferation in vascular smooth muscle cells. Cardiovasc Pathol 19:e221–e231.

Zeng Y, Zhuang S, Gloddek J, Tseng CC, Boss GR, Pilz RB. 2006. Regulation of cGMP-dependent protein kinase expression by Rho and Kruppel-like transcription factor-4. J Biol Chem 281:16951–16961.

RNAi shows PKG type-I promotes Integrin β1 expression, cell attachment and proliferation and prevents spontaneous apoptosis in pleural mesothelioma cells

Mary G. Johlfs, MS and Ronald R. Fiscus, PhD*

Cancer Molecular Biology Section, Nevada Cancer Institute, Las Vegas, NV 89135, USA and College of Pharmacy, University of Southern Nevada, Henderson, NV 89014, USA

*Correspondence: Dr. Ronald R. Fiscus, University of Southern Nevada, Henderson, NV, 89014, USA. Cell: (702) 427-3139, Office: (702) 968-5570, Fax: (702) 968-5573, rfiscus@usn.edu

Abbreviations: PKG, protein kinase G or cGMP-dependent protein kinase; ODQ, 1H-[1,2,4] Oxad-iazolo[4,3-a]quinoxalin-1-one; RNAi, RNA interference; shRNA, Short hairpin RNA; VSMCs, vascular smooth muscle cells; NO, nitric oxide; ANP, atrial natriuretic peptide; eNOS, endothelial nitric oxide synthase; MPM, malignant pleural mesothelioma.

Keywords: Apoptosis, cell proliferation, cell attachment, adhesion, integrin, cGMP-dependent protein kinase, cGMP, PKG, RNA interference.

Introduction

Initially, cyclic GMP-dependent protein kinase (protein kinase G, PKG) was shown to be the key protein kinase activated by nitric oxide (NO) in airway (Fiscus *et al.*, 1984) and vascular smooth muscle cells (Fiscus and Murad, 1988; Fiscus *et al.*, 1983), and was proposed to be the major protein kinase mediating the bronchodilatory and vasodilatory effects of NO. PKG, a serine/threonine kinase, also serves as the main protein kinase activated by atrial natriuretic peptide (ANP, atriopeptin) in vascular smooth muscle cells, mediating ANP-induced vasodilation (Fiscus *et al.*, 1985). In both cases of stimulation, the activation of PKG involves elevations in the intracellular levels of cGMP, an allosteric activator of PKG. PKG has also been shown to be involved in the regulation of platelet aggregation (Massberg *et al.*, 1999; Munzel *et al.*, 2003) and vascular smooth muscle cell (VSMC) proliferation, promoting VSMC proliferation at basal levels of PKG activation (Wong and Fiscus, 2010), but inhibiting VSMC proliferation when PKG is overexpressed or hyperactivated (Chiche *et al.*, 1998; Lincoln *et al.*, 2006).

The effects of NO in mammalian cells are largely dependent on the concentration of this small molecule, the type of cell studied and the environmental conditions (Ridnour *et al.*, 2008). NO has been linked to both the inhibition and the promotion of cancer (Ekmekcioglu *et al.*, 2000; Ekmekcioglu *et al.*, 2006; Hussain *et al.*, 2004; Prueitt *et al.*, 2007). In general, high levels of NO have toxic effects, due in part to the formation of peroxynitrite, a toxic pro-oxidant capable of oxidizing DNA, lipids and proteins (Beckman and Koppenol, 1996). Abnormally high levels of cGMP resulting from pathological levels of NO have also been correlated with cell death in certain types of mammalian cells (Fiscus, 2002; Fiscus *et al.*, 2002; Ridnour *et al.*, 2008). In the photoreceptors in animal models of retinitis pigmentos (Paquet-Durand *et al.*, 2009), toxic effects were a result of severe hyperactivation of the cGMP/PKG signaling pathway caused by a defect in cGMP

degradation, which is characteristic of retinitis pigmentosa. In PC12 cells, cell death in response to high levels of NO is mediated by a mechanism other than hyperactivation of the cGMP/PKG signaling pathway (Wada *et al.*, 1996). In contrast to the toxic effects of high-level NO, lower, physiological levels of NO cause cytoprotective/anti-apoptotic effects in many types of mammalian cells (Fiscus, 2002; Fiscus *et al.*, 2002; Ridnour *et al.*, 2008). This cytoprotective effect of low-level NO is mediated by basal stimulation of soluble guanylyl cyclase activity, which causes moderate increases in cGMP levels and PKG activation. In neural cells, this cytoprotective effect is thought to provide continuous protection against neural cell death, thus limiting the loss of neural cells that may be caused by aging or exposure to stressful conditions, such as inflammation and ischemia (Chiueh *et al.*, 2003; Ciani *et al.*, 2002; Fiscus, 2002; Fiscus *et al.*, 2002).

PKG plays an important role in protecting against apoptosis in many types of mammalian cells, including epithelial cells (Chan and Fiscus, 2003), VSMCs (Wong and Fiscus, 2010), ovarian cancer cells (Leung *et al.*, 2010), B lymphocytes (Kolb, 2000), leukemia cells (Flamigni *et al.*, 2001), rat ovarian follicle (Chun *et al.*, 1995), and many neural cells, including primary cultures of rat hippocampal neurons (Barger *et al.*, 1995), dorsal root ganglion and motor neurons, cerebellar granule cells and PC12 cells (reviewed in Fiscus 2002), as well as N1E-115 and SH-SY5Y human neuroblastoma cells (Chiueh *et al.*, 2003) and NG108-15 neuroblastoma-glioma hybrid cells (Cheng Chew *et al.*, 2003; Fiscus, 2002; Fiscus *et al.*, 2002; Johlfs and Fiscus, 2010). Furthermore, the cGMP pathway has been shown to down regulate p53 in ovarian cancer cells, leading to suppression of apoptosis (Fraser *et al.*, 2006). NO activation of PKG leads to the phosphorylation of specific transcription factors, such as cAMP response element (CRE)-binding protein (CREB), which may contribute to protection from cell death (Fiscus, 2002; Pilz and Casteel, 2003).

Previous studies from our laboratory have shown that PKG, at basal levels of activation, is essential for promoting DNA synthesis and cell proliferation in ovarian cancer cells (Leung *et al.*, 2010). It has also been shown that the cGMP/PKG signaling pathway promotes adhesion of VSMCs via its ability to promote cell-surface expression of integrin β1 (Weinmeister *et al.*, 2008) and NO has been found to upregulate other integrins, such as CD11b in microglial cells (Roy *et al.*, 2006). Adhesion molecules are dysregulated in cancer cells, allowing for growth, migration, and metastasis and are often over-expressed on drug resistant cancer cells and anti-adhesion molecules have recently entered into clinical trials (Schmidmaier and Baumann, 2008). Furthermore, NO- and ANP-induced stimulation of PKG activity triggers subsequent phosphorylation of vasodilator-stimulated phosphoprotein (VASP), which associates with integrin (Lund *et al.*, 2010) and regulates the actin cytoskeleton (Krause *et al.*, 2003; Li Calzi *et al.*, 2008), thus promoting cell proliferation, migration and adhesion.

PKG-I, the focus of this study, can be expressed as two different isoforms, PKG-Iα and PKG-Iβ (Cornwell and Lincoln, 1989; Wolfe *et al.*, 1989). These two isoforms are thought to be a result of alternative splicing and are expressed at various levels, depending on cell type. Placental and lung cells express primarily the PKG-Iα form, whereas urinary bladder, uterus, adrenal gland and fallopian tube cells express primarily PKG-Iβ (Orstavik *et al.*, 1997). Vascular smooth muscle cells express both PKG-Iα and PKG-Iβ, but the expression of the PKG-Iα isoform is typically predominant (Feil *et al.*, 2005; Wong and Fiscus, 2010). Although earlier studies had suggested that PKG expression is absent in many types of cancer cell lines (Hou *et al.*, 2006; Wong *et al.*, 2001), recent studies from our lab have found that PKG-I isoforms are indeed expressed in many types of cancer cells, including ovarian (Leung *et al.*, 2010) lung, breast, bladder, and prostate cancer cell lines (unpublished data). We have also found that

PKG-I is expressed in mesothelioma cells (data of present study), an aggressive form of cancer that is derived from mesothelial cells, which line the thoracic cavity, abdominal cavity and heart sac.

The present study uses pharmacological agents as well as gene knockdown techniques to demonstrate the function of PKG-I in pleural mesothelioma cell lines, MSTO-211H and NCI-H2452. A cGMP/PKG-I pathway inhibitor, ODQ, which inhibits the endoegenous NO-induced activation of soluble guanylyl cyclase and subsequent cGMP synthesis, was used to demonstrate that cGMP/PKG-I activation is critical in preventing spontaneous apoptosis, promoting cell proliferation, and maintaining integrin β1 expression cell attachment in the mesothelioma cell lines. For the first time, RNA interference, using short hairpin RNA (shRNA), was used to directly study PKG-I function in mesothelioma cells. Reverse transcriptase (RT)-PCR and a 12-channel capillary electrophoresis system with a light emitting diode-induced fluorescence detector system was used as a tool for determining the extent of RNA interference in PKG-I specific shRNA transfected cells. We demonstrate that PKG-I expression in MSTO-211H and NCI-H2452 mesothelioma cells is important for integrin β1 expression in these cells, for attachment, for proliferation and for avoiding spontaneous onset of apoptosis.

Results

eNOS and both PKG-I isoforms (PKG-Iα and -Iβ) are expressed in MSTO-211H and NCI-H2452 mesothelioma cells

The endothelial isoform of NO synthase (eNOS) is known to be highly expressed in mesothelioma cells (Soini *et al.*, 2001). Figure 1a demonstrates that both MSTO-211H and NCI-H2452 mesothelioma cell lines express also express eNOS, which can provide an endogenous source of NO capable of activating the downstream cGMP/PKG-I pathway in these cells.

Studies during the 1970's, 1980's and early 1990's suggested that PKG was expressed in only a limited number of cell types, such as smooth muscle cells of airways, blood vessels, intestines and Purkinje neurons of brain (reviewed in Fiscus 2002). However, more recent data have demonstrated that PKG, especially PKG-I, is expressed in many other types of cells (Orstavik *et al.*, 1997). Although a down-regulation of PKG-I expression appears to occur when epithelial cells transform into cancer cells (Hou *et al.*, 2006; Wong *et al.*, 2001), our studies have shown that PKG-I (especially the PKG-Iα isoform) continues to be expressed at detectable levels and this expression is essential for proliferation and cell survival of certain cancer cells, such as ovarian cancer cells (Leung *et al.*, 2010) and neuroblastoma cells (Johlfs and Fiscus, 2010).

Given the technical limitations of detecting the required low levels of PKG-I in these cancer cells using traditional Western blots, we used a highly sensitive immunocytochemistry technique in conjunction with a traditional assessment of protein expression. Figure 1b shows the analysis of PKG-I by traditional Western blot using a PKG-I-specific antibody, capable of recognizing both isoforms of PKG-I. PKG-I

expression is readily detected in the MSTO-211H cell line, but expression in the NCI-H2452 cell line is just at the limit of detection. In-cell westerns were also conducted with the same antibody. This assay proved more sensitive than traditional Western blot analysis and confirmed expression of PKG-I in both mesothelioma cell lines.

In collaboration with Cell Signaling Technology, isoform-specific antibodies, that can discriminate between PKG-Iα and PKG-Iβ, were developed for use in an ultrasensitive immunocytochemistry assay (Duolink technique) from Olink Biosciences, in order to confirm expression of each isoform in both cell lines. Figure 2a shows that the PKG-I isoform-specific antibodies could indeed discriminate between the two targets (though affinity or differences in titer appeared to differ between the two antibodies), using recombinant PKG-Iα and PKG-Iβ versions of each enzyme as the standards. Figure 2b demonstrates, using the ultrasensitive Duolink assay from Olink Biosciences, that both isoforms of PKG-I are expressed in each cell line.

Endogenous NO-induced activation of soluble guanylyl cyclase is necessary for maintaining lower levels of apoptosis and promoting cell proliferation

A proposed model of stimulation of PKG-I by endogenous NO, either NO from eNOS within mesothelioma cells or NO released from nearby endothelial cells, and the subsequent interactions of PKG-I with various downstream targets (VASP, BAD and CREB) can be seen in Figure 2c. We are proposing that the phosphorylations of BAD, CREB and VASP by PKG-I contribute to the stimulation of integrin expression, cell attachment, proliferation and inhibition of apoptosis in mesothelioma cells.

Figure 3a shows a simplified model of the cGMP/PKG-I signaling pathway and its effects on apoptosis, proliferation, and cell attachment, with particular emphasis on selected activators and inhibitors used in the present study. Endogenous NO produced

by eNOS, even at basal levels, has been shown to activate soluble guanylyl cyclase, elevates cGMP and causes continous partial (30-40 % of maximum) activation of PKG (Fiscus *et al.*, 1983). In the present study, we used ODQ, a selective inhibitor of NO-induced activation of soluble guanylyl cyclase (sGC), to determine the role of the NO/sGC/cGMP/PKG-I signaling pathway in regulating cell apoptosis and cell proliferation in MSTO-211H and NCI-H2452 cells. Cells were treated with 25 and 50 μM of ODQ, with or without 1.0 mM of 8-Br-cGMP (a cell permeable cGMP analog that is a direct PKG activator, which can bypass the ODQ-induced block) and were incubated for 24 hours. After the incubation, the cells were assayed for changes in levels of apoptosis and cell proliferation.

ODQ caused significant and concentration-dependent increases in caspase 3/7 activity in both MSTO-211H and NCI-H2452 cells (Figure 3b), indicating an increase in spontaneous apoptosis. The inhibitory effect of ODQ on the cGMP/PKG-I pathway was prevented by stimulating PKG activity directly with 8-Br-cGMP, which brought back the levels of apoptosis closer to that of the control cells. After a 24 hour incubation, cells treated with ODQ also had significant decreases in cell proliferation (Figure 3c). Treating cells with 8-Br-cGMP, in combination with ODQ, restored cell proliferation levels similar to those of the control cells.

Knocking down PKG-I expression using PKG-I-specific shRNA constructs decreases VASP phosphorylation (indicator of endogenous PKG-I kinase activity)

To determine if PKG-I expression directly plays a role in protecting cells from apoptosis, stimulating growth, and promoting adhesion, we developed gene knockdown clones to selectively silence the expression of PKG-I. To assess gene expression in mesothelioma knockdown clones, reverse transcriptase (RT)-PCR products were analyzed on a 12-channel capillary electrophoresis system with a light-emitting diode-

induced fluorescence detector (CE-LED-IF) system to determine relative mRNA levels of the PKG-I isoforms. Previously, our lab has used single channel CE technology to quantify levels of DNA fragmentation indicative of apoptosis in a variety of mammalian cells (Fiscus, 2002; Fiscus *et al.*, 2001; Fiscus *et al.*, 2002) and to determine mRNA expression levels of iNOS in VSMCs (Chan and Fiscus, 2004). The 12-channel capillary electrophoresis system used in this study is also capable of detecting and quantifying apoptotic DNA fragmentation (Johlfs and Fiscus, 2010), but also allows for higher through-put of samples, high resolution and the ability to make relative comparisons among channels while analyzing apoptotic DNA fragments as well as the products of multiplexed PCR reactions (as shown in the present study). Figure 4 shows the analysis of RT-PCR products by CE-LED-IF, indicating PKG-Iα and PKG-Iβ mRNA levels. Figure 4a shows that PKG-Iα was knocked down by 65 and 83%, respectively, by knockdown clones #1 and #2 and PKG-Iβ was knocked down by 79 and 82%, respectively, by knockdown clones #1 and #2 in the MSTO-211H cell line. In the NCI-H2452 cell line (Figure 4b), PKG-Iα was knocked down by 65 and 92%, respectively, by the knockdown clone #1 and #2 and PKG-Iβ was knocked down by 73 and 78%, respectively, by the knockdown clone #1 and #2.

Western blots assessing MSTO-211H and NCI-H2452 knockdown clones and controls show that decreased PKG-I expression leads to lower levels of VASP phosphorylation at serine 239 (Figure 5), one of PKG-I's known substrates within mammalian cells (Butt *et al.*, 1994), indicating that PKG-I activity is, indeed, decreased in these cell lines by the knockdown procedure.

Knocking down PKG-I expression triggers the onset of spontaneous apoptosis and decreases cell proliferation

Levels of apoptosis and cell proliferation were assessed post-transfection, 48 and 72 hours, respectively, after successful knock down was confirmed. Knockdown clones for both mesothelioma cell lines had clear increases in caspase 3/7 activity, an early indicator of apoptosis (Figure 6a). There was only a modest effect on the cells when transfected with a scrambled shRNA expressing vector. MTT assays show that cell proliferation decreased in the knockdown clones, as well, for both cell lines (Figure 6b). It is apparent that cells with decreased PKG-I expression have increased levels of apoptosis and decreased cell proliferation.

Knocking down PKG-I expression leads to decreased cell attachment and colony formation

PKG-I-specific gene knockdowns were used to determine if PKG-I plays an important role in maintaining cell attachment in the MSTO-211H mesothelioma cell line. After 72 hours, the attached and detached populations from the PKG-I-specific shRNA transfected cells were separated and assessed using the Vybrant Cell Adhesion Assay Kit. The cells with decreased PKG-I expression had significantly less cell attachment to the tissue culture plate, indicating that the expression of PKG-I is important for maintaining cell attachment (Figure 7a). Cell attachment did not appear to be affected by the negative control transfection. Microscopic evaluation confirmed that the knockdown clones had dramatically detached from the plate after a 72 hour incubation compared to the control (Figure 7b). Cells with decreased PKG-I expression appeared to round up and many were observed to be floating in suspension. Clonogenic assays with crystal violet staining were also used to show a decrease in colony formation in cell populations with decreased PKG-I expression, shown in Figure 7c. Solubilization of the

stained clones revealed a significant decrease in colony formation in the knockdown cell cultures, compared to the controls (graph in Figure 7c).

ODQ-induced inhibition of PKG-I activity and gene knockdown of PKG-I expression decreases the expression of integrin β1

In primary VSMCs, it has been suggested that PKG-I-induced adhesion is mediated by β1 and β3 integrins, based on experiments using stimulation by cGMP analogs (Weinmeister *et al.*, 2008). In the present study, we used Western blots to assess integrin expression after treatment with ODQ (Figure 8a) and RNA interference of PKG-I expression (Figure 8b). Integrin β1 was chosen for analysis because it is highly expressed in pleural mesothelioma (Koukoulis *et al.*, 1997). In the current study, levels of integrin β1 expression in the two mesothelioma cell lines were decreased compared to the controls, suggesting integrin β1 expression is under the control of the NO/cGMP/PKG-I signaling pathway. These data provide a potential link between PKG-I expression and cell adhesion of mesothelioma cells.

Discussion

This study focused on two pleural mesothelioma cell lines, MSTO-211H and NCI-H2452, and PKG-I's role in regulating apoptosis, cell proliferation and cell attachment. Malignant pleural mesothelioma (MPM) is a rare type of cancer that occurs in the thin layer of cells lining the body's internal organs, known as the mesothelium. Exposure to asbestos is a recognized cause of this cancer and the onset of symptoms does not appear until years after exposure. Crocidolite asbestos increases NO levels in mesothelioma cells, presumably by the stimulation of inducible nitric oxide (iNOS) and eNOS expression (Marrogi *et al.*, 2000; Riganti *et al.*, 2007), potentially stimulating the cGMP/PKG signaling pathway. eNOS is well known to regulate cancer-related events such as angiogenesis, apoptosis, cell cycle progression, invasion, and metastasis (Ying and Hofseth, 2007). Furthermore, our studies show that eNOS plays an important role in preventing spontaneous apoptosis and promoting DNA synthesis and cell proliferation in ovarian cancer cells (Leung *et al.*, 2008; Leung *et al.*, 2010).

PKG-I is expressed in a vast number of normal mammalian cells ((Orstavik *et al.*, 1997) reviewed in Fiscus 2002). Although initially PKG-I expression was thought to be low or even absent in cancer cells cancer cells (Hou *et al.*, 2006; Wong *et al.*, 2001), studies from our lab have shown that PKG-I, especially the PKG-Iα isoform, is expressed in all cancer cell lines studied, including neuroblastoma cells (Fiscus, 2002; Johlfs and Fiscus, 2010), ovarian cancer cells (Leung *et al.*, 2010) and breast, lung and prostate cancer cells (unpublished data from the Fiscus lab). Nitric oxide mediates vasoregulatory function via its ability to increase intracellular PKG activity in VSMCs (Fiscus *et al.*, 1983). Increased inducible nitric oxide (iNOS) is correlated with poor survival in melanoma patients (Ekmekcioglu *et al.*, 2003). Similarly, decreased endogenous nitric oxide (eNOS) expression is correlated with increased sensitivity to

cisplatin-induced apoptosis in melanoma (Grimm *et al.*, 2008) and ovarian cancer cells (Leung *et al.*, 2008). Also, in ovarian cancer cells, our lab has shown that downstream activation of PKG-Iα contributes to Src activation, leading to increased cell proliferation (Leung *et al.*, 2010). In mesothelioma cells, the inhibition of Src kinase activity has been shown to lead to apoptosis, cell cycle arrest, and deceased migration and invasion (Tsao *et al.*, 2007), illustrating an important role of Src activation in mesothelioma cells. Thus, Src activation mediated by PKG-I may be important in the regulation of proliferation and apoptosis in mesothelioma cells. Future studies in our laboratory will determine the potential involvement of Src and the actions of PKG-I in mesothelioma cells.

In the present study, we used reverse transcriptase (RT)-PCR and subsequent analysis on an automated 12-channel capillary electrophoresis with light emitting diode induced fluorescence (12-CE-LED-IF) system to determine the expression of PKG-I mRNA in two mesothelioma cell lines. PKG-I isoforms are expressed in both of these cell lines, albeit at very different levels, i.e. MSTO-211H cells express relatively high levels of both PKG-Iα and PKG-Iβ whereas NCI-H2452 cells express lower levels of the PKG-I isoforms. Nevertheless, in both cell lines, we were able to demonstrate the protective role of PKG-I, using a soluble guanylyl cyclase inhibitor (ODQ) and RNA interference (shRNA targeting PKG-I). Clearly, the levels of PKG-I expressed in these mesothelioma cells are sufficient to mediate the effects (proliferation, cell survival and cell adhesion) measured in the present study.

In the present study, when PKG-I expression was knocked down, these normally adherent cells detach from the plate, presumably as they enter an apoptotic state. Blocking the PKG-I pathway with an inhibitor of soluble guanylyl cyclase, ODQ, also triggers these cells to enter an apoptotic state and detach from the plate. We also found that integrin β1, a receptor that contributes to the attachment between cells and the

tissue around it, are down-regulated in mesothelioma cells in which the cGMP/PKG-I pathway is disrupted or PKG-I expression in knocked down. Integrin β1 promotes a malignant phenotype and cell proliferation in breast cancer (Weaver *et al.*, 1997) and it has been shown that down-regulating the expression of integrin β1 in prostate cancer cells decreases cell proliferation (Goel *et al.*, 2010). Malignant pleural mesothelioma cells are known to express integrin β1 (Koukoulis *et al.*, 1997), therefore this integrin isoform was chosen for the present study. The present study also shows that VASP, a protein that associates with integrin and is important for cell attachment, is constitutively phosphorylated in the mesothelioma cells in a PKG-I-dependent manner. Others have shown, using VASP knockout endothelial cells, that the PKG-I substrate VASP is essential for integrin-mediated cell adhesion and migration (Schlegel and Waschke, 2009), further implicating PKG-I's role in promoting cell adhesion.

It is particularly vital to develop alternative therapies for the treatment of mesothelioma, as these cells are resistant to various chemotherapeutic agents, such as cisplatin and doxorubicin, and the median overall survival (OS) of patients with the disease is 9-17 months (Ahamad *et al.*, 2003; Vogelzang *et al.*, 2003). Although PKG-I is recognized as the key protein kinase mediating the biological responses to nitric oxide (NO) in airway and vascular smooth muscle cells (Fiscus *et al.*, 1983; Fiscus *et al.*, 1984), recent studies from our laboratory have shown that PKG-I also has an important protective role in cancer cells, i.e. preventing the spontaneous onset of apoptosis and promoting cell proliferation in neuroblastoma cells (Johlfs and Fiscus, 2010) and ovarian cancer cells (Leung *et al.*, 2010). The present study, using RNAi gene knockdown techniques, have shown that PKG-I also plays an essential role in promoting integrin β1 expression, cell attachment and proliferation in mesothelioma cells. Selective inhibition of PKG-I in mesothelioma cells may be an effective way to control tumor growth.

Furthermore, the development of inhibitors, that block key downstream targets facilitating the pro-cancer effect of PKG-I may prove to be promising anti-cancer therapeutic agents.

Materials and methods

Materials

The materials used and their suppliers included MSTO-211H, NCI-H2452 and RPMI 1640 (ATCC, Manassas, VA); Fetal bovine serum (Gemini Bio-Products, West Sacramento, CA); ODQ (1H-[1,2,4]Oxad-iazolo[4,3-a]quinoxalin-1-one) (Sigma, St. Louis, MO); 8-Br-cGMP (BioMol, Plymouth Meeting, PA, USA); Crystal violet (Fisher Scientific, Pittsburgh, PA); anti-PKG-I (c-terminal), anti-PKG-Iα, anti-PKG-Iβ, anti-eNOS, anti-phospho VASP (ser239), anti-integrin β1 antibodies (Cell Signaling Technology, Danvers, MA); anti-β-actin (Santa Cruz Biotechnology, Santa Cruz, CA); anti-rabbit-CW800 secondary antibody, and blocking buffer (LI-COR, Lincoln, NE); PKG-I-specific HuSH vectors (Origene, Rockville, MD); FastStart universal master (Roche, Basel, Switzerland); 100bp DNA ladder, Trizol, Superscript® VILO™ cDNA synthesis kit, Lipofectamine 2000; 4-12% Bis-Tris NuPAGE gel system, EZQ protein Quantitation Kit, and Vybrant Cell Adhesion Assay Kit (Invitrogen, Carlsbad, CA); Caspase 3/7 Glo assay and MTT assay (Promega, Madison, WI); QIAxcel System (Qiagen, Germantown, Maryland); PKG-I-specific primers (Integrated DNA Technologies, Coralville, IA); Duolink in situ PLA kit (Olink, Bioscience, Uppsala, Sweden).

ODQ and 8-Br-cGMP treatments

To determine the effects of ODQ, an inhibitor of soluble guanylyl cyclase, on MSTO-211H and NCI-H2452 cells, cells were seeded in 96 well plates, as described above and grown overnight. The following day, cells were treated with ODQ (25 and 50 μM) in the absence or presence of 1.0 mM 8-br-cGMP, a stimulator of the PKG pathway. After a 24 hour incubation, the cells were tested for changes in levels of apoptosis and cell proliferation using Caspase Glo 3/7 and MTT assays, respectively.

Western blot analysis

Western blots were conducted as previously described (Johlfs and Fiscus, 2010).

In-Cell Westerns and Immunocytochemistry

In-cell Westerns were conducted as previously described (Johlfs and Fiscus, 2010). The immunocytochemistry assays with the Duolink in situ PLA assay kit were carried out identically, except after incubation with the primary isoform-specific PKG-I antibodies, cells were washed and incubated with PLUS and MINUS anti-rabbit PLA probes and processed with the Duolink assay kit. Cells were imaged using an EVOS fluorescence microscope (Advanced Microscopy Group, Bothell, WA).

RNA interference

Cells to be tested for induction of apoptosis, inhibition of cell growth, or changes in cell adhesion were seeded in a 96 well plate at a density of 20,000 cells/well in media lacking antibiotics and were incubated for 24 hours. For each test, at least three wells were seeded. The following day, the cells were transfected with PKG-I-specific shRNA containing expression vectors. The following was prepared, depending on the number of treated wells: 3.0% lipofectamine and 1ug of vector in 100 uL of Opti-MEM (Invitrogen) serum free media per 1 million cells. The mixture was incubated at room temperature for 20 minutes. The mixture was then added to the cells drop-wise so that it consisted of 5% of the media volume. Following gentle mixing, the cells were incubated for 48-72 hours and levels of apoptosis, cell proliferation and cell adhesion were assessed. PKG expression levels were monitored using RT-PCR and subsequent analysis on a 12-channel capillary electrophoresis system with a light emitting diode. It should be noted that PKG-II expression was not effected due to low sequence similarity.

Gene expression analysis on a 12-channel capillary electrophoresis system with a light emitting diode-induced fluorescence detector (CE-LED-IF)

RNA was trizol extracted from 50,000 cells and DNAse treated. One microgram of purified total RNA was converted to cDNA using Superscript Vilo reverse transcriptase kit (Invitrogen) and was used in a PCR reaction using a GeneAmp PCR system 9700. Unique forward primers were designed for each isoform (PKG-Iα: 5' GGCGCAGGGCATCTCG 3'; PKG-Iβ: 5' GACCAGCCACCCAGCA 3'). An oligonucleotide sequence common to both isoforms was used as the reverse primer for both (5' ATCCACAATCTCCTGGATCTG 3'). All three primers were used in a multiplexed reaction. Expected product sizes were ~173 and 227 base pairs for PKG-Iα and -Iβ, respectively. After 30 cycles, the PCR products were run on a QIAxcel (originally distributed through eGene, Inc. and subsequently sold to Qiagen), an automated high performance genetic analyzer that utilizes capillary electrophoresis (CE) to resolve, identify and quantify oligonucleotides. The CE-LED-IF has high resolution, up to 3-5 base pairs and is very sensitive, allowing for detection of low levels of PKG-I expression. Products were injected at 8 kV for 20 seconds and separated at 6 kV for 400 seconds. Results were analyzed using BioCalculator 1.6 software. Products were also run on a 1.0 % agarose gel, isolated, purified and sequenced to verify their identity.

Analysis of apoptosis and cell proliferation

To determine levels of apoptosis, caspase 3/7 activity was measured using Caspase Glo 3/7 (Promega). Reagent was added at a ratio of 1:1 and the cells were incubated for one hour at 37°C. Luminescence measurements were then taken and data was plotted using Graphpad Prism (Graphpad Software, Inc., La Jolla, CA). To determine changes in cell proliferation, MTT reagent (Promega) was used. Ten percent total

volume of the reagent was added to each test. After a two hour incubation at 37°C, the formazan product generated in viable cells was solubilized in acid for two hours at 37°C. Absorbance measurements were then taken at 570 nm (650 nm subtraction) and data was plotted using Graphpad Prism.

Analysis of cell adhesion

To determine changes in cell adhesion, Vybrant Cell Adhesion Assay Kit from Invitrogen was used. 72 hours after transfecting the cells with vectors expressing shRNA in 96 well plates, the population of cells in the culture media (detached cells) was removed to a new 96 well plate. Fresh media was replaced in the original plate. The cells were then loaded with 5 μM of calcein AM dye, which fluoresces in the cell upon cleavage by esterases. Fluorescence was measured at 494 nm/517 nm. Light microscope photographs were performed at 10X. To further characterize adhesion, clonogenic assays were performed using crystal violet. After staining, the dye was solubilized with acetic acid and absorbance was measured at 595 nm.

Acknowledgements

This study was supported by a grant from the Department of Defense (grant # W81XWH-07-1-0543) awarded to RRF and Start-up funding provided by the Nevada Cancer Institute.

References

Barger SW, Fiscus RR, Ruth P, Hofmann F, Mattson MP (1995). Role of cyclic GMP in the regulation of neuronal calcium and survival by secreted forms of beta-amyloid precursor. *J Neurochem* **64:** 2087-96.

Beckman JS, Koppenol WH (1996). Nitric oxide, superoxide, and peroxynitrite: the good, the bad, and ugly. *Am J Physiol* **271:** C1424-37.

Butt E, Abel K, Krieger M, Palm D, Hoppe V, Hoppe J *et al* (1994). cAMP- and cGMP-dependent protein kinase phosphorylation sites of the focal adhesion vasodilator-stimulated phosphoprotein (VASP) in vitro and in intact human platelets. *J Biol Chem* **269:** 14509-17.

Chan GH, Fiscus RR (2004). Exaggerated production of nitric oxide (NO) and increases in inducible NO-synthase mRNA levels induced by the pro-inflammatory cytokine interleukin-1beta in vascular smooth muscle cells of elderly rats. *Exp Gerontol* **39:** 387-94.

Cheng Chew SB, Leung PY, Fiscus RR (2003). Preincubation with atrial natriuretic peptide protects NG108-15 cells against the toxic/proapoptotic effects of the nitric oxide donor S-nitroso- N-acetylpenicillamine. *Histochem Cell Biol* **120:** 163-71.

Chiche JD, Schlutsmeyer SM, Bloch DB, de la Monte SM, Roberts JD, Jr., Filippov G *et al* (1998). Adenovirus-mediated gene transfer of cGMP-dependent protein kinase increases the sensitivity of cultured vascular smooth muscle cells to the antiproliferative and pro-apoptotic effects of nitric oxide/cGMP. *J Biol Chem* **273:** 34263-71.

Chiueh C, Lee S, Andoh T, Murphy D (2003). Induction of antioxidative and antiapoptotic thioredoxin supports neuroprotective hypothesis of estrogen. *Endocrine* **21:** 27-31.

Ciani E, Guidi S, Bartesaghi R, Contestabile A (2002). Nitric oxide regulates cGMP-dependent cAMP-responsive element binding protein phosphorylation and Bcl-2 expression in cerebellar neurons: implication for a survival role of nitric oxide. *J Neurochem* **82:** 1282-9.

Ekmekcioglu S, Ellerhorst J, Smid CM, Prieto VG, Munsell M, Buzaid AC *et al* (2000). Inducible nitric oxide synthase and nitrotyrosine in human metastatic melanoma tumors correlate with poor survival. *Clin Cancer Res* **6:** 4768-75.

Ekmekcioglu S, Ellerhorst JA, Prieto VG, Johnson MM, Broemeling LD, Grimm EA (2006). Tumor iNOS predicts poor survival for stage III melanoma patients. *Int J Cancer* **119:** 861-6.

Feil R, Feil S, Hofmann F (2005). A heretical view on the role of NO and cGMP in vascular proliferative diseases. *Trends Mol Med* **11:** 71-5.

Fiscus RR (2002). Involvement of cyclic GMP and protein kinase G in the regulation of apoptosis and survival in neural cells. *Neurosignals* **11:** 175-90.

Fiscus RR, Leung CP, Yuen JP, Chan HC (2001). Quantification of apoptotic DNA fragmentation in a transformed uterine epithelial cell line, HRE-H9, using capillary electrophoresis with laser-induced fluorescence detector (CE-LIF). *Cell Biol Int* **25:** 1007-11.

Fiscus RR, Murad F (1988). cGMP-dependent protein kinase activation in intact tissues. *Methods Enzymol* **159:** 150-9.

Fiscus RR, Rapoport RM, Murad F (1983). Endothelium-dependent and nitrovasodilator-induced activation of cyclic GMP-dependent protein kinase in rat aorta. *J Cyclic Nucleotide Protein Phosphor Res* **9:** 415-25.

Fiscus RR, Torphy TJ, Mayer SE (1984). Cyclic GMP-dependent protein kinase activation in canine tracheal smooth muscle by methacholine and sodium nitroprusside. *Biochim Biophys Acta* **805:** 382-92.

Fiscus RR, Yuen JP, Chan SL, Kwong JH, Chew SB (2002). Nitric oxide and cyclic GMP as pro- and anti-apoptotic agents. *J Card Surg* **17:** 336-9.

Fraser M, Chan SL, Chan SS, Fiscus RR, Tsang BK (2006). Regulation of p53 and suppression of apoptosis by the soluble guanylyl cyclase/cGMP pathway in human ovarian cancer cells. *Oncogene* **25:** 2203-12.

Goel HL, Underwood JM, Nickerson JA, Hsieh CC, Languino LR (2010). Beta1 integrins mediate cell proliferation in three-dimensional cultures by regulating expression of the sonic hedgehog effector protein, GLI1. *J Cell Physiol* **224:** 210-7.

Grimm EA, Ellerhorst J, Tang CH, Ekmekcioglu S (2008). Constitutive intracellular production of iNOS and NO in human melanoma: possible role in regulation of growth and resistance to apoptosis. *Nitric Oxide* **19:** 133-7.

Hou Y, Gupta N, Schoenlein P, Wong E, Martindale R, Ganapathy V *et al* (2006). An anti-tumor role for cGMP-dependent protein kinase. *Cancer Lett* **240:** 60-8.

Hussain SP, Trivers GE, Hofseth LJ, He P, Shaikh I, Mechanic LE *et al* (2004). Nitric oxide, a mediator of inflammation, suppresses tumorigenesis. *Cancer Res* **64:** 6849-53.

Johlfs MG, Fiscus RR (2010). Protein kinase G type-Ialpha phosphorylates the apoptosis-regulating protein Bad at serine 155 and protects against apoptosis in N1E-115 cells. *Neurochem Int* **56:** 546-53.

Kolb JP (2000). Mechanisms involved in the pro- and anti-apoptotic role of NO in human leukemia. *Leukemia* **14:** 1685-94.

Koukoulis GK, Shen J, Monson R, Warren WH, Virtanen I, Gould VE (1997). Pleural mesotheliomas have an integrin profile distinct from visceral carcinomas. *Hum Pathol* **28:** 84-90.

Krause M, Dent EW, Bear JE, Loureiro JJ, Gertler FB (2003). Ena/VASP proteins: regulators of the actin cytoskeleton and cell migration. *Annu Rev Cell Dev Biol* **19:** 541-64.

Leung EL, Fraser M, Fiscus RR, Tsang BK (2008). Cisplatin alters nitric oxide synthase levels in human ovarian cancer cells: involvement in p53 regulation and cisplatin resistance. *Br J Cancer* **98:** 1803-9.

Leung EL, Wong JC, Johlfs MG, Tsang BK, Fiscus RR (2010). Protein kinase G type Ialpha activity in human ovarian cancer cells significantly contributes to enhanced Src activation and DNA synthesis/cell proliferation. *Mol Cancer Res* **8:** 578-91.

Li Calzi S, Purich DL, Chang KH, Afzal A, Nakagawa T, Busik JV *et al* (2008). Carbon monoxide and nitric oxide mediate cytoskeletal reorganization in microvascular cells via vasodilator-stimulated phosphoprotein phosphorylation: evidence for blunted responsiveness in diabetes. *Diabetes* **57:** 2488-94.

Lincoln TM, Wu X, Sellak H, Dey N, Choi CS (2006). Regulation of vascular smooth muscle cell phenotype by cyclic GMP and cyclic GMP-dependent protein kinase. *Front Biosci* **11:** 356-67.

Lund N, Henrion D, Tiede P, Ziche M, Schunkert H, Ito WD (2010). Vimentin expression influences flow dependent VASP phosphorylation and regulates cell migration and proliferation. *Biochem Biophys Res Commun*.

Massberg S, Sausbier M, Klatt P, Bauer M, Pfeifer A, Siess W *et al* (1999). Increased adhesion and aggregation of platelets lacking cyclic guanosine 3',5'-monophosphate kinase I. *J Exp Med* **189:** 1255-64.

Munzel T, Feil R, Mulsch A, Lohmann SM, Hofmann F, Walter U (2003). Physiology and pathophysiology of vascular signaling controlled by guanosine 3',5'-cyclic monophosphate-dependent protein kinase [corrected]. *Circulation* **108:** 2172-83.

Orstavik S, Natarajan V, Tasken K, Jahnsen T, Sandberg M (1997). Characterization of the human gene encoding the type I alpha and type I beta cGMP-dependent protein kinase (PRKG1). *Genomics* **42:** 311-8.

Paquet-Durand F, Hauck SM, van Veen T, Ueffing M, Ekstrom P (2009). PKG activity causes photoreceptor cell death in two retinitis pigmentosa models. *J Neurochem* **108:** 796-810.

Pilz RB, Casteel DE (2003). Regulation of gene expression by cyclic GMP. *Circ Res* **93:** 1034-46.

Prueitt RL, Boersma BJ, Howe TM, Goodman JE, Thomas DD, Ying L *et al* (2007). Inflammation and IGF-I activate the Akt pathway in breast cancer. *Int J Cancer* **120:** 796-805.

Ridnour LA, Thomas DD, Switzer C, Flores-Santana W, Isenberg JS, Ambs S *et al* (2008). Molecular mechanisms for discrete nitric oxide levels in cancer. *Nitric Oxide* **19:** 73-6.

Roy A, Fung YK, Liu X, Pahan K (2006). Up-regulation of microglial CD11b expression by nitric oxide. *J Biol Chem* **281:** 14971-80.

Schlegel N, Waschke J (2009). Impaired integrin-mediated adhesion contributes to reduced barrier properties in VASP-deficient microvascular endothelium. *J Cell Physiol* **220:** 357-66.

Schmidmaier R, Baumann P (2008). ANTI-ADHESION evolves to a promising therapeutic concept in oncology. *Curr Med Chem* **15:** 978-90.

Soini Y, Puhakka A, Kahlos K, Saily M, Paakko P, Koistinen P *et al* (2001). Endothelial nitric oxide synthase is strongly expressed in malignant mesothelioma but does not

associate with vascular density or the expression of VEGF, FLK1 or FLT1. *Histopathology* **39:** 179-86.

Wada K, Okada N, Yamamura T, Koizumi S (1996). Nerve growth factor induces resistance of PC12 cells to nitric oxide cytotoxicity. *Neurochem Int* **29:** 461-7.

Weaver VM, Petersen OW, Wang F, Larabell CA, Briand P, Damsky C *et al* (1997). Reversion of the malignant phenotype of human breast cells in three-dimensional culture and in vivo by integrin blocking antibodies. *J Cell Biol* **137:** 231-45.

Weinmeister P, Lukowski R, Linder S, Traidl-Hoffmann C, Hengst L, Hofmann F *et al* (2008). Cyclic guanosine monophosphate-dependent protein kinase I promotes adhesion of primary vascular smooth muscle cells. *Mol Biol Cell* **19:** 4434-41.

Wong AS, Kim SO, Leung PC, Auersperg N, Pelech SL (2001). Profiling of protein kinases in the neoplastic transformation of human ovarian surface epithelium. *Gynecol Oncol* **82:** 305-11.

Wong JC, Fiscus RR (2010). Protein kinase G activity prevents pathological-level nitric oxide-induced apoptosis and promotes DNA synthesis/cell proliferation in vascular smooth muscle cells. *Cardiovasc Pathol*.

Ying L, Hofseth LJ (2007). An emerging role for endothelial nitric oxide synthase in chronic inflammation and cancer. *Cancer Res* **67:** 1407-10.

Figure Legends

Figure 1 A. Traditional Western blot showing eNOS expression in MSTO-211H and NCI-H2452 cells. B. Traditional Western blot, using a C-terminal anti-PKG-I antibody, capable of recognizing both PKG-I isoforms. Both PKG-I isoforms, PKG-Iα and PKG-Iβ, are expressed in both MSTO-211H and NCI-H2452 mesothelioma cell lines. C. In-cell Westerns showing expression of PKG-I isoforms in both MSTO-211H and NCI-H2452 mesothelioma cell lines. Both PKG-I isoforms are expressed at higher levels in the MSTO-211H cell line, compared to the NCI-H2452 cells, but both cell lines expressed detectable levels of both PKG-Iα and PKG-Iβ. Similar results were obtained in three other experiments.

Figure 2 A. Traditional Western blots, using recombinant human PKG-Iα and human PKG-Iβ as standards, demonstrating the specificity of the PKG-I isoform-specific antibodies. B. Ultrasensitive immunocytochemistry (using Duolink system) showing the expression of PKG-Iα and PKG-Iβ in MSTO-211H and NCI-H2452 cells. C. A proposed cellular model of NO-stimulated PKG-I activity and its interactions with downstream targets, which promotes integrin expression, cell attachment, cell proliferation and inhibits spontaneous apoptosis.

Figure 3 A. A simplified diagram of the NO/cGMP/PKG-I signaling pathway and its downstream effects in mesothelioma cells, emphasizing the activators and inhibitors used in the present study. B. Caspase 3/7 assays show that inhibition of endogenous NO-induced soluble guanylyl cyclase activity with 25 and 50 μM of ODQ increases the levels of apoptosis in both MSTO-211H and NCI-H2452 cells. This effect was

counteracted by treatment with 8-Br-cGMP, a cell permeable cGMP analog that bypasses the ODQ block. Similar results were obtained in three other experiments. C. MTT assays show that inhibition of soluble guanylyl cyclase with 25 and 50 μM of ODQ decreases cell proliferation in MSTO-211H and NCI-H2452 cells. Growth was significantly increased when 8-Br-cGMP was added in the presence of the ODQ block. Similar results were obtained in three other experiments. * P< 0.05, compared to no treatment control (No trmt), ** P< 0.01, compared to no trmt; ***P< 0.001, compared no trmt, # P< 0.05, compared to ODQ alone, ### P< 0.01, compared to ODQ alone, ### P< 0.001, compared to ODQ alone.

Figure 4 A. PKG-Iα and PKG-Iβ isoforms are both expressed at lower levels in MSTO-211H cells treated with shRNAs. Gel images and corresponding electropherograms show (RT)-PCR products analyzed on a 12-channel capillary electrophoresis system, using light emitting diode induced fluorescence, to determine relative mRNA levels. B. PKG-Iα and PKG-Iβ isoforms are both expressed at lower levels in NCI-H2452 cells treated with shRNAs.

Figure 5 Knocking down PKG-I expression levels in MSTO-211H and NCI-H2452 cells decreases the phosphorylation level of VASP, a well established target (intracellular substrate) of PKG-I, at serine 239, thus indicating that the shRNA constructs are effectively reducing not only transcript levels, but also the enzymatic activity of PKG-I in these cells. Similar results were obtained in three other experiments.

Figure 6 A. Caspase 3/7 assays show that PKG-I knockdown clones have higher levels of apoptosis in MSTO-211H and NCI-H2452 cells. Similar results were obtained

in three other experiments. B. MTT assays show that knocking down PKG-I expression leads to decreased cell proliferation in MSTO-211H and NCI-H2452 cells. Similar results were obtained in three other experiments. * P< 0.05, compared to no treatment control (no trmt); ** P< 0.01, compared to no trmt; ***P< 0.001, compared no trmt,

Figure 7 A. Gene knockdown of PKG-I expression in MSTO-211H cells results in detachment of cells from the plate. A Vybrant cell adhesion assay was used to show that when PKG-I expression is decreased, the population of cells attached to the culture plate decreases, and the population of cells that detach increases. Similar results were obtained in three other experiments. B. MSTO-211H cells were photographed at 10X magnification to show the morphological change that occurs after cells are treated with PKG-I specific shRNAs. The cells round up and detach from the culture plate. C. Clonogenic assays with crystal violet also show the PKG-I knockdowns have decreased colony formation. Cells that had detached were removed and those colonies remaining were stained and quantified. * P< 0.05, compared to no treatment control (no trmt), ** P< 0.01, compared to no trmt.

Figure 8 A. MSTO-211H and NCI-H2452 cells treated with ODQ have decreased levels of expression of integrin β1, one of the proteins known to be involved in cell attachment. Similar results were obtained in three other experiments. B. MSTO-211H and NCI-H2452 cells with decreased levels of PKG-I expression (following PKG-I-specific shRNA gene knockdown) also have decreased levels of integrin β1. Similar results were obtained in three other experiments.

a. Western blot of mesothelioma cell lysates showing eNOS expression

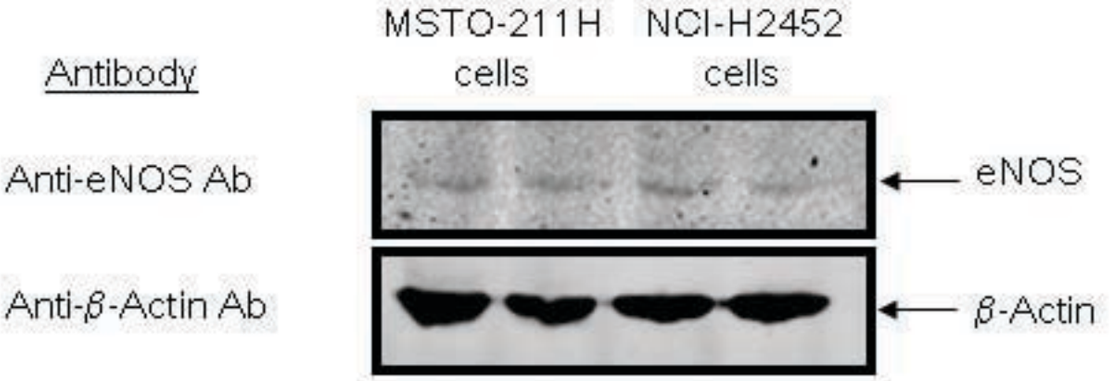

b. Western blot of mesothelioma cell lysates showing PKG-Iα/β expression

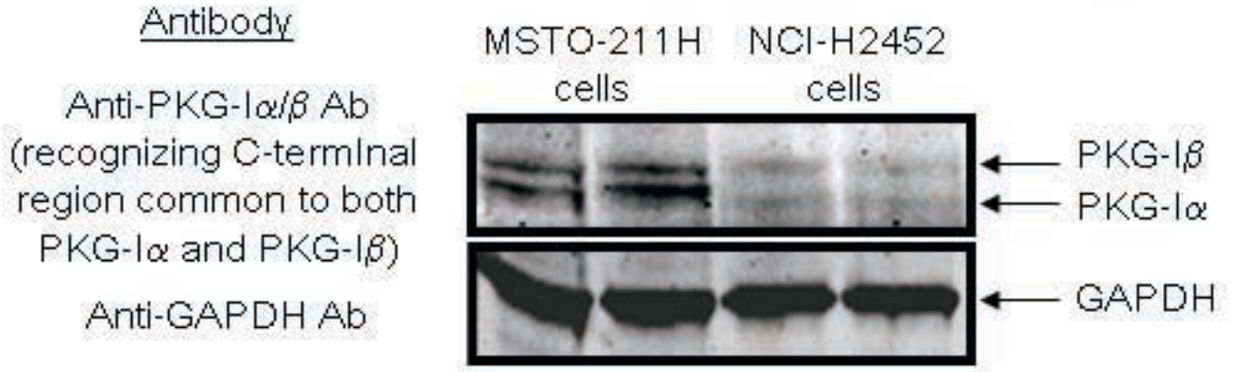

c. In-cell Western

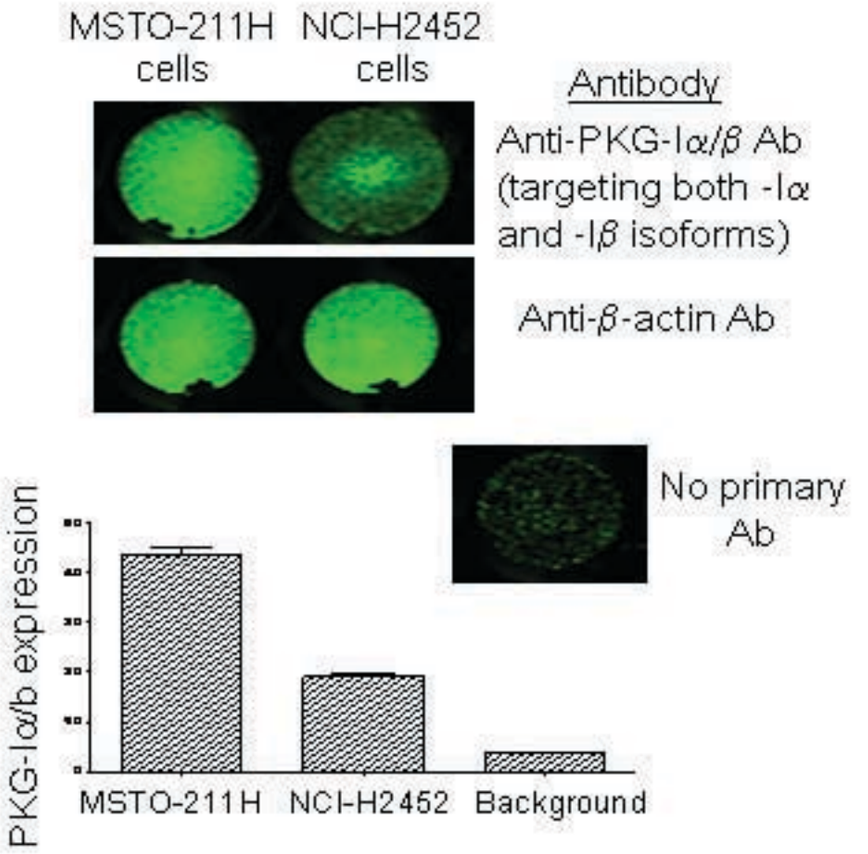

Figure 1

a. Western blots showing specificity of different anti-PKG-I antibodies using recombinant PKG-Iα and PKG-Iβ as standards

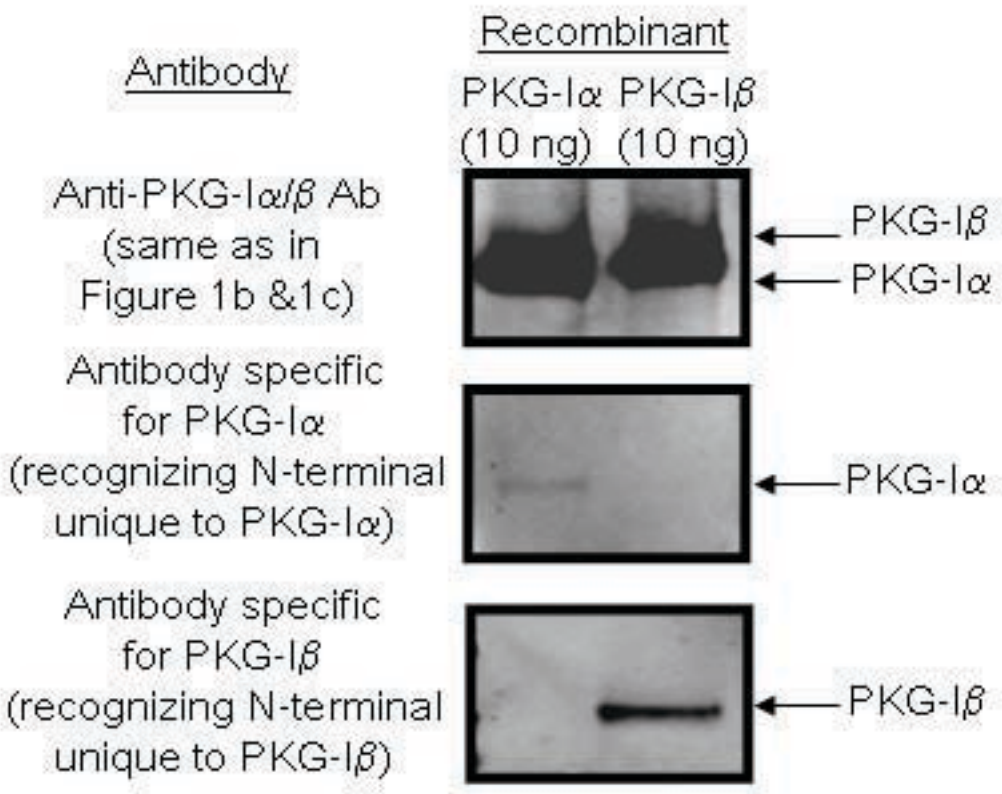

b. Ultrasensitive Immunocytochemistry (Duolink technique)

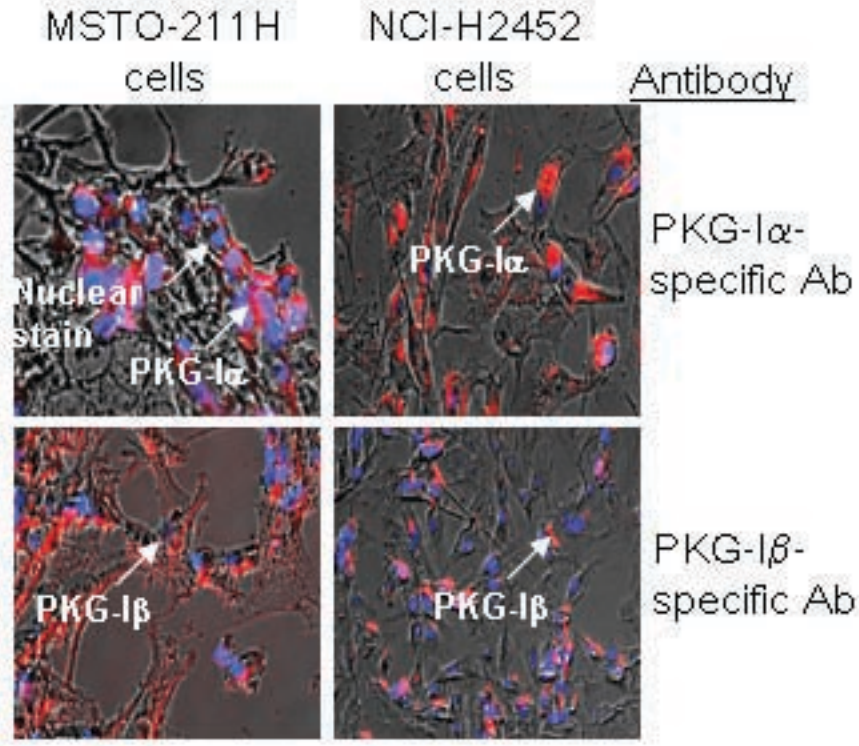

c.

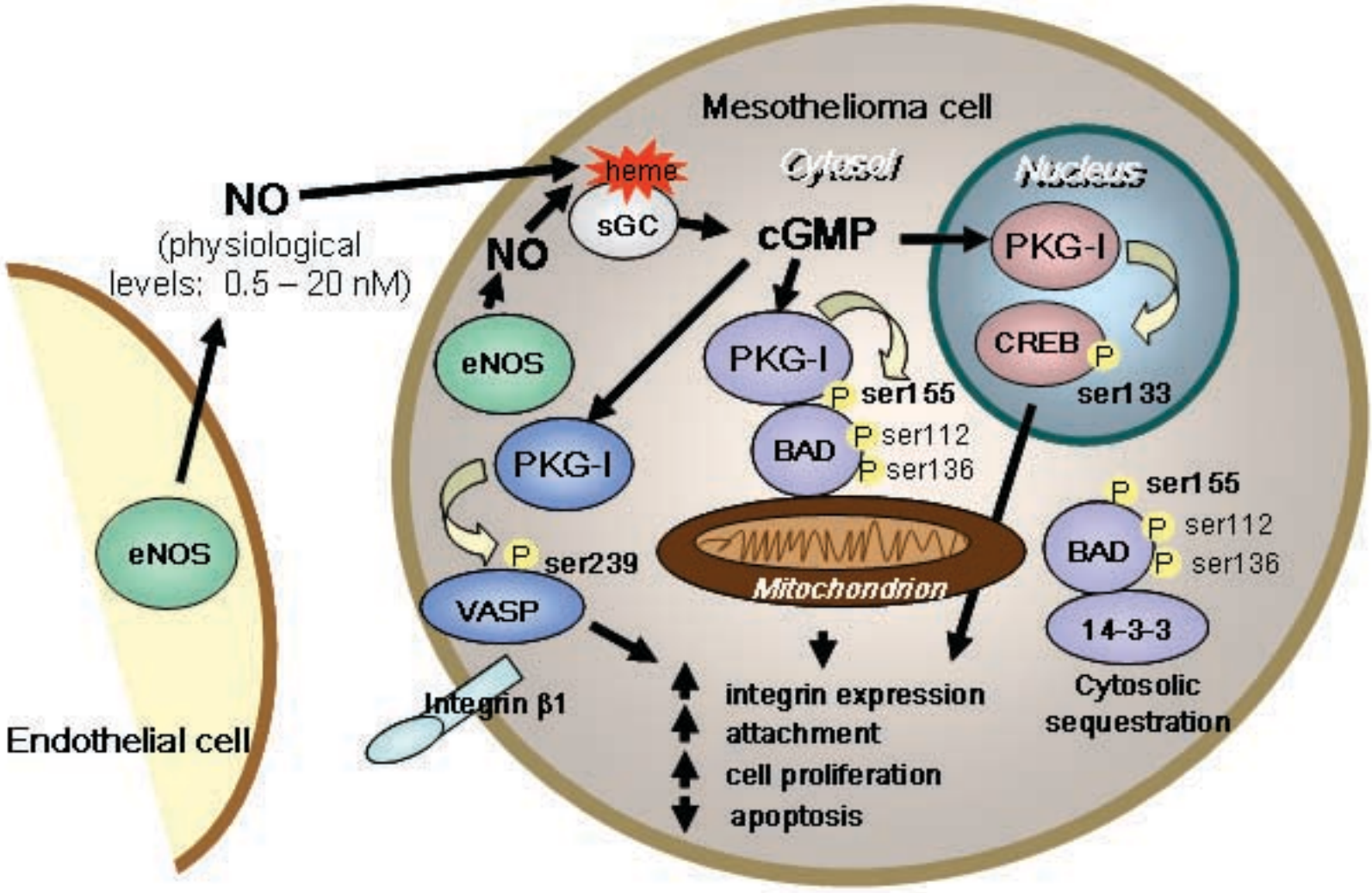

Figure 2

a.

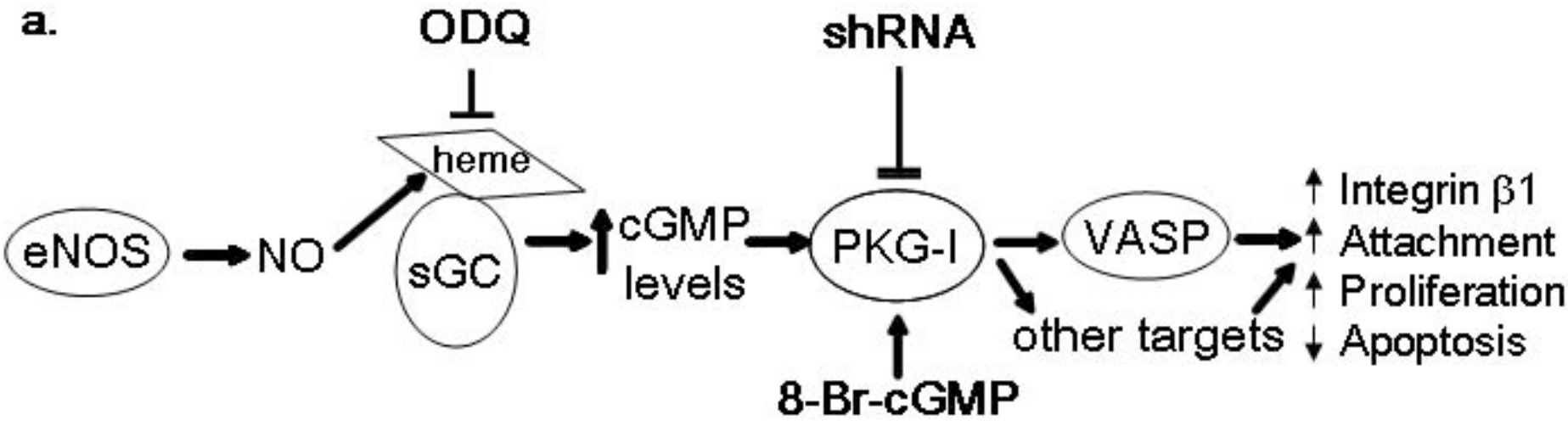

b. MSTO-211H cells

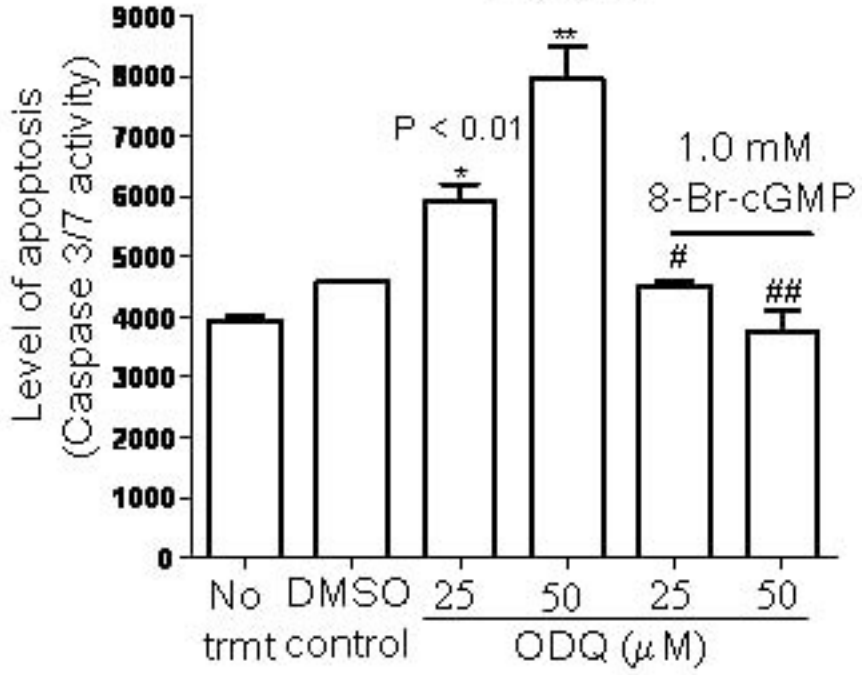

NCI-H2452 cells

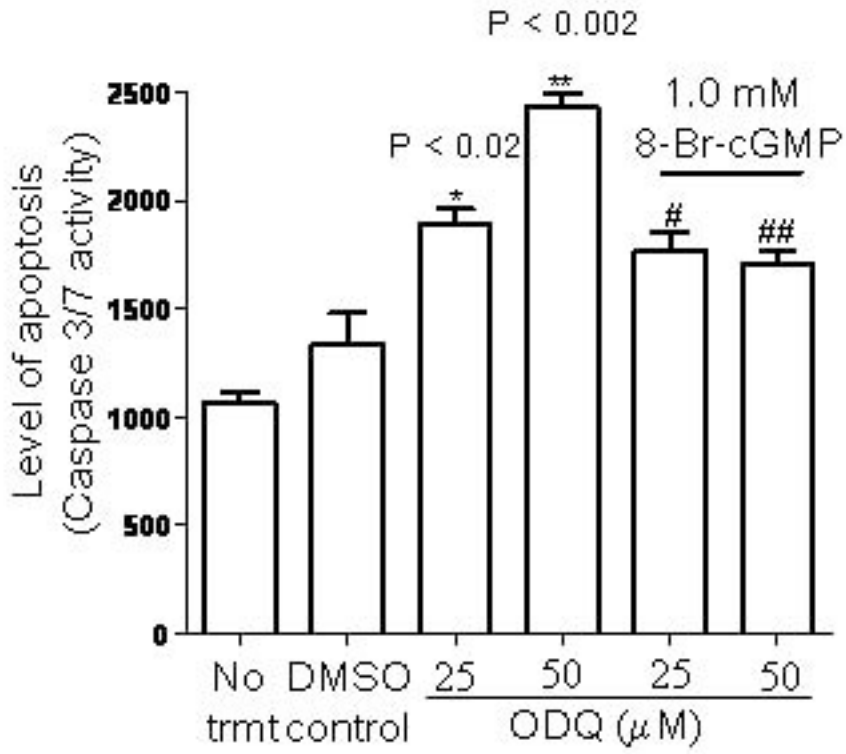

c. MSTO-211H cells

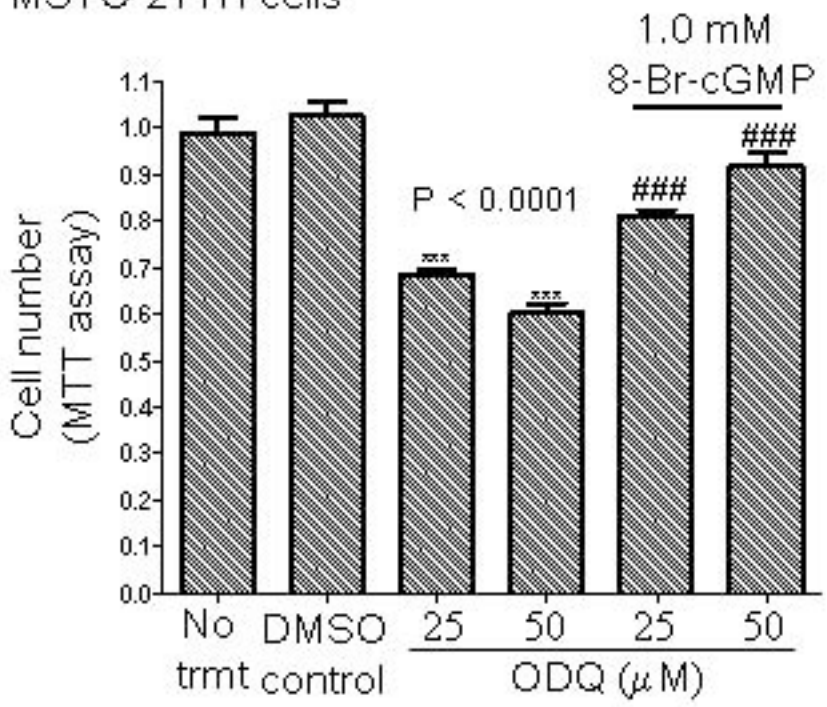

NCI-H2452 cells

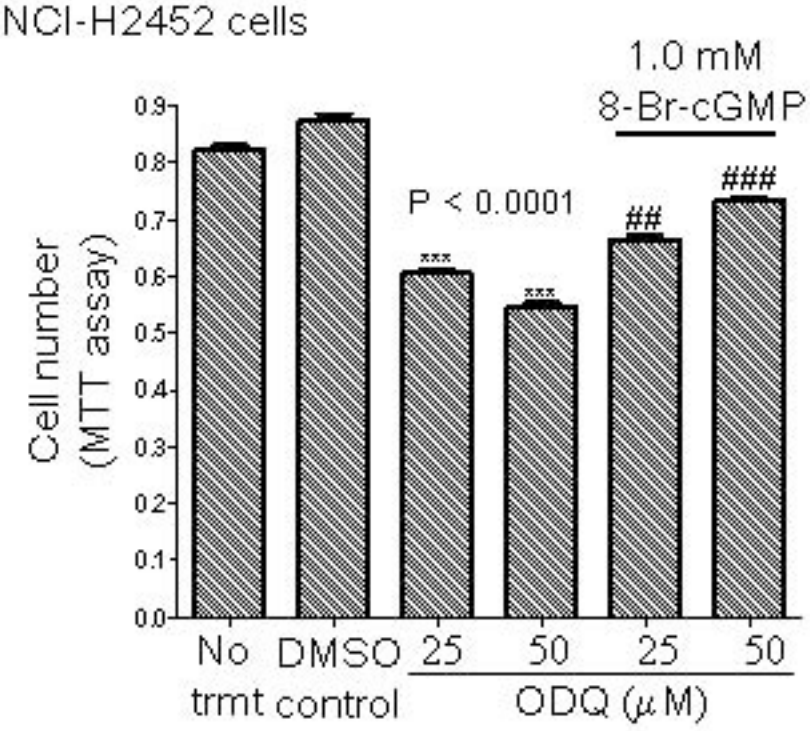

a. MSTO-211H cells (RT-PCR products analyzed by capillary electrophoresis with LED-induced fluorescence detector [CE-LED-IF])

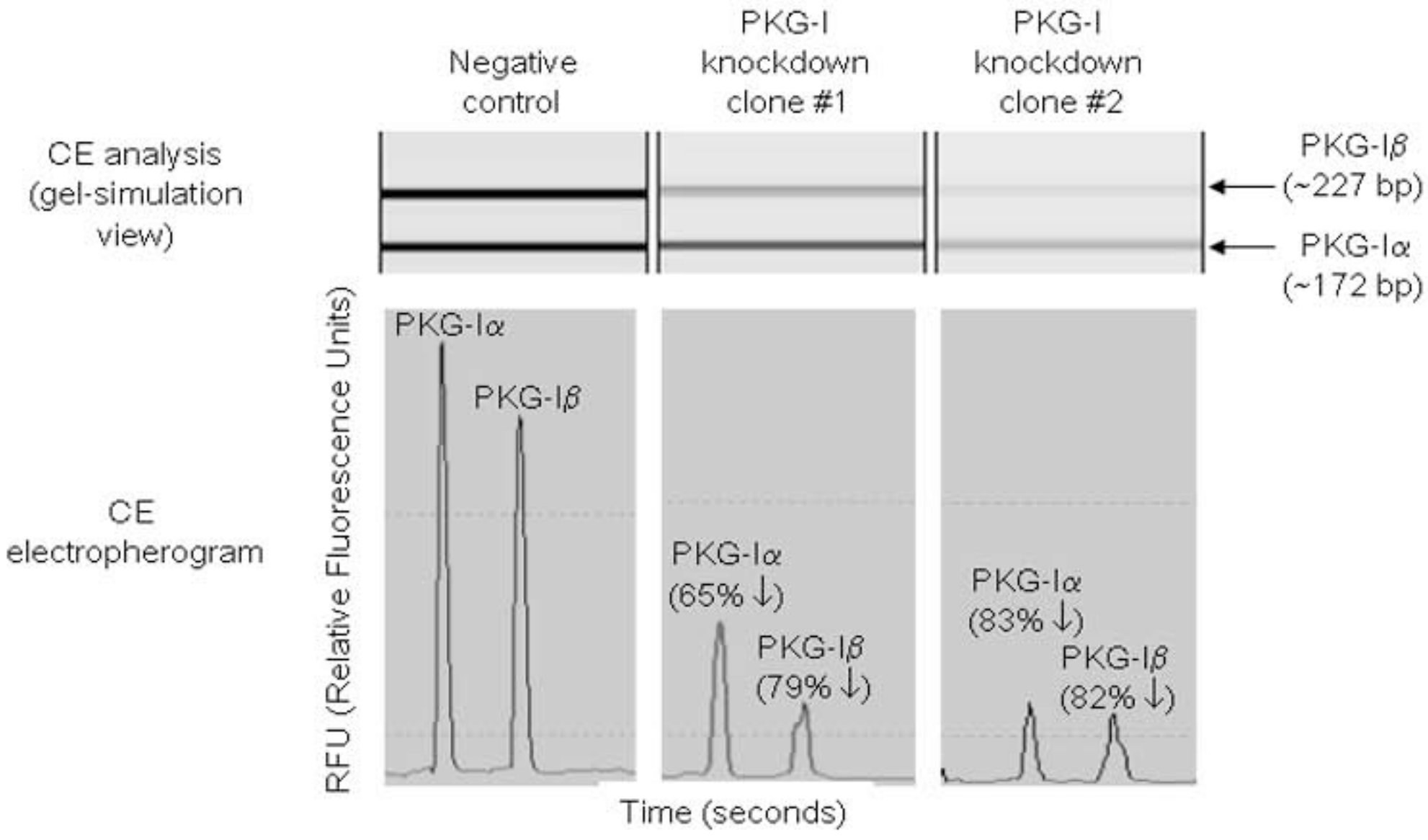

b. NCI-H2452 cells (RT-PCR products analyzed by CE-LED-IF)

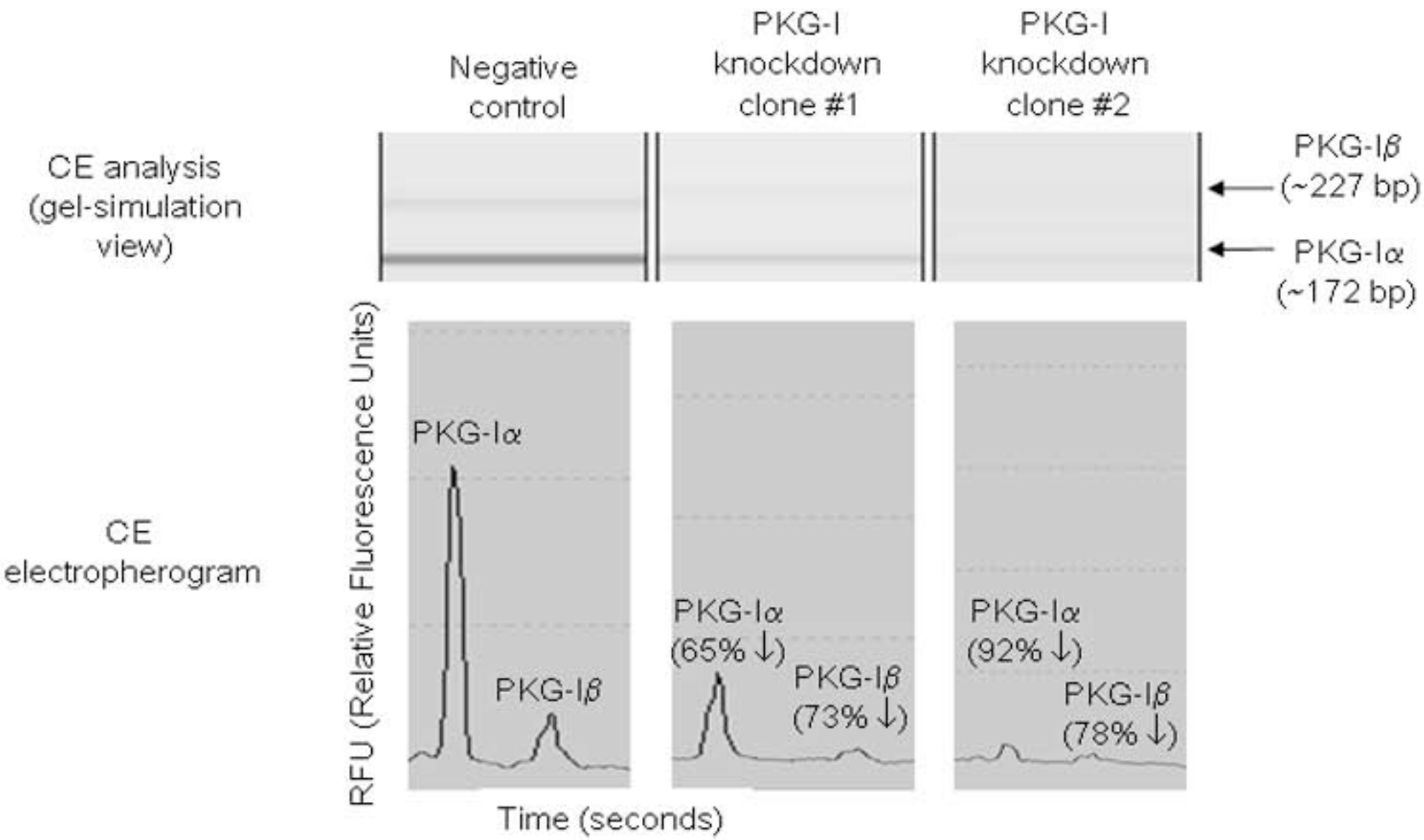

Figure 4

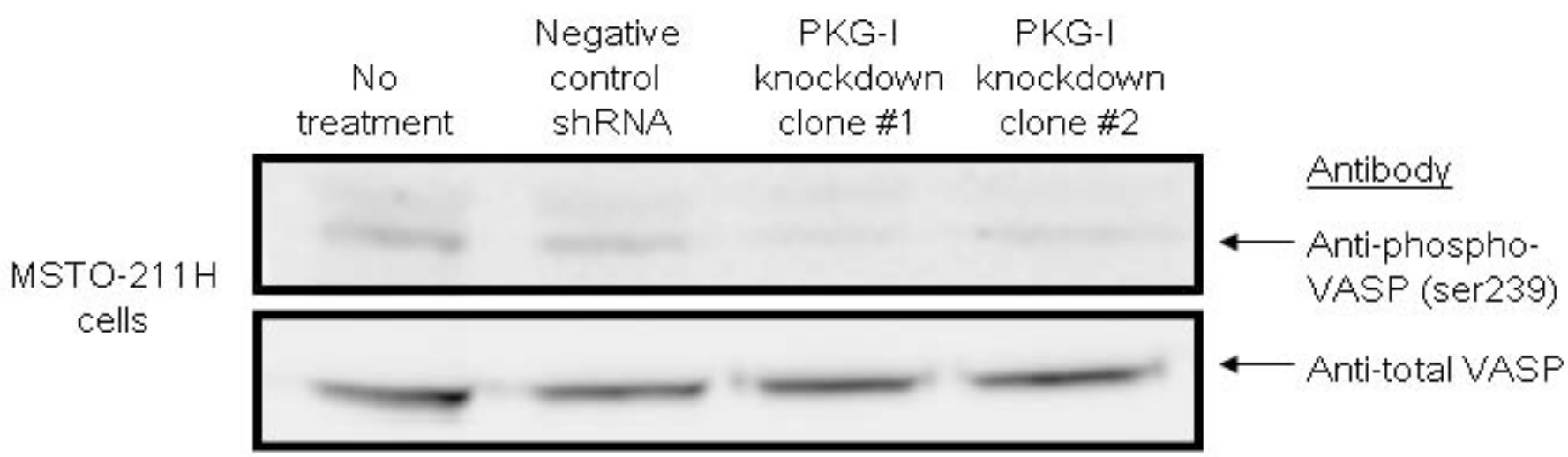
No treatment
Negative control shRNA
PKG-I knockdown clone #1
PKG-I knockdown clone #2
MSTO-211H cells
Antibody
Anti-phospho-VASP (ser239)
Anti-total VASP

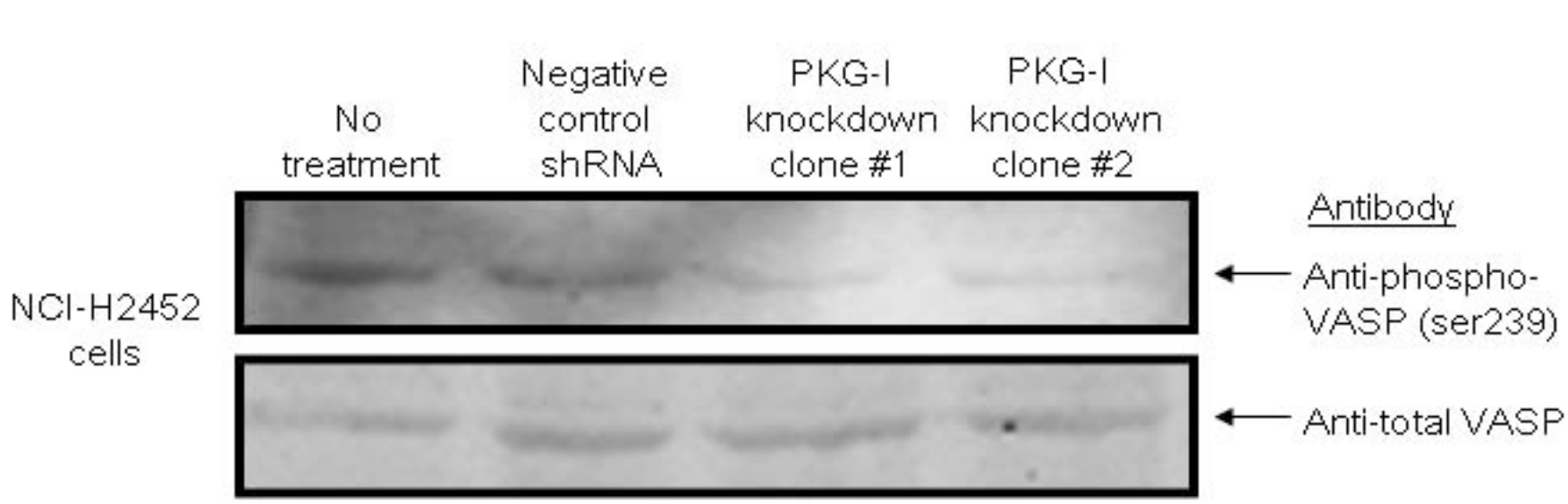
No treatment
Negative control shRNA
PKG-I knockdown clone #1
PKG-I knockdown clone #2
NCI-H2452 cells
Antibody
Anti-phospho-VASP (ser239)
Anti-total VASP

Figure 5

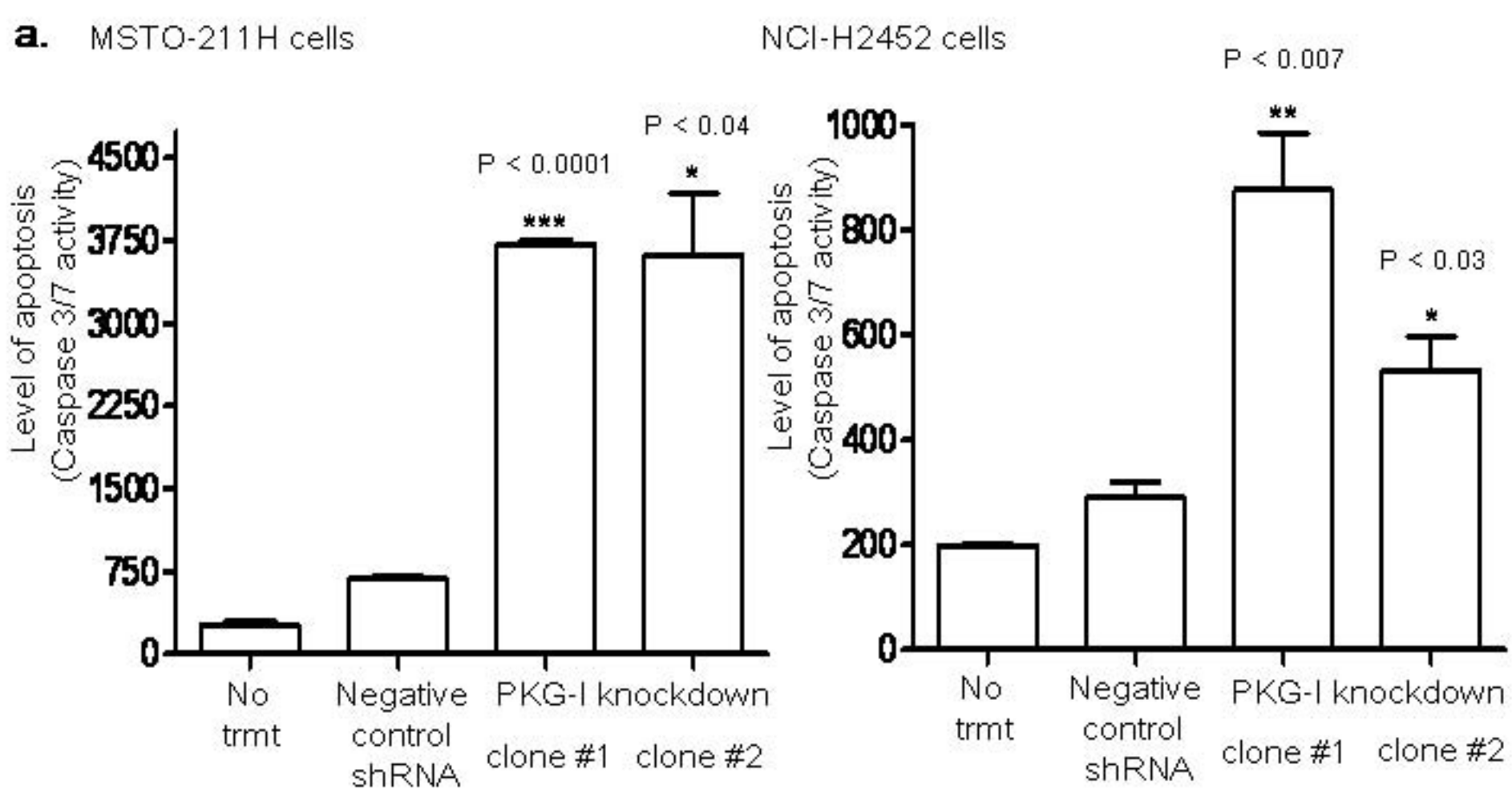
a.
MSTO-211H cells
NCI-H2452 cells
Level of apoptosis (Caspase 3/7 activity)
4500
3750
3000
2250
1500
750
0
P < 0.0001
***
P < 0.04
*
1000
800
600
400
200
P < 0.007
**
P < 0.03
*
No trmt
Negative control shRNA
PKG-I knockdown clone #1
clone #2
b.
MSTO-211H cells
NCI-H2452 cells
Cell number (MTT assay)
0.3
0.2
0.1
0.0
P < 0.04
*
P < 0.0002
***
0.12
0.10
0.08
0.06
0.04
0.02
0.00
P < 0.004
**
P < 0.0003
***
No trmt
Negative control shRNA
PKG-I knockdown clone #1
clone #2

Figure 6

a.

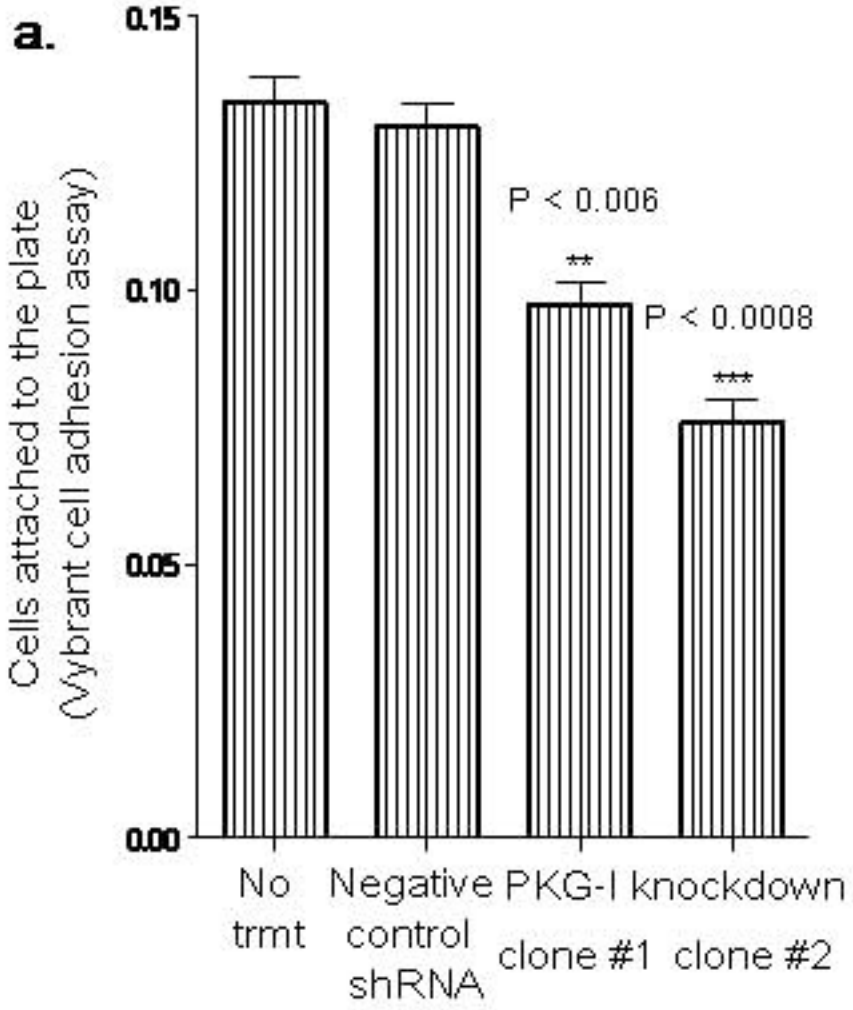
Cells attached to the plate
(Vybrant cell adhesion assay)
0.15
0.10
0.05
0.00
P < 0.006
**
P < 0.0008
***
No trmt
Negative control shRNA
PKG-I knockdown clone #1
clone #2

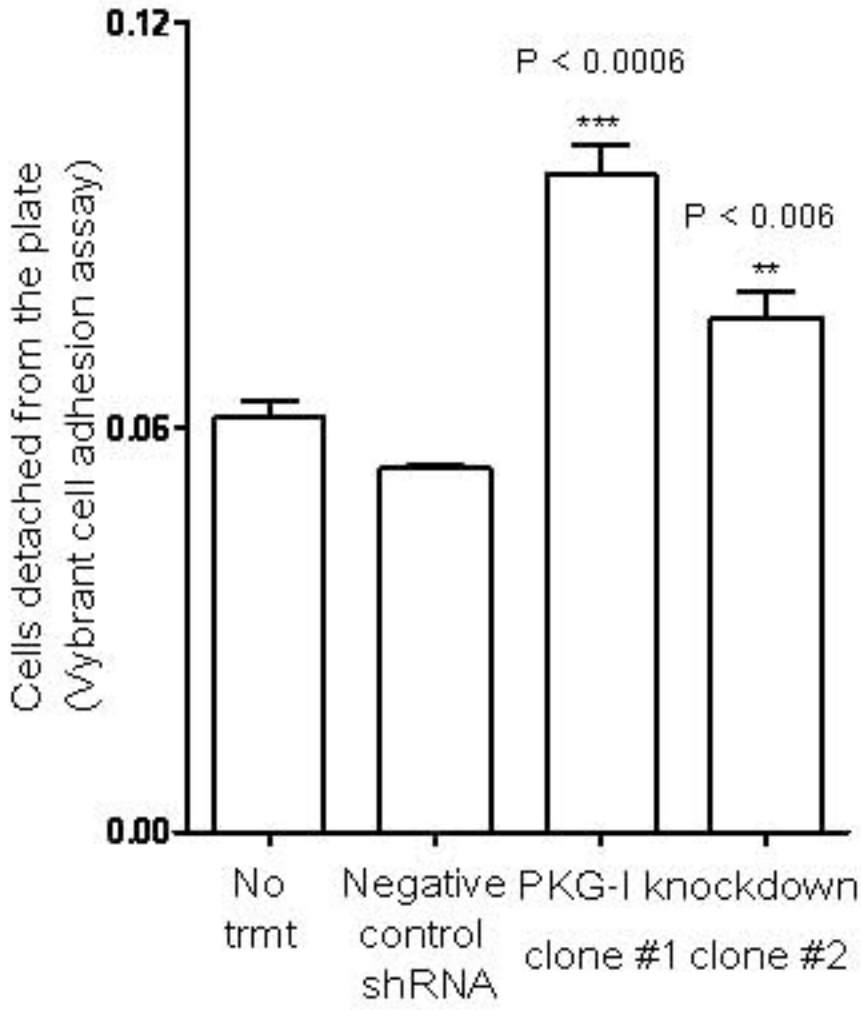
Cells detached from the plate
(Vybrant cell adhesion assay)
0.12
0.06
0.00
P < 0.0006
***
P < 0.006
**
No trmt
Negative control shRNA
PKG-I knockdown clone #1
clone #2

b.

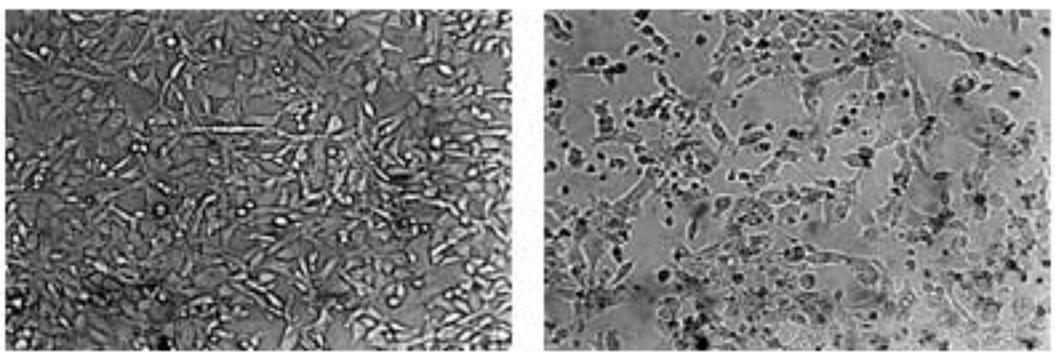
No treatment
PKG-I knockdown clone

c.

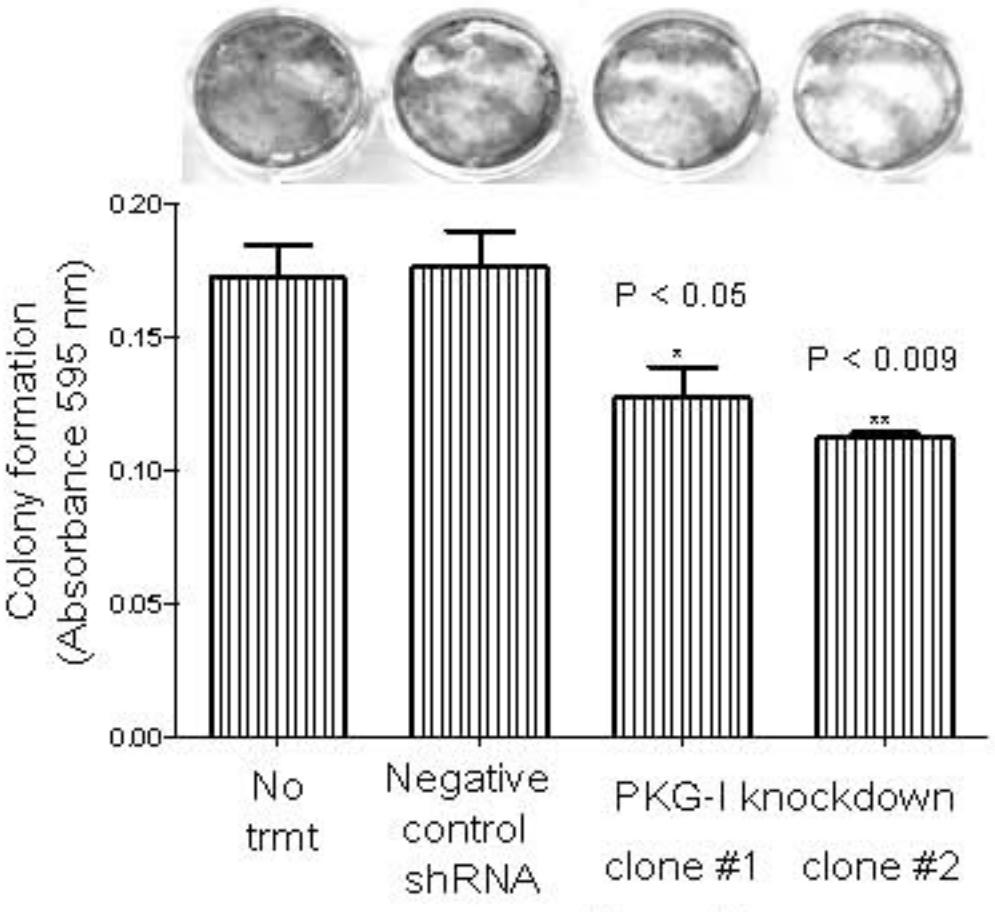
Colony formation
(Absorbance 595 nm)
0.20
0.15
0.10
0.05
0.00
P < 0.05
*
P < 0.009
**
No trmt
Negative control shRNA
PKG-I knockdown clone #1
clone #2

Figure 7

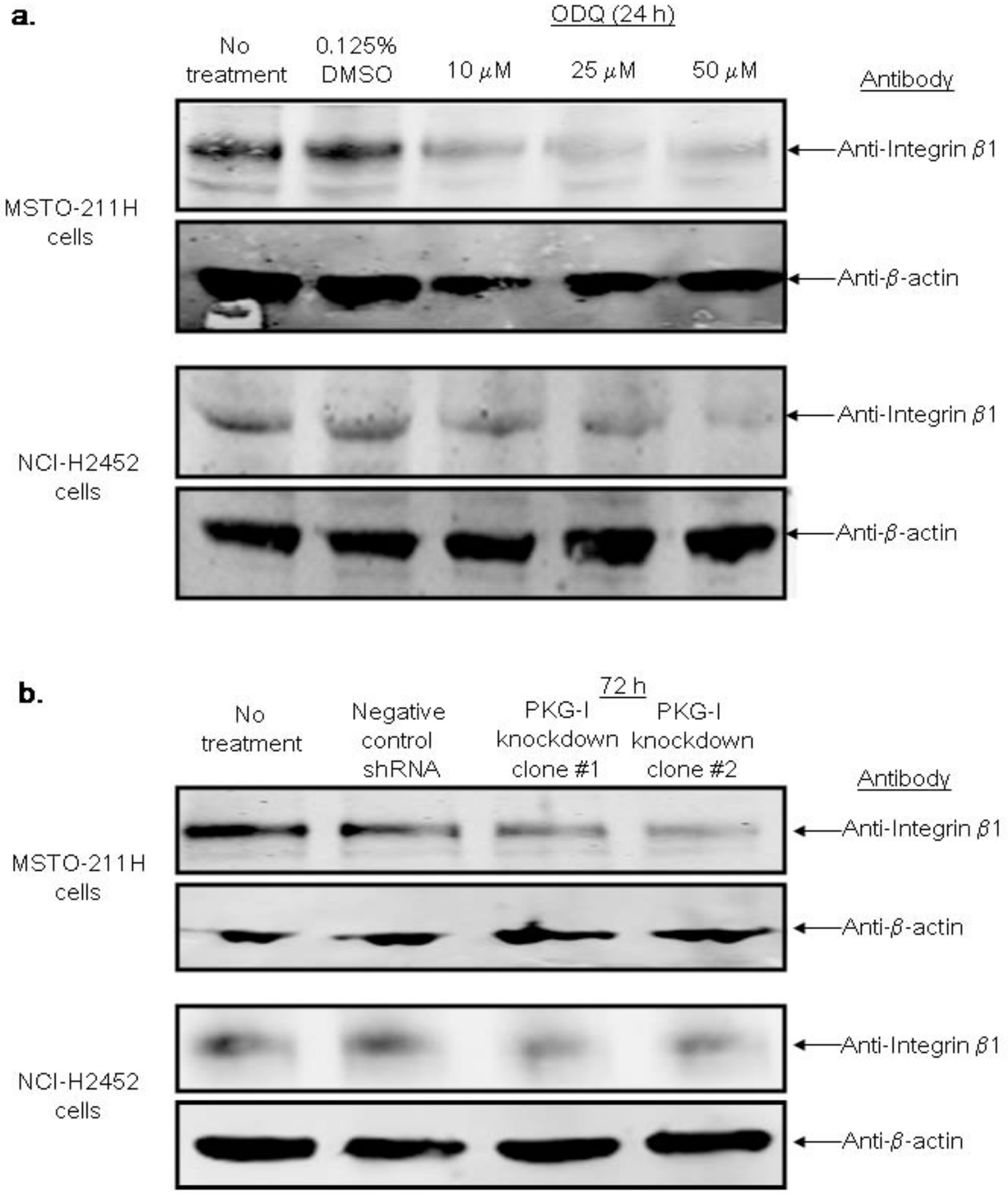
a.
ODQ (24 h)
No treatment
0.125% DMSO
10 μM
25 μM
50 μM
Antibody
MSTO-211H cells
Anti-Integrin β1
Anti-β-actin
NCI-H2452 cells
Anti-Integrin β1
Anti-β-actin
b.
72 h
No treatment
Negative control shRNA
PKG-I knockdown clone #1
PKG-I knockdown clone #2
Antibody
MSTO-211H cells
Anti-Integrin β1
Anti-β-actin
NCI-H2452 cells
Anti-Integrin β1
Anti-β-actin

Figure 8

Involvement of the protein kinase G type-Iα signaling pathway in suppressing apoptotic cell death in prostate cancer cells

Ronald R. Fiscus, Madhavi Bathina, Mary G. Johlfs, Janica C. Wong, Oscar B. Goodman, Jr., Sunil Sharma, Giuseppe Pizzorno and Nicholas J. Vogelzang

Cancer Molecular Biology Section, Nevada Cancer Institute, Las Vegas, Nevada, USA, and
College of Pharmcy, University of Southern Nevada, Henderson, Nevada, USA

Correspondence: Ronald R. Fiscus, University of Southern Nevada, 11 Sunset Way, Henderson, Nevada, USA 89014; Phone: 702-968-5570, Fax: 702-968-5573, email: rfiscus@usn.edu

Abstract

Previously our lab has shown the involvement of nitric oxide (NO), cGMP and protein kinase G (PKG) in the regulation of apoptosis in both normal cells and transformed cells. In the present study, it is hypothesized that PC-3, DU145 and LNCaP prostate cancer cell lines might involve the NO/cGMP/PKG signaling pathway in the regulation of spontaneous apoptosis. To test this hypothesis, apoptosis assays (Cell Death Detection ELISAs, measuring apoptotic DNA fragmentation) and Caspase-3/7 activity assays were used. Western blot analysis has shown that all three of the prostate cancer cell lines express predominantly the PKG-Iα isoform of PKG and endothelial nitric oxide synthase (eNOS), which is a source of endogenous NO. ODQ, an inhibitor of NO-induced activation of cGMP synthesis through selective inhibition of soluble guanylyl cyclase (sGC), induced apoptosis in all the three prostate cancer lines. ODQ also induced caspase-3/7 activity in all the three prostate cancer cells. These pro-apoptotic effects of ODQ were reversed by the cGMP analog 8-Bromo-cGMP, which bypasses the ODQ block. The involvement of PKG-Iα isoform was further confirmed by inhibiting the PKG-Iα using DT-2 and DT-3, both of which induced apoptosis in PC3, DU145 and LNCaP cells. Gene knockdown using PKG-I-specific shRNA in PC-3 cells also lead to induction of apoptotic DNA fragmentation and caspase-3/7 activation, showing a clear role of PKG-I in continually protecting against the spontaneous induction of apoptosis. These data identify a novel signaling pathway in prostate cancer cells that is essential for suppressing the induction of apoptosis. New therapeutic agents that target this signaling pathway may provide a useful, more effective means for stopping the development of prostate cancer.

Introduction

Prostate cancer is the second leading cause of cancer deaths among men in United States. In 2008 an estimated 186,320 new cases of prostate cancer and an estimated 28,660 new prostate cancer deaths occurred in USA (Jemal *et al.*, 2008) Prostate cancer is resistant to chemotherapy, radiation and hormone therapy. Both local and metastatic prostate cancer prognosis is poor (Stearns and McGarvey, 1992) For treating the metastatic prostate cancer, androgen deprivation therapy is commonly employed but, in almost all of the cases the prostate cancer reverts back and becomes resistant (Denis and Murphy, 1993) In many cases chemotherapeutic agents are not 100% effective (Aaltoma *et al.*, 2001) Hormone refractory prostate cancer treatment in combination with chemotherapuetic agents is still not effective and needs further investigation and discovery of more effective treatment methods with less side effects and less chances of the tumor reverting back (Oh and Kantoff, 1998)

The aim in the present study is to determine the role of a novel signaling pathway driven by NO, cGMP and PKG in preventing the prostate cancer cells from undergoing spontaneous apoptosis. NO activates the heme-containing enzyme, sGC which converts GTP in to cGMP. cGMP further activates PKG that leads to phosphorylation of down stream target proteins which are involved in cell proliferation, gene regulation and apoptosis. In mammals the elevation in cGMP levels and the activation of sGC, have been shown to activate the PKG enzyme (Fiscus *et al.*, 1985)

NO plays an important role in neuronal development and is very crucial in regulating the cell death in neurodegenerative diseases such as parkinson's disease, Alzimers and

dementia (Chun *et al.*, 1995; Ciani *et al.*, 2002; Fiscus, 2002; Fiscus *et al.*, 2002; Lohmann *et al.*, 1997) The role of NO as pro-apoptotic or anti-apoptotic molecule depends on its concentration (Jenkins *et al.*, 1995) NO activates sGC and increases the cGMP levels. cGMP activates the PKG which is an intracellular receptor protein. Other receptor proteins activated by cGMP are cGMP-regulated ion channels and cGMP-regulated phosphodiesterases (Lincoln and Cornwell, 1993) cGMP which is activated by NO and the natriuretic peptides has been implicated in regulating gene expression especially in cardio vascular system (Pilz and Casteel, 2003) cGMP via the activation of PKG is involved in relaxation of smooth muscle cells (Fiscus *et al.*, 1983; Fiscus *et al.*, 1985; Murad *et al.*, 1985) Further it has been shown that PKG-Iα isoform is responsible for relaxation of vascular smooth muscle cells via cGMP-dependent pathway (Michael *et al.*, 2008) cGMP also plays a crucial role in regulating the cytosolic calcium levels (Cornwell and Lincoln, 1989; Felbel *et al.*, 1988) Gene deletion studies have suggested that PKG signaling plays an important role in hear physiology, vasorelaxation and platelet function (Hofmann *et al.*, 2006)

There are two forms of PKG: PKG-I and PKG-II. PKG-I has two alternately spliced variants – PKG-Iα and PKG-Iβ (Woodford *et al.*, 1989) The two isoforms of PKG-I, Iα and Iβ differ in the amino terminal region. The amino terminus of PKG-Iα has been shown to be responsible for regulation the binding of cGMP (Pfeifer *et al.*, 1998; Wernet *et al.*, 1989)

The role of cGMP and PKG at the basal levels has been implicated in immortalized uterine epithelial cells. The inhibitors of sGC (ODQ and NS2028) and PKG (KT5823) induce apoptosis in these cells (Chan and Fiscus, 2003) In neuronal cells apoptosis is regulated by cGMP/PKG pathway. BNP (a natriuretic peptide in brain that activates particulate guanylyl cyclase, pGC) elevates cGMP levels in PC12 cells and prevents

spontaneous apoptosis. Also, addition of cGMP analog 8-Bromo-cGMP that activates PKG protected the cells against apoptosis (Fiscus *et al.*, 2001) ANP also induces smooth muscle cell relaxation in rat aorta via cGMP-dependent protein kinase (Fiscus *et al.*, 1985) Both ANP and BNP protected the PC12 cells against spontaneous apoptosis induced by serum-deprivation (Fiscus *et al.*, 2001) ANP also protects the NG108 cells from spontaneous apoptosis (Cheng Chew *et al.*, 2003) It has been also proven in PC12 and NG108 cells that cGMP acts as a prosurvival factor and inhibits apoptosis (Fiscus, 2002) PKG also regulates bone development by inducing IL-6 expression, 8-CPT-cGMP induced nuclear translocation of PKG-I and increased the phosphorylation of CREB at Ser 133 position. Inhibitors of the NO/cGMP/PKG pathway inhibited the IL-6 expression in osteoblasts (Broderick *et al.*, 2007) PKG-I nuclear translocation was also shown to be induced by adrenomedulin and the PKG inhibitor DT-5823 blocks these effects (Berenguer *et al.*, 2008) PKG also regulates gene expression of *fos* (proto Oncogene; AP-1 family protein) and translocates to nucleus where it phosphorylates CREB (Gudi *et al.*, 2000)

The NO/cGMP/PKG signaling pathway has also been studied in the cancer cells. The NO pathway via cGMP-dependent protein kinase has been shown to induce apoptosis (Browning, 2008; Liu *et al.*, 2001) as well as inhibits migration in colon cancer cells (Deguchi *et al.*, 2004) It has been shown previously by Dr. Fiscus' lab that NO/cGMP/PKG-I signaling pathway is hyper activated in ovarian cancer cells that leads to resistance to chemotherapeutic agents. The ovarian cancer cells express two forms of NO synthase, eNOS and nNOS, which is the source of endogenous NO (Fraser *et al.*, 2006; Leung *et al.*, 2008) It has also been shown previously that prostate cancer tissue taken from patients highly express iNOS (Aaltoma *et al.*, 2001) iNOs is expressed highly in human prostate carcinoma but not in the normal prostate tissue (Klotz *et al.*, 1998)

The prostate cancer cell line LNCaP also express eNOS at high levels (Tong and Li, 2004) In this study we hypothesize that in prostate cancer cells like ovarian cancer, the NO induced PKG-I signaling pathway is hyper activated and is involved in protecting the cells from spontaneous apoptosis.

Materials and Methods

Cell cultures and reagents

PC-3, DU145 and LNCaP prostate cancer cell lines were obtained from American type culture collection (Mansassas, VA). PC-3 cells were maintained in F-12K medium, DU145 cells were maintained in Minimum Essential Medium (MEM) and LNCaP cells were maintained in RPMI-1640 medium. All media were supplemented with 10% fetal bovine serum and 1% penicillin-streptomycin (ATCC, Mansassas, VA). All the cells were cultured at 37^0C, at 5% CO_2. Cells were treated with ODQ (Sigma, St. Louis, MO, USA) 8-Bromo-cGMP (Biomol international, Plymouth Meeting, PA, USA) and PKG-Iα inhibitors DT-2 and DT-3 (Biolog, Hayward CA, USA and Calbiochem, Gibbstown, NJ, USA) to measure caspase-3/7 activity and apoptosis.

Apoptosis Assay: Cell Death Detection ELISA

Cell death detection was determined using Cell Death Detection ELSIA kit (Roche Diagnostics Inc. Indianapolis, IN, USA) Ten thousand cells per well of 96 well plates were exposed to the PKG-Iα inhibitors DT-2 and DT-3 at 0, 1, 10 and 30 μM concentrations for 24 h or the sGC inhibitor ODQ at 0, 10, 30, 50 and 100 μM concentrations for 24 h. In some experiments, cells treated with ODQ were pretreated for 4 h with 8-Bromo-cGMP, a direct activator of all isoforms of PKG. At the end of the incubation period, levels of apoptosis in the control and treatment groups were measured following the manufacturer's protocol. Each control and treatment group represents 6 different samples.

Caspase activity by Caspase-Glo 3/7 Assay

Caspase-3/7 activity in all the three of the prostate cancer cells were determined using Caspase-3/7 Glo activity kit (Promega Corporation, Madison, WI, USA). Two thousand cells per well were plated in 384 well plates. The cells were exposed to the sGC inhibitor ODQ at 0, 10, 30, 50 and 100 μM concentrations and PKG-Iα inhibitors DT-2 and DT-3 at 0, 1 and 10 μM concentrations for 24 h. At the end of the incubation period caspase-3/7 activity in the cell lysates was measured according the instructions in the manufacturer's protocol. Each control and treatment group represents 9 different samples.

Cell Lysis and Protein Quantification

For western blot analysis, one million cells were lysed with SDS lysis buffer. The total amount of protein in the lysates was calculated from the fluorescence-based protein Quantitation kit EZQ (Molecular Probes, Carlsbad, CA, USA)

Western blot analysis using Infrared imaging

Equal amounts of protein from all the three prostate cancer cell lines were loaded and resolved by SDS-PAGE. The separated proteins were transferred to a nitrocellulose membrane (Amersham Biosciences, Piscataway, NJ, USA) through a wet transfer at 35Volts overnight at 4^0C. The membrane was blocked at room temperature for one hour in the blocking buffer (LI-COR Biosciences, Lincoln, NE, USA) with 0.1% Tween (Invitrogen, Carlsbad, CA, USA) followed by overnight incubation with the primary antibody, rabbit anti-PKG-I antibody (Cell signaling technology, Beverly, MA, USA) (247.7 μg/ml) at 1:1000 dilution or rabbit anti-eNOS antibody (Calbiochem, Gibbstown, NJ, UAS) at 1:500 dilution and anti α–GAPDH antibody (eGene Inc., Irvine, CA, USA)

Secondary antibodies labeled with infrared dyes were used (LI-COR biosciences). The membranes were scanned on the LI-COR Infrared imaging system for the expression of PKG-I or eNOS in all the three prostate cancer cell lines.

RNA interference

PC-3 cells to be tested for induction of apoptosis were seeded in a 96 well plate at a density of 20,000 cells/well in media lacking antibiotics and incubated overnight. The following day, the cells were transfected with PKG-I-specific shRNA containing expression vectors (Origene, Rockville, MD) as follows: 3.0% Lipofectamine 2000 (Invitrogen) and vector at a ratio of 1ug/100ul were added to Opti-MEM (Invitrogen) serum free media and incubated at room temperature for 20 minutes. The mixture was then added to the cells drop-wise. Following gentle mixing, the cells were incubated for 48-72 hours and levels of apoptosis were assessed. PKG expression levels were monitored using RT-PCR and subsequent analysis on a 12-channel capillary electrophoresis system with a light emitting diode (eGene Inc., Irvine, CA, USA)

Gene expression analyzed on a 12-channel capillary electrophoresis system with a light emitting diode

RNA was trizol (Life Technologies, Grand Island, NY, USA) extracted from 50,000 PC-3 cells. One microgram of purified total RNA was converted to cDNA using Superscript Vilo reverse transcriptase kit (Invitrogen) The cDNA was used in a PCR reaction with the PKG-Iα specific primers (Forward Primer – 5'-GGC GCA GGG CAT CTC G-3' and Reverse Primer – 5'-ATC CAC AAT CTC CTG GAT CTG-3' from Integrated DNA technologies, Coralville, IA, USA) using a GeneAmp PCR system 9700. After 30 cycles, the PCR products were run on a QIAexcel (eGene, Inc.), an automated high

performance genetic analyzer that utilizes capillary electrophoresis (CE). Products were injected at 8 kV for 20 seconds and separated at 6kV for 400 seconds. Products were sequenced to verify their identity.

Statistical Analysis

Results were expressed as the mean ± SEM of at least 6 different samples. Statistical analysis was performed by one way ANOVA followed by Dunnett's post test using PRISM software (Version 3.0; GraphPad) Results were inferred using a statistical significance of $P<0.01$.

Results

Prostate cancer cells express eNOS

To determine whether the prostate cancer cells express the nitric oxide synthase (NOS) which is the potential source of NO in these cells, western blot analysis was carried out using specific antibody against eNOS. All the three prostate cancer cell lines express the eNOS although at different expression levels (Figure 1, Panel A). This proves that eNOS is the source of NO in these cells which activates sGC. sGC is the major enzyme responsible for inducing cGMP synthesis in mammalian cells (Pilz and Casteel, 2003)

ODQ induces caspase-3/7 activity in all the three prostate cancer cell lines

To determine the role of cGMP/PKG-Iα pathway in maintaining low levels of apoptosis in prostate cancer cells, we treated all the three prostate cancer cell lines with ODQ for 24 hours at the concentrations of 0, 10, 30, 50 and 100 μM. ODQ induced caspase-3/7 activity in a dose dependent manner in all the three prostate cancer cell lines (Figure 1, Panel B). This proves that inhibiting the sGC enzyme induces caspase activity, by inhibiting the cGMP synthesis and further decreasing the activity of PKG-Iα.

ODQ induces apoptosis in all the three prostate cancer cell lines

After determining the induction of caspase activity by ODQ, we further tested if inhibiting sGC will induce apoptosis. To determine this Cell Death Detection ELISA was used. Ten thousand cells were plated per well of a 96-well plate, the cells were treated with ODQ the following day, at the concentrations of 0, 10, 30 and 50 μM. After 24 h exposure to ODQ, apoptosis was measured as described in materials and methods section. In PC-3, DU145 and LNCaP cells, ODQ induced apoptosis in a dose dependent manner. In PC-3

cells 30 and 50 μM ODQ significantly induced apoptosis, almost 4 fold increase compared to the control (Figure 2, panel A) In DU145 cells, 30 and 50 μM ODQ induced 3 fold and 3.2 fold increase in apoptosis respectively compared to the control (Figure 3, panel A) In LNCaP cells, 30 and 50 μM ODQ induced 2.5 fold and 4.0 fold increase in apoptosis respectively compared to the control (Figure 4, panel A) This further provides an evidence for the role of cGMP mediated induction of apoptosis in the prostate cancer cell lines.

8-Bromo-cGMP reverses the apoptosis induced by ODQ in prostate cancer cell lines

To determine the role of PKG-Iα which is the downstream protein kinase activated by cGMP, we used 8-Bromo-cGMP which is a direct activator of PKG-Iα to bypass the ODQ-induced block in the NO/cGMP/PKG-Iα signaling pathway. To show that the proposed signaling pathway is mediated by PKG-Iα, we treated all the three prostate cancer cell lines, with 8-Bromo-cGMP prior to the treatment with sGC inhibitor ODQ. This will allow the accumulation of enough PKG-Iα activity that would allow the cells to bypass the ODQ induced inhibition of sGC and its effects (lowering of PKG-Iα activity via decreasing the cGMP levels) 8-Bromo-cGMP was added at the concentration of 1000 μM at least one hour before the addition of 30 μM ODQ. After 24 h incubation apoptosis was measured in these cells using Cell Death Detection ELISA. In both DU145 cells and LNCaP cells, 8-Bromo-cGMP pre treatment reversed the effects of ODQ almost completely, indicating the involvement of PKG-Iα in inducing apoptosis in these cells. (Figure 3, panel B and Figure 4, panel B respectively) In PC-3 cells the effects of 8-Bromo-cGMP was not significantly seen (Figure 2, Panel A). This difference in the response to 8-Bromo-cGMP can be attributed to the type of PKG-I isoforms expressed in this cell line. The basal levels of PKG-Iα and Iβ isoforms have opposite effects on cells. PKG-Iα basal activation protects the cells whereas basal PKG-Iβ activation promotes

apoptosis. Since PC-3 cells express both isoforms of PKG-I, (Figure 5, panel A) the 8-Bromo-cGMP effects are not totally uncovered.

Differential expression of PKG-I isoforms in prostate cancer cells

Now that we have confirmed the role of PKG-Iα isoform in maintaining low levels of apoptosis, we then looked at the expression levels of PKG-Iα in all the three prostate cancer cell lines. Western blot analysis was carried out using Odyssey infrared imaging system as described in materials and methods. 70 µg of total protein was used for each cell line. PC-3 cells express both the isoforms of PKG-I, with PKG-Iα predominantly than PKG-Iβ. (Figure 5, panel A) The digitally enhanced image shows the expression of PKG-Iα isoform in DU145 cells and LNCaP whereas PKG-Iβ isoform is not detectable. (Figure 5, panel A) The Odyssey Infrared imager allows quantifying the western blot signal which is shown in Figure 5, panel B. The relative levels of PKG-Iα isoform expression are different in the three prostate cancer cell lines. PC-3 cells express 4.4 times more than DU145 and LNCaP cells.

PKG-Iα inhibitors DT-2 and DT-3 induce caspase-3/7 activity

The role of PKG-Iα basal activity in preventing spontaneous apoptosis was elucidated by using direct PKG-Iα inhibitors DT-2 and DT-3, both of which induced caspase-3/7 activity. The cells are treated with the peptides DT-2 and DT-3 at the concentrations 0, 1 and 10 µM each for 24 h. After the incubation caspase activity was measured using Caspase-3/7 Glo assay as described in materials and methods. In PC-3 and DU145 both DT-2 and DT-3 significantly induced caspase-3/7 activity in a dose dependent manner (Figure 6, panel A and panel B respectively). In LNCaP cells DT-2 induced caspase-3/7 activity in a dose dependent manner (Figure 6, panel C), whereas DT-3 induced caspase-3/7 activity at 10 µM concentration.

PKG-Iα inhibitors DT-2 and DT-3 induce apoptosis

Both the PKG-Iα inhibitors DT-2 and DT-3 induce apoptosis in prostate cancer cells. The cells were treated with DT-2 and DT-3 at the concentrations of 0.0, 1.0 and 10.0 μM. After 24 h treatment the cells were lysed and the apoptotic DNA fragments were measured using a Cell Death Detection ELISA. In PC-3 cells, 1.0 μM DT-2 and DT-3 did not induce statistically significant increase in apoptosis, but 10.0 μM DT-2 and DT-3 induced 4.5 fold and 1.6 fold increases in apoptosis compared to the control (Figure 7, Panel A). In DU145 cells, both DT-2 and DT-3 induced dose dependent increase in apoptosis. With 1.0 and 10.0 μM, DT-2 induced 1.9 fold and 2.0 fold increase in apoptosis respectively. DT-3 at lower concentration of 1.0 μM did not induce statistically significant level of apoptosis, but with 10.0 μM concentration it induced 1.7 fold increase in apoptosis compared to the control (Figure 7, Panel B). In LNCaP cells both DT-2 and DT-3 showed statistically significant and dose dependent increase in apoptosis compared to the control. DT-2 induced 1.75 fold, 3.0 fold and 6.25 fold increases in apoptosis compared to the control (Figure 7, Panel C). DT-3 induced 1.26 fold, 1.31 fold and 3.6 fold increases in apoptosis compared to the control (Figure 7, Panel D). The difference in responses with DT-2 and DT-3 can be attributed to the way these peptides are transported into the cells as well as their resistance to be degraded by the cellular components before they could inhibit the PKG. These responses might also be attributed to differences in the cell lines. These results with the direct PKG-Iα inhibitors suggests that in all the three prostate cancer cell lines, PKG signaling pathway is involved in maintaining low levels of apoptosis and is important for prolonged survival of prostate cancer cells.

Gene knockdown using PKG-I-specific shRNA induce apoptosis and caspase activation in PC-3 prostate cancer cell line

To further confirm the role of PKG-Iα in inducing apoptosis, PC-3 cells were transfected with PKG-I-specific shRNA containing expression vector for 48-72 hours as described in materials and methods. At the end of the incubation period the PKG-I knockdown is confirmed by gene expression analysis on a 12-channel capillary electrophoresis system (as described in materials and methods) (Figure 8, Panel A) PC-3 cells after transfection, were lysed and the apoptotic DNA fragments were measured using a Cell Death Detection ELISA. Compared to the control and the negative control, the PKG-I knockdown showed a significant increase in the level of apoptosis (Figure 8, Panel B) PC-3 cells transfected with PKG-I-specific shRNA were also analyzed for the induction of caspase-3/7 activity using caspase-3/7 Glo assay. The PKG-I knockdown showed a significant increase in caspase-3/7 activity compared to the no treatment and the negative control (Figure 8, Panel C) The results with gene knockdown / transfection studies strongly suggests that PKG-Iα isoform is involved in preventing spontaneous apoptosis in PC-3 prostate cancer cell line.

Discussion

In this study we demonstrated that NO/cGMP/PKG signaling pathway plays a significant role in maintaining low levels of apoptosis in PC-3, DU145 and LNCaP cell lines. Here we showed that prostate cancer cells express eNOS which is a source of NO and PKG-Iα isoform using western blotting technique. Our data using highly specific sGC enzyme inhibitor ODQ and selective PKG-Iα inhibitors DT-2 & DT-3 showed induction of apoptosis in all the three prostate cancer cell lines. This is further confirmed by gene knockdown studies using PKG-I-specific shRNA which induced caspase-3/7 activity and apoptosis in PC-3 prostate cancer cell line. Further the data showed that addition of 8-Bromo-cGMP, which is a direct activator of PKG, reverses the induction of apoptosis by ODQ. This strongly suggests that basal levels of NO/cGMP/PKG are involved in preventing spontaneous apoptosis in prostate cancer cell lines.

Low levels of NO activates the sGC enzyme by binding to its heme group, this inturn elevates the cGMP levels which increases the enzyme activity of PKG. This is thought to be mediating anti apoptotic effects in mammalian cells (Fiscus, 2002; Fiscus *et al.*, 2002) In 2002 Fiscus et al have shown that nNOS is constitutively expressed in neural cells (Fiscus, 2002; Fiscus *et al.*, 2002) Later it has been found that iNOs, eNOS and nNOS are expressed in many different cell types. eNOS and nNOS function has been demonstrated as an important factor in regulating cardiovascular and neuronal systems (Fiscus, 2002; Fiscus *et al.*, 2002) Previous reports showed the expression of all 3 isoforms of NOs and their role in chemoresistance (Leung *et al.*, 2008) NO can show protumor or antitumor activity depending on it's concentration (Xie *et al.*, 1996) NOS expression and NO production has been observed in a number of different cancer types. Thomsen et al showed that NO synthase activity is related to malignancy in

gynecological cancers (Thomsen *et al.*, 1994) It has also been shown that high levels of NO (from enhanced activity of iNOS) is involved in sustaining tumor growth via enhanced blood flow and vascular permeability in solid tumors (Doi *et al.*, 1996) Inhibition of NOS by L-NAME (NG-nitro-L-arginine methylester) and the resulting low NO production caused a decrease in tumor growth and lung metastasis (Orucevic and Lala, 1996) Over expression of eNOS and the resulting high levels of NO was shown to contribute to the tumor angiogenesis in oral squamous cell carcinoma (Shang and Li, 2005) It has been shown that iNOS is highly expressed in prostate carcinoma tissues compared to the benign tissue (Klotz *et al.*, 1998), but further investigations have not been done to study the role of NO or the associated downstream pathway in prostate cancer progression. To our knowledge we are the first to show the down stream signaling pathway from NO production (sGC/cGMP/PKG) that is involved in promoting survival of prostate cancer cells.

cGMP activates PKG both in vitro (Lincoln and Cornwell, 1993) and in vivo (Fiscus *et al.*, 1983) In vivo the cGMP activates the PKG in response to either NO or natriuretic peptides. NO activates the sGC and the natriuretic peptides such as ANP and BNP activate pGC (Fiscus *et al.*, 1983; Fiscus *et al.*, 1985) Here we have shown that the prostate cancer cell lines express eNOS, which is the source of NO. We hypothesized that NO activates sCG which activates the cGMP/PKG signaling pathway in these cells. This is confirmed by using highly specific inhibitor of ODQ which induced apoptosis in prostate cancer cells. We have found that PC-3 cells express both the isoforms of PKG, Iα and Iβ, whereas the DU145 and LNCaP cells express the Iα isoform. PKG-Iα & Iβ isoforms have opposite effects on the cells. Basal levels of PKG-Iα are responsible for maintaining low levels of apoptosis, where as basal levels of PKG- Iβ isoform induces apoptosis. This is clearly seen in our data, when the prostate cancer cells were treated

with 8-Bromo-cGMP, the direct activator of PKG, the apoptosis induced by ODQ was reversed to a greater extent in DU145 and LNCaP cells which express only the PKG-Iα isoform, but in PC-3 cells which express both the isoforms of PKG the reversal of ODQ induced apoptosis by 8-Bromo-cGMP was not as significant as in the DU145 and LNCaP cells. This suggests that in PC-3 cells the reversal of apoptosis by 8-Bromo-cCMP is masked by the effects of PKG-Iβ which induces apoptosis at the basal levels.

In summary our findings using the specific sGC inhibitors, PKG-Iα inhibitors and gene knockdown studies prove that the basal NO/cGMP/PKG-Iα signaling pathways is necessary in preventing spontaneous apoptosis in PC-3, DU145 and LNCaP cell lines. Our future studies will be focused on the downstream signaling proteins (apoptosis proteins and transcription factors) which are directly or indirectly activated by PKG-Iα that are responsible for mediating low levels of apoptosis in these cells. Our ultimate goal is to develop inhibitors of PKG-Iα that would be specific for only cancer cells.

Acknowledgements: This research was supported by a Department of Defense grant (# W81XWH-07-1-0543) and Nevada Cancer Institute Startup Funding, awarded to Ronald R. Fiscus, Nicholas J. Vogelzang, Sunil Sharma and Giuseppe Pizzorno.

References

Aaltoma SH, Lipponen PK, Kosma VM (2001). Inducible nitric oxide synthase (iNOS) expression and its prognostic value in prostate cancer. *Anticancer Res* **21:** 3101-6.

Berenguer C, Boudouresque F, Dussert C, Daniel L, Muracciole X, Grino M *et al* (2008). Adrenomedullin, an autocrine/paracrine factor induced by androgen withdrawal, stimulates 'neuroendocrine phenotype' in LNCaP prostate tumor cells. *Oncogene* **27:** 506-18.

Broderick KE, Zhang T, Rangaswami H, Zeng Y, Zhao X, Boss GR *et al* (2007). Guanosine 3',5'-cyclic monophosphate (cGMP)/cGMP-dependent protein kinase induce interleukin-6 transcription in osteoblasts. *Mol Endocrinol* **21:** 1148-62.

Browning DD (2008). Protein kinase G as a therapeutic target for the treatment of metastatic colorectal cancer. *Expert Opin Ther Targets* **12:** 367-76.

Chan SL, Fiscus RR (2003). Guanylyl cyclase inhibitors NS2028 and ODQ and protein kinase G (PKG) inhibitor KT5823 trigger apoptotic DNA fragmentation in immortalized uterine epithelial cells: anti-apoptotic effects of basal cGMP/PKG. *Mol Hum Reprod* **9:** 775-83.

Cheng Chew SB, Leung PY, Fiscus RR (2003). Preincubation with atrial natriuretic peptide protects NG108-15 cells against the toxic/proapoptotic effects of the nitric oxide donor S-nitroso- N-acetylpenicillamine. *Histochem Cell Biol* **120:** 163-71.

Chun SY, Eisenhauer KM, Kubo M, Hsueh AJ (1995). Interleukin-1 beta suppresses apoptosis in rat ovarian follicles by increasing nitric oxide production. *Endocrinology* **136:** 3120-7.

Ciani E, Guidi S, Bartesaghi R, Contestabile A (2002). Nitric oxide regulates cGMP-dependent cAMP-responsive element binding protein phosphorylation and Bcl-2 expression in cerebellar neurons: implication for a survival role of nitric oxide. *J Neurochem* **82:** 1282-9.

Cornwell TL, Lincoln TM (1989). Regulation of intracellular Ca2+ levels in cultured vascular smooth muscle cells. Reduction of Ca2+ by atriopeptin and 8-bromo-cyclic GMP is mediated by cyclic GMP-dependent protein kinase. *J Biol Chem* **264:** 1146-55.

Deguchi A, Thompson WJ, Weinstein IB (2004). Activation of protein kinase G is sufficient to induce apoptosis and inhibit cell migration in colon cancer cells. *Cancer Res* **64:** 3966-73.

Denis L, Murphy GP (1993). Overview of phase III trials on combined androgen treatment in patients with metastatic prostate cancer. *Cancer* **72:** 3888-95.

Doi K, Akaike T, Horie H, Noguchi Y, Fujii S, Beppu T *et al* (1996). Excessive production of nitric oxide in rat solid tumor and its implication in rapid tumor growth. *Cancer* **77:** 1598-604.

Felbel J, Trockur B, Ecker T, Landgraf W, Hofmann F (1988). Regulation of cytosolic calcium by cAMP and cGMP in freshly isolated smooth muscle cells from bovine trachea. *J Biol Chem* **263:** 16764-71.

Fiscus RR (2002). Involvement of cyclic GMP and protein kinase G in the regulation of apoptosis and survival in neural cells. *Neurosignals* **11:** 175-90.

Fiscus RR, Rapoport RM, Murad F (1983). Endothelium-dependent and nitrovasodilator-induced activation of cyclic GMP-dependent protein kinase in rat aorta. *J Cyclic Nucleotide Protein Phosphor Res* **9:** 415-25.

Fiscus RR, Rapoport RM, Waldman SA, Murad F (1985). Atriopeptin II elevates cyclic GMP, activates cyclic GMP-dependent protein kinase and causes relaxation in rat thoracic aorta. *Biochim Biophys Acta* **846:** 179-84.

Fiscus RR, Tu AW, Chew SB (2001). Natriuretic peptides inhibit apoptosis and prolong the survival of serum-deprived PC12 cells. *Neuroreport* **12:** 185-9.

Fiscus RR, Yuen JP, Chan SL, Kwong JH, Chew SB (2002). Nitric oxide and cyclic GMP as pro- and anti-apoptotic agents. *J Card Surg* **17:** 336-9.

Fraser M, Chan SL, Chan SS, Fiscus RR, Tsang BK (2006). Regulation of p53 and suppression of apoptosis by the soluble guanylyl cyclase/cGMP pathway in human ovarian cancer cells. *Oncogene* **25:** 2203-12.

Gudi T, Casteel DE, Vinson C, Boss GR, Pilz RB (2000). NO activation of fos promoter elements requires nuclear translocation of G-kinase I and CREB phosphorylation but is independent of MAP kinase activation. *Oncogene* **19:** 6324-33.

Hofmann F, Feil R, Kleppisch T, Schlossmann J (2006). Function of cGMP-dependent protein kinases as revealed by gene deletion. *Physiol Rev* **86:** 1-23.

Jemal A, Siegel R, Ward E, Hao Y, Xu J, Murray T *et al* (2008). Cancer statistics, 2008. *CA Cancer J Clin* **58:** 71-96.

Jenkins DC, Charles IG, Thomsen LL, Moss DW, Holmes LS, Baylis SA *et al* (1995). Roles of nitric oxide in tumor growth. *Proc Natl Acad Sci U S A* **92:** 4392-6.

Klotz T, Bloch W, Volberg C, Engelmann U, Addicks K (1998). Selective expression of inducible nitric oxide synthase in human prostate carcinoma. *Cancer* **82:** 1897-903.

Leung EL, Fraser M, Fiscus RR, Tsang BK (2008). Cisplatin alters nitric oxide synthase levels in human ovarian cancer cells: involvement in p53 regulation and cisplatin resistance. *Br J Cancer* **98:** 1803-9.

Lincoln TM, Cornwell TL (1993). Intracellular cyclic GMP receptor proteins. *FASEB J* **7:** 328-38.

Liu L, Li H, Underwood T, Lloyd M, David M, Sperl G *et al* (2001). Cyclic GMP-dependent protein kinase activation and induction by exisulind and CP461 in colon tumor cells. *J Pharmacol Exp Ther* **299:** 583-92.

Lohmann SM, Vaandrager AB, Smolenski A, Walter U, De Jonge HR (1997). Distinct and specific functions of cGMP-dependent protein kinases. *Trends Biochem Sci* **22:** 307-12.

Michael SK, Surks HK, Wang Y, Zhu Y, Blanton R, Jamnongjit M *et al* (2008). High blood pressure arising from a defect in vascular function. *Proc Natl Acad Sci U S A* **105:** 6702-7.

Murad F, Rapoport RM, Fiscus R (1985). Role of cyclic-GMP in relaxations of vascular smooth muscle. *J Cardiovasc Pharmacol* **7 Suppl 3:** S111-8.

Oh WK, Kantoff PW (1998). Management of hormone refractory prostate cancer: current standards and future prospects. *J Urol* **160:** 1220-9.

Orucevic A, Lala PK (1996). NG-nitro-L-arginine methyl ester, an inhibitor of nitric oxide synthesis, ameliorates interleukin 2-induced capillary leakage and reduces tumour growth in adenocarcinoma-bearing mice. *Br J Cancer* **73:** 189-96.

Pfeifer A, Klatt P, Massberg S, Ny L, Sausbier M, Hirneiss C *et al* (1998). Defective smooth muscle regulation in cGMP kinase I-deficient mice. *EMBO J* **17:** 3045-51.

Pilz RB, Casteel DE (2003). Regulation of gene expression by cyclic GMP. *Circ Res* **93:** 1034-46.

Shang ZJ, Li JR (2005). Expression of endothelial nitric oxide synthase and vascular endothelial growth factor in oral squamous cell carcinoma: its correlation with angiogenesis and disease progression. *J Oral Pathol Med* **34:** 134-9.

Stearns ME, McGarvey T (1992). Prostate cancer: therapeutic, diagnostic, and basic studies. *Lab Invest* **67:** 540-52.

Thomsen LL, Lawton FG, Knowles RG, Beesley JE, Riveros-Moreno V, Moncada S (1994). Nitric oxide synthase activity in human gynecological cancer. *Cancer Res* **54:** 1352-4.

Tong X, Li H (2004). eNOS protects prostate cancer cells from TRAIL-induced apoptosis. *Cancer Lett* **210:** 63-71.

Wernet W, Flockerzi V, Hofmann F (1989). The cDNA of the two isoforms of bovine cGMP-dependent protein kinase. *FEBS Lett* **251:** 191-6.

Woodford TA, Correll LA, McKnight GS, Corbin JD (1989). Expression and characterization of mutant forms of the type I regulatory subunit of cAMP-dependent protein kinase. The effect of defective cAMP binding on holoenzyme activation. *J Biol Chem* **264:** 13321-8.

Xie K, Dong Z, Fidler IJ (1996). Activation of nitric oxide synthase gene for inhibition of cancer metastasis. *J Leukoc Biol* **59:** 797-803.

Titles and legends to figures

Figure 1 (a) Expression of eNOS in Prostate cancer cell lines. Western blot analysis of three prostate cancer cell lines PC-3, DU145 and LNCaP using LI-COR infrared imaging system shows the expression of eNOS. (b) Inhibition of sGC by the selective inhibitor ODQ induced Caspase 3/7 activity in all the three prostate cancer cell lines. The cells were treated with ODQ for 24 h and the caspase activity was detected by Caspase 3/7 Glo Assay. Results were analyzed using statistical analysis software graph pad prism and ANOVA test with Dunnett's post test showed significant increase in apoptosis in the treatment groups with a p-value of <0.01.

Figure 2 Inhibition of sGC by the selective inhibitor ODQ induced apoptosis in PC-3 prostate cancer cell line. (a) The cells were treated with ODQ for 24 h and the apoptotic DNA fragments in the cell lysate was measured using a cell death detection ELISA from Roche diagnostics, Inc. (b) The combined treatment with 8-Br-cGMP involved 1 h pre incubation. Results were analyzed using statistical analysis software graph pad prism and ANOVA test with Dunnett's post test showed significant increase in apoptosis in the treatment groups with a p-value of <0.01.

Figure 3 Inhibition of sGC by the selective inhibitor ODQ induced apoptosis in DU145 prostate cancer cell line. (a) The cells were treated with ODQ for 24 h and the apoptotic DNA fragments in the cell lysate was measured using a cell death detection ELISA from Roche diagnostics, Inc. (b) The combined treatment with 8-Br-cGMP involved 1 h pre incubation. Results were analyzed using statistical analysis software graph pad prism

and ANOVA test with Dunnett's post test showed significant increase in apoptosis in the treatment groups with a p-value of <0.01.

Figure 4 Inhibition of sGC by the selective inhibitor ODQ induced apoptosis in LNCaP prostate cancer cell line. (a) The cells were treated with ODQ for 24 h and the apoptotic DNA fragments in the cell lysate was measured using a cell death detection ELISA from Roche diagnostics, Inc. (b) The combined treatment with 8-Br-cGMP involved 1 h pre incubation. Results were analyzed using statistical analysis software graph pad prism and ANOVA test with Dunnett's post test showed significant increase in apoptosis in the treatment groups with a p-value of <0.01.

Figure 5 Protein expression levels of PKG-I isoform in LNCaP DU145 and PC-3 prostate cancer cell lines was determined using western blot analysis with infrared imaging system. (a) PC-3 cells express both isoforms of PKG, PKG-Iα and PKG-Iβ with PKG-Iα isoform predominantly. LNCaP and DU145 cells express PKG-Iα isoform. PKG-Iβ isoform is not detectable in LNCaP and DU145 cells. In the digitally enhanced image, the PKG-Iα isoform expression is more clearly seen in LNCaP and DU145 cells. (b) Basal levels of PKG-Iα isoform expression are different in the three prostate cancer cell lines, with PC-3 cells expressing 4.4 times more than LNCaP and DU145 cells.

Figure 6 Inhibition of PKG-Iα by the specific PKG-Iα inhibitors DT-2 and DT-3 induced Caspase 3/7 activity in (a) PC-3 (b) DU145 and (c) LNCaP prostate cancer cell lines. The cells were treated with DT-2 and DT-3 for 24 h and the Caspase activity was detected by Caspase 3/7 Glo Assay. Results were analyzed using statistical analysis

software graph pad prism and ANOVA test with Dunnett's post test showed significant increase in apoptosis in the treatment groups with a p-value of <0.01.

Figure 7 Inhibition of PKG-Iα by the specific PKG-Iα inhibitors DT-2 and DT-3 induced apoptosis in (a) PC-3 (b) DU145 and (c,d) LNCaP prostate cancer cell line. Cells were treated with DT-2 and DT-3 for 24 hours and the apoptotic DNA fragments in the cell lysate were measured by cell death detection ELISA. Graphs represent Mean ± SEM for each treatment and control group with an n value of 6. Statistical analysis was performed using Prism software and ANOVA test with Dunnett's post test showed significant increase in apoptosis in the treatment groups with a p-value of <0.01.

Figure 8 Gene knockdown using PKG-I-specific shRNA vector induced apoptosis and caspase-3/7 activation in PC-3 cell line (a) Gene expression levels of PKG-Iα using 12-channel capillary electrophoresis system after 48-72 hours of PKG-I-specific shRNA transfection. Negative control shRNA represents transfection of the cells with the vector carrying non specific gene. PKG-I knockdown shRNA #1 and shRNA # 2 represent two different clones of the vector (b) Knockdown of PKG-I induces apoptosis in PC-3 prostate cancer cells. Cells were lysed after 48-72 hours of gene transfection and the apoptotic DNA fragments were analyzed using cell death detection ELISA. A significant increase in the level of apoptosis was observed in the knockdown clones compared to the no treatment and the negative control (c) Knockdown of PKG-I induce caspase-3/7 activation in PC-3 cells. After 48-72 h transfection the caspase-3/7 activity was measured using Caspase-3/7 Glo assay. Compared to no treatment and the negative control the knockdown clones show significant increase in caspase-3/7 activity. Graphs represent Mean ± SEM for each treatment and control group with an n value of 6.

Statistical analysis was performed using Prism software and ANOVA test with Dunnett's post test showed significant increase in apoptosis in the treatment groups with a p-value of <0.01.

Figure 9 Model of PKG-Iα mediated induction of apoptosis by blocking the NO/cGMP/PKG pathway at various steps.

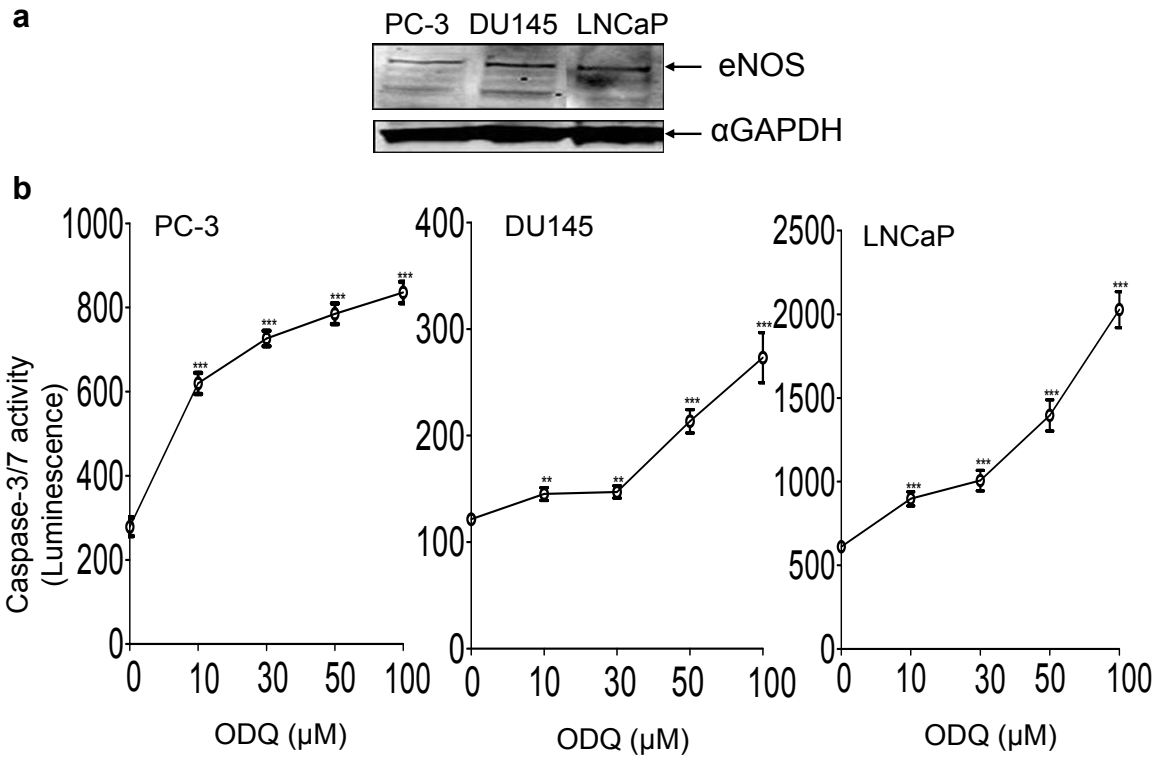

Figure 1

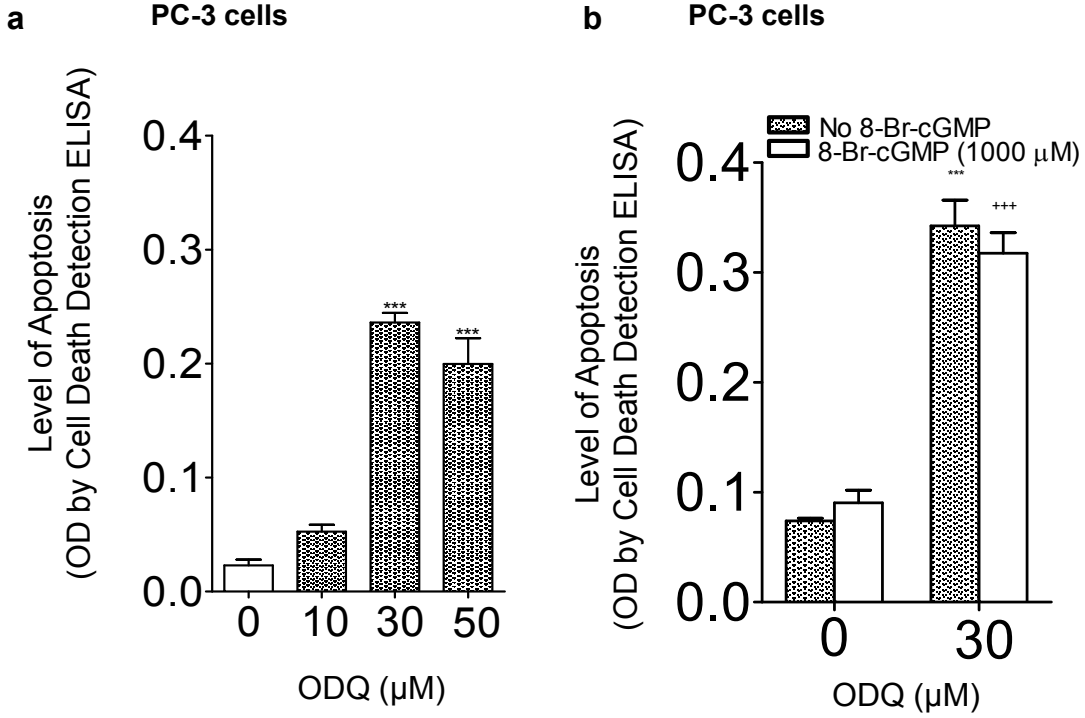

Figure 2

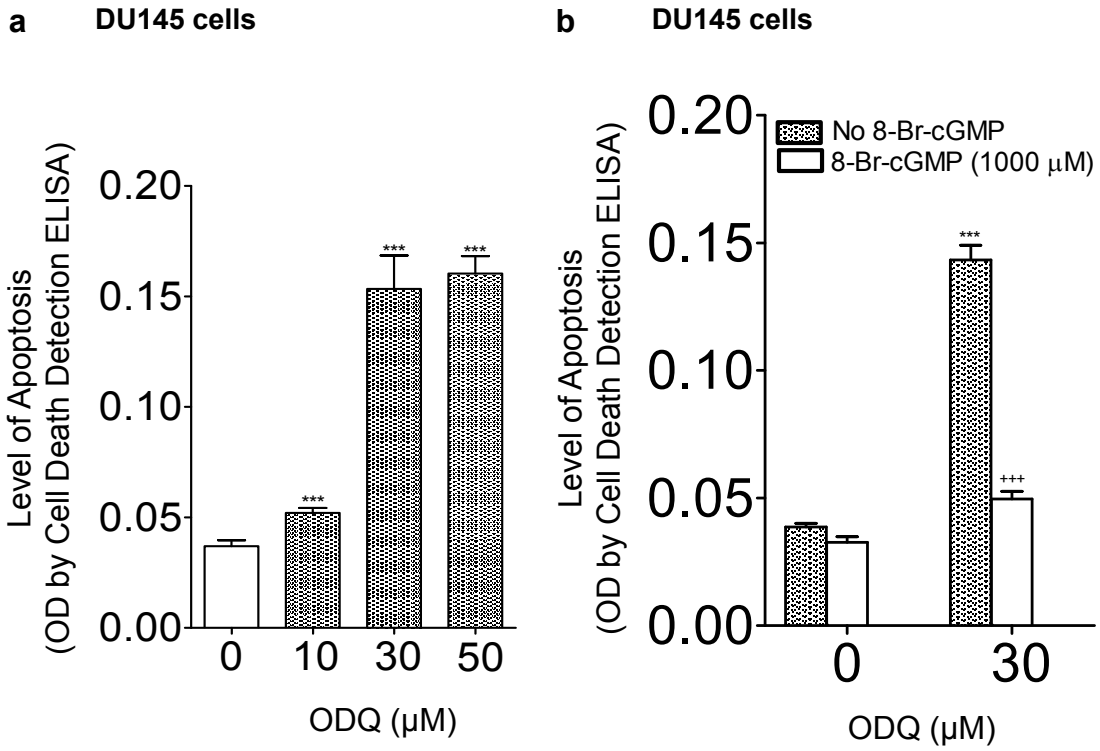

Figure 3

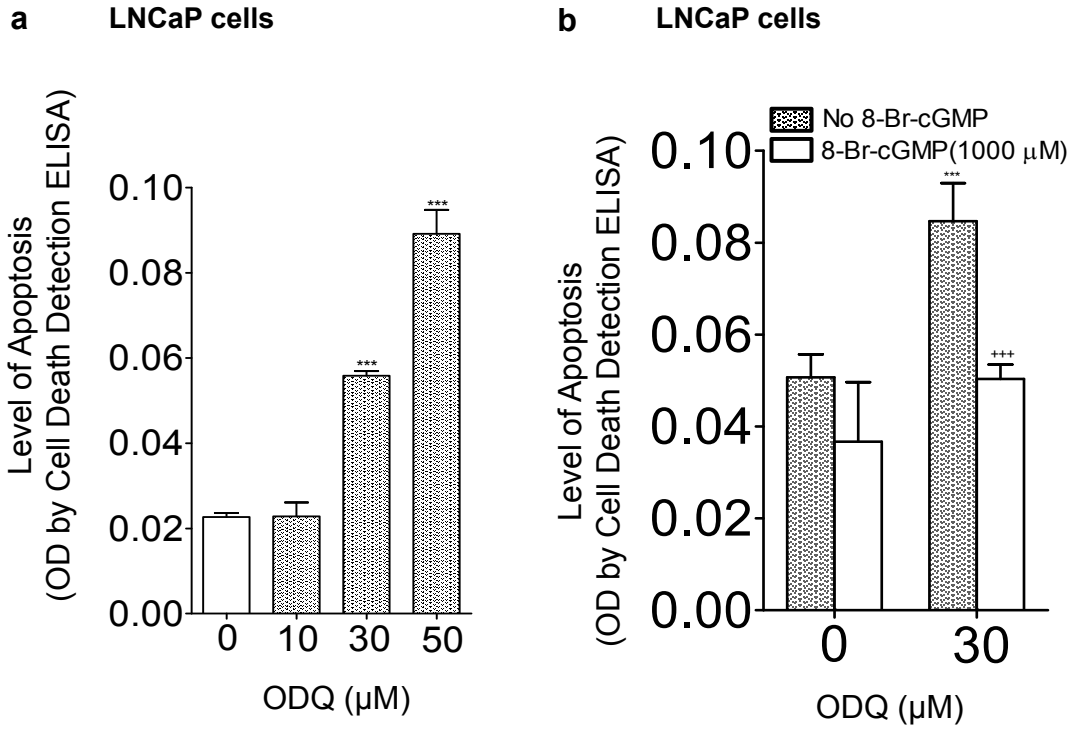

Figure 4

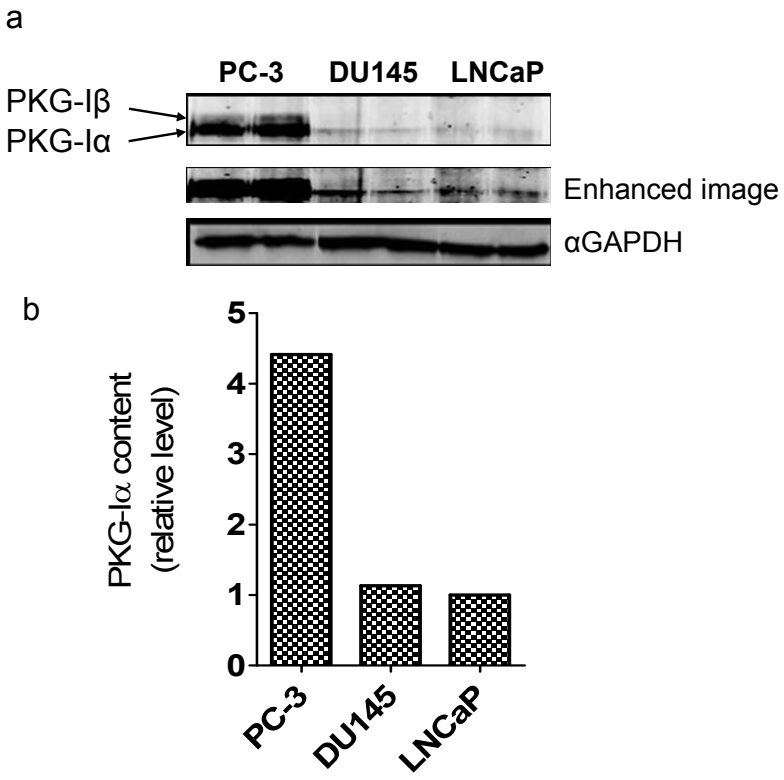

Figure 5

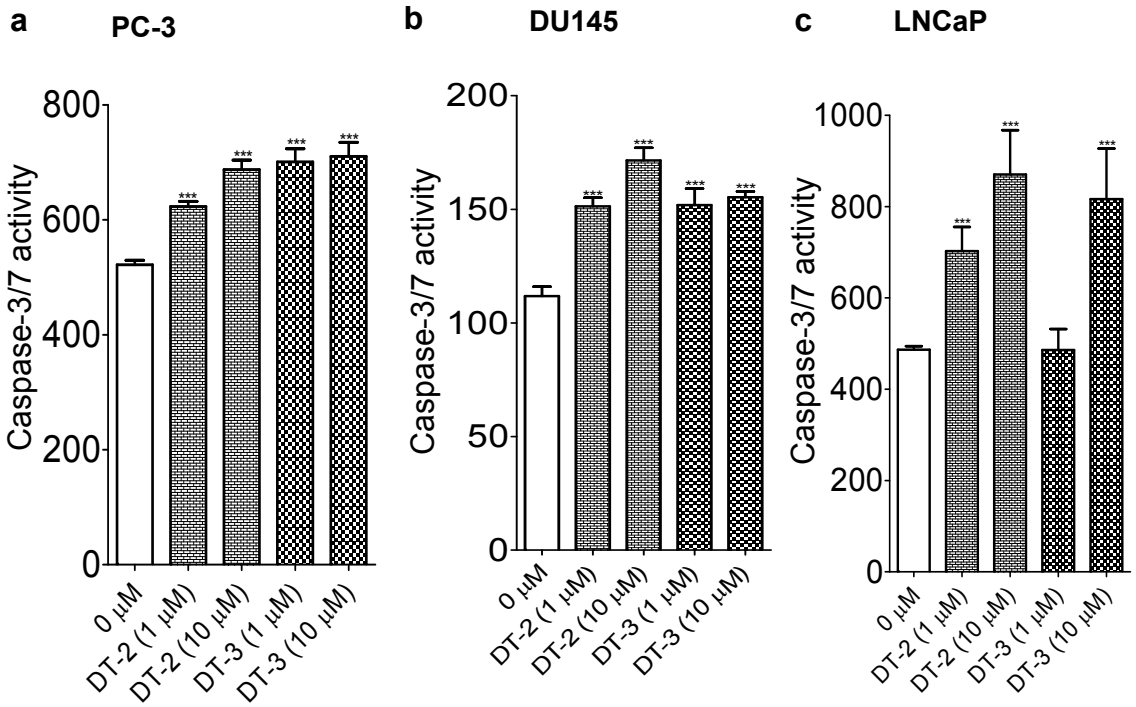

Figure 6

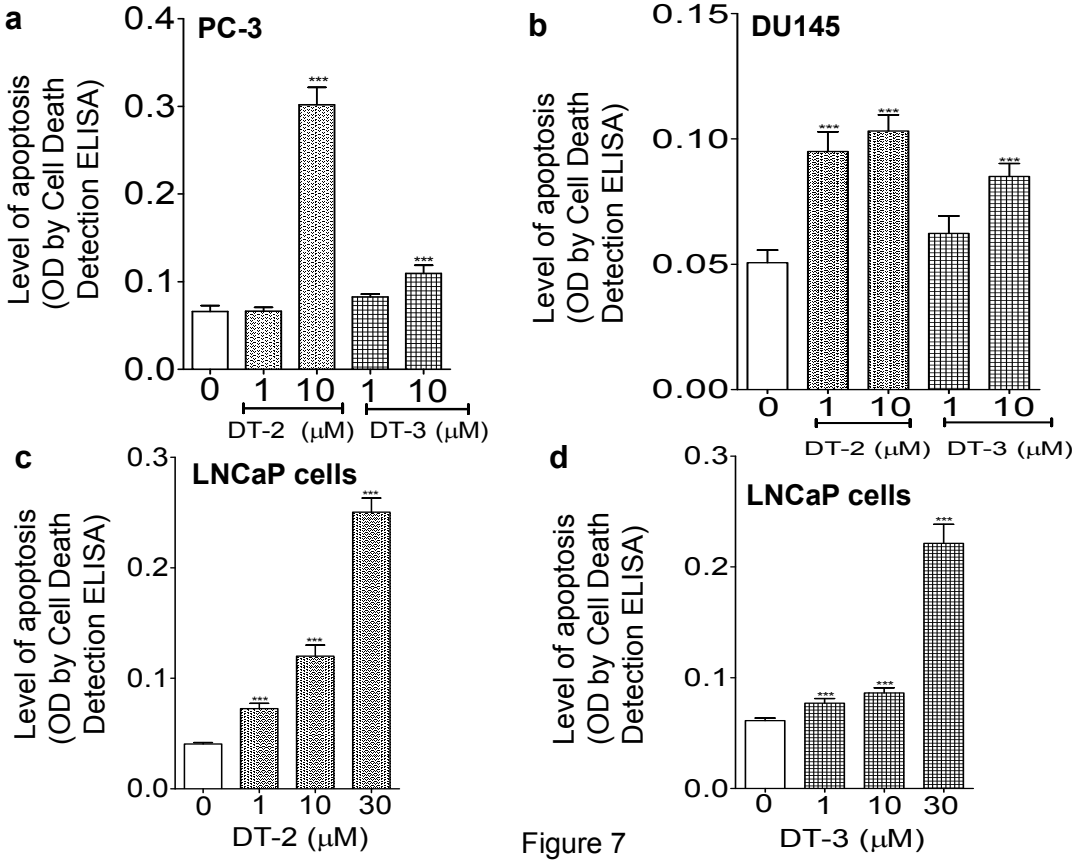

Figure 7

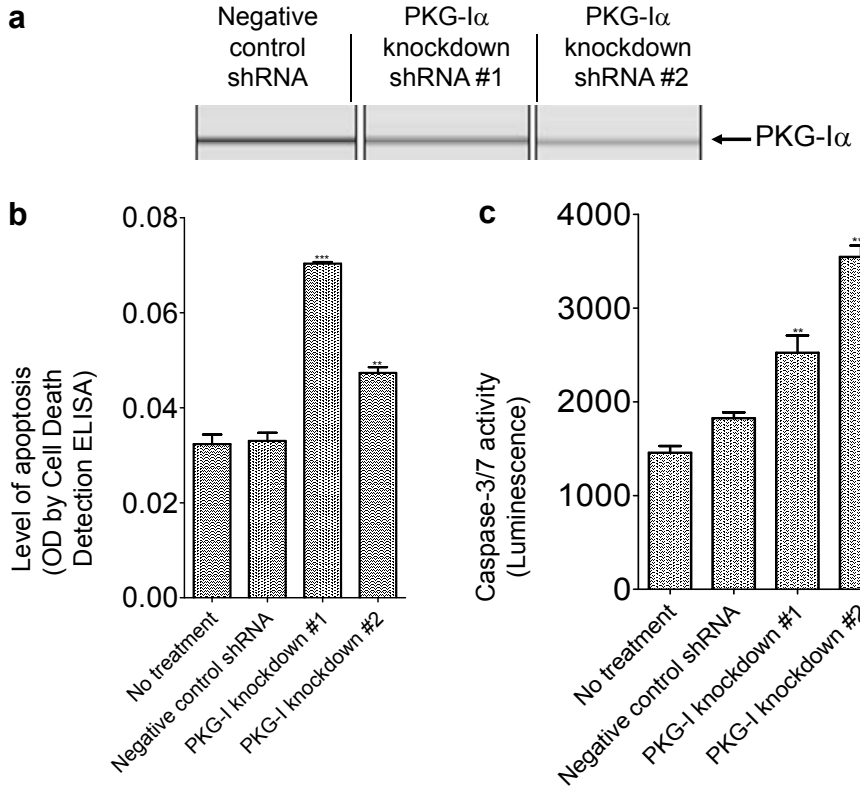

Figure 8

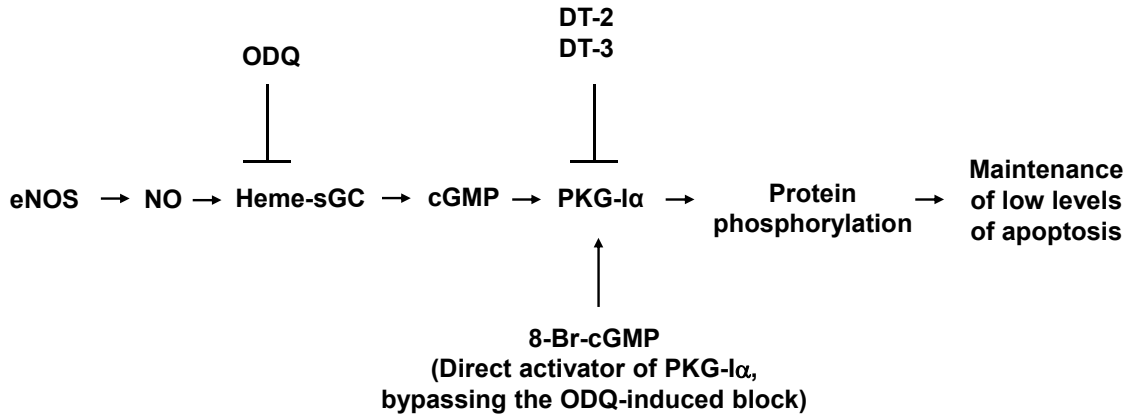
DT-2
DT-3
ODQ
eNOS
NO
Heme-sGC
cGMP
PKG-Iα
Protein phosphorylation
Maintenance of low levels of apoptosis
8-Br-cGMP
(Direct activator of PKG-Iα, bypassing the ODQ-induced block)

Figure 9

Basal cyclic GMP levels and protein kinase G type-Iα activity play an essential role in promoting cell proliferation in prostate cancer cells

Ronald R. Fiscus, Madhavi Bathina, Mary G. Johlfs, Janica C. Wong, Oscar B. Goodman, Jr., Sunil Sharma, Giuseppe Pizzorno and Nicholas J. Vogelzang

Cancer Molecular Biology Section, Nevada Cancer Institute, Las Vegas, Nevada, USA, and College of Pharmacy, University of Southern Nevada, Henderson, Nevada, USA.

Correspondence: Ronald R. Fiscus, University of Southern Nevada, 11 Sunset Way, Henderson, Nevada, USA 89014; Phone: 702-968-5570, Fax: 702-968-5573, email: rfiscus@usn.edu

Abstract

Radiation therapy and chemotherapy often result in side effects and the potential of relapse of the tumor. There is a need to identify the molecular mechanisms in the prostate cancer cells that are responsible for disease progression, continued cell proliferation, which in turn would aid in better treatment options for prostate cancer patients. In this study, we propose the involvement of a novel protein kinase G signaling pathway in regulating the proliferation of prostate cancer cell lines, PC-3, DU145 and LNCaP. Previous studies from our laboratory have shown that nitric oxide (NO)/cGMP/PKG signaling pathway plays an essential role in suppressing apoptosis and promoting DNA synthesis/cell proliferation in both normal (e.g. vascular smooth muscle cells) and transformed cells (e.g. ovarian cancer cells). There is supporting evidence in the literature that prostate cancer cell lines express enzymes that synthesis endogenous NO. We hypothesized that the endogenous NO drives the NO/cGMP/PKG pathway in prostate cancer cells, promoting their proliferation. The present study, using radioimmunoassay for cGMP, shows that sGC inhibition by the selective inhibitor ODQ decreases the cGMP levels in all three of the prostate cancer cell lines. Western blot analysis shows that all three of the prostate cancer cell lines express predominantly the PKG-Iα isoform. Furthermore, gene knockdown of PKG-Iα using specific shRNA decreases the cell proliferation of PC-3 prostate cancer cells. sGC inhibition by ODQ and PKG-Iα inhibition by the highly selective inhibitors DT-2 and DT-2 decreased the DNA synthesis in all the prostate cancer cell lines. The decrease in the colony formation ability of cells treated with ODQ

and DT-2 further supports our hypothesis that sGC/cGMP/PKG-Iα signaling pathways is involved in regulating cell proliferation in PC-3, DU145 and LNCaP prostate cancer cell lines.

Introduction

Prostate cancer is one of the leading causes of cancer deaths after lung and bronchus, among men in the United States. In 2008 an estimated 186,320 number of new prostate cancer cases and an estimated 28,660 number of new deaths were expected (1) Prostate cancer is typically treated with radiation therapy, hormonal therapy and chemotherapy. Radiation therapy has side effects on normal cells if used in higher doses (2) Hormone therapy or androgen depletion is rarely effective (3) Metastasis prostate cancer to multiple sites is increasingly difficult to treat (4)

Here in this study we elucidate the molecular mechanism which is responsible for the continued proliferation of the prostate cancer cells. Both hormone dependent (LNCaP) and hormone independent (PC-3 and DU145) prostate cancer cell lines were studied for the expression of a protein kinase G. Protein kinase G is a serine-threonine kinase extensively studied in vascular smooth muscle cells, endothelial cells and bone marrow derived stromal cells (5, 6) In these cell the PKG plays a wide range of important roles such as bone development (7), muscle relaxation, regulation of calcium levels (5) regulation of gene expression and regulation of apoptosis in neuronal cells (8)

The role of PKG has also been studied in cancer cells. PKG activation induces apoptosis in colon cancer cells (9, 10) In ovarian cancer cells, PKG has been shown to suppress apoptosis (11, 12) sGC enzyme activates cGMP which inturn

increases the enzymatic activity of PKG (13) Nitric oxide activates the sGC by binding to its heme group (14) NO activated sGC enzyme increases the intracellular levels of cGMP (15) cGMP regulates ion channels, cGMP-regulated phosphodiesterases, and cGMP-dependent protein kinases (PKGs) (13, 16) NO regulates gene expression via cGMP and PKG (17) NO and the subsequently activated cGMP act as pro apoptotic and anti apoptotic factors depending on their concentrations (8)

NO is a signaling molecule produced by the enzymes called Nitric oxide synthases (NOS) NOS have been found to be expressed in various tumor cells. Human prostate cancer cells express eNOS (endothelial nitric oxide synthase) (18) eNOS expression is also found in oral squamous cell carcinoma (19) iNOS (inducible nitric oxide synthase) has been found in human prostate carcinoma tissues from patients (20) iNOS expression is directly related to the cancer cell proliferation rate in prostate cancer (21) In prostate cancer cell lines (PC-3 DU145 and LNCaP) it was shown that NO donors sensitizes the cells to apoptosis through TRAIL, Bcl-2 and Bcl-xL (18)

Though some background data is available in the literature about the role of NO in prostate tumor cells, the exact molecular mechanism through which the NO induces the proliferation of these cells is not yet elucidated. We hypothesize that NO is produced within the prostate cancer cells by NOS (In this study we show that PC-3 cells express eNOS; the data with DU145 and LNCaP is not shown)

and this would activate the sGC enzyme which increases the levels of cGMP, the activated cGMP increases the enzymatic activity of PKG. According to our hypothesis, PKG-Iα activity is important for cell survival of the prostate cancer. To prove the involvement of PKG-Iα we used highly specific inhibitors DT-2 and DT-3 and also the specific PKG-I gene knock down, and studied the inhibition of PKG-Iα on cell proliferation and DNA synthesis in all the three prostate cancer cell lines.

Materials and Methods

Cell cultures and reagents

PC-3, DU145 and LNCaP prostate cancer cell lines were obtained from American type culture collection (Mansassas, VA). PC-3 cells were maintained in F-12K medium, DU145 cells were maintained in Minimum Essential Medium (MEM) and LNCaP cells were maintained in RPMI-1640 medium. All media were supplemented with 10% fetal bovine serum and 1% penicillin-streptomycin (ATCC, Mansassas, VA). All the cells were cultured at 37^0C, at 5% CO_2. Cells were treated with ODQ (Sigma, St. Louis, MO, USA) PKG-Iα inhibitors DT-2 and DT-3 (Biolog, Hayward CA, USA and Calbiochem, Gibbstown, NJ, USA) to measure cell proliferation by BrdU cell proliferation kit (Roche Diagnostics Inc., Indianapolis, IN, USA) cGMP levels by radioimmunoassay (Biomedical Technologies Inc., Stoughton, MA, USA) and Clonogenic Survival using crystal violet dye (Sigma)

Protein Quantification & Western blot analysis using Infrared imaging

For western blot analysis, approximately one million cells were lysed with SDS lysis buffer and the protein concentration was measured by fluorescence-based protein Quantitation kit EZQ (Molecular probes, Carlsbad, CA, USA) Protein was resolved by SDS-PAGE and then transferred to a nitrocellulose membrane (Amersham Biosciences, Piscataway, NJ, USA) through a wet transfer at 35Volts overnight at 4^0C. The membrane was blocked at room temperature for one hour in the LI-COR buffer, with 0.1% Tween, followed by overnight

incubation with the rabbit anti-PKG-I primary antibody (Cell signaling technology, Beverly, MA, USA) (247.7µg/ml) at 1:1000 dilution and anti-GAPDH antibody (eGene Inc., Irvine, CA, USA) Following day membrane was incubated with secondary antibody labeled with IR Dye800 for one hour at room temperature. The membrane is then scanned on the LI-COR Infrared imaging system for the expression of PKG-I in all the three prostate cancer cell lines.

Radioimmunoassay

To determine the levels of cGMP in prostate cancer cell lines treated with sGC inhibitor ODQ, a radioimmunoassay was performed using cyclic GMP RIA kit. Approximately 3 million cells were plated in 60mm tissue culture plates for each cell line. The cells were treated with ODQ (0µM, 10 µM, 30 µM and 50 µM) for 20 minutes and lysed with ice cold ethanol. The cGMP levels in the control and treatment groups were measured using I^{125} labeled cGMP and specific cGMP antiserum following manufacturer's recommendations. Results are represented as cGMP in pmole/million cells compared to the control.

BrdU cell proliferation assay

To determine the cell proliferation in prostate cancer cell lines treated with sGC inhibitor ODQ or PKG-Iα inhibitors DT-2 and DT-3, a colorimetric immunoassay was performed, which measures the cell proliferation based on the measurement of BrdU incorporation during DNA synthesis. Approximately thousand cells were exposed to ODQ at 0, 10, 30 and 50 µM or DT-2 and DT-3 at 0, 1 and 10µM

concentrations for 24hours. At the end of the incubation period cell proliferation was measured following the manufacturer's protocol.

Colonogenic survival assay

For clonogenic survival assay, approximately 500 cells were plated in 6-well plates and treated with ODQ or DT-2 for 24 hours. At the end of incubation period, the cells were washed with 1X PBS twice and fresh media was added, the cells were let grow and form colonies for about 10 days or until the control wells become confluent. At the end of the incubation time, the colonies were stained with crystal violet (5mg/ml in 95% ethanol) for 10 minutes. The numbers of colonies in the treatment groups were counted and compared to the controls.

RNA interference

PC-3 cells were seeded in a 96 well plate at a density of 20,000 cells/well in media lacking antibiotics and incubated overnight. The following day, the cells were transfected with PKG-I-specific shRNA containing expression vectors (Origene, Rockville, MD, USA) as follows: 3.0% Lipofectamine 2000 (Invitrogen, Carlsbad, CA, USA) and vector at a ratio of 1ug/100ul were added to Opti-MEM (Invitrogen) serum free media and incubated at room temperature for 20 minutes. The mixture was then added to the cells drop-wise. Following gentle mixing, the cells were incubated for 48-72 hours and cell proliferation was assessed. PKG expression levels were monitored using RT-PCR and

subsequent analysis on a 12-channel capillary electrophoresis system with a light emitting diode (eGene Inc., Irvine, CA, USA)

Gene expression analyzed on a 12-channel capillary electrophoresis system with a light emitting diode

RNA was trizol (Life Technologies, Grand Island, NY, USA) extracted from 50,000 PC-3 cells. One microgram of purified total RNA was converted to cDNA using Superscript Vilo reverse transcriptase kit (Invitrogen) The cDNA was used in a PCR reaction with the PKG-Iα specific primers (Forward primer – 5'-GGC GCA GGG CAT CTC G-3' and Reverse primer – 5'-ATC CAC AAT CTC CTG GAT CTG-3' from Integrated DNA technologies, Coralville, IA, USA) using a GeneAmp PCR system 9700. After 30 cycles, the PCR products were run on a QIAexcel (eGene, Inc.), an automated high performance genetic analyzer that utilizes capillary electrophoresis (CE). Products were injected at 8 kV for 20 seconds and separated at 6kV for 400 seconds. Products were sequenced to verify their identity.

Statistical Analysis

Results were expressed as the mean ± SEM of at least 3, 6 or 8 different samples. Statistical analysis was performed by one way ANOVA followed by Dunnett's post test using PRISM software (Version 3.0; GraphPad) Results were inferred using a statistical significance of $P<0.01$.

Results

Prostate cancer cells express PKG-Iα isoform:

Western blot analysis using highly specific antibody for PKG-I from cell signaling technology showed that all the three prostate cancer cell lines express the PKG-Iα isoform (Figure 1, Panel B) Western blot analysis was carried out using Li-Cor infrared imaging system that utilizes secondary antibodies directly tagged with infrared dyes. PC-3 cells express both isoforms of PKG, Iα and Iβ. DU145 and LNCaP cells express PKG-Iα isoform which can be clearly seen in the digitally enhanced image. The α–GAPDH was used as a loading control.

Radioimmunoassay: cGMP levels in prostate cancer cell lines:

Radioimmunoassay (Biomedical Technologies Inc.,) which involves the competitive binding of cGMP in the sample and the radioactive I125 cGMP for a highly specific antibody was used to measure the cGMP levels in response to the sGC inhibitor ODQ. The concentrations of cGMP (pmoles/ml) in the samples were calculated from the standard curve. Within 20 minutes of treatment, ODQ at 0, 10, 30 and 50 μM concentrations caused a concentration dependent decrease in the cGMP levels in all the three prostate cancer cell lines (Figure 2, Panel A) these results suggest that in prostate cancer cells sGC activates the basal levels of cGMP.

sGC inhibitor ODQ decreases DNA synthesis in prostate cancer cell lines:

After determining the decrease in cGMP levels in response to ODQ treatment, we next examined the effects of sGC inhibition on cell proliferation. All the three prostate cancer cell lines were treated with 0, 10, 30 and 50 μM ODQ for 24 hours and the DNA synthesis was measured using BrdU labeling reagent. In all the three prostate cancer cell lines ODQ decreased DNA synthesis in a concentration dependent manner (Figure 2, Panel B)

Clonogenic survival assay: sGC inhibitor (ODQ) and PKG-Iα inhibitor decrease colony formation ability in all the three prostate cancer cell lines:

ODQ treatment for 24 hours (Figure 3, Panel A) and PKG-Iα inhibitor DT-2 (Figure 3, Panel B) decrease the colony formation ability of the prostate cancer cell lines. ODQ at 0, 10, 30, 50 and 100 μM caused a dose dependent effect in decreasing the colony formation ability. The highly selective PKG-Iα inhibitor DT-2, at 0, 1 and 10 μM concentration also caused a dose dependent effect in decreasing the colony formation ability in all the three prostate cancer cell lines. Taken together these results prove the involvement of a novel signaling pathway – sGC/cGMP/PKG-Iα in the regulation of cell proliferation in prostate cancer cells.

PKG-Iα inhibitors DT-2 and DT-3 decreases DNA Synthesis:

To confirm the role of PKG-Iα in the regulation of cell proliferation of prostate cancer cells, we used highly selective inhibitors of PKG-Iα to measure the DNA

synthesis through BrdU incorporation. DT-2 and DT-3 at concentrations 0, 1 and 10 μM caused a dose dependent decrease in the DNA synthesis (Figure 4)

Gene knock down studies of PKG-Iα confirms its role in regulation of cell proliferation:

To further confirm the role of PKG-Iα signaling pathway in cell proliferation regulation in prostate cancer cells, we used PKG-I specific shRNA gene knockdown and measured the cell proliferation in PC-3 cells using MTT assay (Roche Diagnostics Inc.,) shRNA #1 and shRNA # 2 caused 54% and 68% of PKG-Iα knockdown respectively. shRNA # 1 and #2 are two different cloned of shRNA vector. A negative control shRNA was included which carries a non specific gene. Figure 5, Panel A represents the mRNA levels of PKG-Iα in relative fluorescent units (RFU) the graph in Panel B represents the cell proliferation in the controls and the PKG-Iα knockdown groups using MTT assay. The PKG-Iα knockdown decreased the cell proliferation in PC-3 prostate cancer cell line.

Discussion

Our findings suggest an important role of PKG-Iα in regulation the cell proliferation of prostate cancer cell lines. In the present study we propose that in prostate cancer cells the sGC enzyme active cGMP which increases the activity of PKG-Iα. PKG-Iα mediates the regulation of cell proliferation. This is thought to be mediated by the phosphorylation of downstream proteins or transcription factors that are involved in cell proliferation and/or apoptosis. Our future studies would concentrate in finding out which proteins are involved downstream to PKG-Iα which mediates its effects.

The results in the present study with the prostate cancer cell lines PC-3, DU145 and LNCaP, proves the role of a novel signaling pathway involving PKG-Iα in the regulation of cell proliferation. Previous studies in our lab have shown that PKG-I play a critical role in regulation apoptosis in ovarian cancer cells (11) The role of sGC/cGMP/ PKG-Iα signaling pathway has not yet been elucidated in the prostate cancer cells. Data in the literature shows that various cancer cells express different isoforms of nitric oxide synthase enzymes and their role in the tumor growth (22)

Our data using highly selective inhibitors of sGC/cGMP/PKG-Iα pathway show that basal levels of sGC/cGMP/PKG-Iα signaling pathway is involved in maintaining the cell proliferation in all the three prostate cancer cell lines. The

role of PKG-Iα is further confirmed using gene knockdown studies with PKG-I specific shRNA, which decreased the cell proliferation in PC-3 prostate cancer cell line. Further studies will be carried out to determine which downstream signal proteins are involved in mediating the effects of PKG-Iα.

References

1. Jemal A, Siegel R, Ward E, et al. Cancer statistics, 2008. CA Cancer J Clin 2008;58:71-96.

2. Hanks GE, Martz KL, Diamond JJ. The effect of dose on local control of prostate cancer. Int J Radiat Oncol Biol Phys 1988;15:1299-305.

3. Bubendorf L, Kolmer M, Kononen J, et al. Hormone therapy failure in human prostate cancer: analysis by complementary DNA and tissue microarrays. J Natl Cancer Inst 1999;91:1758-64.

4. Cheng L, Zincke H, Blute ML, Bergstralh EJ, Scherer B, Bostwick DG. Risk of prostate carcinoma death in patients with lymph node metastasis. Cancer 2001;91:66-73.

5. Cornwell TL, Lincoln TM. Regulation of intracellular Ca2+ levels in cultured vascular smooth muscle cells. Reduction of Ca2+ by atriopeptin and 8-bromo-cyclic GMP is mediated by cyclic GMP-dependent protein kinase. J Biol Chem 1989;264:1146-55.

6. Murad F, Rapoport RM, Fiscus R. Role of cyclic-GMP in relaxations of vascular smooth muscle. J Cardiovasc Pharmacol 1985;7 Suppl 3:S111-8.

7. Broderick KE, Zhang T, Rangaswami H, et al. Guanosine 3',5'-cyclic monophosphate (cGMP)/cGMP-dependent protein kinase induce interleukin-6 transcription in osteoblasts. Mol Endocrinol 2007;21:1148-62.

8. Fiscus RR, Yuen JP, Chan SL, Kwong JH, Chew SB. Nitric oxide and cyclic GMP as pro- and anti-apoptotic agents. J Card Surg 2002;17:336-9.

9. Deguchi A, Thompson WJ, Weinstein IB. Activation of protein kinase G is sufficient to induce apoptosis and inhibit cell migration in colon cancer cells. Cancer Res 2004;64:3966-73.

10. Liu L, Li H, Underwood T, et al. Cyclic GMP-dependent protein kinase activation and induction by exisulind and CP461 in colon tumor cells. J Pharmacol Exp Ther 2001;299:583-92.

11. Leung EL, Fraser M, Fiscus RR, Tsang BK. Cisplatin alters nitric oxide synthase levels in human ovarian cancer cells: involvement in p53 regulation and cisplatin resistance. Br J Cancer 2008;98:1803-9.

12. Fraser M, Chan SL, Chan SS, Fiscus RR, Tsang BK. Regulation of p53 and suppression of apoptosis by the soluble guanylyl cyclase/cGMP pathway in human ovarian cancer cells. Oncogene 2006;25:2203-12.

13. Fiscus RR, Rapoport RM, Waldman SA, Murad F. Atriopeptin II elevates cyclic GMP, activates cyclic GMP-dependent protein kinase and causes relaxation in rat thoracic aorta. Biochim Biophys Acta 1985;846:179-84.

14. Boxall AR, Garthwaite J. Long-term depression in rat cerebellum requires both NO synthase and NO-sensitive guanylyl cyclase. Eur J Neurosci 1996;8:2209-12.

15. Lin HC, Wan FJ, Tseng CJ. Modulation of cardiovascular effects produced by nitric oxide and ionotropic glutamate receptor interaction in the nucleus tractus solitarii of rats. Neuropharmacology 1999;38:935-41.

16. Lincoln TM, Cornwell TL. Intracellular cyclic GMP receptor proteins. FASEB J 1993;7:328-38.

17. Idriss SD, Gudi T, Casteel DE, Kharitonov VG, Pilz RB, Boss GR. Nitric oxide regulation of gene transcription via soluble guanylate cyclase and type I cGMP-dependent protein kinase. J Biol Chem 1999;274:9489-93.

18. Tong X, Li H. eNOS protects prostate cancer cells from TRAIL-induced apoptosis. Cancer Lett 2004;210:63-71.

19. Shang ZJ, Li JR. Expression of endothelial nitric oxide synthase and vascular endothelial growth factor in oral squamous cell carcinoma: its correlation with angiogenesis and disease progression. J Oral Pathol Med 2005;34:134-9.

20. Klotz T, Bloch W, Volberg C, Engelmann U, Addicks K. Selective expression of inducible nitric oxide synthase in human prostate carcinoma. Cancer 1998;82:1897-903.

21. Aaltoma SH, Lipponen PK, Kosma VM. Inducible nitric oxide synthase (iNOS) expression and its prognostic value in prostate cancer. Anticancer Res 2001;21:3101-6.

22. Jenkins DC, Charles IG, Thomsen LL, et al. Roles of nitric oxide in tumor growth. Proc Natl Acad Sci U S A 1995;92:4392-6.

Figure Legends

Figure 1. A, Model showing the hypothesis of PKG-Iα mediated stimulation of cell proliferation in prostate cancer cells. B, Expression levels of PKG-Iα and Iβ in prostate cancer cell lines PC-3, DU145 and LNCaP. Cells were lysed with SDS lysis buffer and the western blot analysis was performed using Li-Cor infrared imaging system. For all the three cell lines 80 µg of total protein was loaded per lane. All the three prostate cancer cell lines express the PKG-Iα isoform. Digitally enhanced image shows the expression of PKG-Iα isoform more clearly in DU145 and LNCaP cell lines. PC-3 cell line also expresses PKG-Iβ isoform. The Iβ isoform is not detectable in DU145 and LNCaP cell lines. The α-GAPDH is used as a loading control.

Figure 2. A, Inhibition of sGC by the specific inhibitor ODQ decreases the cGMP levels in all the three prostate cancer cell lines. Cells were treated with ODQ for 20 minutes and lysed with ice cold ethanol. cGMP levels in the treatment and control groups were measured using radioimmuno assay. Graphs represent Mean ± SEM for each treatment and control group with an n value of 3. B, Inhibition of sGC by the specific inhibitor ODQ decreases the DNA synthesis in all the three prostate cancer cell lines. Cells were treated with ODQ for 24 hours; the BrdU labeling reagent was added at the time of ODQ treatment. DNA synthesis was measured using BrdU cell proliferation kit. Graphs represent Mean ± SEM for each treatment and control group with an n value of 8. Statistical

analysis was performed to using GraphPad prism software and ANOVA test with Dunnett's post test showed significant decrease in the colony formation ability in the treatment groups with a p-value of <0.01.

Figure 3. A, Inhibition of sGC by ODQ and B, Inhibition of PKG-Iα with the selective inhibitor DT-2 decreases the colony formation ability of all the three prostate cancer cell lines. Cells were treated with the inhibitors for 24 hours and the colony forming ability was assessed by growing the cells in fresh media for about 10 days. The graphs show the number of colonies in the treatment groups compared to the control. Graphs represent Mean ± SEM for each treatment and control group with an n value of 3. Statistical analysis was performed to using GraphPad prism software and ANOVA test with Dunnett's post test showed significant decrease in the colony formation ability in the treatment groups with a p-value of <0.01.

Figure 4. Inhibition of PKG-Iα by the selective inhibitors DT-2 and DT-3 decreases the DNA synthesis in PC-3, DU145 and LNCaP prostate cancer cell lines. Cells were treated with the inhibitors for 24 hours. The BrdU labeling reagent was added at the time of treatment. DNA synthesis was measured using BrdU cell proliferation kit from Roche Diagnostics Inc., Graphs represent Mean ±

SEM for each treatment and control group with an n value of 6. Statistical analysis was performed using Prism software and ANOVA test with Dunnett's post test showed significant decrease in DNA synthesis in the treatment groups with a p-value of <0.01.

Figure 5. PKG-I-specific Gene knockdown using shRNA vectors in PC-3 cell line decreases DNA synthesis. A, Gene expression levels of PKG-Iα were measured using a 12-channel capillary electrophoresis system after 48-72 hours of PKG-I-specific shRNA transfection. Negative control shRNA represents transfection of the cells with the vector carrying non specific gene. PKG-I knockdown shRNA #1 and shRNA # 2 represent two different clones of the vector. B, Knockdown of PKG-I decreases cell proliferation in PC-3 prostate cancer cells. Cells were lysed after 48-72 hours of gene transfection and the cell proliferation was measured. significant decrease in proliferation was observed in the knockdown clones compared to the no treatment and the negative control. Graphs represent Mean ± SEM for each treatment and control group with an n value of 6. Statistical analysis was performed using Prism software and ANOVA test with Dunnett's post test showed significant decrease in proliferation in the treatment groups with a p-value of <0.01.

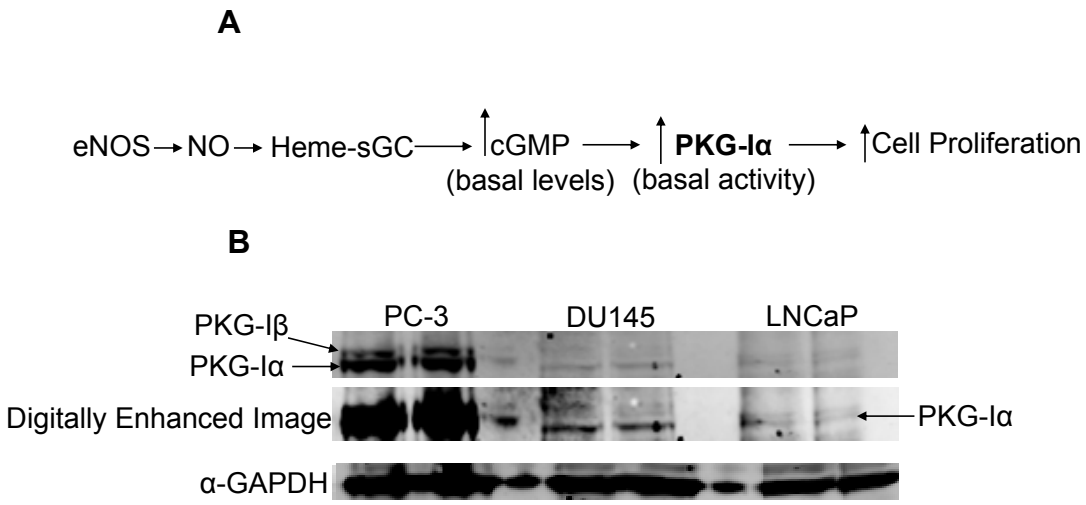

Figure 1.

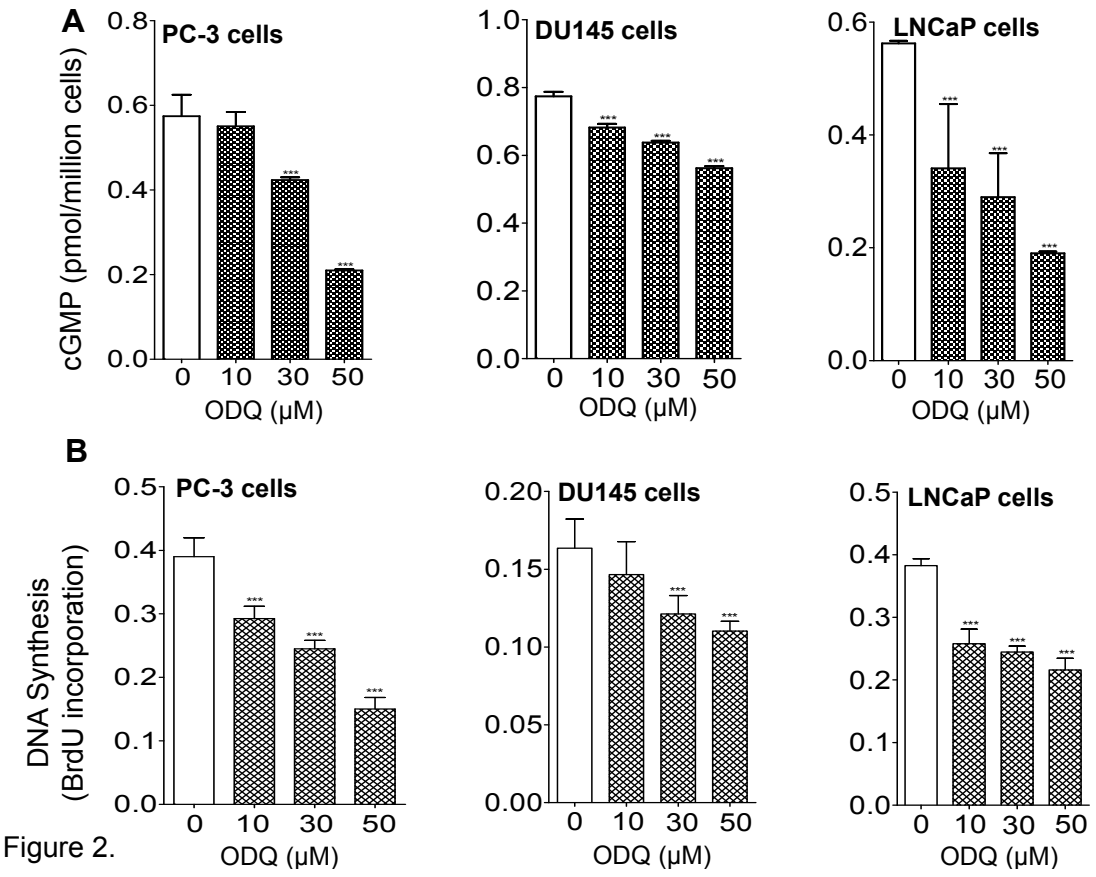

Figure 2.

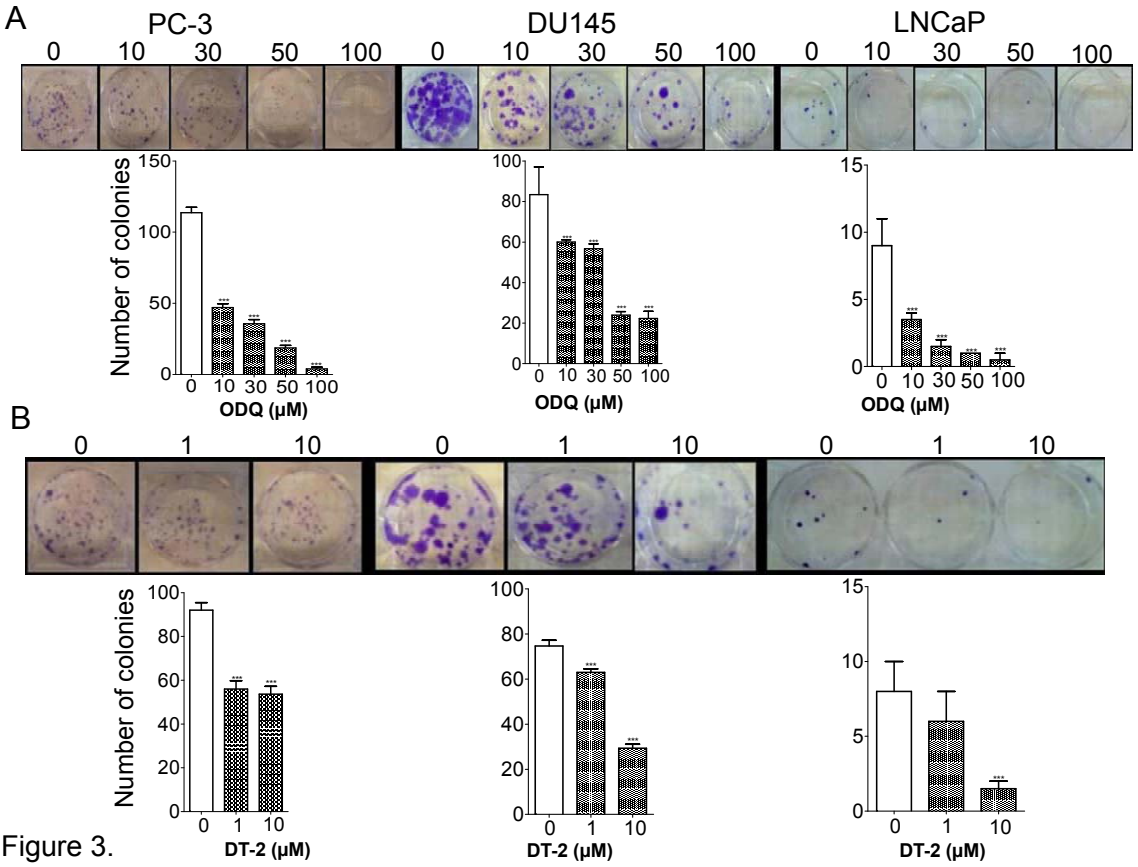

Figure 3.

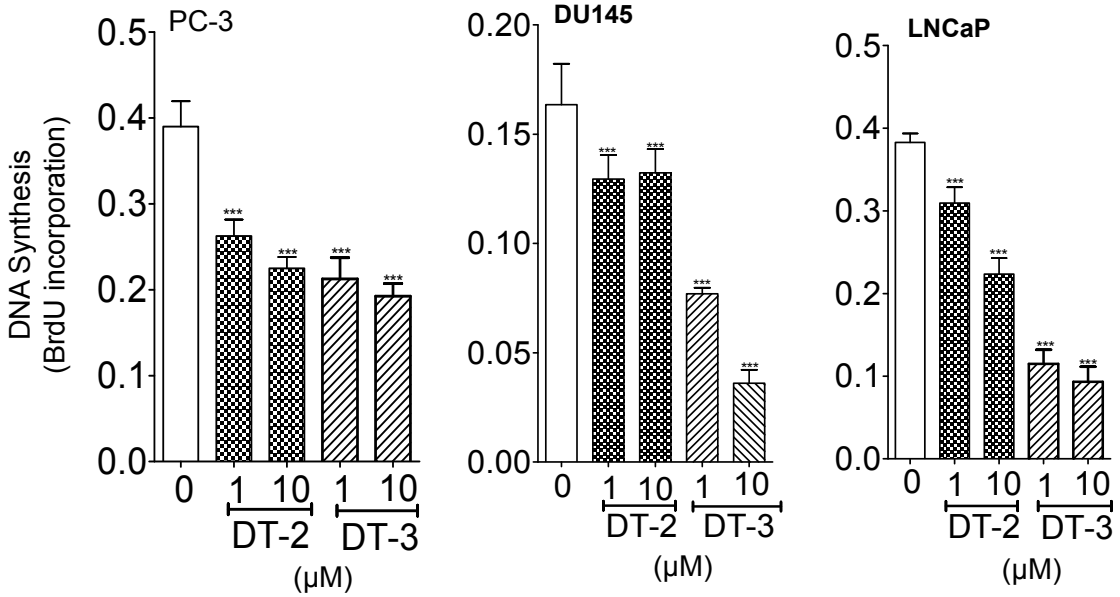

Figure 4.

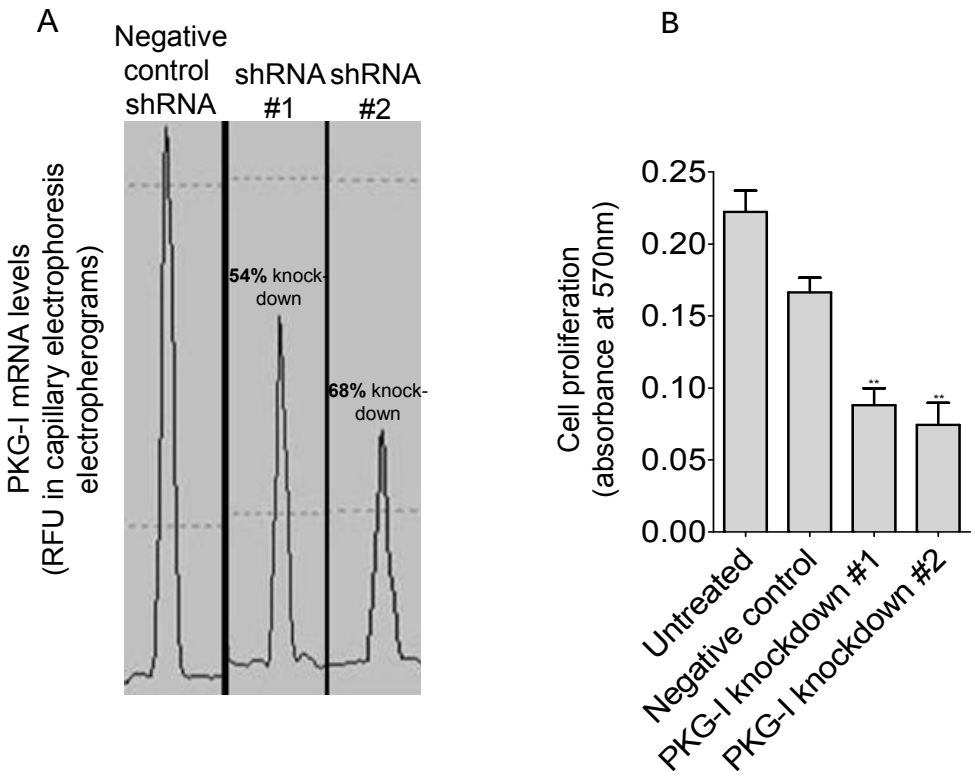
A
Negative control shRNA
shRNA #1
shRNA #2
PKG-I mRNA levels (RFU in capillary electrophoresis electropherograms)
54% knock-down
68% knock-down
B
Cell proliferation (absorbance at 570nm)
0.25
0.20
0.15
0.10
0.05
0.00
**
**
Untreated
Negative control
PKG-I knockdown #1
PKG-I knockdown #2

Figure 5.

Direct serine-17 phosphorylation of Src by protein kinase G type-1 as a cellular mechanism mediating anti-apoptotic and growth-stimulatory effects in malignant mesothelioma cells and non-small cell lung cancer cells

Mary G. Johlfs and Ronald R. Fiscus*

Cancer Molecular Biology Section, Nevada Cancer Institute, Las Vegas, Nevada, and College of Pharmacy, University of Southern Nevada, Henderson, Nevada

*Correspondence: Ronald R. Fiscus, University of Southern Nevada, 11 Sunset Way, Henderson, Nevada, 84014. Cell: (702) 427-3139, Office: (702) 968-5570, Fax: (702) 968-5573, rfiscus@usn.edu

Abstract

Previous data from our laboratory have shown that activation of the cGMP/protein kinase G (PKG) signaling pathway, by basal (low) levels of nitric oxide, prevents apoptosis and stimulates cell proliferation in both normal and malignant mammalian cells, including neural cells, vascular smooth muscle cells, and ovarian cancer cells; however, how PKG interacts with anti-apoptotic and growth-stimulating downstream targets is not yet clear. Src, a non-receptor tyrosine kinase, is known to be important for preventing apoptosis and promoting proliferation in many types of mammalian cells, especially cancer cells. In ovarian cancer cells, our laboratory has shown that a PKG isoform, PKG-Iα, is able to activate Src via a mechanism that involves enhanced autophosphorylation at tyrosine- 416 (mouse sequence)/tyrosine-419 (human sequence), a known activation site in Src, ultimately resulting in enhanced proliferation. However, the exact mechanism by which PKG-Iα is able to enhance Src autophosphorylation/activation is not known. Several previous studies have shown that phosphorylation of Src at the serine 17 site can be catalyzed by protein kinase A (PKA), in response to elevations in cAMP levels, in CHO and PC12 cells, resulting in enhanced activation (tyrosine kinase activity) of Src. Our previous studies have shown that PKG-Iα/β can often phosphorylate the same substrate proteins (at the same phosphorylation sites) as PKA, because of the similar consensus sequence preference of PKA and PKG, e.g. phosphorylation of BAD at serine-155 by both PKA and PKG-Iα.The present study determines whether PKG-I (either PKG-Iα or PKG-Iβ) is capable of both phosphorylating Src at serine-17 and stimulating Src autophosphorylation at tyrosine-419, leading to activation and subsequent increase in cell proliferation and inhibition of apoptosis in malignant mesothelioma cells and non-small cell lung cancer cells. Three malignant mesothelioma cell lines, ME-13, MSTO-211H and NCI-H2052 cells, and a non-small cell lung cancer cell line, NCI-H23 cells, were used. Both in vitro and intact-cell experiments showed that serine-17 and tyrosine-419 phosphorylation was dependent

on PKG-I, using shRNA gene knockdown techniques and highly-selective pharmacological agents known to stimulate (8-Br-cGMP, a cell-permeable cGMP analog that directly activates PKG-Iα/β) or inhibit (ODQ, inhibitor of soluble guanylyl cyclase; DT-2, a PKG-I-specific cell-permeable peptide inhibitor) the cGMP/PKG-I signaling pathway. These pharmacological agents and shRNA were also used to show that inhibition of basal PKG activity leads to increased apoptosis and decreased cell proliferation, as well as decreased cell adhesion. The data indicate that basal kinase actvitiy of PKG-I is essential for preventing spontaneous apoptosis as well as promoting cell proliferation and cell adhesion via the ability of PKG-I to directly phosphorylate Src at serine-17, which in turn enhances Src autophosphorylation at tyrosine-419 and Src activation, in malignant mesothelioma cells and non-small cell lung cancer cells.

Figure 1. A. A control western blot showing the total amount of Src loaded from an in vitro kinase assay. B. A western blot showing serine 17 phosphorylation of recombinant Src by recombinant PKG-Is after an in vitro kinase assay, using a P-Src (ser17)-specific antibody. C. A western blot showing auto-phosphorylation of Src at tyrosine 416 (tyrosine 419 in human Src) in the presence of recombinant PKG-I in an in vitro assay, using a P-Src (Tyr416)-specific antibody.

Figure 2. A. Western blot showing that treatment with ODQ in non-small cell lung cancer cells leads to a decrease of phosphorylation at serine position 17 of Src, indicating that endogenous Src serine-17 phosphorylation is dependent on the endogenous activity of the NO/cGMP/PKG-I signaling pathway. Similar results are found in three malignant mesothelioma cell lines, ME-13, MSTO-211H and NCI-H2052.

Figure 3. A. RT-PCR showing that both of the PKG-I isoforms are knocked down by PKG-I-specific shRNA complexes. B. Western blot demonstrating a decrease in serine 17 phosphorylation in PKG-I-specific knockdown non-small cell lung cancer cells.

Figure 4. A. Caspase 3/7 activity assay showing levels of apoptosis in PKG-I-specific shRNA-treated NCI-H23 non-small cell lung cancer cells are significantly increased compared to no treatment (No trmt) or negative control shRNA. B. Levels of cell proliferation are decreased in PKG-I-specific shRNA-treated NCI-H23 non-small cell lung cancer cells compared to no treatment or negative control shRNA.

Figure 5. A. Western blot showing that treatment with 8-Br-cGMP, a cell-permeable analog of cGMP that can directly activate PKG-Iα/β, leads to increased phosphorylation at serine position 17 of Src.

In vitro experiment using recombinant human Src and recombinant human PKG-Iα and PKG-Iβ showing phosphorylation of Src at serine-17 site and autophosphorylation/activation of Src

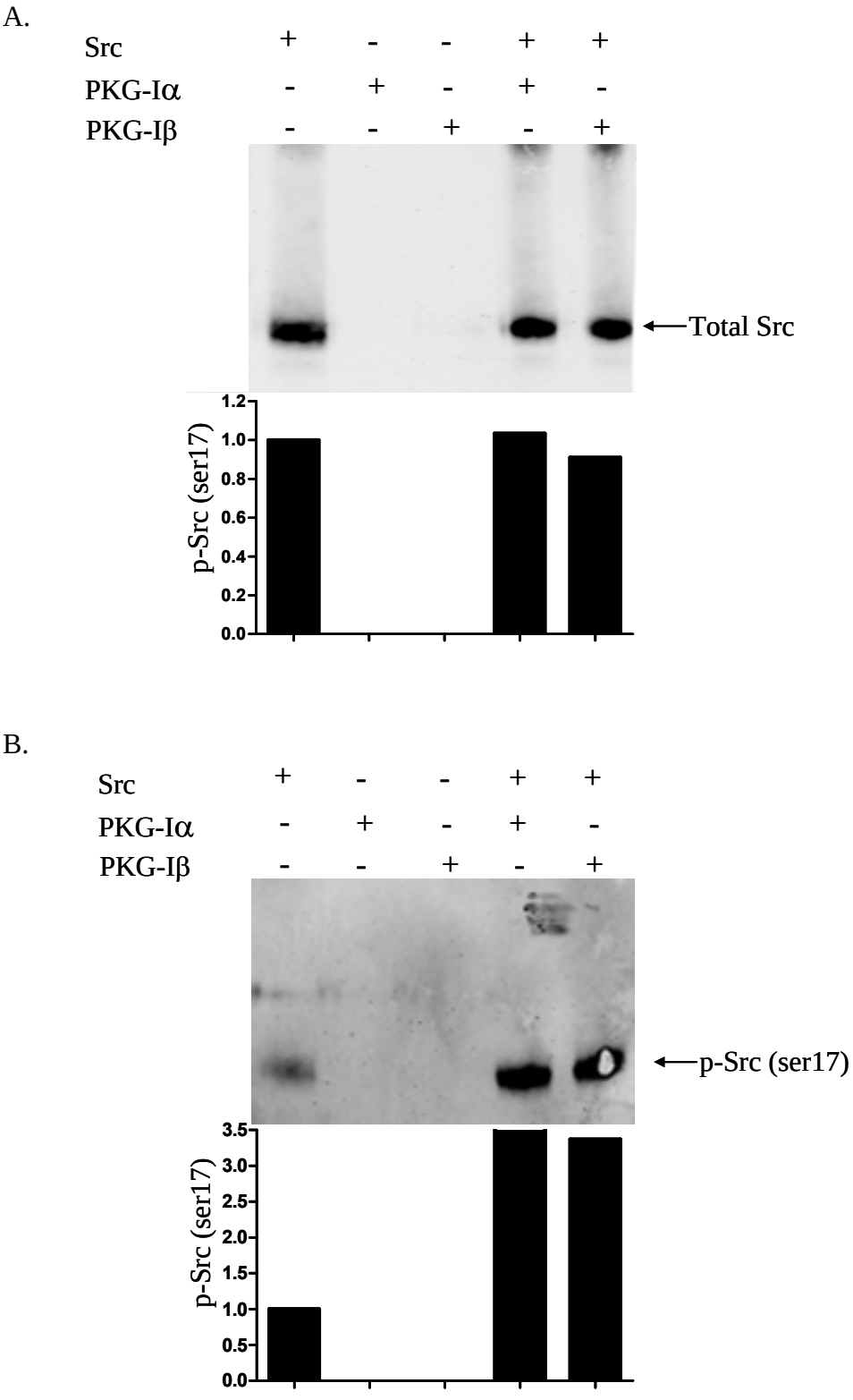

Figure 1

C.

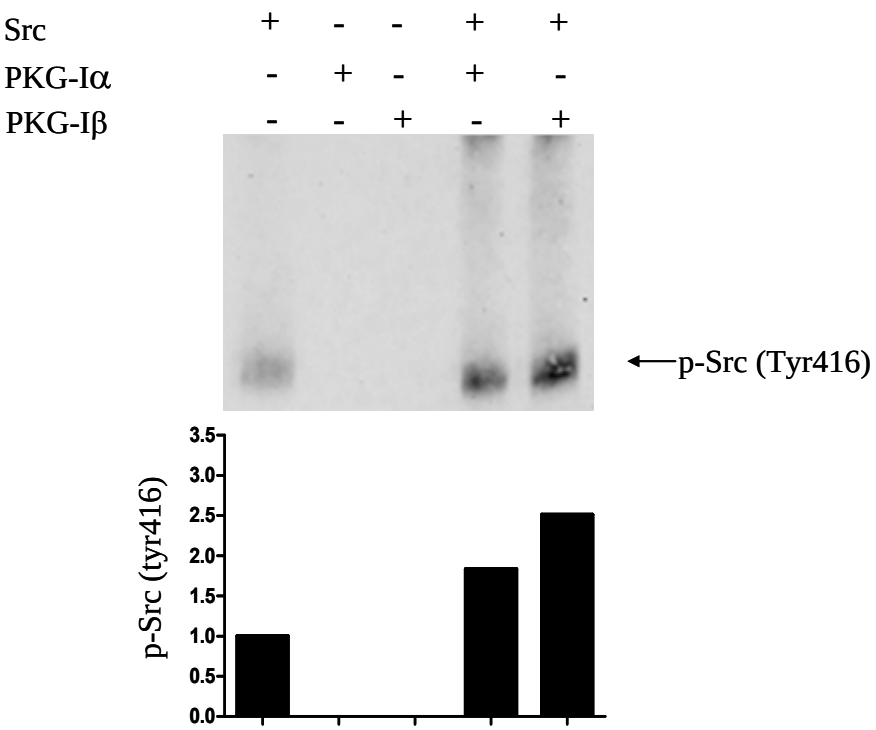

Figure 1 (cont.)

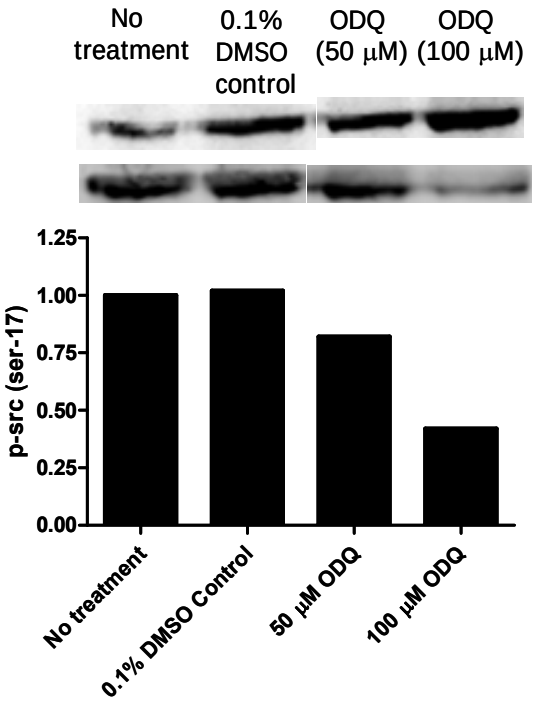
No treatment
0.1% DMSO control
ODQ (50 μM)
ODQ (100 μM)
p-src (ser-17)
1.25
1.00
0.75
0.50
0.25
0.00
No treatment
0.1% DMSO Control
50 μM ODQ
100 μM ODQ

Figure 2

A.

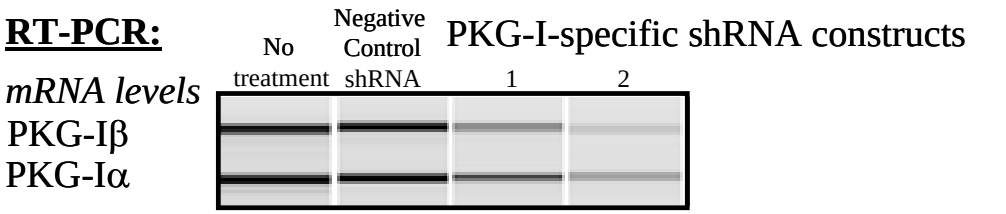
RT-PCR:
No treatment
Negative Control shRNA
PKG-I-specific shRNA constructs
1
2
mRNA levels
PKG-Iβ
PKG-Iα

B.

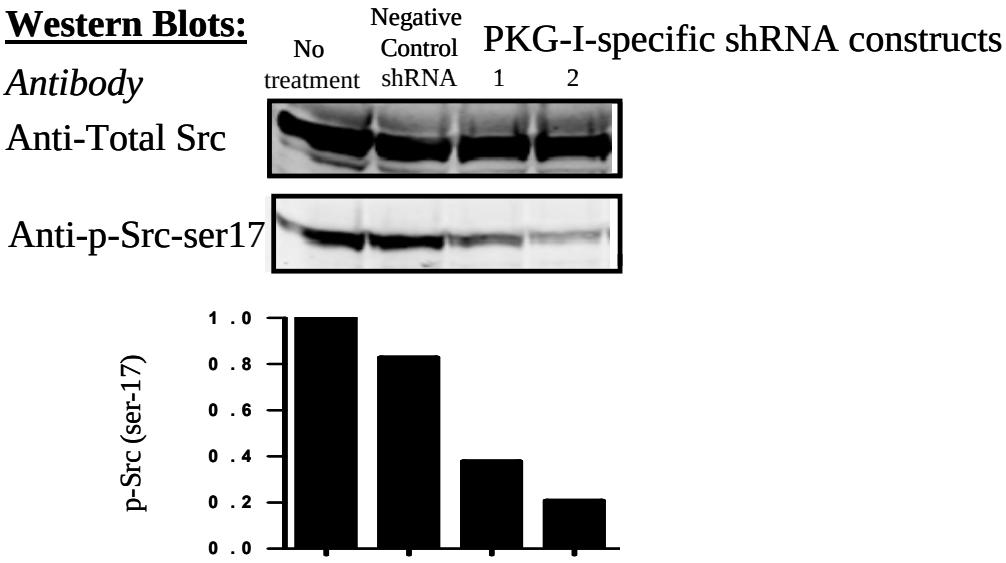
Western Blots:
No treatment
Negative Control shRNA
PKG-I-specific shRNA constructs
1
2
Antibody
Anti-Total Src
Anti-p-Src-ser17
p-Src (ser-17)
1.0
0.8
0.6
0.4
0.2
0.0

Figure 3

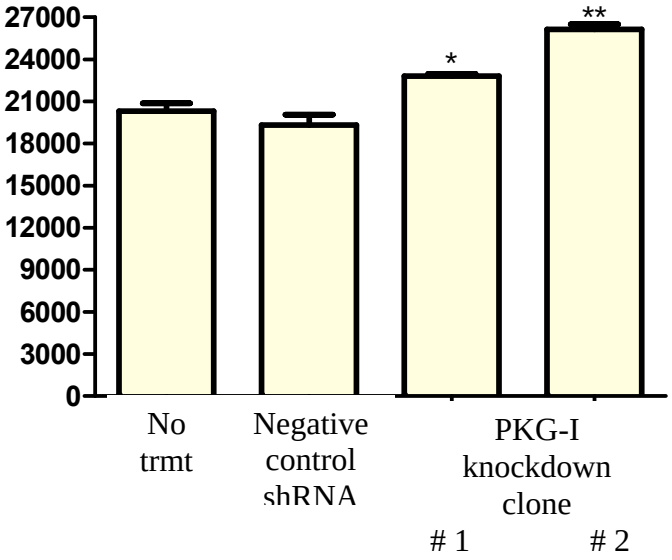
27000
24000
21000
18000
15000
12000
9000
6000
3000
0
*
**
No trmt
Negative control shRNA
PKG-I knockdown clone
1
2

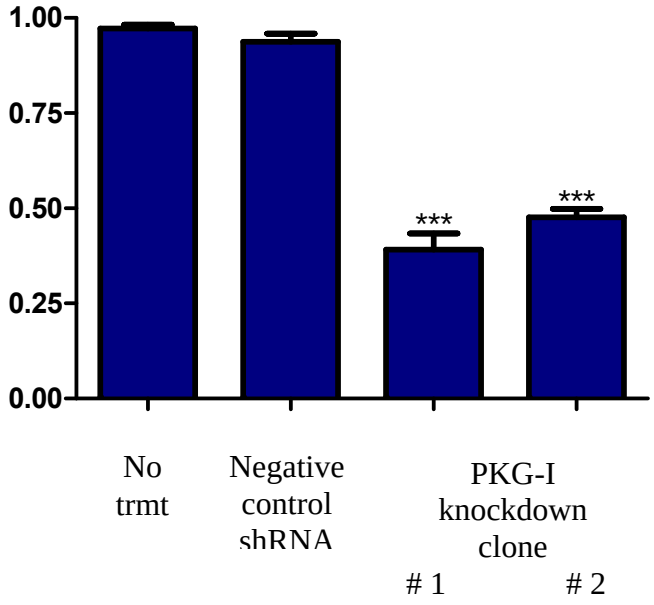
1.00
0.75
0.50
0.25
0.00
***
***
No trmt
Negative control shRNA
PKG-I knockdown clone
1
2

Figure 4

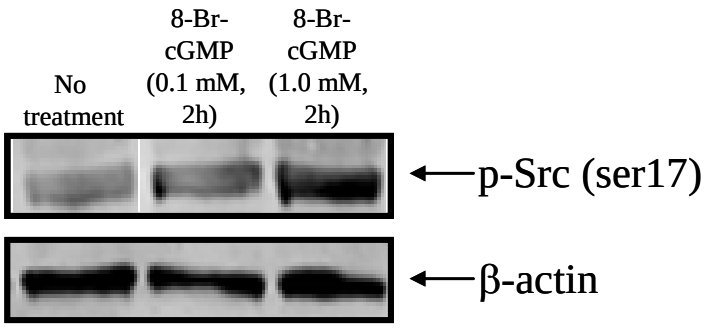
No treatment
8-Br-cGMP (0.1 mM, 2h)
8-Br-cGMP (1.0 mM, 2h)
p-Src (ser17)
β-actin

Figure 5